Evaluation of Shelf Life in Post-Tensioning Grouts

Final Report **August 2018**

Principal investigators:
H. R. Hamilton
Christopher C. Ferraro

Research assistants:
Eduardo Torres
Marcelino Aguirre

Department of Civil and Coastal Engineering
University of Florida
P.O. Box 116580
Gainesville, Florida 32611

Sponsor:
Florida Department of Transportation (FDOT)
Project Manager:
Harvey DeFord, PhD

Contract:
UF Project No. 00115788
FDOT Contract No. BDV31-977-31

University of Florida
Engineering School of Sustainable Infrastructure and Environment
Department of Civil and Coastal Engineering
University of Florida
P.O. Box 116580
Gainesville, Florida 32611

Disclaimer

The opinions, findings, and conclusions expressed in this publication are those of the authors and not necessarily those of the State of Florida Department of Transportation

Unit of Measurement Conversions

SI* (MODERN METRIC) CONVERSION FACTORS

*APPROXIMATE CONVERSIONS **TO** SI UNITS*

SYMBOL	WHEN YOU KNOW	MULTIPLY BY	TO FIND	SYMBOL
LENGTH				
in	inches	25.4	millimeters	mm
ft	feet	0.305	meters	m
yd	yards	0.914	meters	m
mi	miles	1.61	kilometers	km
AREA				
in^2	square inches	645.2	square millimeters	mm^2
ft^2	square feet	0.093	square meters	m^2
yd^2	square yard	0.836	square meters	m^2
ac	acres	0.405	hectares	ha
mi^2	square miles	2.59	square kilometers	km^2
VOLUME				
fl oz	fluid ounces	29.57	milliliters	mL
gal	gallons	3.785	liters	L
ft^3	cubic feet	0.028	cubic meters	m^3
yd^3	cubic yards	0.765	cubic meters	m^3
NOTE: volumes greater than 1000 L shall be shown in m^3				
MASS				
oz	ounces	28.35	grams	g
lb	pounds	0.454	kilograms	kg
T	short tons (2000 lb)	0.907	megagrams	Mg (or "t")
TEMPERATURE (exact degrees)				
°F	Fahrenheit	5(F-32)/9 or (F-32)/1.8	Celsius	°C
ILLUMINATION				
fc	foot-candles	10.76	lux	lx
fl	foot-Lamberts	3.426	candela/m^2	cd/m^2
FORCE and PRESSURE or STRESS				
kip	1000 pound force	4.45	kilonewtons	kN
lbf	pound force	4.45	newtons	N
lbf/in^2	pound force per square inch	6.89	kilopascals	kPa

*SI is the symbol for the International System of Units. Appropriate rounding should be made to comply with Section 4 of ASTM E380.

SI* (MODERN METRIC) CONVERSION FACTORS

*APPROXIMATE CONVERSIONS **FROM** SI UNITS*

SYMBOL	WHEN YOU KNOW	MULTIPLY BY	TO FIND	SYMBOL
LENGTH				
mm	millimeters	0.039	inches	in
m	meters	3.28	feet	ft
m	meters	1.09	yards	yd
km	kilometers	0.621	miles	mi
AREA				
mm^2	square millimeters	0.0016	square inches	in^2
m^2	square meters	10.764	square feet	ft^2
m^2	square meters	1.195	square yards	yd^2
ha	hectares	2.47	acres	ac
km^2	square kilometers	0.386	square miles	mi^2
VOLUME				
mL	milliliters	0.034	fluid ounces	fl oz
L	liters	0.264	gallons	gal
m^3	cubic meters	35.314	cubic feet	ft^3
m^3	cubic meters	1.307	cubic yards	yd^3
MASS				
g	grams	0.035	ounces	oz
kg	kilograms	2.202	pounds	lb
Mg (or "t")	megagrams (or "metric ton")	1.103	short tons (2000 lb)	T
TEMPERATURE (exact degrees)				
°C	Celsius	1.8C+32	Fahrenheit	°F
ILLUMINATION				
lx	lux	0.0929	foot-candles	fc
cd/m^2	candela/m^2	0.2919	foot-Lamberts	fl
FORCE and PRESSURE or STRESS				
kN	kilonewtons	0.225	1000 pound force	kip
N	newtons	0.225	pound force	lbf
kPa	kilopascals	0.145	pound force per square inch	lbf/in^2

*SI is the symbol for the International System of Units. Appropriate rounding should be made to comply with Section 4 of ASTM E380.

Technical Report Documentation Page

1. Report No.	2. Government Accession No.	3. Recipient's Catalog No.

4. Title and Subtitle	5. Report Date
Evaluation of Shelf Life in Post-Tensioning Grouts	August 2018
	6. Performing Organization Code
7. Author(s)	8. Performing Organization Report No.
Torres, E., Aguirre, M., Ferraro, C. C., and Hamilton, H. R.	
9. Performing Organization Name and Address	10. Work Unit No. (TRAIS)
University of Florida Department of Civil & Coastal Engineering P.O. Box 116580 Gainesville, FL 32611-6580	11. Contract or Grant No. BDV31-977-31
12. Sponsoring Agency Name and Address	13. Type of Report and Period Covered
Florida Department of Transportation 605 Suwannee Street, MS 30 Tallahassee, FL 32399	Final Report Oct. 2014-Aug. 2018
	14. Sponsoring Agency Code

15. Supplementary Notes

16. Abstract

Post-tensioning (PT) grout is commonly used in post-tensioned bridge girders to create a bond between the prestressing strands in the tendon and the surrounding concrete; it also provides corrosion protection to the prestressing strands. In recent years, however, soft grout has been found in several bridges in Florida and around the world. Soft grout has the potential to cause severe corrosion of the prestressing strands.

The purpose of this study was to investigate the shelf life of proprietary prepackaged grout along with limited testing of their respective constituents under various levels of exposure to humidity and heat. Prehydration of the fresh portland cement, when exposed to high humidity, causes an increase in mass and a change in the cement particle size; Modified Inclined Tube Test (MITT) results have shown that prolonged exposure to high temperature and humidity increased the susceptibility of prepackaged grout to the formation of soft grout, thus linking prehydration to soft grout.

In this research, MITT was conducted on large-volume samples to evaluate the effect of exposure on the susceptibility to soft grout formation. Mixtures were prepared using a water dosage that was 15% higher than the maximum recommended by the manufacturer. All commercial PT grouts, if given sufficient exposure time, eventually formed soft grout. MITT testing was conducted along with a number of other test methods that evaluated the effects of prehydration on mass and particle size, including mass gain, particle size analysis, Blaine fineness, loss on ignition, thermogravimetric analysis, and microwave moisture content.

In addition, behavior of individual PT grout constituents such as portland cement, supplementary cementitious materials (SCM), and admixtures under high humidity and temperature was investigated. It was found that each PT grout constituent was susceptible to either physical and/or chemical changes during exposure to adverse levels of temperature and humidity. These changes in properties of PT grout constituents contribute to the formation of soft grout; prehydration of portland cement appears to be the primary cause.

Finally, this report provides a proposed screening protocol for field determination of the condition of a PT grout prior to use. If a PT grout performs adequately in the screening tests, it should perform as expected in the grouting operations. This would provide a more convenient and economical method for evaluating exposure of the bagged material than the MITT method.

17. Key Words	18. Distribution Statement
PT grout, shelf life, soft grout, prehydration, grout constituents, post-tensioned concrete,	No restrictions

19. Security Classif. (of this report)	20. Security Classif. (of this page)	21. No. of Pages	22. Price
Unclassified	Unclassified	280	

Form DOT F 1700.7 (8-72) Reproduction of completed page authorized

Acknowledgments

The authors would like to thank the Florida Department of Transportation (FDOT) State Materials Office and Structural Lab for their support in materials testing assistance with experimental testing. In particular, the authors would like to thank Dr. DeFord, Mike Bergin, and Richard DeLorenzo for their help with technical suggestions and Patrick Carlton for helping with the experimental process in the laboratory.

Furthermore, the authors would like to the thank Sumiden Wire for donating post-tensioning strand for experimental research, the Major Analytical Instrumentation Center (MAIC) at the University of Florida, especially Dr. Carpinone for his insight and testing, and PSI-Orlando engineering services for their assistance along with the use of laboratory testing equipment. The authors would also like to thank those grout manufacturers who donated pallets of PT grout and portland cement for this project.

Additionally, the authors would like to thank the many contributors to the project, including Devon Minich, Marlo Chumioque, Kapil Salokhe, Dong Wang, Pablo Soto Lopez, William Broxton, Eugene Peter Cho, Kaimian Yang, Satyajeet Patil, Ming Li, and Jacob Montgomery for assistance with experimental testing, data collection and analysis, and report preparation.

Executive Summary

This report contains a summary of research performed to reproduce and determine the cause of soft grout, which has been discovered in several bridges in the state of Florida and elsewhere, both in the U.S. and abroad. In these bridges, the grout located in the post-tensioning (PT) ducts was found to be unhydrated (soft) and possibly contained high levels of moisture and potentially damaging chemicals, several years after construction was complete.

The objective of this research project was to explore the causes of bleed and segregation of commercially produced prepackaged PT grout. A portion of the study explored the sensitivity of mass and particle size change to prehydration of the portland cement, which is the chief constituent of typical PT grouts, by means of exposing the specimens to elevated temperature and humidity. A secondary objective involved the development of test methods to evaluate relative mass and particle size change, which may serve as a screening method to track the susceptibility of a particular PT grout formulation to formation of soft grout.

The research involved the investigation of the effects of time, temperature, and humidity on grout formation. Prepackaged grout, portland cement, supplementary cementitious materials (SCM), and admixtures from various sources were collected and tested. Samples of both small and large volumes of material were conditioned at four different combinations of temperature and humidity to evaluate any adverse reactions among the grout constituents. Exposure to 95˚F and 95% relative humidity (RH) was denoted as *Extreme;* exposure to 85˚F and 85% RH was denoted as *Field*; exposure to 65˚F and 50-70% RH was denoted as *Laboratory*; and exposure to 65˚F and 45-65% RH was denoted as *Control*.

Modified Inclined Tube Tests (MITTs) were conducted on large-volume samples to evaluate the effect of exposure on the potential for soft grout formation. Mixtures were prepared using a water dosage that was 15% higher than the maximum recommended by the manufacturer. All commercial PT grouts, if given sufficient exposure time after injection into the tube, eventually formed soft grout. *Field* exposure resulted in an average time required to form soft grout of 8 days, with values ranging from 4-13 days, and *Extreme* exposure resulted in an average time-to-formation of 3 days, with values ranging from 1-7 days. This behavior was due to a combination of excess mixing water and the segregation of partially hydrated portland cement particles and low-density, low-reactivity fillers. Very fine particles of these materials were suspended in the bleed water, which was displaced as the larger particles settled due to gravity and collected in the high point of the tube.

A number of test methods were used or developed to measure and track PT grout's sensitivity of portland cement particle mass gain under *Control, Laboratory, Field,* and *Extreme* exposures. The test methods used to measure particle change included small-scale mass gain (MG), particle size analysis (PSA), Blaine fineness (BF), loss on ignition (LOI), thermogravimetric analysis (TGA), and microwave moisture content (MMC). While these test methods could detect changes in the portland cement as a result of prehydration, their sensitivities varied significantly. The most sensitive methods were loss on ignition (mass loss), and Blaine fineness (particle size); however, Blaine fineness accuracy was found to be highly dependent on the operator performing the test.

The ultimate goal is to implement one of these methods to test the shelf life (suitability for use) of PT grout in the field before grouting operations. This would provide a more convenient and economical method for tracking exposure of the bagged material than MITT. This study provides indicators of soft grout formation applicable only to the PT grouts tested

during this study. Also, an implementation process is recommended to select a screening test for any PT grout.

Individual PT grout constituents were also investigated to determine their sensitivity to moisture. These materials included portland cement, supplemental cementitious materials (fly ash class C and class F, slag, and silica fume), and water reducer/anti-bleeding powdered admixtures. Each of these materials exhibited physical and/or chemical changes during exposure. While these materials were affected by exposure, the primary cause of the soft grout formation appeared to be the prehydration of the portland cement. In addition, from the limited constituent work conducted, there appeared to be some potential for synergistic affects that amplify the deleterious effect of moisture on the PT grout. More work is needed to identify these effects.

Table of Contents

List of Figures

List of Tables

1 Introduction

This report covers research that is a continuation of the prepackaged post-tensioning grout shelf life study (Piper et al., 2014). In the previous study, the effects of shelf life and adverse storage conditions on the susceptibility of soft grout formation in a variety of Post-Tensioning (PT) grouts were investigated. In particular, the effects of time, temperature, and humidity were evaluated by the use of environmental chambers. PT grout was conditioned and then tested using the Modified Inclined Tube Test (MITT). MITT was developed to address the issue of soft grout. The original Euronorm test (EN445-07) focuses on determining bleeding and change in volume of grout after injection. The modifications will be described later in the report. It was concluded that prehydration of the portland cement constituent of PT grout was the primary cause of increased soft grout susceptibility.

The study reported herein focused on two goals. The primary goal was to develop test methods that indirectly tracked particle size growth or other prehydration mechanisms so that the quality of PT grout could be verified prior to use. The secondary goal was to explore the sensitivity of various PT grouts, and their corresponding cements, SCMs, and admixtures, to exposure conditions likely to be experienced in the field. The effects of a range of elevated temperatures and humidities were evaluated based on changes to particle size and rheology. After exposure, MITT was used to evaluate the susceptibility to soft grout formation. As in the previous study, DSR, PSA, and Blaine Fineness testing were used to evaluate the effects of exposure. Other test methods such as nominal shear rate (NSR) viscosity, small-scale mass gain (MG), loss on ignition (LOI), thermogravimetric analysis (TGA), and microwave moisture content (MMC) were used to measure the sensitivity of the PT grout constituents to prehydration.

This report contains a literature review covering typical grout constituents and their behavior when exposed to moisture. Hydration and prehydration of portland cement is also discussed along with prepackaged grout storage, packaging, and injection. Chapter 3 covers the approach taken in the research project. Materials used in testing are detailed in Chapter 4. Details regarding the exposure of the samples are covered in Chapter 5. Chapter 6 covers the sample preparation for all testing. Chapter 7 describes the modified inclined tube test setup and procedures. Fluidity of PT grout and individual admixtures is covered in Chapter 8. Chapter 9 describes the test methods and results of heat of hydration using isothermal calorimetry. Chapter 10 covers mass gain results of PT grout, portland cement, SCMs, and admixtures. Particle size test methods, including laser particle size analysis and Blaine fineness, are described in Chapter 11 and 12 respectively. Chapter 13 through Chapter 15 provide the summary of each test method and results of tests associated with mass loss by means of heating; the methods covered include loss on ignition (LOI), thermogravimetric analysis (TGA), and microwave moisture content (MMC). Chapter 16 incorporates all findings to propose deterioration mechanisms that can result in soft grout formation. Chapter 17 discusses individual PT grout shelf life limits for each test method. In Chapter 18, a process is presented to combine the results of MITT and the other test methods conducted in this research into limits for shelf life screening test limits. Chapter 19 provides the summary and conclusions. Chapter 20 describes recommendations for future research. The experimental test methods are further discussed in Appendix A through K.

2 Literature Review

In post-tensioned (PT) bridge construction, design engineers use the forces imparted by post-tensioning tendons to limit deflections and cracking of the structures. PT allows for greater span lengths, which reduces the number of supports to provide a more economical design. Portland cement-based PT grout is used to transfer bond stresses generated between the concrete and tendon during load application. In addition, the grout provides a cementitious layer that protects the steel strand from corrosion. Post-tensioning grout is typically a proprietary prepackaged material that is composed primarily of portland cement. It is generally specified by performance rather than by prescription. PT grout has traditionally been stored and transported in bags of a size that can be handled by a single worker.

In the last 15 years, Florida has had several issues with PT grouts not performing as they should and ultimately not providing the protection they are intended to provide. Examples of this include the failure of a tendon in the Niles Channel Bridge in 1999, the failure of two tendons and replacement of 11 others in the Mid-Bay Bridge in 2000, the failure of a tendon in a precast segmental column in the Skyway Bridge in 2000, the failure of two tendons in the Ringling Causeway Bridge in 2011, and the discovery of soft grout and corrosion in the Wonderwood Connector in 2012 (Goldsberry, 2013). In addition, soft grout has been found near corroded tendons and has been attributed to grout segregation as shown in Figure 2-1 (Bertolini and Carsana, 2011).

This corrosion resulting from soft grout in bridges is not unique to Florida and has been identified in other parts of the United States and abroad. Therefore, further PT grout research was initiated after soft grout was found at anchors or crest points in many PT bridges several years after completion of construction.

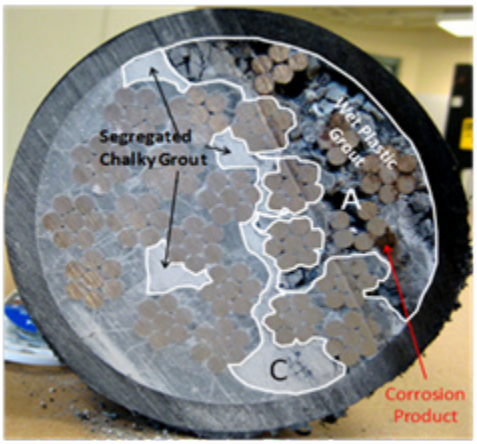

Figure 2-1 Tendon from a bridge in Florida showing severe corrosion (Theryo et al., 2013)

An initial study of the susceptibility of soft grout formation, which focused on the effects of shelf life and adverse storage conditions, was done by Piper et al. (2014). The initial results indicated that hydration of the portland cement component of PT grout, while stored in the original unopened bags, was a significant factor in the formation of soft grout. For this study, the term prehydration was used to indicate any reactions that occurred in the cement contained in the grout, from the time the grout was produced until the time it was prepared for use. The type and degree of the reactions depend on the environmental storage conditions (primarily relative humidity and temperature). The local atmosphere can provide water vapor and carbon dioxide,

leading to hydration of the cement and carbonation. Daily ambient temperature and relative humidity variations can result in condensation and adsorption on exposed surfaces, providing moisture for hydration. It is well known that ambient temperature can significantly affect the rate of hydration reactions.

The preliminary study determined that prehydration may occur as a result of adverse storage conditions of the bagged grout materials, including elevated temperature or humidity, or both. Preliminary testing also indicated that extended storage time after bagging the material increased the susceptibility to form soft grout. Finally, PT grout manufacturers use expiration dates; however, it appears there are no standards or methods to determine a grout's expiration date based on how long it is expected to maintain acceptable performance under specified storage conditions.

Similarly, in this study prehydration is defined as any hydration reaction or moisture absorption that occurs in the grout components from the time the grout is produced to the time prior to actual production mixing with water for permanent use. The prehydration definition includes any detrimental reactions with carbon dioxide or water, in either liquid or vapor form, during exposure to typical environmental ranges of temperature and humidity.

2.1 Grout Constituents

Post-tensioning grouts are typically specified on a performance rather than a prescriptive basis. For instance, FDOT specifications provide a series of laboratory tests that the grout must satisfy to be considered for approval. These tests include performance requirements such as flowability, bleeding, segregation, chloride content, compressive strength, and surface resistivity. Although not directly specified, it is understood that the PT grout will be formulated with portland cement as the primary constituent.

PTI M55.1-12 (2012) is also a performance specification, but with some restrictions on constituent type and proportions. The specification states that the ingredients of grouts intended for use in bonded, post-tensioned concrete work can include portland cement, mineral additives, admixtures, aggregates, and water. PTI M55.1-12 (2012) provides different suggestions depending the grout class used. Class A grout is for use in applications of non-aggressive exposure. Class B grout is for aggressive exposures. Class C grout is prepackaged grout suitable for aggressive and non-aggressive exposures. Finally, Class D grouts are specially designed for critical applications. This section will discuss Class C (prepackaged) requirements in terms of individual constituents.

One consequence of the use of a performance specification is that the formulation is proprietary. While initial approval of the material is relatively straightforward, ensuring quality during construction can be a challenge. This is because the material is typically supplied in bagged form on pallets; mixtures are typically prepared on site where the water dosage is controlled by the plant operator. If conditions are hot or pumping is difficult, then there is temptation to add water to improve pumpability, but this may exceed the manufacturer's limitations that are typically printed on the bags. Post-injection testing is not feasible because of the extreme difficulty in removing and replacing PT grout. Therefore, it must be done correctly the first time. Another factor in quality control is the environmental conditions under which the grout is stored. The product will typically change hands several times and may be inadvertently stored in humid conditions, which can severely degrade the PT grout performance. Investigating the effects of adverse storage conditions is the focus of this research project.

Before investigating the sensitivity of PT grout and the corresponding portland cement used in the grout, it is helpful to start with the constituents typically used in the PT grout mix, starting with portland cement as described by PTI M55.1 (2012) and FDOT Standard Specifications for Road and Bridge Construction (2018).

2.1.1 Portland Cement

Portland cement is manufactured from raw materials such as lime, iron, silica, and alumina. These materials are often obtained from common sources like limestone, clay, shale, iron ore, etc. After the manufacturing process, clinker nodules contain distributions of these phases: dicalcium silicate (C_2S), tricalcium silicate (C_3S), tricalcium aluminate (C_3A), and ferroaluminate (C_4AF). These compounds account for over 90% of the weight of portland cement. Individual proportions of each phase vary, and each phase reacts in the presence of water. Portland cement derives its compressive strength from the formation of hydration products due to the reaction of the clinker phases. PTI M55.1 (2012) section 2.2 requires that PT grouts use portland cements that meet ASTM C150/C150M requirements, and it allows the use of either Type I or Type II cements. ASTM C150/C150M sets ingredient requirements for portland cement Type II, with limitations of limestone and inorganic processing additions usage to less than 5% by mass, and (C_3A) to less than 8% by mass.

2.1.2 Supplemental Cementitious Materials

The next constituents described in the PTI M55.1 (2012) specification are mineral additives. PTI allows for the following mineral additives in PT grouts: 1) fly ash (Class C and Class F), conforming to ASTM C618; 2) slag cement conforming to ASTM C989/C989M (only Grade 120 slag shall be specified for use in PT grouts); and 3) silica fume conforming to ASTM C1240.

The benefits of using these mineral additives in PT grouts are to reduce the maximum temperature developed during the cement hydration reaction, increase the long-term strength of the PT grout, decrease the permeability of the PT grout, slow the rate of chloride ion migration, and reduce bleeding and segregation. Despite all these advantages, PTI does mention in their commentary (C2.3) that the properties of all these mineral additives and their interactions with other grout constituents can vary depending on what other components are present in the mixture. More explicitly, the specification suggests to carefully consider the interaction between admixture and supplemental cementitious materials, and potential changes in expected properties.

2.1.3 Admixtures

The third constituent mentioned in the PTI specification is admixtures. PTI M55.1 (2012) specifies that for Class C (prepackaged) grouts the following admixtures are allowed: high-range water reducers (HRWRs), corrosion inhibitors, anti-bleed admixtures, pumping aids, and air-entraining agents based on manufacturer recommendations. The type and quantity are not specified, but rather, the specification provides limitations on the dosages. For example, an HRWR can be added at a maximum dosage of 3 kg per 100 kg of cement, as long as the grout performs adequately according to the specification section 4.4.1 through 4.4.9. In addition to providing specifications for the use of admixtures in all these various applications, the PTI manual states that compatibility with the cement, mineral additives, and other admixtures being considered shall be established during specified grout trial mixes. FDOT Standard

Specifications for Road and Bridge Construction Section 938 Duct Filler for Post-Tensioned Structures also is a performance-based specification, where properties such as efflux time, bleeding, setting time, compressive strength, and permeability must meet specified criteria.

2.1.4 Aggregates and Water

According to PTI M55.1 (2012), if any aggregates are used in PT grout, they must have a maximum size of 1 mm to facilitate movement of the grout through the duct and provide total encapsulation of the prestressing elements. With the exception of gradation, aggregates used in PTI grouts must meet the requirements of ASTM C33/C33M. The PTI manual states that potable water shall be used in PT grouts, and in cases when potable water is not available, the proposed water shall meet the requirements of ASTM C1602/C1602M and have a maximum of 500 ppm of chloride ions, and no organic materials.

2.2 Hydration of Cement

Understanding the hydration mechanisms was necessary, for this study, to investigate the effect of exposure on the PT grout hydration process. Hydration of cement begins with the first interaction of cement particles with water.

The first cement phase to dissolve or react with water is C_3S, which comprises 50-80% of the material in portland cement (Scrivener and Nonat, 2011). Hydration of C_3S and C_2S results in production of calcium-silicate- hydrate (C-S-H), which is responsible for providing the majority of strength found in hydrated cement paste (Figure 2-2). C_2S contributes very little to the early-age strength, and C_3A and C_4AF have minor contributions to the early-age strength of hardened cement.

C_3S has both a higher reaction rate and heat of hydration than C_2S, and is responsible for providing initial set early in the hydration process. C_2S, on the other hand, contributes significantly to the strength of the hardened cement paste in the long term (Mehta and Monteiro, 2006). Both the aluminates (C_3A and C_4AF) also undergo a hydration process that results in two byproducts known as ettringite (which has a needle-like crystalline shape) and monosulfate (which has a crystalline structure resembling thin hexagon-shaped plates), respectively. Tricalcium aluminate (C_3A), liberates the largest amount of heat among all cement phases during the very early stage of hydration as shown in Figure 2-3. Iron is commonly used as a fluxing agent to reduce the melting temperature of the raw materials in the kiln during cement production, which results in the formation of tetracalcium alumino ferrite (C_4AF). During hydration, C_4AF has a small contribution to the strength. The most significant effect of this cement phase is its influence in the gray color of the cement powder.

In addition to the four main clinker phases, gypsum $C\bar{S}H_2$ is added in small percentages to the clinker materials to reduce the hydration rate of C_3A and helps with the resistance to sulfates (Sidney et al., 2003).

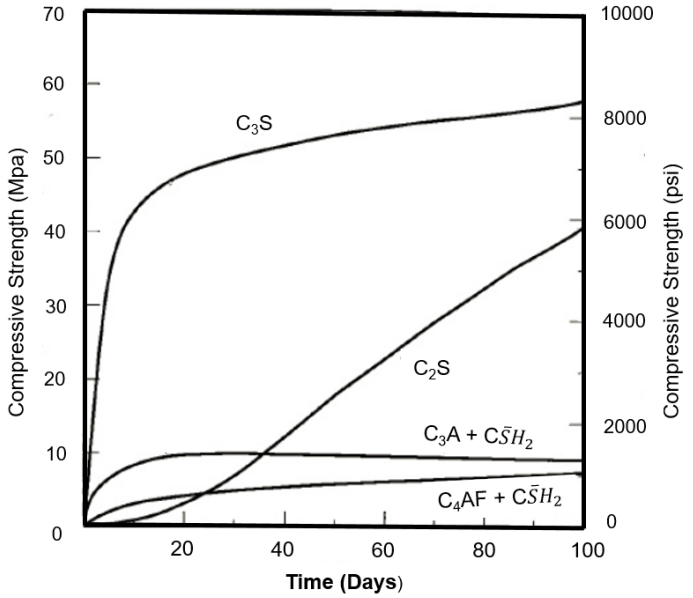

Figure 2-2 Compressive strength attributed to specific hydration of cement phases (data from Mindess et al., 2003)

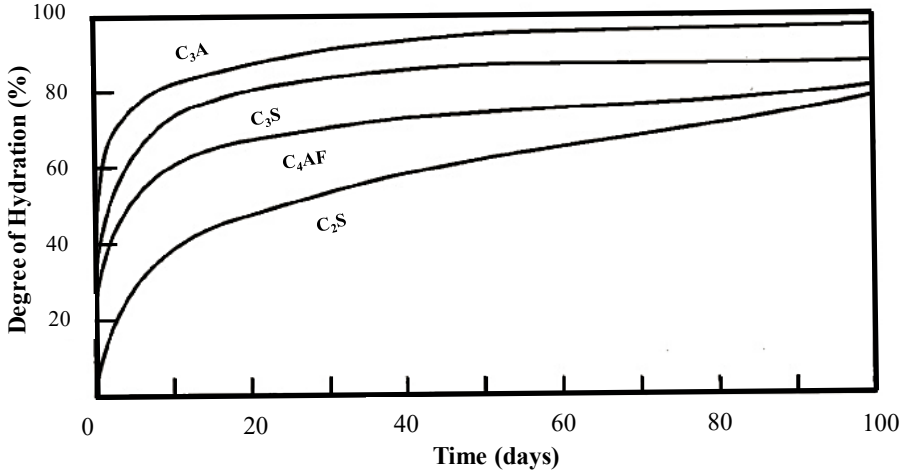

Figure 2-3 Degree of hydration attributed to specific clinker materials (data from Mindess et al., 2003)

Hydration reactions of cement phases occur by stages. The hydration process consists of 5 stages as shown in Figure 2-4. During the first stage, dissolution at the surface of the smallest cement particles occurs, which results in rapid evolution of heat within the first 5-10 minutes of the reaction. The initial interaction of cement with water results in release of ions into the pore solution. This initial heat evolution occurs due to ettringite formation and aluminate hydration. This rapid aluminate hydration is typically controlled by the presence of calcium sulfates, which derive from the addition of gypsum, which is interground with clinker to form portland cement (Bullard et al., 2011). The second stage is called the induction period. The induction period can take several hours depending on mixture constituents e.g., admixtures. During the induction period, the hydration reaction rate is low, resulting in little heat evolution. In a previous study,

Randell and Hamilton (2013) showed that exposure of PT grout bags can result in a delay of setting or retardation, meaning that the induction period lasts longer. In the third stage, heat evolution increases for several hours until it reaches a peak. This stage is known as acceleration period and is mainly attributed to the growth of C-S-H (Bazzoni, 2014). Initial and final set are expected to occur during the acceleration period. The fourth stage, or deceleration period, consists of a slow rate of hydration mainly attributed to the lack of space or water to continue hydration (Bullard et al., 2011). Similarly, Bazzoni (2014) proposed that C-S-H needles can grow quickly (acceleration period), which changes once the surface of cement grains are completely covered, limiting further growth (deceleration period). This mechanism of C-S-H needle growth is shown in Figure 2-5. Also, following the consumption of calcium sulfates, the hydration of C_3A reactivates, which generally occurs after the main hydration peak. Finally, the fifth stage, or steady-state stage, continues with the hydration at a lower rate.

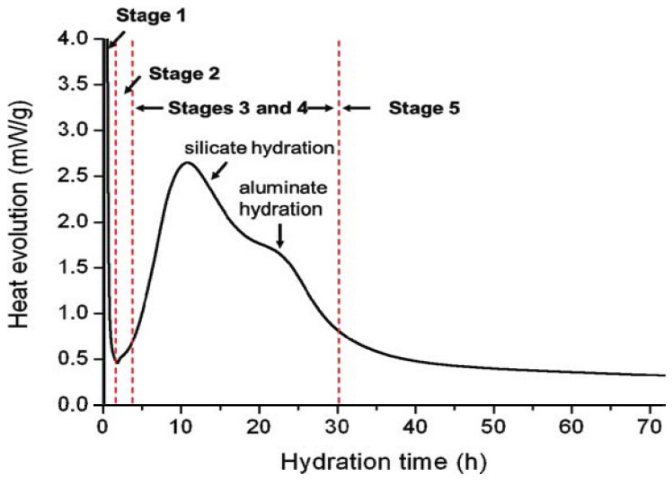

Figure 2-4 Cement hydration heat evolution during hydration (Whittaker et al., 2013)

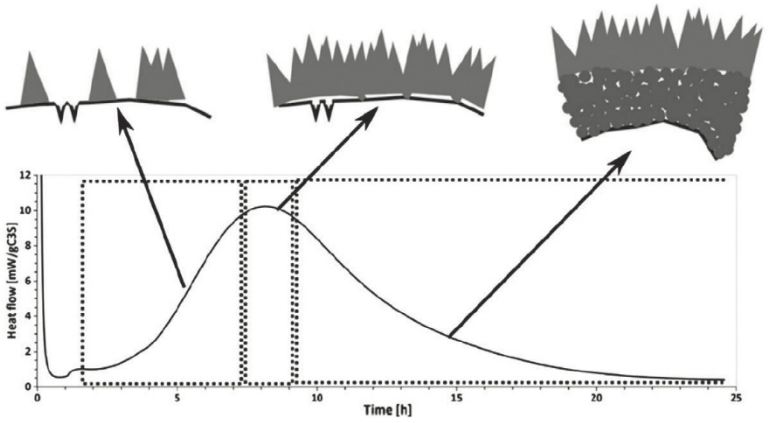

Figure 2-5 Formation and growth of C-S-H "needles" during hydration (Bazzoni, 2014)

Prepackaged PT grout consists of pre-blended portland cement, SCMs, and admixtures. SCMs can contribute to fluidity, bleeding resistance, and higher strength. SCM effects on cement hydration are divided into three mechanisms. Most SCMs react very little at early ages,

but have the effect of dispersing the cement particles, which allows a higher degree of early-age reaction (since the SCMs are not initially reacting, there is temporarily more water available for reaction than there would be if some of the portland cement had not been replaced with SCM) (Scrivener et al., 2015). SCMs provide additional surface area for hydration products to grow, during early hydration. The second mechanism uses the siliceous content of SCMs to provide a continued reaction with the free calcium (from the portland cement hydration) within the microstructure to further produce C-S-H at later ages (Ferraro et al. 2017). The third mechanism occurs at a later age, where the SCM particles serve as nucleation sites for hydrate products. This mechanism is more significant for SCMs of small particle size, such as silica fume (Berodier and Scrivener, 2014).

2.3 Prehydration Characterization

Portland cement undergoes hydration in the presence of water that results in the formation of C-S-H, which is responsible for providing the hardened properties of hydrated cement. Other byproducts of cement hydration include calcium hydroxide (CH), ettringite ($C_6A\bar{S}_3H_{32}$), and monosulfate. The prehydration process increases the amount of inert material in the cementitious mixture, those portions of the mixture that are prehydrated experience a delay before hydration starts, which is due to a layer of hydration products surrounding cement grains (agglomerations) that impede the ingress of water to hydrate the particles. Therefore, those portions of the mixture that experience prehydration essentially become an inert "filler," or aggregate material during mixing, injection, and initial hydration. A previous study found that an overabundance of filler material (limestone powder) in PT grout increased the grout's susceptibility to the formation of soft grout (Randell and Hamilton, 2013). Studies have also shown that the hydration reactions that take place during the intentional mixing of water with cement also take place when cement is exposed to humidity (Hunt et al., 1958; Dubina et al., 2008; Lopez-Arce et al., 2011; Whittaker et al., 2013; Starinieri et al., 2013; Paper et al., 2013; Stoian et al., 2015).

Water sorption of individual clinker phases was investigated in a series of studies (Dubina et al., 2011; Dubina et al., 2012; Dubina et al., 2015). These studies found that free lime was the most hygroscopic material, whose sorption started at 14% RH. C_3A sorption started at 55% RH and at 80% RH for the orthorhombic and cubic phases, respectively. Silicate phases C_3S and C_2S sorb water above 63% RH. Consider that humidity levels above 55% are beyond RH percentages normally seen in indoor storage conditions. However, higher RH levels are often found on field sites in Florida and can result in prehydration of the cementitious materials. Jensen et al. (1999) also found that C_3A was the first clinker phase to hydrate followed by C_3S and C_2S, which had the highest resistance to relative humidity prehydration.

Dubina et al. (2008) investigated the prehydration of cement particles in high relative humidity (85%) and found that water molecules adsorbed onto the surfaces of C_3S molecules and reacted with the C_3S to form C-S-H, $C_6A\bar{S}_3H_{32}$ (ettringite), and CH, thus making the prehydration process irreversible (Figure 2-6).

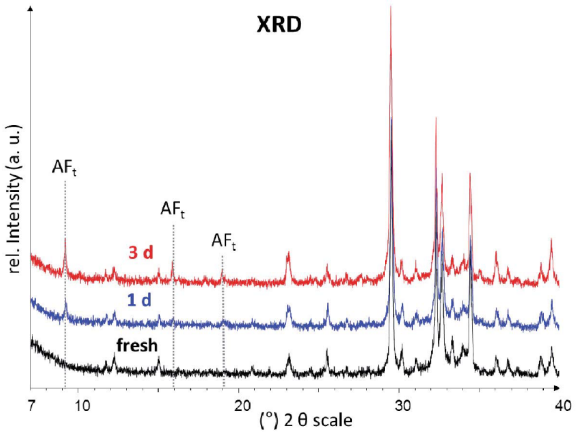

Figure 2-6 XRD analysis showing ettringite (shown as AF_t in the figure) formation during exposure (Dubina et al., 2008).

The degree of hydration or chemical reaction that occurred due to the change in relative humidity was studied by scanning electronic microscope. The study determined that the chemical reaction between the water and the cement varied by particle structure, each of the cement phases had a unique sensitivity to relative humidity. SEM results showed that ettringite crystals were formed on the surfaces of cement particles when exposed to 85% RH (Figure 2-7).

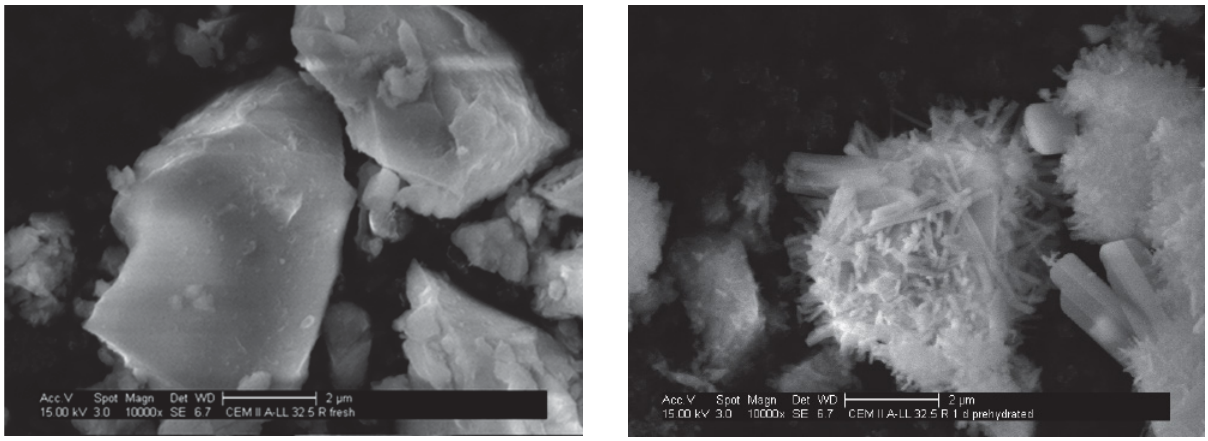

(a) (b)

Figure 2-7 SEM images (Dubina et al., 2008): (a) Fresh cement, (b) Cement prehydrated for 1 d at 35°C and 90% RH

Beyond simply turning fresh, unhydrated cement particles into temporarily inert byproducts, the prehydration of cement, in the study performed by Dubina et al. (2008), unveiled an interesting effect that prehydration has on the setting time of cement. It was discovered that when cement particles undergo prehydration, C-S-H and CH form a thin layer on the surface of C_3S grains, and this layer acts as a barrier between C_3S and water at the time of mixing. This was demonstrated by Dubina et al. (2008) when they showed that a prehydrated cement took two hours longer for water to reach the bulk C_3S than for fresh C_3S samples (Figure 2-8a). This will delay the setting time for prehydrated cements and may lead to insufficient hydration of the cement and possibly aid the formation of soft grout. In the study, portland cements were

prehydrated at 68°F in relative humidities ranging from 10% to 100%. Similar behavior was observed by Stoian et al. (2015), where portland cement Type I/II was exposed to 55% RH or sprayed with water at a dosage of 2.5%-5.0% mass of cement (Figure 2 8b). It was observed that in all cases the main hydration peak decreased in intensity. Also, the samples exposed to 55% humidity exhibited a longer induction period compared to the control and sprayed samples.

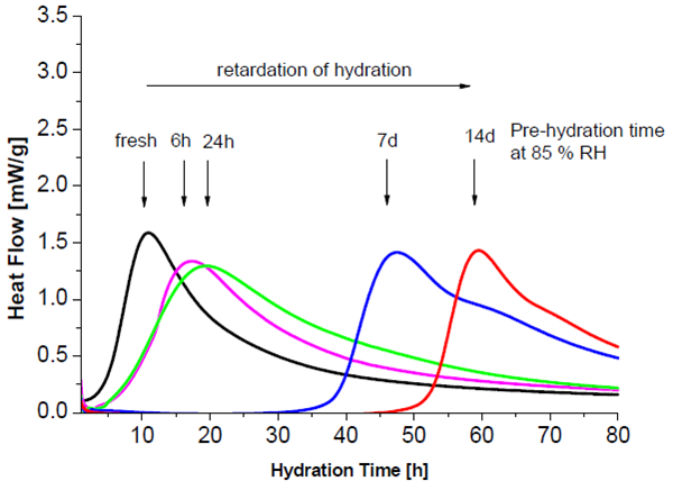

(a)

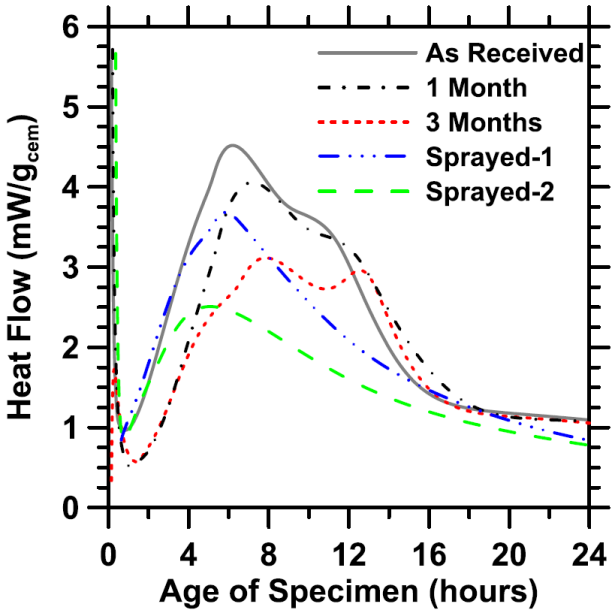

(b)

Figure 2-8 Heat of hydration curves after exposing cement to high levels of humidity (Dubina and Plank, 2012; Stoian et al., 2015): (a) C_3S samples exposed to 90% RH, and (b) Portland cement Type I/II exposed to 55% RH or sprayed with water at a dosage between 2.5%-5.0% of mass of cement.

Van Breugel (1992) conducted a study on simulation modeling taking into consideration mutual interferences between the hydration process and the development of microstructure. The hydration mechanisms of portland cement known as topochemical and through-solution

mechanisms were defined in this study. Topochemical hydration occurs immediately after the first contact of cement with water, in which a calcium-rich siliceous phase liberates Ca^{++} ions into the solution. This is accompanied by swelling of the hydration products relative to the original volume of the anhydrous cement. The reaction is then limited to the available surface of cement particles. The through-solution hydration concept involves dissolution from the cementitious surfaces after contact with water, and the reaction of aqueous components, followed by precipitation of the reaction product (C-S-H) onto the cement particles. For low water/solid ratios, the reaction would be predominantly topochemical, whereas for high water/solid ratios, the through-solution mechanism would be more important. Both reactions occur simultaneously. The concept of simultaneously operating mechanisms is plausible indeed if the outer products, i.e., the products which are formed outside the original grain boundaries in a relatively water-rich environment, are formed by a through-solution mechanism, while the inner products, formed inside the original grain boundaries, are formed topochemically (Figure 2-9).

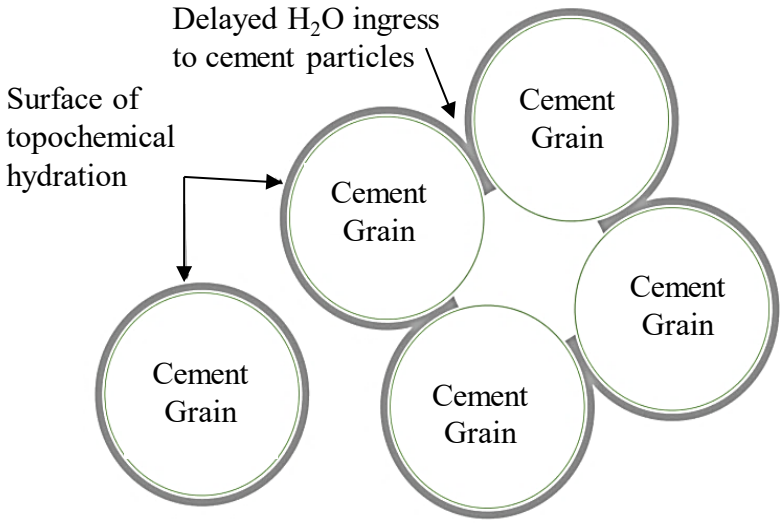

Figure 2-9 Formation of agglomerations due to prehydration and water absorption

In a hydrating water-cement system, the water is present in roughly three different forms; chemically bound, physically bound, and free or capillary water (van Breugel, 1992). Chemically bound water, which includes water molecules that are most tightly adhered to the surfaces of reaction products, is considered an inherent part of the solid matter. Physically bound water is the water adsorbed by the surface of the particles and depends on the relative humidity in the pore system. Water that is removed by heating of cement paste up to 105°C is generally identified as free water or physically bound. Water molecules of this free water are considered to behave like bulk water and are often equated with evaporable water. This free water is assumed to be available for further hydration of the cement.

Thermogravimetric analysis has been used to identify and quantify the decomposition reactions that occur when a cement paste is heated to high temperatures. Temperature regions of weight loss during heating can be used to determine the hydration phases present. Alarcon-Ruiz et al. (2004) described five regions of weight loss when cement was heated from 0°C to 950°C in TGA testing. The first region, between 30°C and 105°C, corresponded to the loss of evaporable

water, which was complete by 120°C. The second region, between 110°C and 170°C, corresponded mainly to the decomposition of gypsum (with a double endothermal reaction), the decomposition of ettringite, and the loss of water from part of the carboaluminate hydrates. In the range between 180°C –300°C, the loss of bound water from the decomposition of the C-S-H and carboaluminate hydrates occurs. Next, the region between 450°C and 550°C corresponded to the dehydroxylation of portlandite (calcium hydroxide). The final region was between 700°C and 900°C and corresponded to the decarbonation of calcium carbonate. The study concluded that TGA data curves can be used as tracers for determining the reaction temperature history of cement.

Whittaker et al. (2013) studied portland cement exposed to relative humidities of 60%-85% for 7, and 28 days and measured prehydration using thermogravimetric analysis (TGA) in the range of 0°C to 950°C (Figure 5-5). Based on the TGA weight loss data shown in Figure 2-10, it was apparent that 7 days of exposure to 85% RH had triggered silicate prehydration that produced calcium hydroxide, based on the weight loss in the temperature range that corresponds to dehydroxylation of portlandite. Also, weight loss in the temperature range corresponding to decarbonation of calcium carbonates indicated that some of the calcium hydroxide produced by prehydration had undergone carbonation. Using the presence of portlandite as a measure of alite prehydration, the TGA data showed that at 60% RH alite was not affected, but 85% RH led to alite prehydration. The study concluded that prehydration is characterized by the formation of a barrier of hydrates covering the surfaces of the cement grains, and the thickness of the barrier depended on the relative humidity.

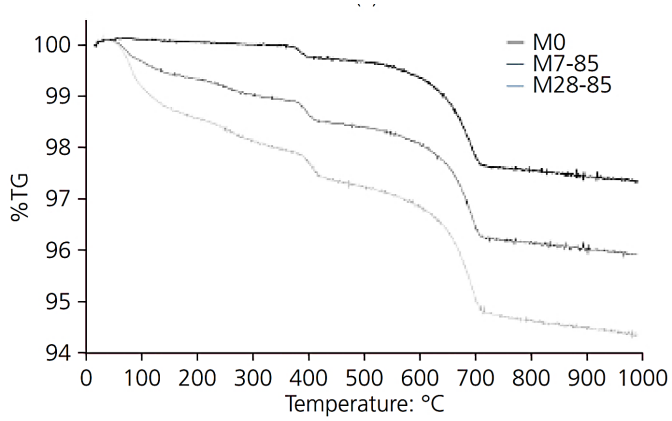

Figure 2-10 TGA curve of the as-received cement and the prehydrated cement at 85% RH for 7 and 28 days (Whittaker et al., 2013).

In addition to prehydration of cementitious constituents such as portland cement and slag, exposure to elevated temperature and humidity may also affect the ability of other pozzolanic constituents to perform as they should. Pozzolans are defined as a siliceous or a siliceous and aluminous material, which possesses no cementing capability on its own, but will react with calcium hydroxide (byproduct of portland cement hydration process) in the presence of water to form a cementitious product. Fly ash and silica fume are two pozzolanic materials commonly used in PT grout. Currently, no studies discuss the effect of prehydration on pozzolans; however, based on their non-cementitious nature, pozzolans can store physically bound water on the particle surfaces, which would be available for further portland cement prehydration.

On the other hand, Stoian et al. (2015) investigated the influence of fine limestone to mitigate the effect of prehydration. Isothermal calorimetry results showed that fine limestone can offset the prehydration effects as shown in Figure 2-11. Limestone's ability to mitigate prehydration can be attributed to the small particle size and corresponding large surface area that can serve as a catalyst for silicate reaction, enhancing the nucleation of hydration products during the acceleration stage of hydration.

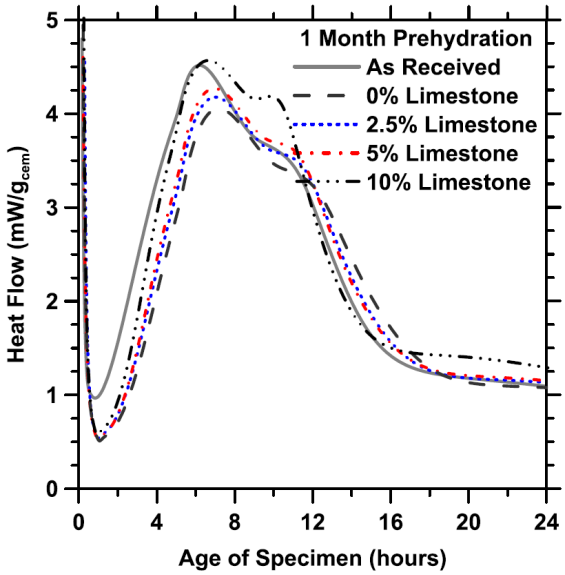

Figure 2-11 Heat flow results of cement pastes with limestone as a mitigator of prehydration (Stoian et al., 2015)

The changes at the surface of the cement particles due to the formation of hydration phases can affect the performance of the admixtures. Winnefeld et al. (2009) studied the interaction of superplasticizers with hydration products such as ettringite and C-S-H. The study reported that viscosity of ettringite suspensions decreases even with increasing dosage of superplasticizer compared to suspensions of pure C-S-H, and C_3S.

Suspensions of these materials were analyzed using zeta potential. Zeta potential is determined according to the concentration of calcium and sulfate ions in the solution. Zeta potential values increase when the $CaSO_4$ concentration is high (Lowke and Gehlen, 2017). Zeta potential results showed that ettringite tended to reduce zeta potential levels, while for the suspensions with other hydration products it remained consistent. These results agree with the Dubina and Plank (2012) findings, where it was reported that zeta potential values decreased for cement pastes having prehydrated cement as shown in Figure 2-12 Measurements were taken 4 min and 20 min after mixing; the change in zeta potential with exposure time was more evident for the measurements taken at 20 min. The change in zeta potential was attributed to the ettringite formation on the cement particles due to prehydration. This also relates to soft grout characteristics with high sulfates concentration reported by Carsana and Bertolini (2016).

Fluidity of cement pastes was studied using the same parameters of zeta potential. Dubina and Plank, (2012) found that the effect of polycarboxylate ether, naphthalene sulfonic, and casein-based superplasticizers decreased with the prehydration of cement, resulting in less

fluidity. Finally, the conclusion of the study was that the effectiveness of superplasticizers in prehydrated cement decreases, especially after 3 days of exposure.

In another study, Meier et al. (2017) proposed that the performance of superplasticizer on aged cement is controlled by two processes. The first process is agglomeration of cement particles due to ageing or prehydration, which results in a decrease of surface area. This process takes place prior to adding water and superplasticizers. The second process is the formation of hydration products, especially ettringite, which leads to an increase of surface area. The governing process will depend on the composition of the cement relative to C_3A. Recall that orthorhombic C_3A is the clinker material with more sorption tendency starting at 55% RH.

No literature was available to determine the effect of aged or deteriorated admixtures on the performance of cement pastes.

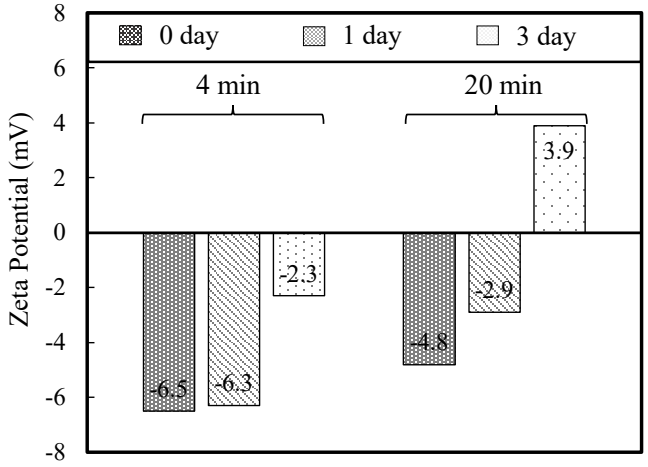

Figure 2-12 Zeta potential values of cement pastes made from prehydrated cement (data from Dubina and Plank, 2012).

2.4 Defective Grout

Thus far, this report has described PT grout constituents, hydration mechanisms, and prehydration of cementitious materials, which aimed to provide a starting point to understand the effects of prehydration and its implications that can result in defective grout.

Defective grout is often described as soft grout, which consists of chalky, unhardened material or sedimented silica fume (Figure 2-13), having high moisture content, and often accompanied by bleed-water. Defective grout is often found in the upper section of the tendon, which suggests that segregation or inadequate grouting operations can be reasons for defective grout, although soft grout has also been found at the end caps (Theryo et al., 2013). In another study, Ghorbanpoor and Madathanapalli (1993) stated that the bleed-water in the tendon would eventually dissipate; although, significant corrosion can occur at the grout-water interface.

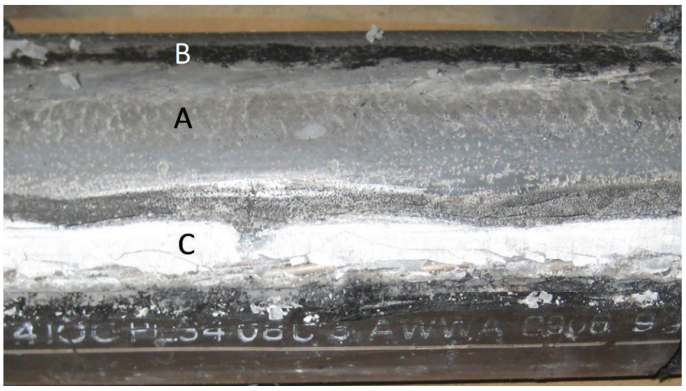

Figure 2-13 PT tendon profile showing: A: Wet plastic grout, B: Sedimented silica fume, and C: White chalky soft grout (Lau et al., 2016).

Several studies (Lau et al., 2016; Powers et al., 2016; Lee and Zielske, 2014; and Rafols et al., 2013) have attempted to characterize soft grout and relate its properties to the corrosion mechanism occurring in the PT tendons. These studies utilized samples of corroded PT tendons obtained from different bridges in Florida, as well as laboratory made samples.

Rafols et al. (2013) reported that the grout samples, obtained from bridges with cored tendons, typically are characterized by having high moisture content, high pore solution pH, low chloride concentration, and high sulfate concentrations. The study also found significant corrosion in the regions having deficient grout by using electrochemical testing and visual examination. At the end of the study the authors recommended further work to understand the mechanisms causing grout segregation, and the role of sulfates, oxygen content, and pore water pH in terms of corrosion development.

Lau et al. (2016) continued this work by investigating the effects of sulfates in terms of corrosion. The study reported that the grout causing corrosion was characterized by having low levels of chlorides, pH above 11 and high amounts of sulfates. Therefore, the study focused on the effect of the sulfates as an initiation agent for corrosion in strands. The study suggested that early exposure of the strands to grout having sulfates can result in an impairment of the formation of the passive layer to protect the strands. Finally, the authors concluded that the propensity to corrosion initiation cannot be defined by sulfates content alone, but that changes in pore water chemistry need to be investigated.

Powers et al. (2016) considered samples with corrosion in the immediate proximity to the anchorage. The study showed that the post-tensioned strands are mostly anodic to the anchorage system when grout bleed water is present. These preliminary results were followed with electrochemical measurements of laboratory-made specimens representing the anchorage system. These measurements indicated that portions of the strand and of the anchorage component surfaces became active upon water recharge and stayed active for extended periods afterwards, even without addition of chloride ions. Also, it was found that corrosion took place in the transition zone between grout and air space, while the metal completely embedded in grout remained in the passive condition.

Lee and Zielske (2014), investigated the required chloride concentration levels to start corrosion in high-strength post-tensioning strands. Their samples consisted of single-wire, single-strand and multi-strand configurations. The electrochemical testing results suggested that the PT strand can tolerate chloride contamination without significant corrosion up to 0.6 percent by weight of cement in carbonation-free (high pH) grout, whereas a chloride content as low as

0.04 percent by weight of cement can initiate active corrosion in the carbonated (low pH) grout. These chloride levels are under the level of 0.08 recommended by AASHTO (2011).

2.5 Grout Storage and Transportation

Although much has been said about PT grout itself and the potential effects its various constituents may have on the grout's susceptibility to forming soft grout, there are also other factors independent of any PT grout's compositional makeup that affect the grout's susceptibility to forming soft grout. One these factors is the environmental conditions in which the PT grout is stored. PT grouts may be stored indoors where the bags are completely protected from any precipitation, and humidity levels and temperatures are regulated, but PT grouts may also be stored outdoors where bags are exposed to the ambient temperature and humidity, and bags may or may not be completely protected from precipitation. It is also possible that a bag of PT grout will experience conditions similar to both of the above-mentioned environments in its lifetime.

An example of this situation would be when bags on a pallet are initially stored in an air-conditioned warehouse for the first several months after manufacture. Then the pallet of bags is placed on a truck with little protection from precipitation throughout the duration of its travel to the construction site (Figure 2-14), and then dropped off at the site where sufficient protection from precipitation exists, but in which the grout is still exposed to ambient temperature and humidity for the final days leading up to mixing.

The number of environmental variables for such an example is large, which makes predicting the effects of such conditions on the grout performance extremely difficult. Because of the complexity of this issue and the fact that there is currently little known about all the potential effects of various environmental conditions on the shelf life of PT grouts, many manufacturers simply state that PT grouts should be "stored in a cool dry place" and denote a seemingly arbitrary shelf life in the range of 6-12 months.

Figure 2-14 PT grout protection during transportation to storage facility

One grout manufacturer did not provide a shelf life, but instead chose to designate that after one year a bag should be returned to the manufacturer for recertification of the grout produced in that lot. PTI M55.1-12 and FDOT Standard Specifications for Road and Bridge Construction Section 462-6.4, Filler (revised 2018) state that prepackaged grouts should not be stored on site for more than one month before use. It is recommended that the onsite storage of the materials be in a building or shed that is both weatherproof, and located convenient to the work to be performed. However, the construction engineer can allow storage in an open environment as long as the grout bags are raised on a platform and have adequate waterproof covering. PTI M55.1-12 specification also specifies certain conditions for admixtures and silica fume. For admixtures, care should be taken when grouts are exposed to temperatures below 32°F, which is generally unlikely for most of Florida. Safety measures should be taken when silica fume is used as a slurry or when dry silica fume is added separately to the mix. In the case of prepackaged PT grout the silica fume is blended with the cement, which has not shown to cause issues with agglomeration.

2.6 Grout Packaging

The other major variable outside of grout composition that plays a role in the shelf life of PT grouts is the packaging of the grout. Despite changes in the packaging of cementitious materials over the years, most PT grout manufacturers seem to have settled on similar bag sizes and the use of similar packaging materials. The PT grout manufacturers investigated in this shelf life study had average bag weights between 49 lb. and 57 lb., and all PT grout manufacturers utilized a similar packaging material scheme that employed the use of one layer of waterproof plastic positioned between multiple layers of paper. Despite these material similarities across all grout manufacturers, there are differences in the bagging and closing procedures employed by each manufacturer.

Figure 2-15 shows that all the PT grout manufacturers involved in this study use similar packaging materials. Three of the six manufactures utilized a layer of plastic between two layers of paper, and three of the manufacturers used an additional layer of paper. In every case that the additional layer of paper was used, it was an external layer white in color. It is possible that the only reason this additional layer was used, was for marketing purposes.

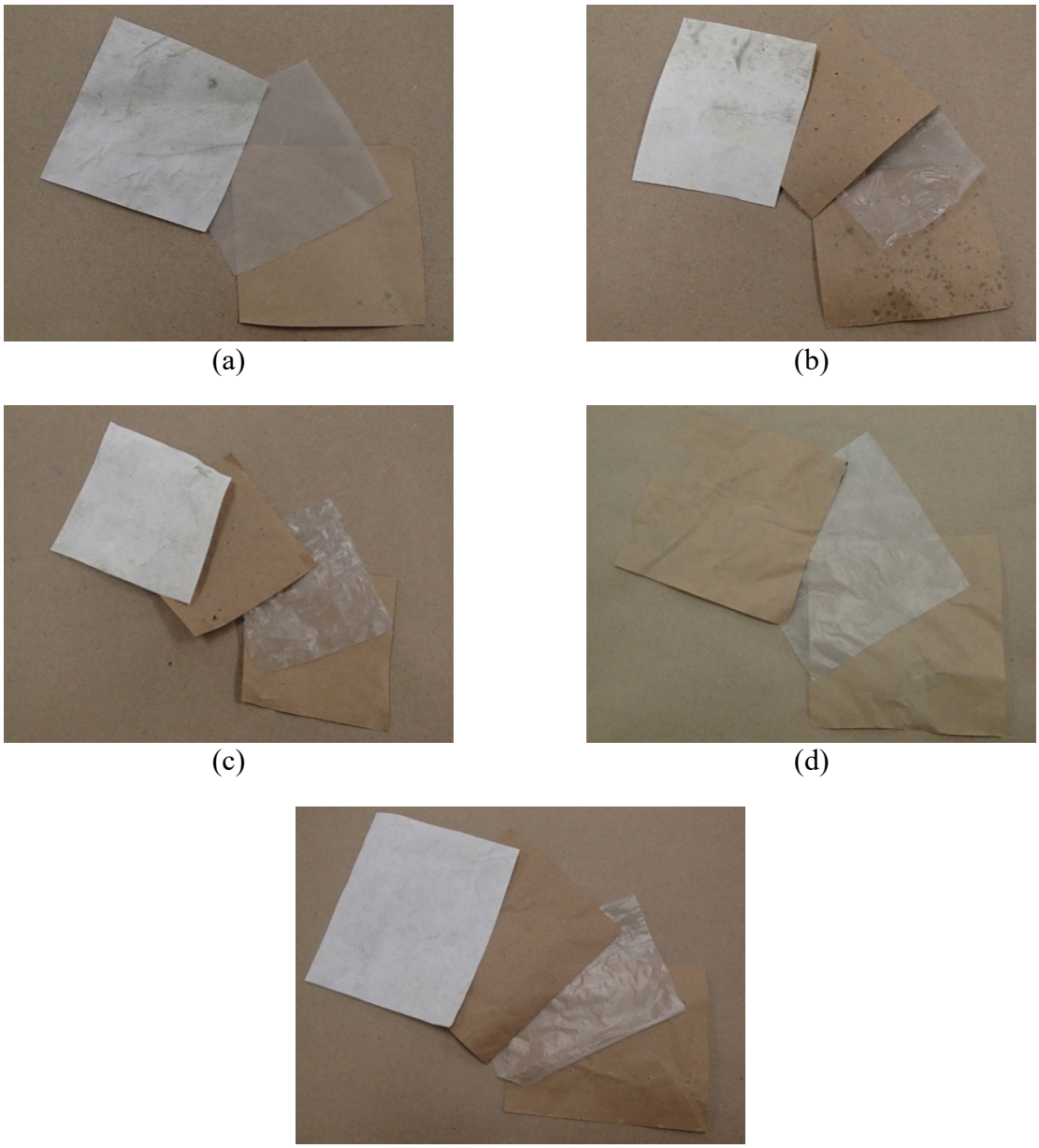

Figure 2-15 Packaging materials for grout: (a) PT1, (b) PT2, (c) PT3, (d) PT4, and (e) PT5

An interesting aspect of the packaging materials that is not clearly depicted in Figure 2-15 is the perforation of the plastic layer in the bags. These perforations varied from one manufacturer to another, but perforations of some sort existed in the plastic layer for all manufacturers except PT1. Figure 2-16 shows some closer views of these layers of plastic. When it comes to the packaging of cementitious materials, perforation of the bags prevents the flying of cement from the bag during the packing process. Flying of cement from the bag occurs when cement is quickly dropped into an open bag, thus trapping air at the bottom of the bag without a pathway out of the bag except upwards through the layers of grout that is trapping it in the bag. As gravity pulls the grout down into the bag, it forces the trapped air up through the layer of grout and causes the fine cement particles to shoot out of the top of the bag in a dust

cloud. Perforation of the bags allows for the air to escape from the side of the bags during this filling process and prevents this dust flying. This allows for the material to be packed more efficiently and the reduction of dust flying also results in a cleaner environment within the production area. Despite its advantages to efficient packing and cleanliness, perforations in the bags of PT grout reduce the bags defense against moisture ingress into the PT grout within. Even in the case of a micro-perforation system, such as the one used by PT7, the protective barrier is made less effective against moisture.

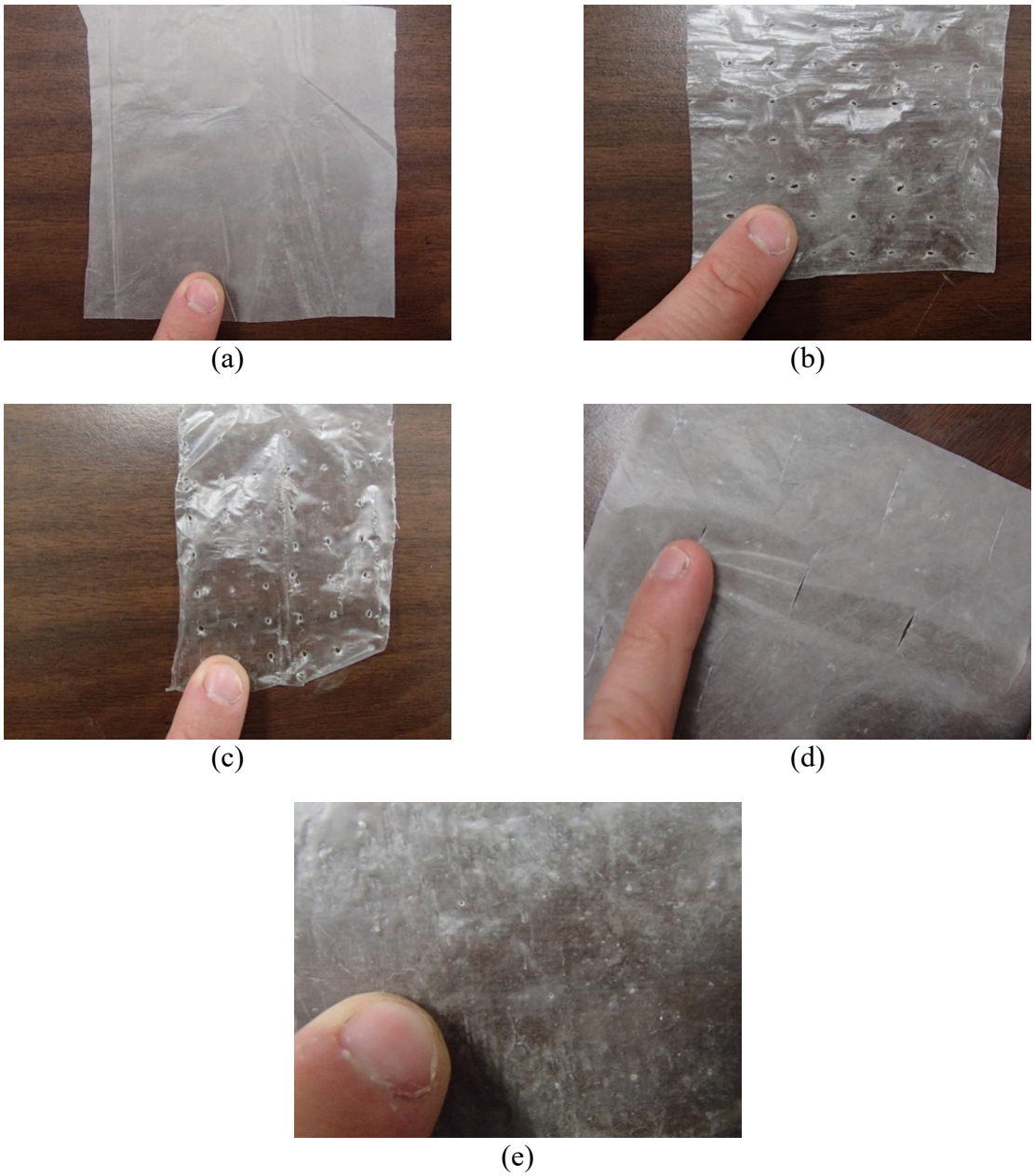

(a) (b) (c) (d) (e)

Figure 2-16 Perforation in plastic layer part of packaging bag: (a) PT1, (b) PT2, (c) PT3, (d) PT4, and (e) PT5

Despite the similarities in bag size and packaging material, there were noticeable differences in the corners of the bags depending on the manufacturer. These differences are likely due to the use of different packaging machines, which use different methods for closing the bags after the cement has been placed within the bag. The most noticeable difference was that the bag corners of one manufacturer allowed for grout to trickle out from the corners of the bags. Figure 2-17 shows grout trickling from the corner of one of these bags. This lack of a complete seal poses a threat to the performance of the PT grout stored within these bags. Even if the packaging material for these bags performs as it should and prevents the humidity in the ambient air from penetrating the material and being transferred to the PT grout within the bag, this lack of an air-tight seal will allow for the moisture to simply enter the bags at the corners. This could lead to prehydration of the material first at the corner of the bag, and then throughout the rest of the bag. This will increase the PT grout's susceptibility to the formation of soft grout.

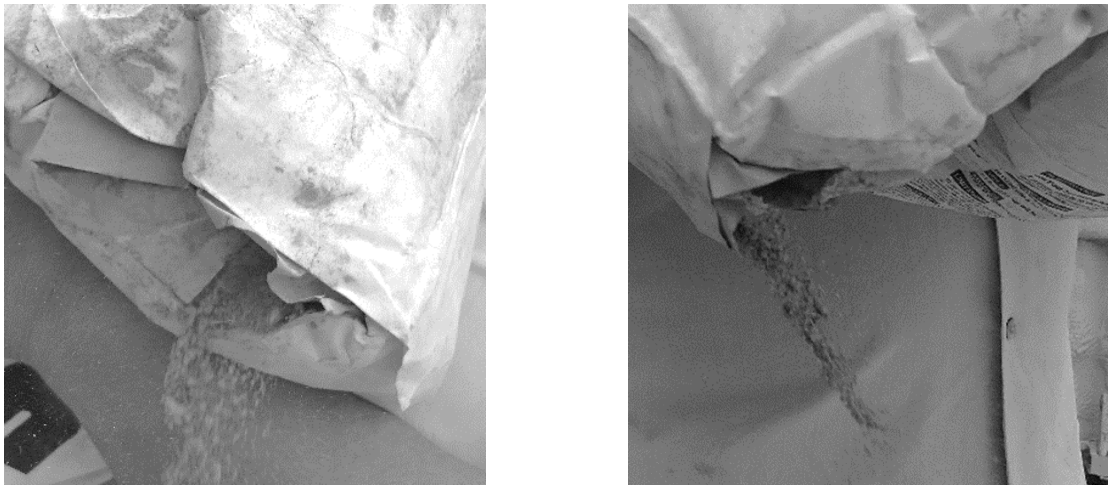

Figure 2-17 Dry grout trickling from the corner of a PT grout bag

Figure 2-17 shows the same bag corner. This is important to note, because only one of the four bag corners allowed grout to trickle from within. The other three bag corners appeared to be completely sealed (Figure 2-18). This same pattern of having three tightly sealed corners and one loosely sealed corner was seen for all the remaining manufacturers.

It appears that each manufacturer has tightly sealed corners for both of the bottom corners, but one of the top corners is usually not sealed as tightly. This corner is easy to spot as the folds made at this corner are different than the folds made at the other three corners. It appears that these unique corners with different folds, are the closing corners in which the final folds are made, and the closing of the bag is completed after being filled with grout.

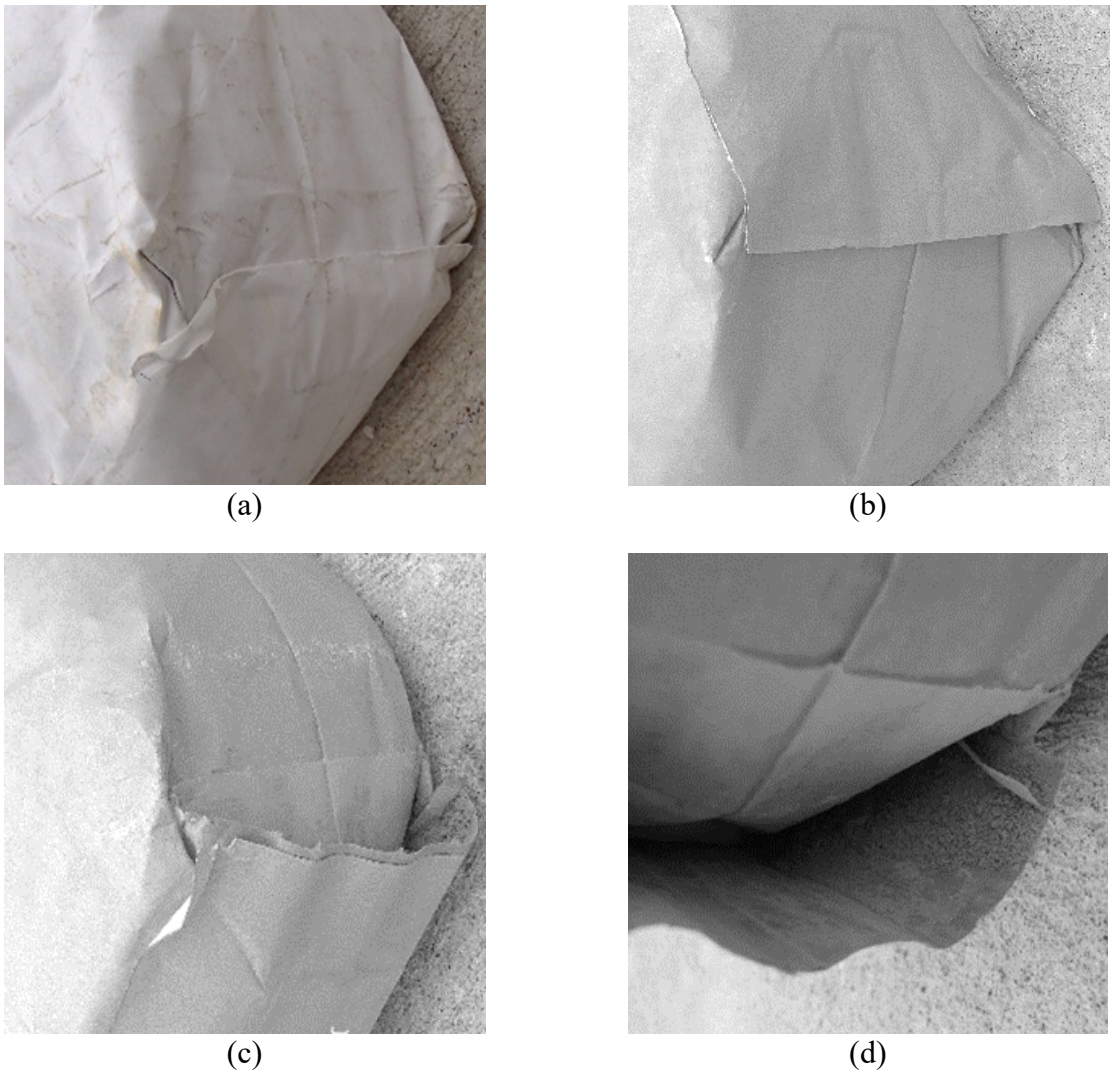

Figure 2-18 Images of each corner of a PT grout bag: (a) Bottom right corner, (b) Bottom left corner, (c) Top right corner, and (d) Top left corner.

2.7 Grouting of PT Tendons

With the purpose of improving the quality of grouted post-tension tendons, several agencies, organizations, and private contractors have developed guidelines for grouting procedures (FDOT 2002; VSL 2002; PTI M55.1-12 2012; and FHWA 2013). These guidelines describe post-tensioning system set up, PT grout constituents, mixing, injection, quality control, and post-grouting inspection and repairs. Problems with defective grout resulting in expensive repairs, have been addressed in these guidelines and other specifications to reduce the likelihood of this occurring again. For instance, past practice included flushing the tendons to remove any debris inside the ducts. Nowadays, flushing should be avoided, as it is almost impossible to remove all the excess water in the tendon, which can affect the quality (water-to-solids) of the grout during injection (FHWA 2013). Similarly, the guidelines for outlet testing have been

reformed to provide more strict performance in terms of fluidity and bleeding, which has also been accompanied with the development of high-performance non-shrink and no-bleed grouts that incorporate SCMs and admixtures to meet desired performance (Schokker et al., 1999).

However, PT grout formulation changes did not provide a solution to the bleed water problem; corrosion-caused tendon failures on relatively new PT bridges have occurred (Theryo et al., 2013). Therefore, the aforementioned specifications (FDOT 2002; VSL 2002; PTI M55.1-12 2012; and FHWA 2013) have included guidelines for inspection and repair. Inspection techniques vary whether it is an internal or external tendon; however, for both cases, the critical points of interest are void localization and changes of electrochemical resistance, which are associated with bleeding or defective grout. Voids can often be repaired by injecting new grout, although it is very important to measure the volume of grout used to fill the grout. This repair technique can be successfully applied when corrosion is not found in the strands. Theryo et al. (2013) recommended that when defective grout is localized either at the end caps or along the tendon (Figure 2-19), a sample of approximately 75 g should be collected to perform the following analysis: X-ray florescence, energy-dispersive X-ray spectroscopy, ion chromatography, wet chemistry analysis for total Cl, and wet chemistry analysis for soluble Cl. Also, measuring the potential of the strands is recommended to calculate corrosion rate, which can be helpful to determine the repair technique.

(a) (b)

Figure 2-19 Sampling of defective grout in different locations: (a) End cap and (b) Internal tendon (Theryo et al., 2013).

3 Research Approach

This research project aims to determine the effect that adverse storage conditions and ageing have on the susceptibility to form soft grout, bleeding, or segregation. PT grout manufacturers typically place expiration dates on their products, yet there are no standards or rational process to determine the shelf life of the product. Therefore, the purpose of this research was to develop or modify a test method that can be used to determine if a prepackaged grout is beyond its shelf life or capable of meeting performance requirements during grouting of PT tendons.

Full-scale modified inclined tube tests (MITT) were conducted in conjunction with a number of small-scale bench-top laboratory tests to monitor the change in the material with exposure and age. To evaluate all the factors affecting grout shelf life, the study was divided into three tasks as shown in Figure 3-1. The first task was the characterization of PT grout and portland cement in terms of particle size and mass change, and to determine their variation due to prehydration. The test methods used to characterize the PT grout dry powder provide limits regarding soft grout formation during MITT, which were used to evaluate the sensitivity to soft grout formation after exposure.

The second task concentrated on the degradation due to adverse exposure and ageing of admixtures or SCMs used in PT grout. The goal was to develop a classification of grout constituents based on susceptibility to degradation under adverse exposure. Identifying the susceptibility of all constituents can provide guidance to develop improved mix designs and decrease the likelihood of PT grout susceptibility.

The third task consisted of evaluating the fresh properties of PT grout before and after formation of soft grout in MITT due to adverse exposure conditions. Fresh properties evaluation also included NSR viscosity of exposed PT grout and powdered admixtures, bleeding of exposed admixtures, and heat of hydration of all PT grouts.

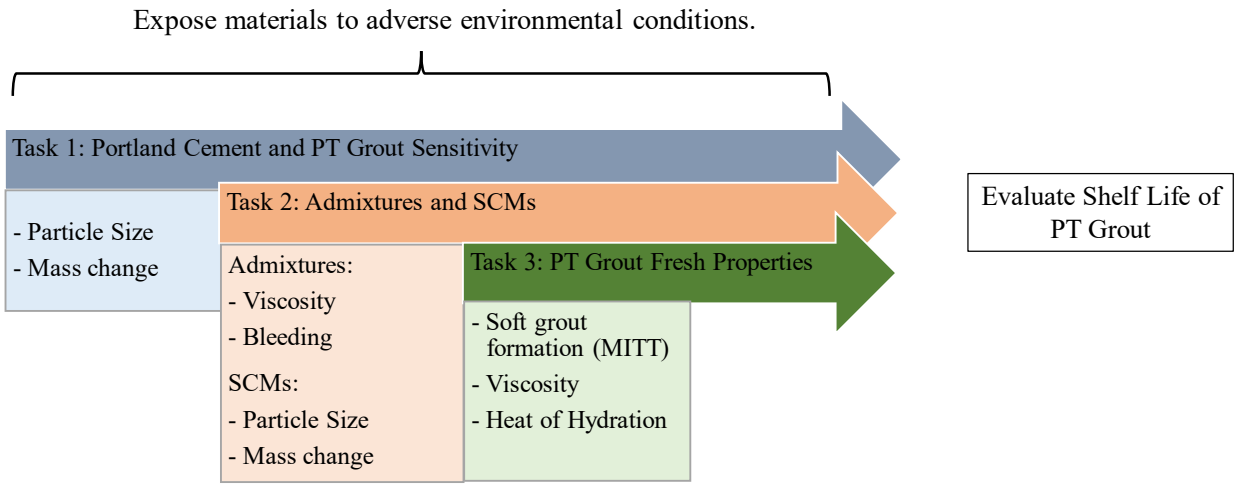

Figure 3-1 Diagram of research approach to evaluate PT grout shelf life.

4 Materials

4.1 PT Grouts and Cements

In this study, tests were performed on five different prepackaged grouts. Each grout mixture was prepared using a full-scale grout plant and four bags of the prepackaged grout material in parallel to small-scale testing. Constituent materials of the prepackaged grouts and their respective proportions were unknown due to the proprietary nature of the product. In addition, each of the prepackaged grout manufacturers provided two bags of the portland cement Type I/II used in their grout mixture, these cements were small-scale tested only. Table 4-1 summarizes the PT grouts and portland cements tested. Testing identification PTx is used to distinguish between specific manufacturers (x). The portland cement used in the PT grout was provided to the manufacturer from a third-party producer in some cases, the cements received were not labeled for commercial use; therefore, no additional background data were provided other than cements met class Type I/II as required by PTI-M55 for PT grout manufacturing. It should be noted that PT2 and PT3 were manufactured by the same company at the same manufacturing plant, one set of cement was delivered with PT3 therefore this cement will be described as C3.

Table 4-1 Summary of PT grout and portland cement tested

Testing ID	Date manufactured	Expiration Date
PT1	5/26/2015	11/26/2015
PT2	5/22/2015	11/22/2015
PT3	7/3/2015	1/3/2016
PT5	7/2/2015	7/2/2016
PT7	7/7/2015	1/7/2016
Testing ID	Date manufactured	Received Date
C1	5/26/2015	6/9/2015
C3	7/3/2015	7/21/2015
C5	7/2/2015	7/15/2015
C7	7/7/2015	7/14/2015

4.2 SCMs

In this study, tests were performed on several SCMs and admixtures. The SCMs were selected from those allowed by the PTI M55 (2012) specification for grouting of post-tensioned structures, and the FDOT Standard Specifications for Road and Bridge Construction Section 938 Duct Filler for Post-Tensioning Structures (revised 2018). Pictures of SCM samples are shown in Figure 4-1, and product details are listed in Table 4-2. All SCMs also comply with FDOT Standard Specifications for Road and Bridge Construction Section 929 Pozzolans and Slag

(2018), and the respective producers are part of the Materials Acceptance and Certification System of FDOT.

(a) (b)

(c) (d)

Figure 4-1 SCMs tested: (a) Fly ash class F (FAF), (b) Fly ash class C, (c) Slag (S), and (d) Silica fume (SF)

Table 4-2 Details of tested SCMs

Materials	As received LOI (%)	LOI limit (%)	ASTM Standard	PTI M55 maximum cement replacement (%)
FAC	0.22	6	C618	30
FAF	1.45	6	C618	25
SF	2.91	6	C1240	15
S	0.39	4	C989	55

4.3 Admixtures

PTI M55 (2012) allows the use of high-range water reducers (HRWRs), corrosion inhibitors, anti-bleed admixtures, pumping aids, and air-entraining agents based on manufacturer recommendations. For Class C grouts, PTI M55 (2012) allows the use of SCMs and chemical admixtures. The type and quantity are not specified, but the specification provides limitations on the dosages. For example, an HRWR can be added to a maximum of 3 kg per 100 kg of cement, as long as the grout performs adequately according to the specification section 4.4.1 through 4.4.9. FDOT Standard Specifications for Road and Bridge Construction Section 938 Duct Filler for Post-Tensioned Structures is also a performance-based specification, where properties such as efflux time, bleeding, setting time, compressive strength, and permeability must meet specified criteria.

Three admixtures, shown in Figure 4-2, from different manufacturers were selected to investigate the susceptibility to adverse exposure. All admixtures were limited to powder form to investigate the effect of adverse exposure and ageing. Also, admixtures used in PT prepackaged grouts are typically blended in powder form with other grout constituents. Admixtures intended to control fluidity and bleeding were of primary interest. Therefore, the final selection included three admixtures with either HRWR or anti-bleeding properties. Each admixture was provided by a different manufacturer. Furthermore, these admixtures were not on the FDOT Approved Product List. Admixture 1 (A1) and Admixture 2 (A2) were HRWRs based on a polycarboxylate polymer. Both admixtures are used to lower w/c and improve pumpability. A1 is intended for use in high-performance concrete or buried concrete. A2 is generally used in grouts and screeds. A3 provides both HRWR and anti-bleeding properties, and is intended for use in producing flowable, non-shrink, non-segregating, high-strength grout.

In terms of shelf life, all admixtures are required to be stored in a dry storage room with temperatures within 45°F -80°F (7°C -27°C). Also, manufacture dates were important to assess the effect of age in the admixtures performance. The date of manufacture and expiration are listed in Table 4-3.

Table 4-3 Posted shelf life and expiration date of admixtures used in testing

	Admixture 1	Admixture 2	Admixture 3
Expiration	10/2018	09/2018	09/2018
Shelf life	12 months	12 months	12 months

(a) (b)

(c)

Figure 4-2 Tested admixtures: (a) A1, (b) A2, and (c) A3

5 Sample Exposure

To address the lack of test protocols, a test program was designed in which *Control*, *Laboratory*, *Field*, and *Extreme* exposure conditions were created. The specific exposure testing program was designed with the following assumptions. The study hypothesized that the portland cement used in the PT grout was the component that was most affected by prehydration degradation prior to mixing. Prior research done at The Technical University of Munich by Dubina et al. (2008) stated that in portland cement, C_3S has proven to be particularly sensitive to humidity. The study on the prehydration of cement particles found that in high relative humidity (85%), water molecules adsorbed onto the surface of C_3S molecules and reacted with the C_3S to form $C_3S_2H_3$ and CH, thus making the prehydration process irreversible. Prehydration sensitivity behavior of C_3S was also studied by Jensen et al. (1999); the research focused on the hydration of the C_3A, C_2S, and C_3S in portland cement by exposing them to different relative humidities ranging from 10% RH to 100% RH and at a constant temperature of 20°C. The study concluded that each cement phase material had a different sensitivity to hydration; C_3A began to hydrate at 60% RH while C_2S hydrated at 80% RH, and C_3S at 90% RH. Using the knowledge acquired from the previous studies, this study set up a testing program to account for the range of hydration reactions occurring for the portland cement phases between 45% RH to 95% RH. Four levels of exposure were chosen to simulate a wide range of temperature and humidity that a grout may be exposed to in the field, and each exposure is detailed below.

- ***Control (C)***—65˚F, 45%-65% RH
- ***Laboratory (L)***—65˚F, 50%-70% RH
- ***Field (F)***—85˚F, 85% RH
- ***Extreme (E)*** —95˚F, 95% RH

Control exposure was implemented by placing the material in the FDOT structural materials lab storage area as shown in Figure 5-1. Climate was maintained by the central air-conditioning system in the building. PT grouts and cements were stored in this condition prior to commencing any testing or exposure to minimize any premature exposure to high temperature and humidity. *Laboratory* exposure was implemented in an insulated portable storage container of 8 ft x 8 ft x 8 ft (2.44 m x 2.44 m x 2.44 m) equipped with a portable air-conditioning unit and dehumidifier as shown in Figure 5-2.

(a)

(b)

Figure 5-1 PT grout and cements in *Control* exposure: (a) PT grout bags and (b) Small-scale containers

(a)

(b)

Figure 5-2 PT grout and cements in Laboratory exposure: (a) PT grout bags and (b) Small-scale containers

Field exposure was implemented with a walk-in environmental chamber at the FDOT State Materials Office. For the MITT tests and small-scale containers, the same environmental chamber was used to expose the material to consistently elevated temperature and humidity. Figure 5-3 illustrates the *Field* exposure chamber used. This environmental chamber maintained a near constant 85˚F and an average relative humidity of approximately 85%. Relative humidity was regulated using a large water tray placed inside the chamber. During the exposure period from May 2015 to September 2015, the average monthly temperature and humidity in the *Field* exposure were recorded, as shown in Table 5-1.

Extreme exposure was imposed on MITT tests and small-scale containers using a second environmental chamber; this chamber was maintained at a constant 95˚F and 95% RH, and was located in Weil Hall at the University of Florida. Figure 5-4 shows the *Extreme* environmental chamber used. The chamber was equipped with a self-regulating temperature and relative

humidity system. During the imposed exposure period from May 2015 to September 2015, the average monthly temperature and humidity in the *Extreme* exposure were recorded, as shown in Table 5-2. To facilitate comparison, the letters C, L, F, and E were used to differentiate between exposure conditions, and will be used along with PT-x labels (previously defined) for identification of tested samples. For example, PT1-E-14 refers to a grout from manufacturer 1 that was subjected to *Extreme* exposure for 14 days.

(a) (b)

Figure 5-3 Walk-in chamber used to impose the *Field* exposure on grout and cement

(a) (b)

Figure 5-4 Walk-in chamber used to impose the *Extreme* exposure on grout and cement

Table 5-1 Mean temperature and relative humidity values for *Field* exposure

	Mean Temperature (˚F)			Mean RH (%)		
	High	Average	Low	High	Average	Low
May	88	86	78	90	86	80
June	90	87	76	94	86	70
July	92	85	78	92	84	64
August	93	86	70	90	87	72
September	94	87	73	95	87	67

* Values taken from Omega Model HH314A digital temperature and humidity meter

Table 5-2 Mean temperature and relative humidity values for *Extreme* exposure

	Mean Temperature (˚F)			Mean RH (%)		
	High	Average	Low	High	Average	Low
May	100	97	88	98	96	88
June	100	96	92	99	97	90
July	102	96	89	99	98	93
August	91	97	93	97	97	94
September	97	95	92	97	96	92

* Values taken from Omega Model HH314A digital temperature and humidity meter

6 Sample Preparation Procedures

6.1 MITT Samples

Five commercially available prepackaged PT grouts were conditioned in intentionally damaged bags at elevated temperature and humidity. Next, representative samples were tested using MITT to determine the amount of soft grout produced. Companion small-scale samples of PT grout and its respective cement were conditioned alongside the MITT samples and tested in selected small-scale tests as an alternative to MITT testing.

Prior to *Field* or *Extreme* exposures, three 18-in. long incisions were made through the top face of each prepackaged grout bag as shown in Figure 6-1. These incisions exposed the grout directly to the high humidity during exposure to accelerate the degradation of the grout and to eliminate the variation in exposure caused by varying packaging techniques used by the manufacturers. It is very likely that packaging does play a major role in the shelf life of PT grouts, so this topic should certainly not be ignored, but this study was more concerned with the constituents of various PT grout manufacturers and their sensitivity to the adverse storage exposure. Packaging used by the manufacturers was previously discussed in the literature review section.

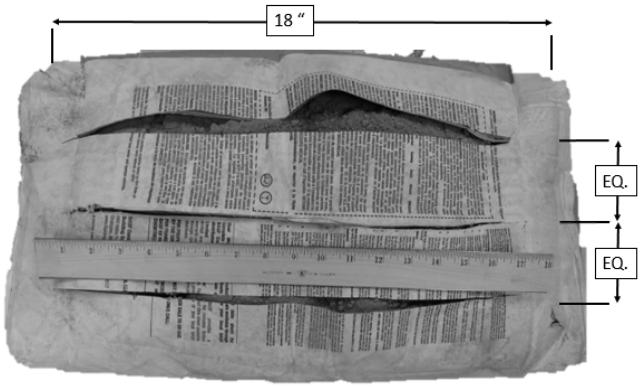

Figure 6-1 PT grout bag incision geometry

6.2 Small-Scale Samples

Small-scale samples consisted of 1.5-inch deep by 3-inch diameter plastic containers filled with material. After exposure, the small-scale containers were mixed with a glass rod for 60 seconds and shaken for 60 seconds in a 3-inch by 6-inch diameter plastic container. One container was used for high shear blending and DSR testing. For the remaining containers, every time a sample was removed, it was taken from four spots to ensure a representative sample. A relatively small sample (roughly 50 g) of cementitious material was removed after mixing and placed in a small plastic vial. The same sampling approach was used for obtaining small-scale samples for Blaine fineness and TGA. Samples for microwave moisture-content testing were prepared by collecting material from a small-scale container (roughly 200 g), which was then mixed with a glass rod for 60 seconds and shaken for 60 seconds using a 3-inch tall by 6-inch diameter plastic container, then returned to the original container.

LOI depth testing consisted of removing, after exposure, 0.5-inch deep layers of material from a small-scale container in sequence and mixing each layer separately with a glass rod for 30

seconds prior to removing a 20-g sample, which was placed in a plastic container as shown in Figure 6-2. All the test methods mentioned in this section are detailed further along in this chapter and in Appendix B.

Figure 6-2 Plastic containers used for LOI layered-material sampling

7 Modified Inclined Tube Test (MITT)

7.1 Summary of Test Method

The Modified Inclined Tube Test (MITT) was used to investigate the formation of soft grout in PT grouts. MITT was developed to determine the susceptibility of a material to form soft grout. The original Euronorm test (EN445-07) focuses on determining bleeding and change in volume of grout after injection (Piper et al., 2014). Modifications to the original test method include:

1. After 24 h, the tube is dissected at the top of the inclined tube and visually inspected for segregated or soft grout. Masses of collected samples are measured and moisture contents of soft grout are determined using ASTM C566.
2. Grout is sampled at selected locations along the length of the tube and at the top and bottom of the cross-section. The samples are tested for moisture content using ASTM C566.
3. Strand bundles are shortened to 14-ft lengths to allow unimpeded sampling of the grout near the top of the inclined tube.

The first step in this test was to blend the dry PT grout. Then, a batch of PT grout was mixed using a full-scale colloidal mixer. The mixing procedures used for dry blending and MITT are discussed in more detail in Appendix A, Appendix I, and Appendix J. After mixing, the grout was then injected into a 15-ft long by 3-in. diameter PVC duct filled with twelve 0.6-in. diameter post-tensioning strands. This PVC duct sits on a stand at an inclination of 30 degrees from horizontal. Figure 7-1 shows the MITT setup.

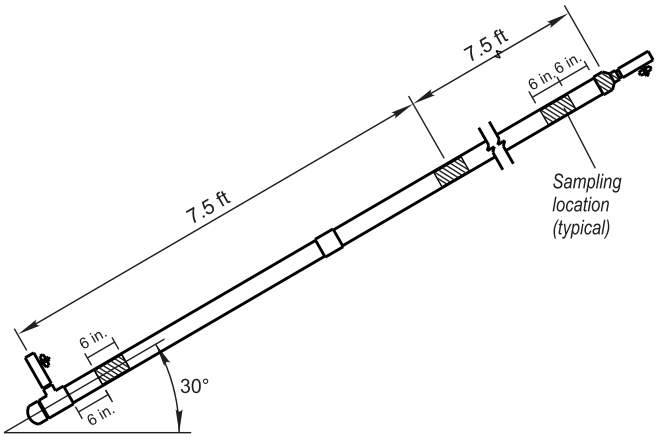

Figure 7-1 MITT setup and sampling locations

The MITT procedure also involves the dissection of the duct at 24 ± 1 h after the time of injection. The purpose of this dissection process is to find any soft grout that may have formed, as well as measure the moisture content of the grout at various locations along the duct. These locations of interest are shown in the four shaded regions along the duct in Figure 7-1.

As discussed in the exposure section, prepackaged bags of PT grouts from various manufacturers were subjected to both the *Field* and *Extreme* exposure conditions, then v-blended

and tested using the MITT testing tube. This section will focus on the measured amounts of bleed water, soft grout, moisture content after dissection, and the unit weight.

7.2 Results and Discussion

7.2.1 Bleed Water

The MITT procedure was used in this study to investigate many different characteristics of the PT grouts; the two primary concerns of the test were to determine the quantities of bleed water and soft grout produced by each manufactured grout after various lengths of exposure to the *Field* and *Extreme* conditions.

Figure 7-2 shows the volume of bleed water measured in both *Field* and *Extreme* exposures. For all PT grouts investigated, as exposure time increased, the volume of bleed water also increased for both *Field and Extreme* exposures. While it is clear that elevated temperature, humidity, or both influenced the susceptibility of PT grouts to bleed, it is not clear why. One possibility is that exposure may adversely affect admixtures that inhibit bleed. Another possibility is that prehydration and water absorption during exposure affected the density and surface characteristics of the portland cement and additional SCM constituents present in the PT grout mixtures.

In all grouts that exhibited bleed water, soft grout was also found. Figure 7-3a shows the collected bleed water found in PT7 after 10 days in the *Extreme* exposure. Figure 7-3b shows the soft grout and bleed water being removed from PT7 after 10 days in the *Extreme* exposure.

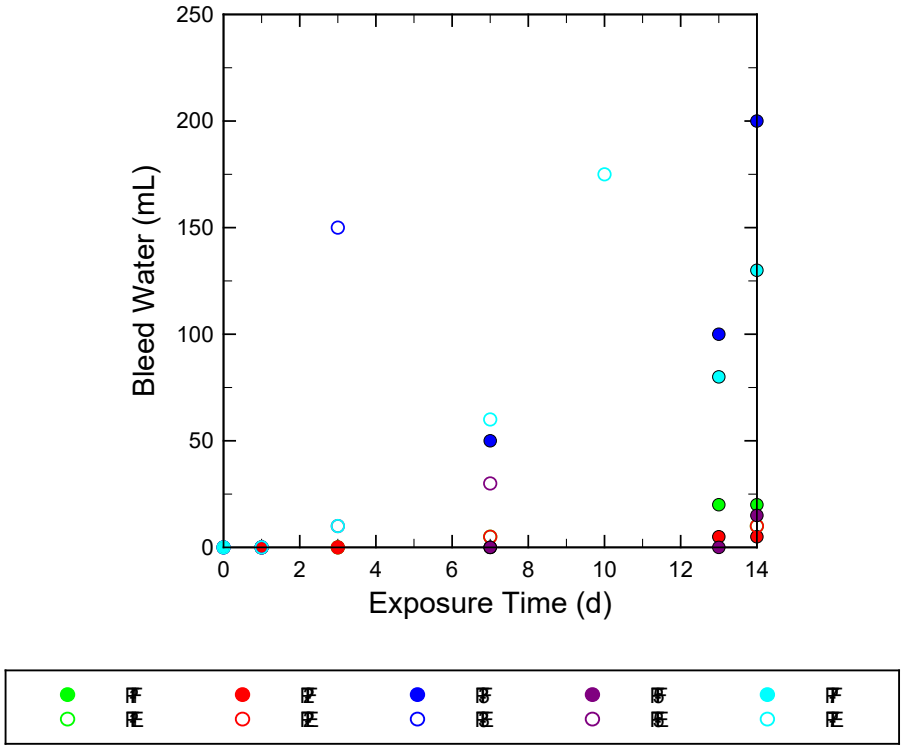

Figure 7-2 Amount of bleed water found in grout MITT testing from the *Field* and *Extreme* exposures

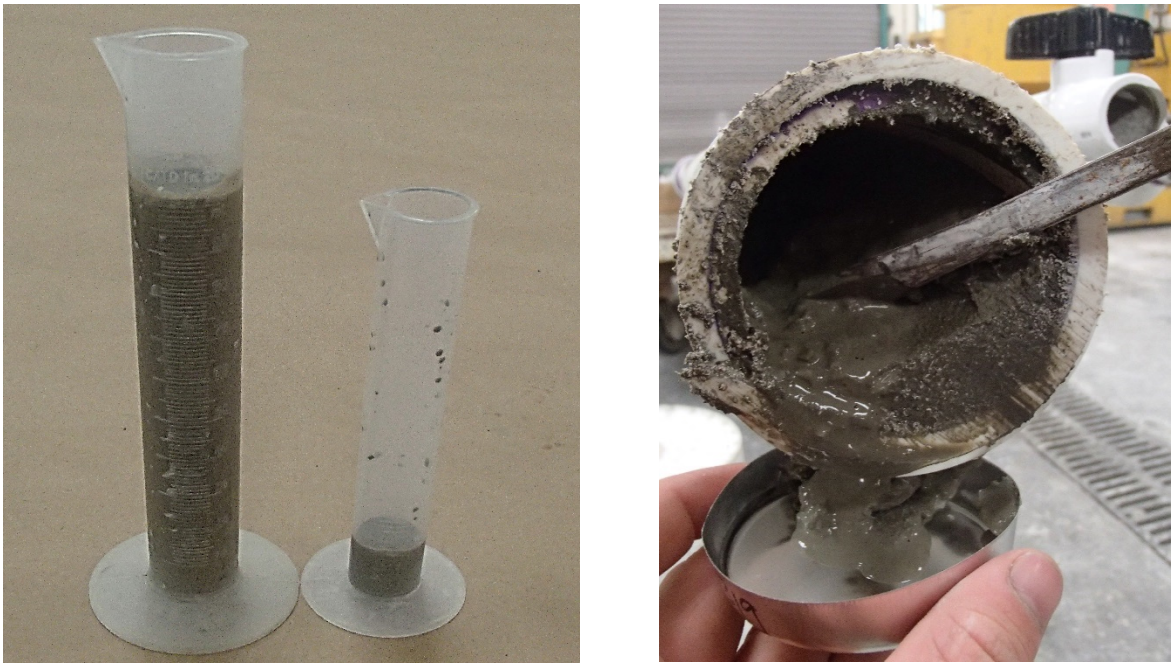

(a) (b)

Figure 7-3 Example of (a) bleed water and (b) soft grout recovered following MITT dissection of PT7 after 10 days in the *Extreme* exposure

7.2.2 Soft Grout

Given sufficient time, both conditions eventually caused soft grout in all grout tests. Figure 7-4 through Figure 7-8 show soft grout results for all PT grouts under *Field* and *Extreme* exposures. Further, more soft grout was found in the *Extreme* exposure compared to the *Field* exposure at comparable exposure times. In some cases, *Extreme* exposure of only 3 days resulted in soft grout formation during testing.

Since it was not practical to conduct tests daily, a single test was unlikely to capture the exact day on which exposure was sufficient to cause soft grout formation during testing. To provide a rudimentary estimate of the time to soft grout, linear regressions were conducted on the mass of soft grout collected. Although the assumption of linear growth in soft grout with time may not be accurate in all cases, the x-intercept of the regression provides a single point in time at which the grout begins to produce soft grout, which should be proportional to the shelf life of the grout. To provide a more general idea, all PT grouts produced soft grout after 14 days of *Field* exposure. The amount of soft grout collected from MITT varied from 15g to 280g. Similarly, for *Extreme* exposure the amount of soft grout collected after 7 days of exposure ranged from 30g to 145g, except for PT1, which only produced soft grout (250g) after 11 days.

Table 7-1 indicates the amount of soft grout collected from MITT at specific exposure times. The total amount of soft grout collected was higher for MITT using *Extreme* exposure samples compared to *Field* exposure, which was expected due to the higher levels of temperature and humidity. However, it was found that when comparing both exposure types, the percent difference of total soft grout was only 13%, which indicates that the effect of temperature and humidity decreases with increase of exposure time.

Table 7-1 Amount of soft grout collected from all PT grouts during MITT

Time of Exposure	Total Soft Grout (g)		% Difference
	Field	*Extreme*	
3 Days	0	210	NA
7 Days	200	315	58%
14 Days	630	710	13%

Figure 7-4 through Figure 7-8 show the trend lines in the *Field* and *Extreme* exposures; the trends projected that soft grout formation may potentially first occur in the *Extreme* exposure at a range from 1 day for PT3 to 7 days in PT1. The trend lines in the *Field* exposure projected that soft grout formation may potentially first occur in a range from 3 days for PT7 to 13 days of exposure in PT2 and PT5.

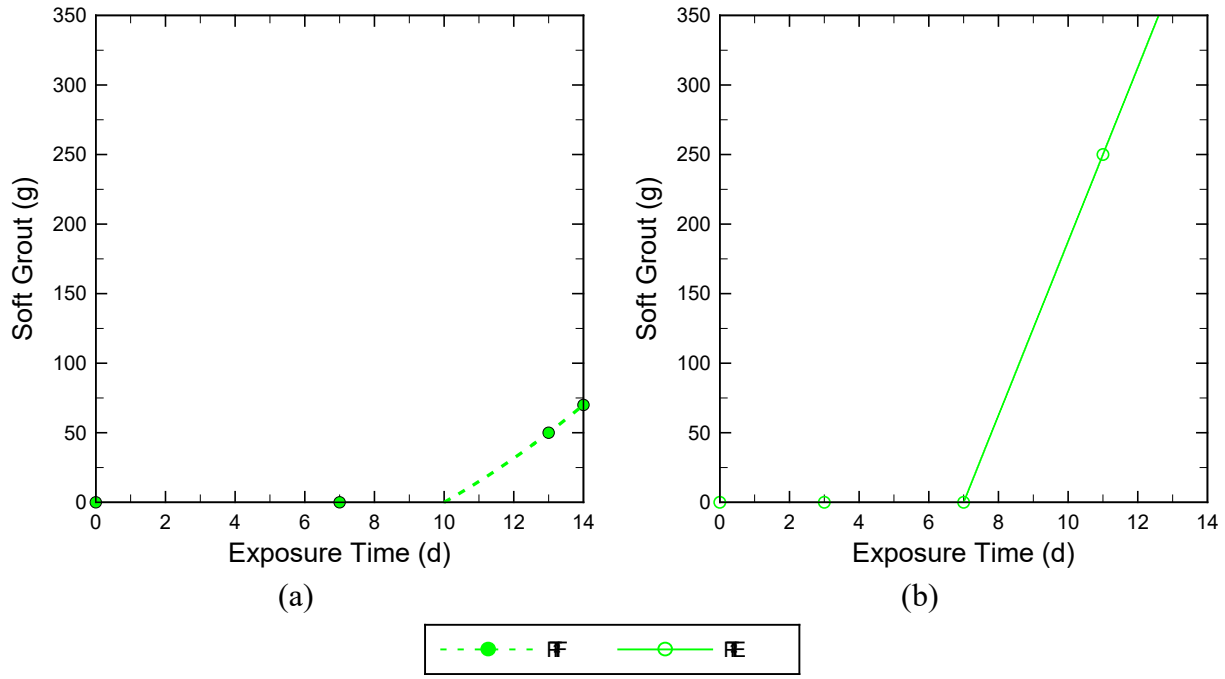

Figure 7-4 PT1 soft grout points and trend lines for both the (a) *Field* and (b) *Extreme* exposure MITT tested

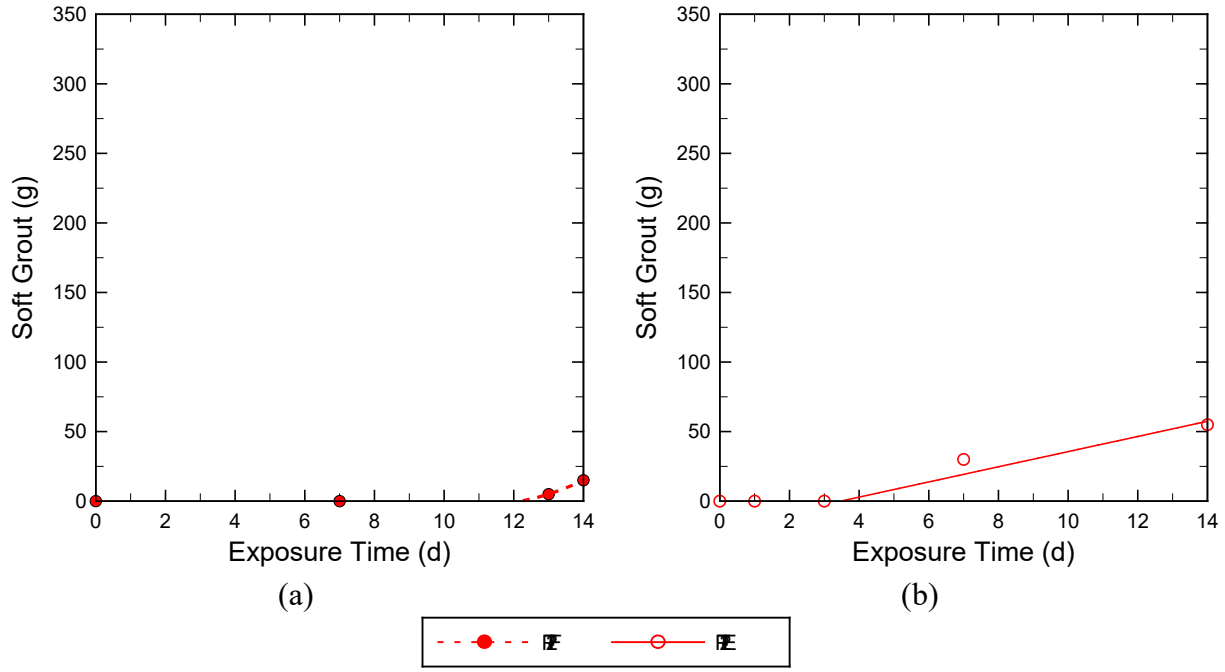

Figure 7-5 PT2 soft grout points and trend lines for both the (a) *Field* and (b) *Extreme* exposure MITT tested

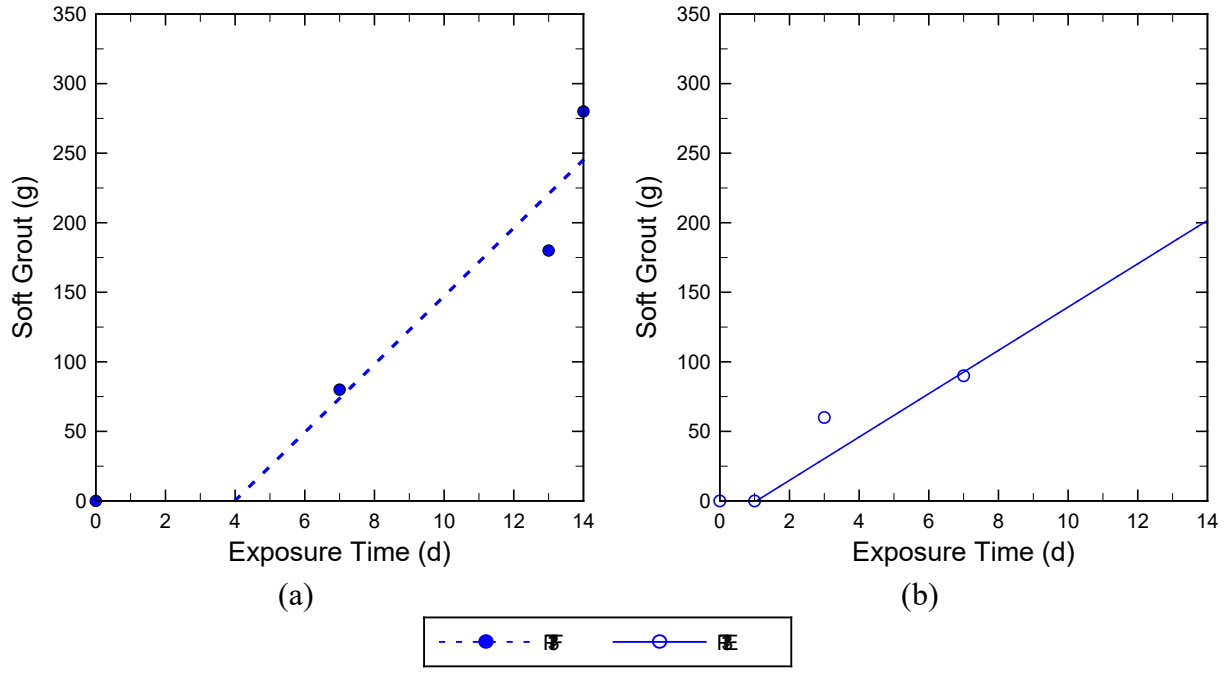

Figure 7-6 PT3 soft grout points and trend lines for both the (a) *Field* and (b) *Extreme* exposure MITT tested

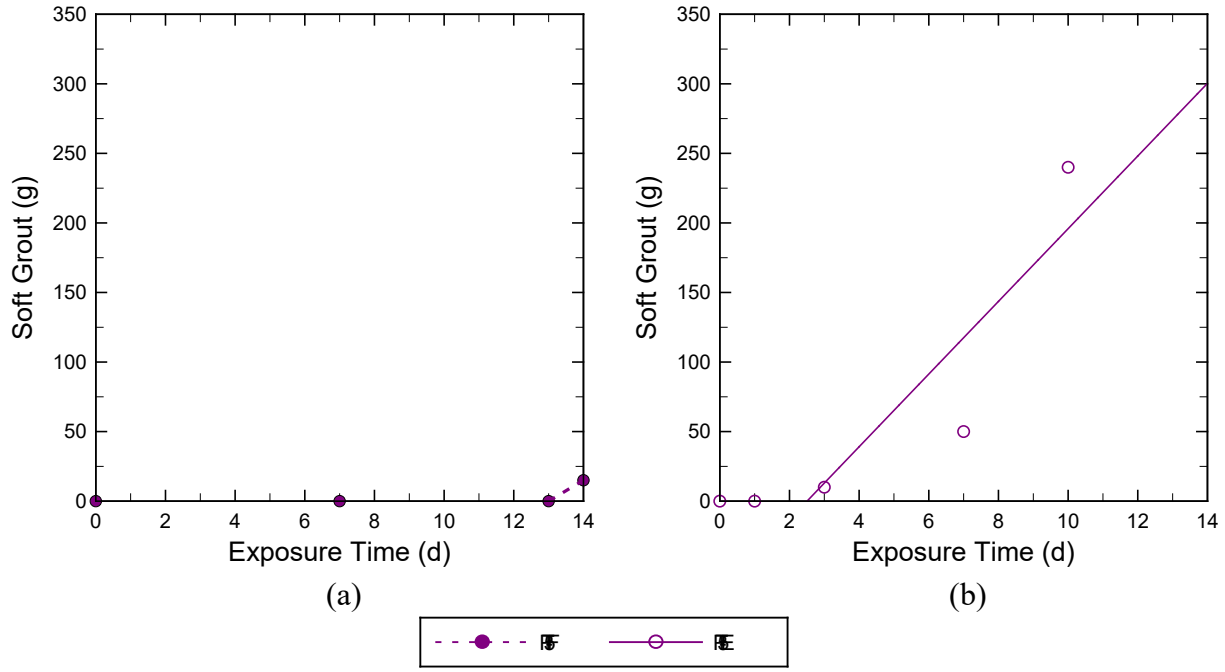

Figure 7-7 PT5 soft grout points and trend lines for both the (a) *Field* and (b) *Extreme* exposure MITT tested

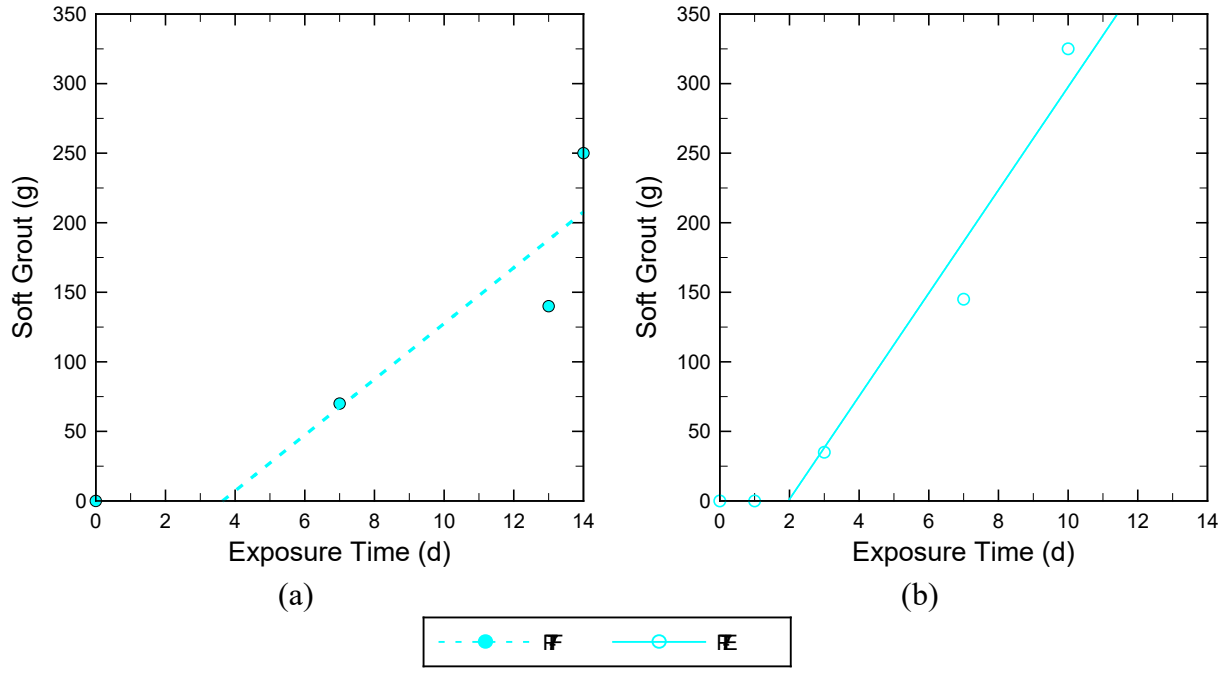

Figure 7-8 PT7 soft grout points and trend lines for both the (a) *Field* and (b) *Extreme* exposure MITT tested

Figure 7-9 summarizes MITT results with respect to the initiation of soft grout formation. For each PT grout, there are two sets of data that were collected from the tests of grout with *Extreme* and *Field* exposures. For each exposure, three times are plotted. The bar labeled *no soft grout* is the shortest test time in which soft grout was not produced. For example, PT1-E formed soft grout at the eleven-day test, but not at the seven-day test. Hence, the *no-soft-grout* point is seven days. The *theoretical limit* is the x-intercept of the regression, which represents the number of days of exposure required to form soft grout for that particular grout under the indicated exposure. Finally, bars labeled soft grout show the earliest test day on which soft grout was discovered. This bar chart, then provides a bracketing of the time to soft grout formation for each PT grout. PT3 and PT7 have the shortest exposure periods.

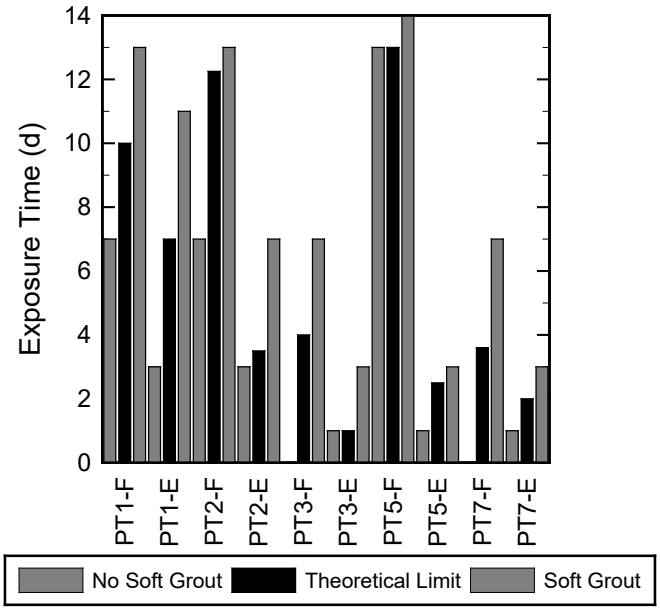

Figure 7-9 Exposure time necessary to form soft grout

Although there are a number of possible explanations for the degradation of the PT grout, it is hypothesized that the primary mechanism responsible for this sensitivity was prehydration of the portland cement and possibly other reactive SCM constituents.

Following injection of conditioned grout into the inclined tube, partially hydrated cement materials that have a reduced density compared to unhydrated material would tend to migrate to the top of the tube prior to and during setting (Figure 7-10). Low-reactivity filler materials of lower density would also be migrating. Similarly, very fine particles such as ground limestone, silica fume, and the finest cement particles tend to stay in suspension longer. As the larger particles settle, the solution is displaced upward resulting in the rise of the bleed layer. Excess mixing water is also present due to the moisture absorbed by the grout during exposure, which will increase the propensity to bleed. During the 24 hours following injection, soft grout recovered from the specimen will likely be a mixture of the filler materials, partially hydrated cement, and bleed water. The bleed water may contain excess concentrations of chemical admixtures or other additives depending on the grout formulation. If a relatively large quantity of partially hydrated cement particles is present in soft grout recovered at 24 hours after injection, then it is possible that the delayed hydration process will continue and perhaps

chemically bind the excess moisture. On the other hand, if the soft grout is predominately filler material, then hydration will not occur, and the excess moisture and perhaps corrosive chemicals will remain inside the tendon.

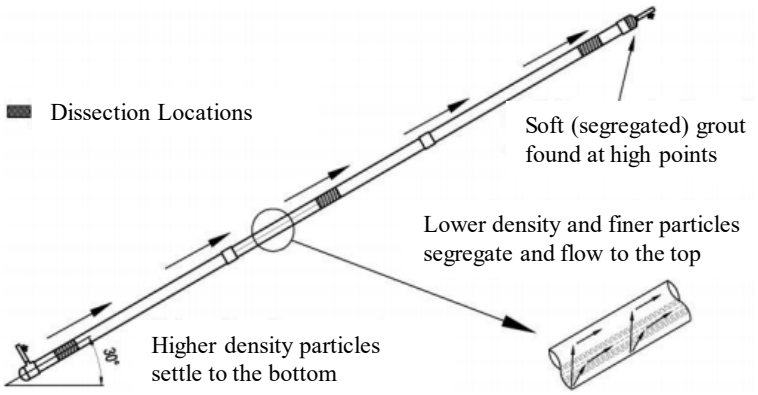

Figure 7-10 Segregation mechanism occurring inside the inclined test tube

7.2.3 Moisture Content

Figure 7-11 through Figure 7-15 show the change in grout moisture gradient related to the position of the test sample within the MITT specimen. Each plot represents the resulting moisture gradient for a particular grout age, with the black plots designating tests in which soft grout was recovered. The dashed line at 35% moisture content is based on previous research (Brunner and Hamilton, 2014), in which soft grout was recovered when measured moisture content exceeded 35%. Moisture content is sampled at the top and bottom of the cross-section at each location shown in Figure 7-1; however, only the highest moisture content is plotted at each location.

The results presented here agree with previous research done by Brunner and Hamilton (2014), where similar trends were noted in the dissection results. Generally, PT grouts showed a nearly uniform moisture content that remained between 12% and 22% for the middle and bottom sample locations. In addition, the moisture content at the bottom sampling location showed little variation with the varying lengths of exposure in both the *Field* and *Extreme* exposures. Conversely, the sample locations at the middle, top, and exit point showed significant increases in moisture gradient as the exposure duration increased. In *Extreme* cases, the moisture content increase by a factor of 2.4. This trend is directly related to the pre-set movement of lower-density, partially hydrated cement particles and unreactive fillers to the top of the tube prior to set. Bleeding due to settlement of larger particles in combination with movement of excess mixing water can also worsen this movement. The migration of partially hydrated cement particles, low reactive fillers, and excess mixing water all contribute to the increase in moisture content at the sample locations at the middle, top, and exit point after grout is conditioned.

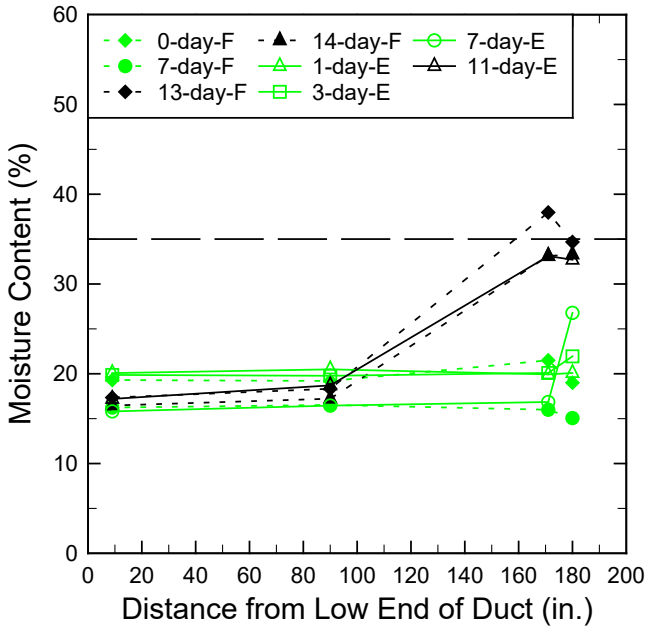

Figure 7-11 Moisture gradient along length of duct for PT1

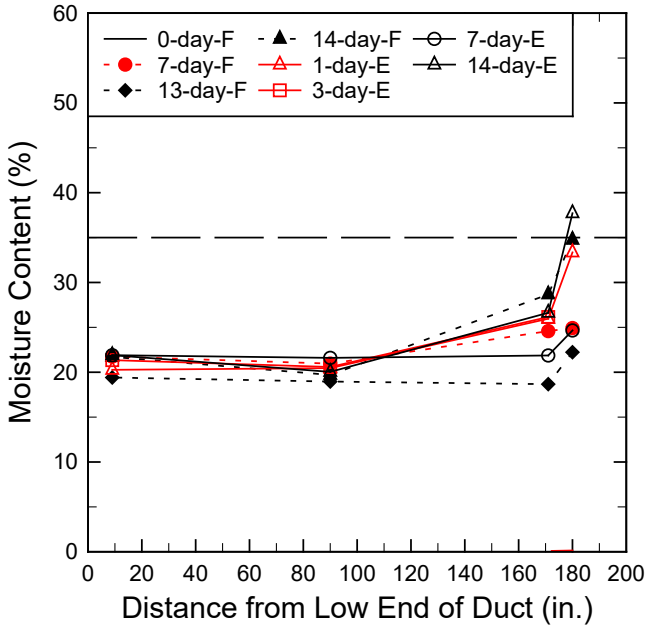

Figure 7-12 Moisture content along length of duct for PT2

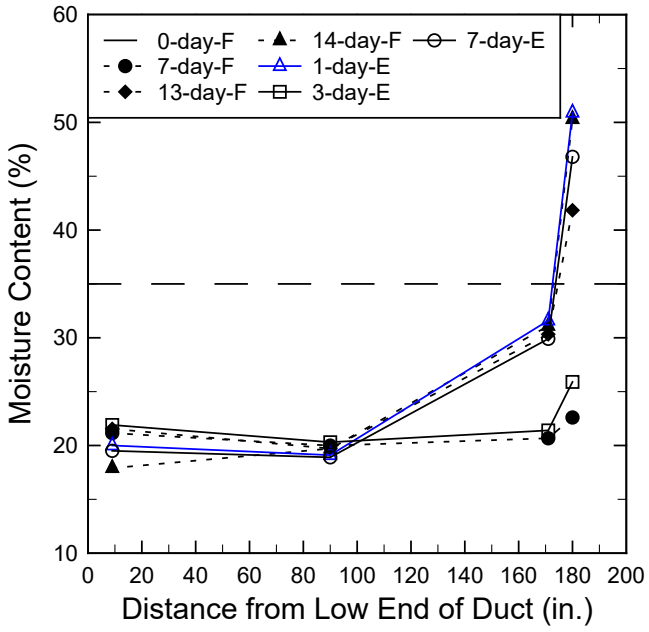

Figure 7-13 Moisture content along length of duct for PT3

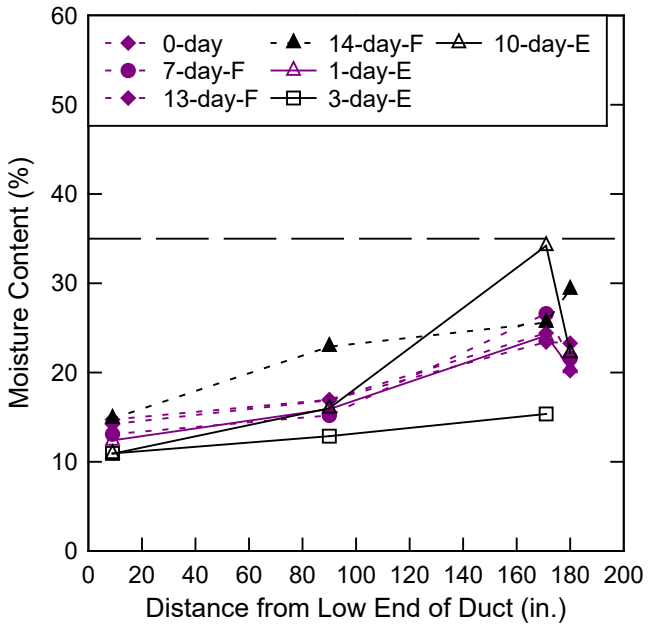

Figure 7-14 Moisture content along length of duct for PT5

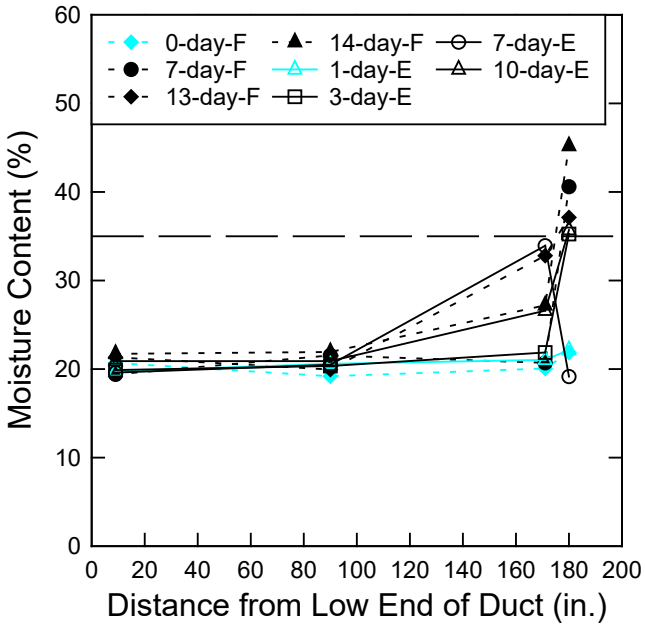

Figure 7-15 Moisture content along length of duct for PT7

7.2.4 Unit Weight

Figure 7-16 shows the unit weight results immediately after mixing and Figure 7-17 shows the unit weight results immediately after injection. Overall, the results varied from 108 pcf to 122 pcf [1,730 kg/m^3 to 1,954 kg/m^3] for all PT grouts exposed to the *Field* and *Extreme* exposures. In general, the trend shows that unit weight decreased with increasing duration of exposure with the exception of PT1, PT2 at 1 day and PT7 at 3 days in the *Extreme* exposure.

Figure 7-18 shows the relative mass gain in grout caused by water absorption during exposure. When measuring the grout proportion for the water-to-solid ratio (w/s) recommended by the manufacturer, absorbed water displaced grout, which in turn reduced the mixed grout unit weight and increased the w/s.

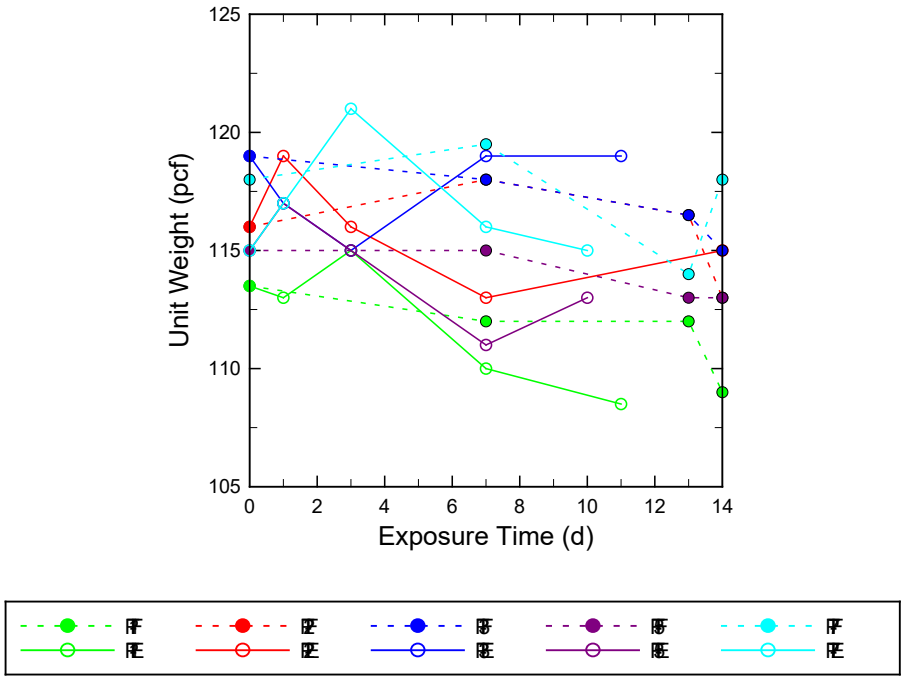

Figure 7-16 Post-mixing unit weight

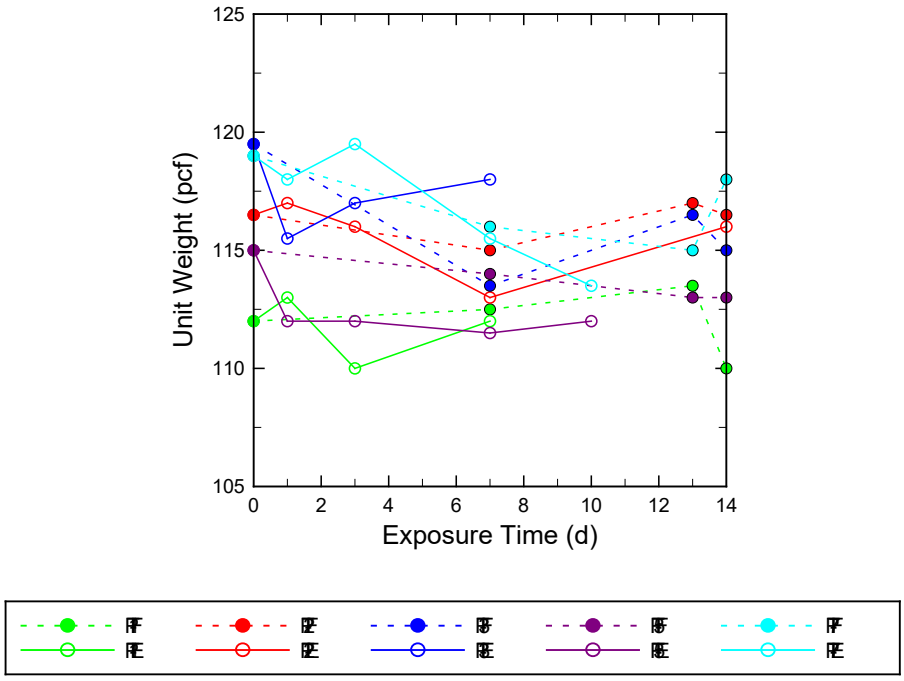

Figure 7-17 Post-injection unit weight

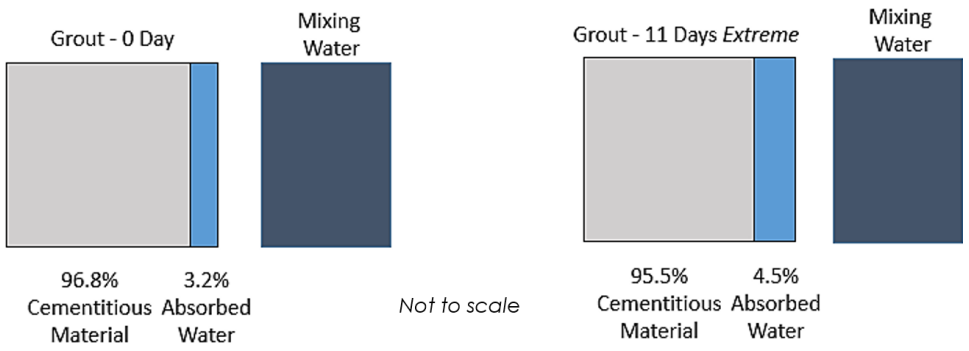

Figure 7-18 Grout relative mass gain due to water absorption

8 Grout Fluidity

8.1 Summary of Test Method

8.1.1 PT Grout

The nominal shear rate (NSR) viscosity of the grout was measured before and after injection using a dynamic shear rheometer (DSR) (Figure 8-1). A helical ribbon geometry and cup were used to test the grout (Figure 8-2 and Figure 8-3). The rheometer measures the torque that results when the ribbon is submerged into fluid grout and rotated at a specified rate. The torque is then converted to shear stress based on a factor that must be determined by testing a standard reference material provided by NIST to calibrate the machine. The standard reference material consists of corn syrup and limestone powder. The shear strain is determined by multiplying the angular velocity by a known shear strain factor that can be obtained from the manufacturer of the cup and ribbon. For this project, the calibration was performed for the cup and ribbon geometry according to Piper et al. (2014). The NSR viscosity is then calculated by dividing the measured shear stress values by the calculated shear strain.

Figure 8-1 Dynamic shear rheometer

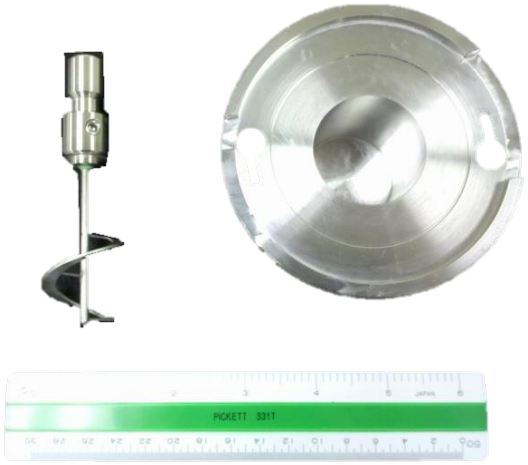

Figure 8-2 Helical ribbon and cup

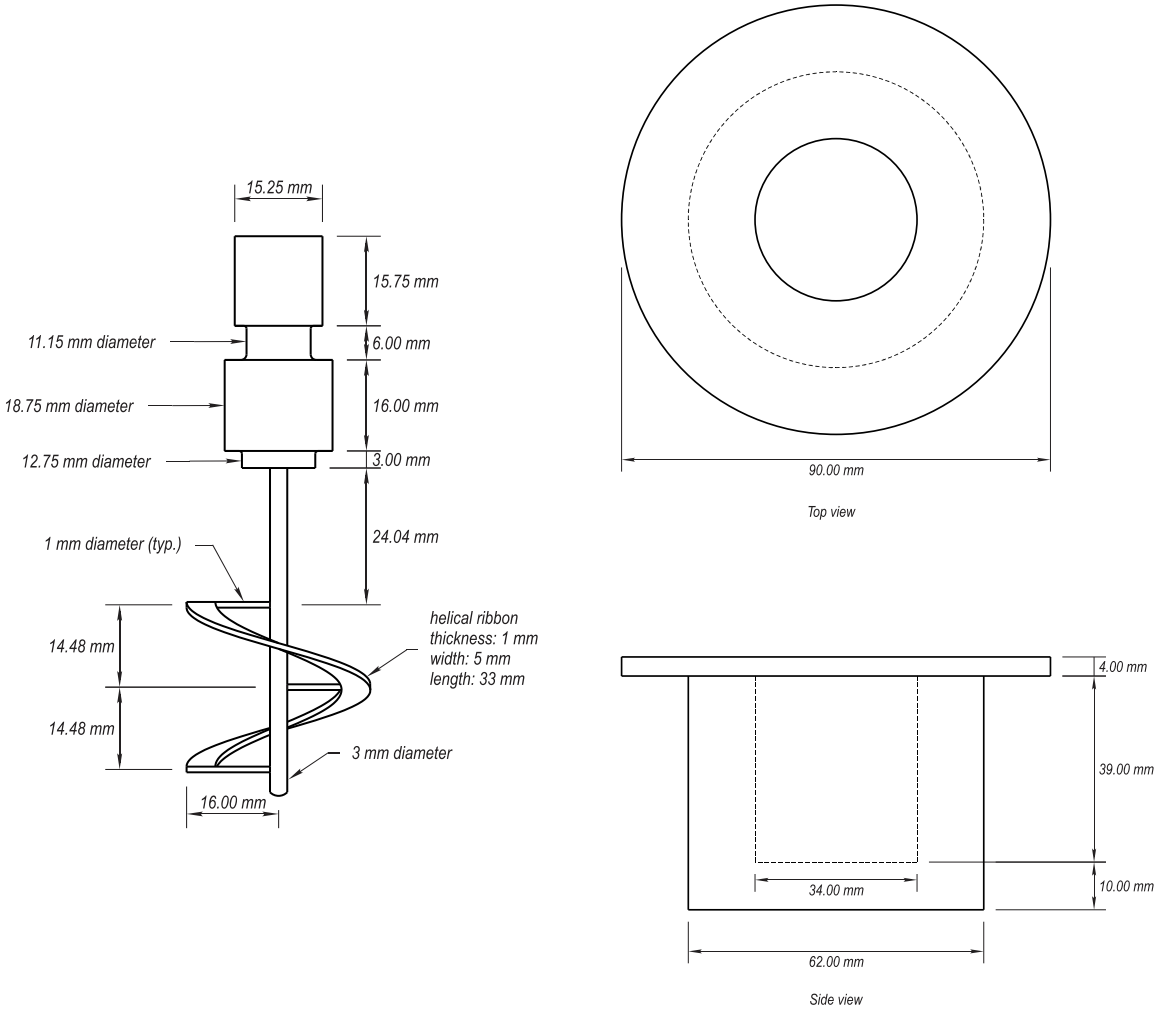

Figure 8-3 Helical ribbon schematic; DSR cup schematic

8.1.2 Admixtures

Similar to the PT grout samples, NSR viscosity and bleeding were used to evaluate the degradation of the admixtures exposed to heat and humidity. Admixture samples were placed in small containers and exposed to *Control*, *Field*, and *Extreme* exposures. It should be noted that these tests were performed in the absence of prehydrating cement, which would have exposed the admixtures to hydration products that could have had synergistic effects on the degradation of the admixtures. For instance, prehydration of the cement will likely create a higher pH environment, which could exacerbate the deterioration. Manufacturers usually label their admixtures with the recommended storage conditions and suggested shelf life. No information, however, is typically provided on the grout properties affected by high temperature and humidity due to the deterioration of admixtures or other constituents.

To evaluate the effect of exposure on the viscosity of neat cement paste, several mixtures were investigated using the same mixture parameters using the admixtures exposed to *Control*, *Field*, and *Extreme* exposures. Portland cement Type I/II was used for all the mixtures, loss on ignition on this cement was 1.96%, showing that the cement had no prehydration that could affect the overall results. Water-cement ratio for all mixtures was 0.30, and the cement content for all mixtures was maintained at 500 g. The admixture dosages were selected using trial batches. For A1 and A3, the dosage was the minimum value suggested by the manufacturer. For admixture A2, the manufacturer provided a range of 0.05% to 0.5% of the total cement content; however, no w/c ratio was provided. Therefore, the final dosage was selected by trial batches to obtain viscosity properties similar to the mixtures using the other admixtures. Table 8-1 summarizes the main parameters used for all mixtures.

Table 8-1 Mixture details

Material	Quality	Dosage (% of cement mass)	Cement Content (g)	w/c
A1	HRWR	0.025	500	0.30
A2	HRWR	0.15	500	0.30
A3	HRWR/Anti-Bleeding	6	500	0.30

Dry admixture samples were placed in small containers and subjected to the specified exposure. Following exposure, admixture samples were used to prepare a neat cement paste for use in NSR viscosity testing. The mixing method utilized was high shear mixing described in Appendix F. This mixing method consists of two mixing cycles of 4,000 and 10,000 rpm. After mixing, NSR viscosity was tested using an AR2000 (see Figure 8-1). For this section of the study, the calibration and NSR viscosity setup was established for the cup and ribbon geometry according to Piper et al. (2014).

In summary, the grout was initially subjected to a pre-shear rate of $165 s^{-1}$ for 30 seconds. After, the grout was subjected to a shear rate of 50 $s^{-1}$for a period of 60 minutes. The NSR viscosity was then calculated by dividing the measured shear stress values by the calculated shear strain. In the study performed by Piper et al. (2014), NSR viscosity was calculated after the first minute of the sustained 50 s^{-1} shear rate to emulate flow cone viscosity or the viscosity after 5 minutes; these were found to characterize the viscosity of the sample for an hour under the predetermined shear rate.

Bleeding of neat cement paste prepared with exposed admixtures was also tested. Because the cement paste volume prepared in the high-shear mixer was insufficient to perform typical bleed tests such as the pressure bleed or wick-induced bleed, researchers elected to use a centrifuge to generate bleeding. This approach was selected to ensure viscosity and bleed tests were conducted on the same sample batch.

After the NSR viscosity test was initiated, 30 mL of cement paste was collected from the high shear mixes and placed into a centrifuge tube (Figure 8-4). The model of centrifuge used to conduct the bleed tests was Accuspin 400 from Fisher Scientific that allows up to 8,500 rpm (Figure 8-5). The sample was then centrifuged for 5 minutes at 5,000 rpm. Next, the tube was removed from the centrifuge and the supernatant was decanted to a graduated cylinder (Figure 8-6). Two samples were tested with the reported result being the average.

Figure 8-4 Centrifuge tube containing 30 mL of cement paste

Figure 8-5 Centrifuge model Accuspin 400

Figure 8-6 Graduated cylinder used to measure bleeding

8.2 Results and Discussion

8.2.1 PT Grout

Figure 8-7 shows DSR results for PT grout samples from post-mixing, and Figure 8-8 shows results for grout samples taken after injection. To allow comparison among PT grouts, the results were normalized to the DSR results from the unconditioned samples (0 days MITT). The general trend shows that the NSR viscosity increased with increased duration of exposure, with the exception of PT2 and PT3, which show relatively constant results, and PT5 in the post-mixing results showed unpredictable variation for the *Extreme* exposure results.

When NSR viscosity results (Figure 8-7 and Figure 8-8) were compared to the amount of soft grout formed (Figure 7-4 through Figure 7-8), an interesting pattern was found. The two grouts (PT5, PT7) that experienced the largest increases in NSR viscosity from 0 days to 14 days of exposure also experienced the greatest amount of soft grout formed.

NSR viscosity results can be interpreted from two perspectives. First, NSR viscosity can decrease due to moisture present in the prehydrated materials. In other words, mixtures having prehydrated material would have more water and less cement compared to mixtures of materials that have not been exposed. Second, decrease in viscosity can result in segregation of particles, i.e., fillers. Segregation of particles will result in an increase of torque needed in the lower portion of the helical ribbon to maintain the constant angular velocity. This increase of torque then will increase the NSR viscosity. Both behaviors can explain the reason that some PT grouts show peaks or pitfalls as exposure time changes. Figure 7-18 shows dry grout material that absorbed water during exposure, which in turn increased the w/s ratio during mixing thus increasing the available water. The use of SCM and admixtures in the grout may also affect the NSR viscosity.

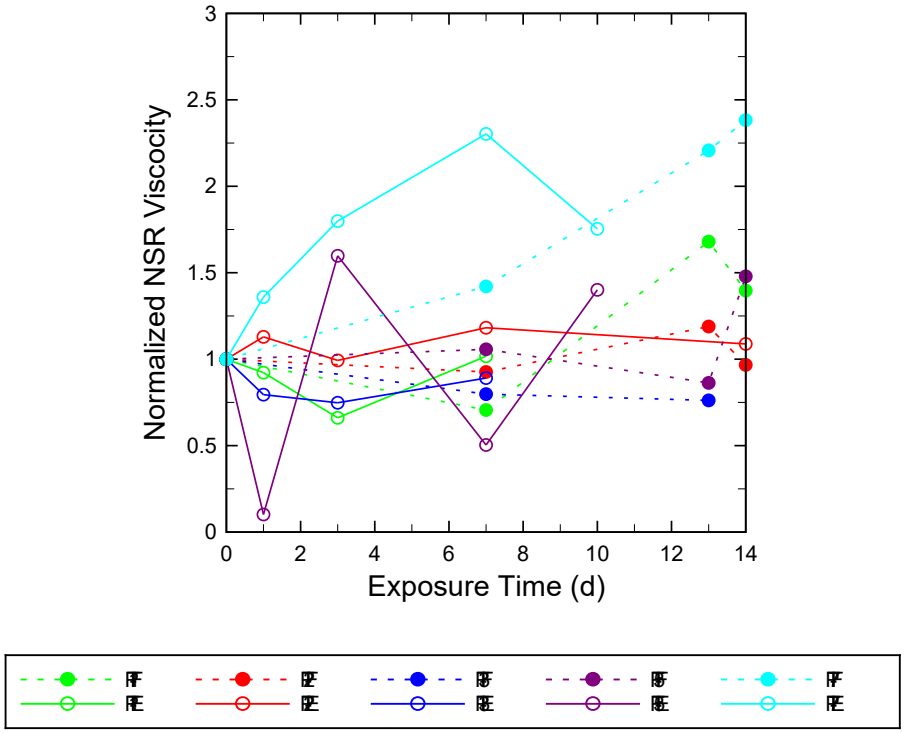

Figure 8-7 Post-mixing normalized NSR viscosity for *Field* and *Extreme* exposures

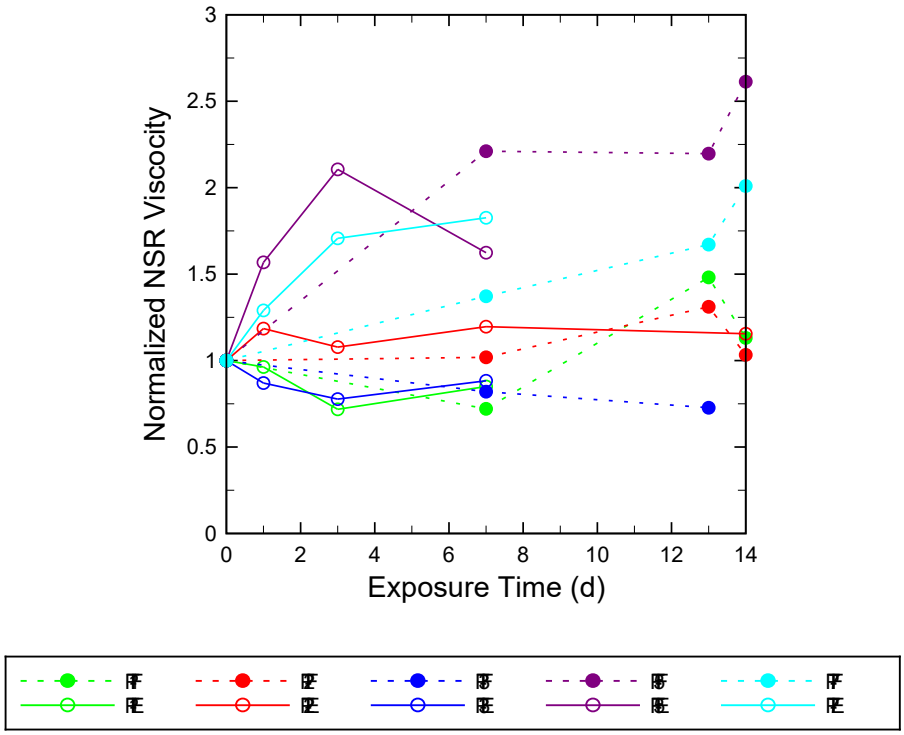

Figure 8-8 Post-injection normalized NSR viscosity for *Field* and *Extreme* exposures

Figure 8-9 and Figure 8-10 show the normalized NSR viscosity for small-scale grout and portland cement samples from *Field* and *Extreme* exposures. The small-scale samples were normalized to the NSR viscosity of the cementitious material (0-day MITT). PT2 and PT3 show relatively constant results with exposure time. The remaining grouts and all cement samples, however, show no clear trends in the variation of viscosity with exposure period. Dry material agglomeration caused by moisture exposure may have erratically affected the DSR results.

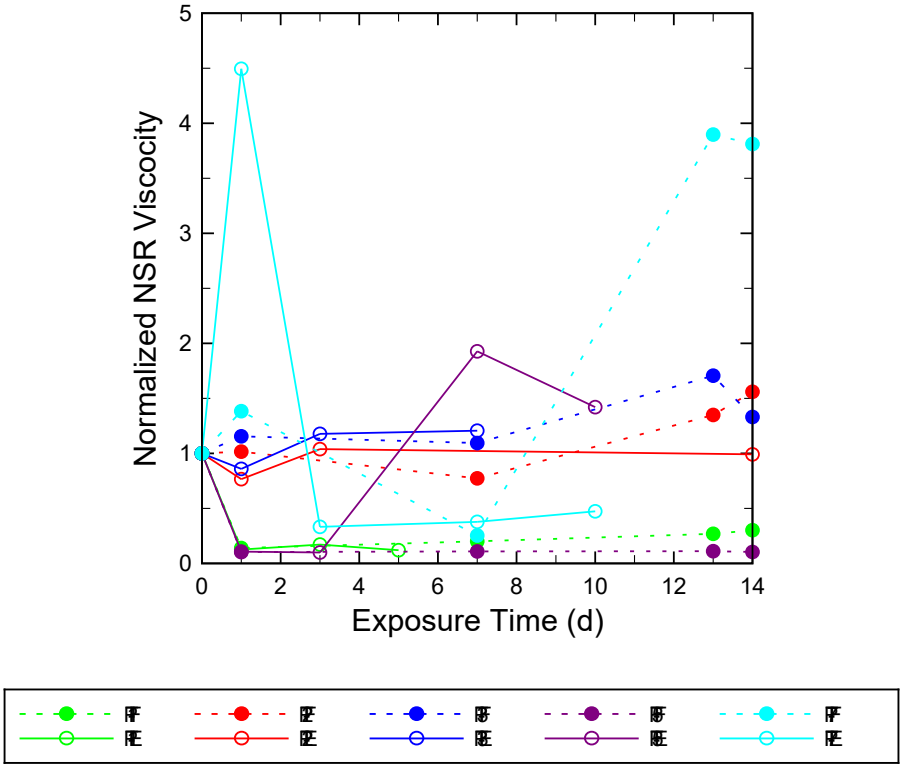

Figure 8-9 Normalized NSR viscosity small-scale grout samples from *Field* and *Extreme* exposures

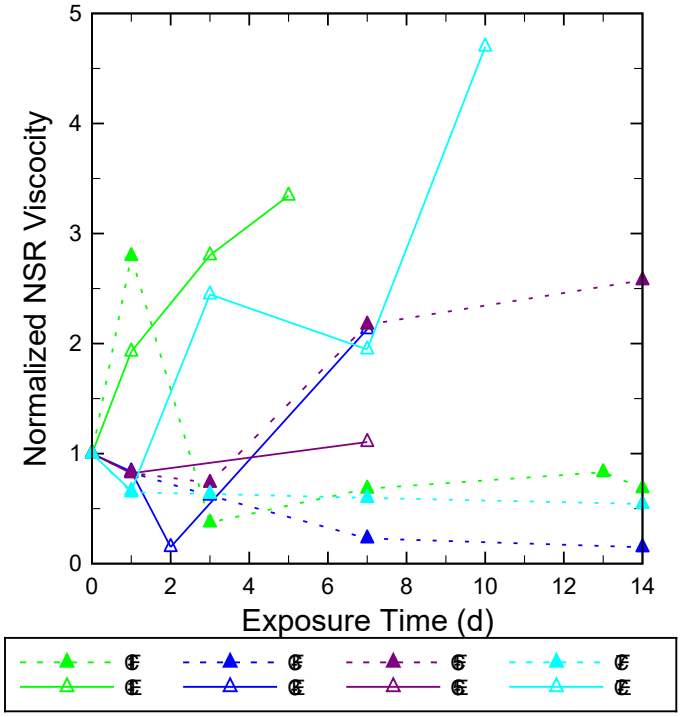

Figure 8-10 Normalized NSR viscosity small-scale portland cement samples from *Field* and *Extreme* exposures

8.2.2 Admixtures

The trend of NSR viscosity after exposure was unique for each admixture. Exposure of A1 and A2 caused severe changes in physical properties, which were due primarily to the adsorption of moisture. To ensure consistent results, a sampling technique was developed for each admixture. For instance, during exposure, A2 changed from powder form to a transparent solution on the surface (see Figure 8-11a) and a thin layer of gluey paste formed in the lower part of the container (see Figure 8-11b). Trial tests were conducted on both the solution and the gluey paste to determine their individual effect. In the case of samples prepared with the transparent solution, the resulting mixture was dry so it could not be tested for viscosity. Clearly the admixture sampled for this test had failed. For the sample prepared with the gluey paste, a higher degree of fluidity was obtained, which gave similar results to that of the unexposed sample. The main challenge with the gluey paste was to distribute the material through the cement prior to mixing, and ensure that the admixture dissolved. To improve the distribution, the material was formed into round pellets (Figure 8-11c) and evenly dispersed in the cement powder prior mixing.

A1 also suffered changes during exposure. During *Extreme* exposure, a crust formed on the surface of the admixture that rapidly hardened (Figure 8-12a); this crust protected the underlying sample from moisture intrusion (Figure 8-12b). The protected portion of the sample preserved its powder form, with the exception of some agglomerations similar to what was observed in cement exposed to moisture. Next, a similar approach to the sampling technique developed for A2 was used. Both the hard layer formed on the surface and the powder underneath were tested independently. The crust material did not dissolve during mixing, which

resulted in poor workability or a dry mixture. The material under the crust, however, provided better workability. Finally, A3 did not undergo any physical changes during exposure that affected sample preparation.

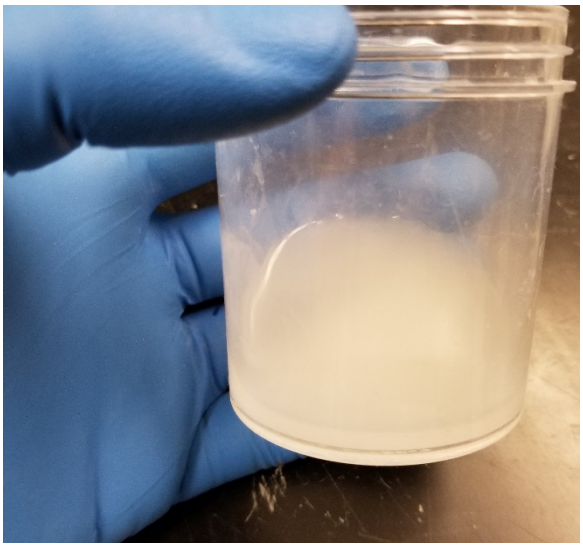

(a)

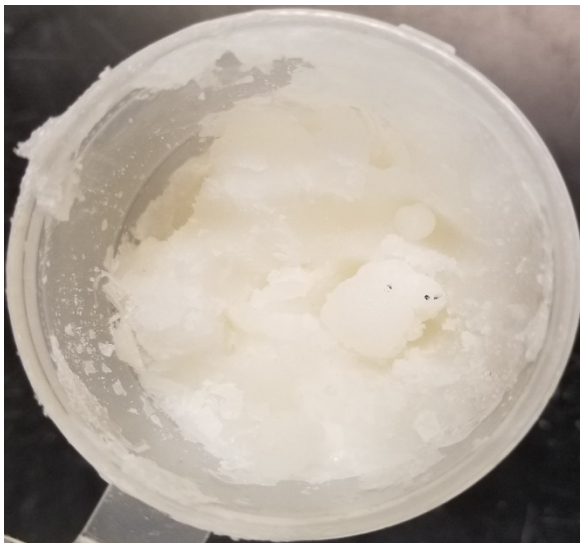

(b)

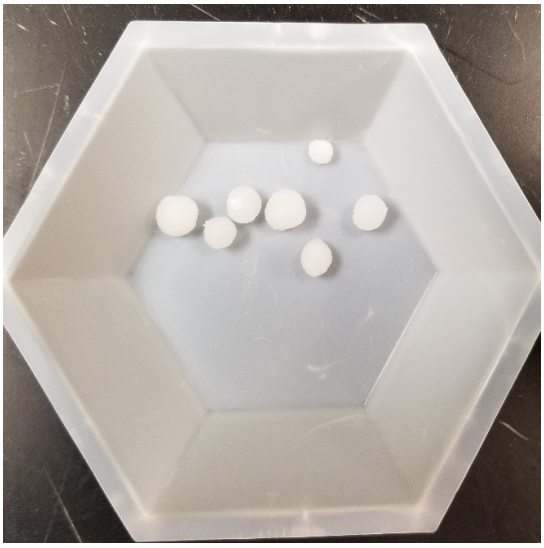

(c)

Figure 8-11 A2 after both *Field* and *Extreme* exposure: (a) Transparent solutions often found in the surface of the admixture A2 container, (b) Gluey paste found in the lower part of the container, and (c) Admixture 2 prepared to mix with the cement.

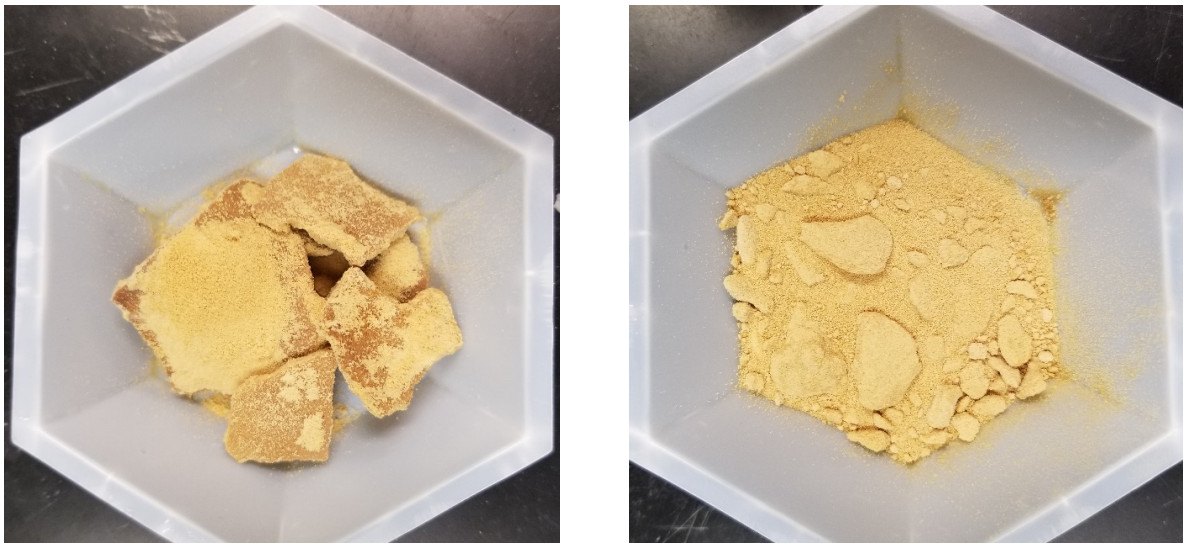

(a) (b)

Figure 8-12 A1 after *Extreme* exposure: (a) Sections of the layer formed on the surface and (b) Powder under the surface layer showing the formation of clumps.

Figure 8-13 shows the normalized values of NSR viscosity for all admixtures subjected to both *Field* and *Extreme* exposure. Initially it was expected that viscosity would increase due to the deterioration of admixtures. For instance, admixtures A1 and A2, which are HRWRs, are used to reduce mixture viscosity, reduce flocculation, and improve flowability. During exposure, however, moisture activated the charge neutralization, which deteriorated its properties. One sign of degradation was the dissolution that occurs at the surface of the admixture sample immediately after exposure began. However, it is unclear how an admixture dispersed in a dry grout powder would react to moisture exposure.

A1 shows a continuous decrease in NSR viscosity with increase of exposure time for both *Field* and *Extreme* conditions. The change in physical characteristics (agglomerations) and increase in mass gain indicate that moisture was adsorbed during exposure. While this would result in additional water present during mixing, it was in relatively small quantities and was unlikely to have an apparent effect. This suggests that this additional water might not be the only contribution to the decrease in viscosity.

A2 NSR viscosity increased during exposure time for both *Field* and *Extreme* exposures. These results were expected as the deterioration of the admixtures due to exposure may result in a reduction of performance. Also, the change in physical properties from powder form before exposure to the gluey paste after exposure could have decreased the dissolution rate during mixing resulting in higher viscosity; however, this was minimized due to the high shear rates used for mixing.

Finally, A3 NSR viscosity increased for both *Field* and *Extreme* exposures. Note that after 7 days of exposure, no more values were recorded. This was due to the lack of workability of the mixtures after exposure as shown in Figure 8-14.

Ageing of admixtures was examined for 28 days under *Control* exposure. The storage conditions were within the recommendations of the manufacturers, so consistency in viscosity

values were expected. Figure 8-15 shows the results of all admixtures during the 28 days. Note that minimal differences exist, especially when comparing the 0 and 28 days. The decrease in viscosity at 7 days for A1 and A3 can be attributed to slight temperature differences during mixing due to heating from high shear mixing. It can be concluded that under recommended storage conditions the admixtures will not deteriorate or suffer physical changes as happened with high temperature and humidity. The effects of longer ageing times can be investigated in future work.

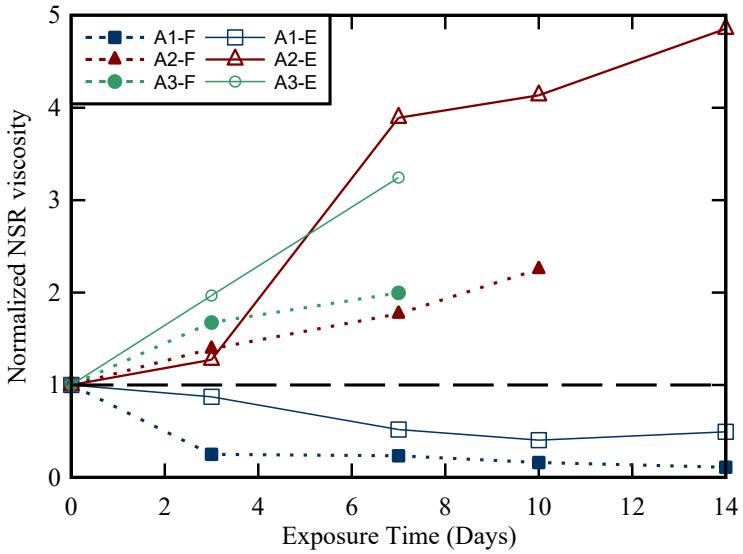

Figure 8-13 Normalized NSR viscosity of all admixtures during both *Field* and *Extreme* exposure

Figure 8-14 A3 mixture after mixing shows lack of fluidity after 10 days of exposure.

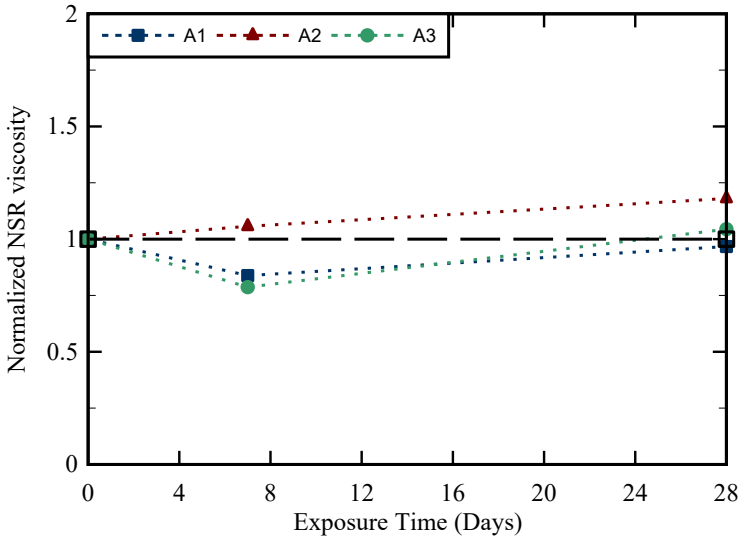

Figure 8-15 Normalized NSR viscosity of all admixtures during *Control* exposure for ageing effects

Figure 8-16 shows the change in bleeding for all admixtures subjected to both *Field* and *Extreme* exposures. A1 showed atypical results for *Field* and *Extreme* exposure. For instance, bleeding tends to increase for the mixture with the material in *Field* exposure, while for the mixture in the *Extreme* exposure bleeding remains similar to the initial value during the first 7 days and continues to slightly increase up to 14 days of exposure. This effect is attributed to the changes that the admixture underwent during exposure; recall that for *Extreme* exposure a layer formed in the surface of admixture A1, which protected the material underneath.

The amount of bleed water collected for the admixture A2 samples generally increased with exposure time for mixtures in both *Field* and *Extreme* exposures. These results were expected because the viscosity decreased with exposure time, making the sedimentation of larger particles easier, which would increase bleeding.

The amount of bleeding for mixtures containing admixture A3 remained consistent during the exposure interval. For both *Field* and *Extreme* exposures, the material was not fit to use after seven days of exposure.

Figure 8-17 shows bleeding results for admixtures under *Control* exposure. Ageing under *Control* exposure slightly increased bleeding with exposure time for admixtures A1 and A2. Admixture A3 showed a 0.1ml decrease in the amount of bleeding at 28 days relative to the amount of bleeding at 0 days of exposure. Results of all admixtures indicate that there was essentially no deterioration for the *Control* exposure during the testing period.

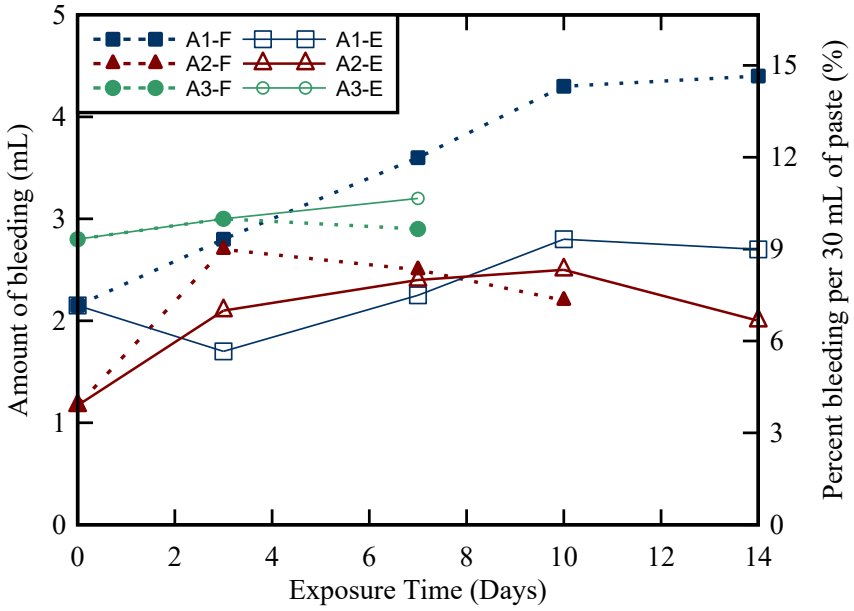

Figure 8-16 Bleeding results for all admixtures during both *Field* and *Extreme* exposure

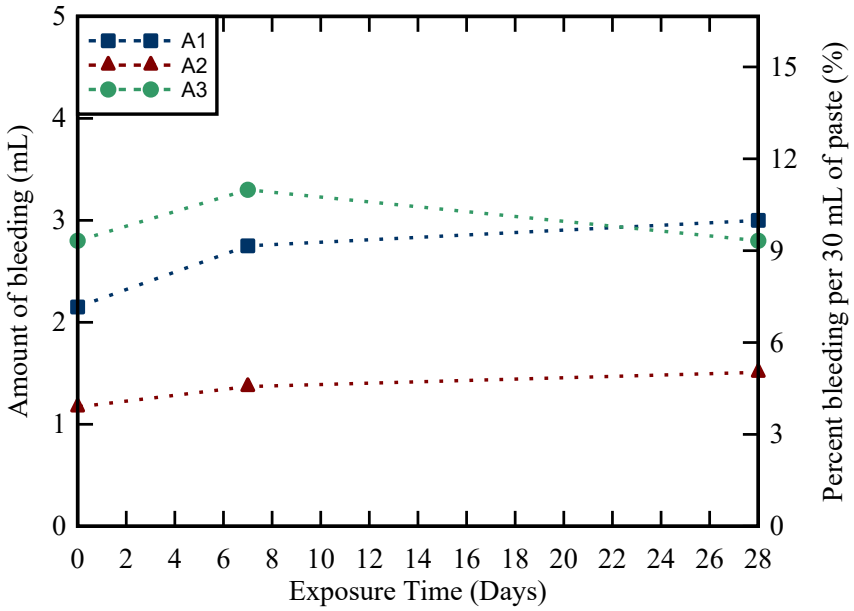

Figure 8-17 Bleeding results for all admixtures during *Control* exposure

9 Heat of Hydration

9.1 Summary of Test Method

Heat of hydration is the heat generated due to the exothermic chemical reactions that takes place when portland cement and water are mixed. Heat release starts from the moment water is added to the cement powder and can continue for years as a result of the hydration process.

The method commonly used to measure the heat of hydration of a material is called isothermal calorimetry. Isothermal calorimetry consists of capturing the heat production of a sample by measuring the thermal power (or heat flow) conducted between the sample and the heat sink. A reference sample of the same thermal mass is necessary to reduce the noise of the measurements. The thermal mass of a sample includes the material of the container (glass) and the sample itself. Reference samples consist of any material that does not generate heat fluctuations such as water, glass beads, or oil.

To determine equivalent thermal masses of PT grout samples and the reference sample, the heat capacity of all samples must be known. The heat capacity of each PT grout was obtained using differential scanning calorimeter (DSC) following the guidelines of ASTM E1269. This technique measures the difference in the amount of energy needed to heat a sample and standard material to a known temperature. ASTM E1269 suggests the use of a standard sample with known heat capacity, such as a sapphire disk.

DSC testing was performed at the FDOT State Materials Laboratory using a Q-20 Differential Scanning Calorimeter manufactured by TA instruments. This instrument was connected to an external refrigerator to control temperature. The first step was to place the material in an aluminum crucible and record the weight with a precision of 0.01 mg. Then, the specimen was placed in the DSC unit. The temperature range was set from 64°F (18.0°C) to 131°F (55°C). Initially, the specimen was held at 64°F (18°C) for five minutes to allow for equilibration of the material. After the initial five minutes, the sample was heated at 36°F/min (20°C/min) until reaching 131°F (55°C). To compute the heat capacity, the heat flow is plotted against temperature (Figure 9-1), and then, Equation 1 is used to calculate the heat capacity at a specific temperature.

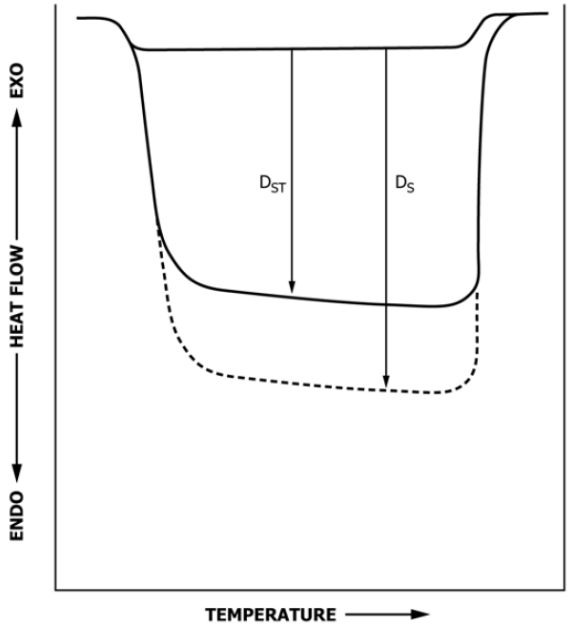

Figure 9-1 Heat flow curves of empty holder, sapphire disk, and specimen.

$$C_p\,(s) = C_p(st) \cdot \frac{D_s \cdot W_{st}}{D_{st} \cdot W_s} \qquad \text{Equation 1}$$

Where:
$C_p\,(s)$ = specific heat capacity of the specimen (J/g·°C)
$C_p\,(st)$ = specific heat capacity of the standard (sapphire) (J/g·°C)
D_s = Vertical displacement between the specimen holder and the specimen (mW)
D_{st} = Vertical displacement between the specimen holder and the sapphire standard (mW)
W_s = mass of specimen (mg)
W_{st} = mass of sapphire standard (mg)

This procedure was used to determine the specific heat of all PT grouts. Figure 9-2 shows the specific heat curve for the PT grouts and the sapphire disk from 68°F (20°C) to 113°F (45°C). For isothermal calorimetry, the temperature of interest was at 73.4°F (23°C). Specific heat values for all PT grouts varied from 0.71 to 0.86 as listed in Table 9-1. The mean values are the result of three replicates, with a maximum coefficient of variation of 5.43% in PT7.

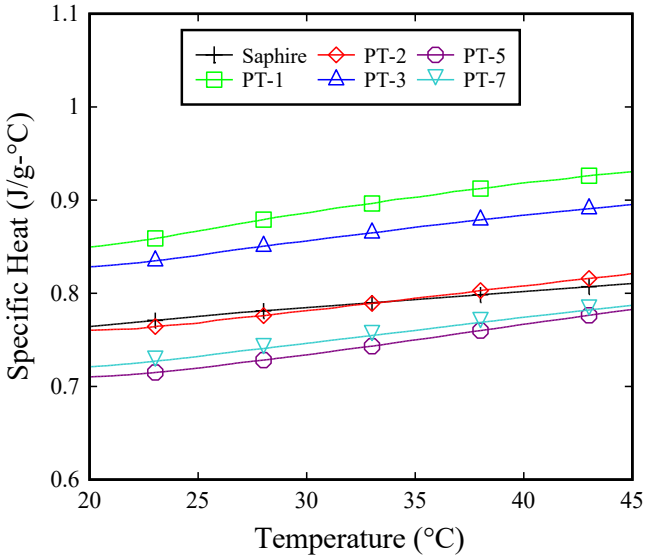

Figure 9-2 Specific heat curves for all PT grouts

Table 9-1 Specific heat values for all PT grouts.

Specific Heat at 73.4°F (23°C)		
Material	Mean	% Coefficient of Variation
Sapphire	0.77	NA
Duratherm	1.92	NA
Water	4.13	NA
Glass	0.68	NA
PT1	0.86	4.09
PT2	0.76	4.36
PT3	0.83	1.74
PT5	0.71	5.40
PT7	0.73	5.43

Heat of hydration of all PT grouts was measured for both *Field* and *Extreme* exposure. For exposure purposes, PT grout samples of approximately 400 g were placed in small containers (Figure 9-3). The small containers were then placed in the environmental chamber and tested at 3, 7, 10, and 14 days of exposure. To accommodate equipment scheduling, some of the samples were removed from exposure on the specified day and were placed in a freezer until the calorimeter became available.

ASTM C1702 prescribes the steps for isothermal calorimetry test of a cementitious mixture of known w/c. For the purpose of this project, w/s (water-to-solids) was used in the analysis because the cement content of the commercial PT grout blends used in this study was unknown. The w/s used in the mix designs corresponded to 1.15 times the recommended dosage of water by the respective manufacturer.

ASTM C1702 allows either internal or external mixing. Internal mixing consists of placing the cement and water in the calorimeter separately and allowing the materials to reach equilibrium at the desired temperature. Cement and water are then mixed manually inside the

calorimeter. Mixing time and velocity are specified by the operator and should be consistent for all mixtures. Best results are obtained when the same operator performs the mixing for all mixes. One drawback from internal mixing is that it is impossible to verify that the materials have been mixed thoroughly as no visual verification can be made until the end of the test.

External mixing can be performed by several methods such as hand mixing, overhead mixing, vacuum mixing or high shear mixer. For the purpose of this project high-shear mixing (Figure 9-4a) was selected because it provides similar mixing energy to that of a full-scale grout plant. High shear mixing procedures were adopted from ASTM C 1738, which are described in Appendix F.

After mixing the grout, the next step was to place the specified mass of paste in the glass vial. The paste in the glass vial was weighed to an accuracy of 0.1 mg (Figure 9-5) in Mettler-Toledo analytical balance with 0.01 mg precision. Once the desired mass was obtained, the glass vial was sealed and placed in one of the "A" channels in the calorimeter (Figure 9-6). The reference sample of same thermal mass was placed in the "B" channel, and was not removed from the calorimeter until test termination.

Figure 9-3 Small containers used for exposure in the environmental chamber

(a) (b)

Figure 9-4 High shear mixing method: (a) High shear mixer and (b) PT grout after mixing

Figure 9-5 Weight of PT grout for isothermal calorimetry

Figure 9-6 Isothermal calorimeter

9.2 Results and Discussion

Isothermal calorimeter results are presented as the thermal power and the cumulative heat of the sample after 70 h. All results were normalized to the total mass of solids because the percent of cement was unknown. Also, the time of testing was adjusted to incorporate the time between the start of mixing and when the sample was placed in the calorimeter. The initial peaks of the thermal power curves occurred within the first two hours and were due to the heat flow driven by the initial temperature differential between the sample and the standard. Recall that with the external mixing method, the initial heat released due to the dissolution of the cement with water is not captured. To obtain the total cumulative heat, the thermal power curve was integrated over time.

All PT grouts have multiple constituents and varying water dosage requirements, which will cause differences in the final w/s. Therefore, analysis of results will be focused on the effect of the exposure to the PT grout rather than a direct comparison of PT grouts. Heat of hydration results will provide an understanding of the effect of exposure on the characteristics of the portland cement reactions. Unfortunately, the effect of admixtures in terms of retardation or acceleration of setting was unable to be investigated due to the unknown admixtures used in each PT grout prepackaged blend. Wang et al. (2006) and Scrivener and Nonat (2011) suggest that initial and final set occur during the accelerating phase (Figure 9-7). Initial set occurs at the beginning of the accelerating phase and final set near the peak rate (slope) around the inflection point. Measured heat of hydration can also be used to predict compressive strength of concrete mortar within 10% accuracy (Bentz et al., 2012). Also, compressive strength is proportional to maturity, and maturity can be estimated by the percent of cumulative heat at a given age (degree of reaction).

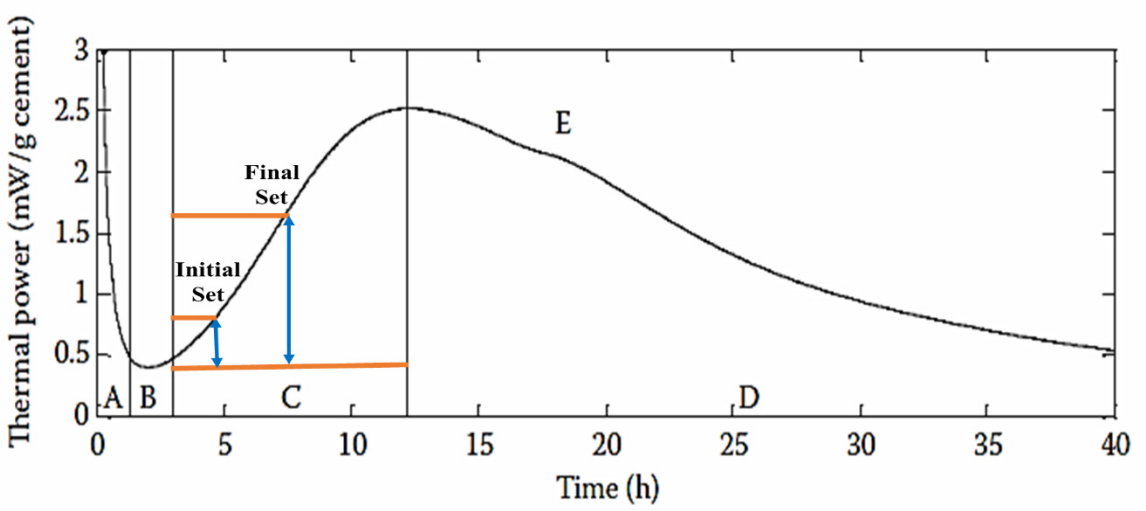

Figure 9-7 Cement hydration phases: Four cement hydration phases: A – initial period; B – induction period; C – accelerating period; and D – decelerating period. E is the sulfate depletion peak. (Scrivener and Nonat 2011)".

The curve in Figure 9-7 will serve as a benchmark for comparison and evaluation of the results of the heat of hydration test results on the PT grout samples. Variations are expected in the heat curves from those shown in the benchmark because the PT grouts contain materials other than portland cement, such as SCMs and admixtures. Furthermore, standard external mixing methods for cement pastes call for hand mixing, overhead mixing, vacuum mixing, or high-shear mixing. For the PT grout tests, high-shear mixing was recommended due to the high mixing energy that obtained from the use of a full-scale grout mixing plant in the *Field*. This mixing method can result in an acceleration of the hydration reactions. Steps were taken, however, to maintain the consistency of sample preparation including: (a) maintaining the temperature of the paste at 73.4°F (23°C) by using a water bath to control the heating effects of high-shear mixing, and (b) limit the time between the end of mixing and of placing the sample into the calorimeter to 20 min.

PT1 results (Figure 9-8) show a marked decrease in the thermal power peak (or degree of reaction) for all exposed samples compared to the unexposed samples. This was expected as the degree of reaction decreases with an increase in particle size, and less cementitious material to react due to prehydration; this will be further discussed in the particle size analysis section. It was also observed that for the exposed samples the accelerating stage of hydration shifted up to 11 hr. compared to those of the unexposed samples. This difference can be attributed to the delay in water reaching unhydrated material in prehydrated cement particles, or due to chemical changes occurring in the admixtures during prehydration, which can affect the reaction kinetics. In terms of hydration phases shown in Figure 9-7, the induction period increases with exposure, which indicates an apparent delay of the accelerating phase or setting.

Figure 9-9 shows cumulative heat measured over the first 70 h of heat of hydration test duration. The cumulative heat curves for the exposed samples shows a delay of approximately 10 h compared to the unexposed samples. By 24 h, the unexposed sample had released about 70% of its total heat, whereas the exposed samples had only released about 20% of their total heats. Deterioration of the PT grouts due to exposure not only delayed the hydration reaction,

but also reduced the total amount of material that had reacted during the 70-h test time. This reduction ranged from 19% to 28%, depending on the exposure conditions (Table 9-2).

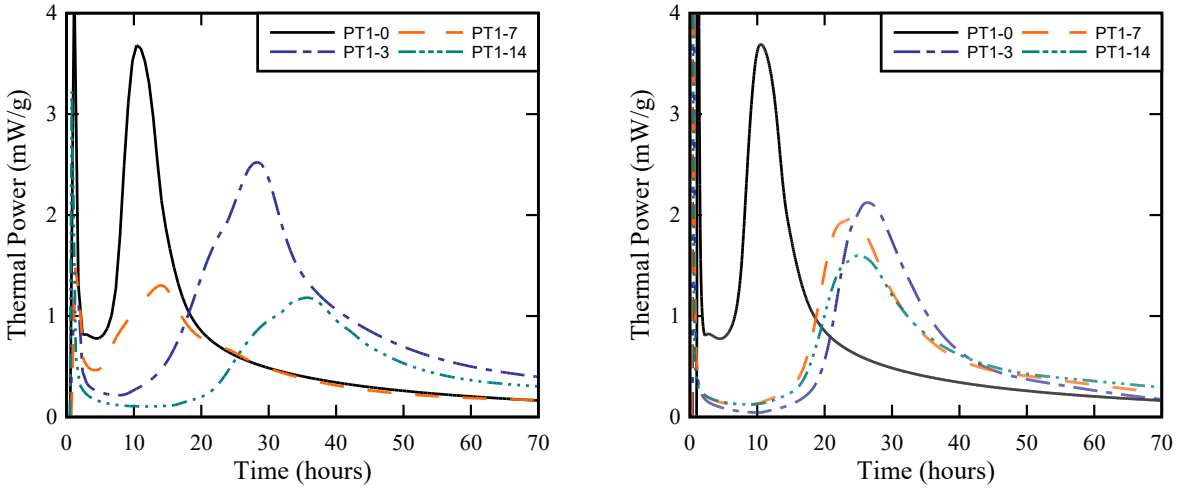

Figure 9-8 Heat flow curves for PT1: (a) *Field* exposure; (b) *Extreme* exposure.

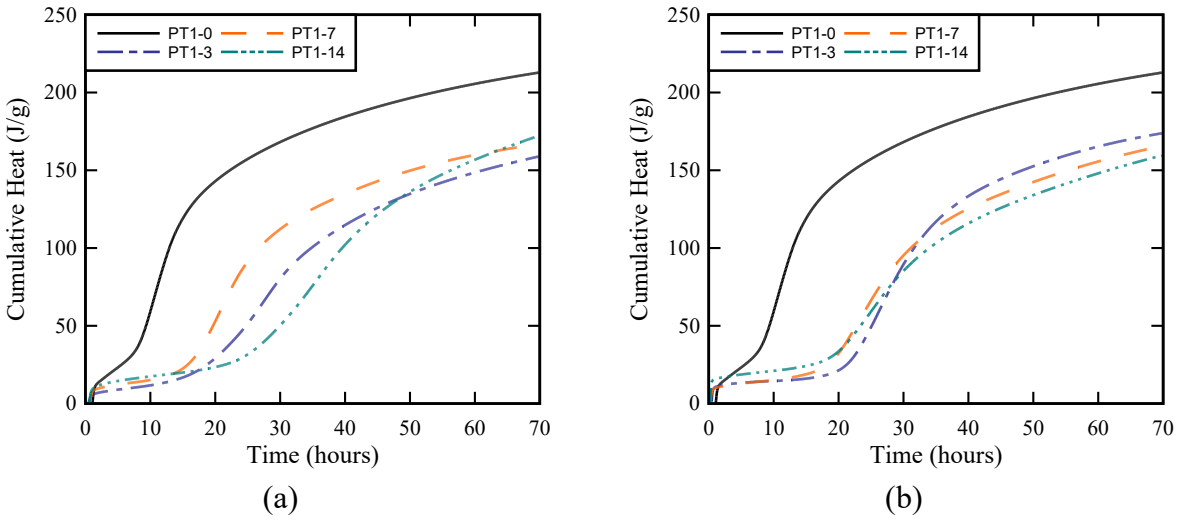

Figure 9-9 Cumulative heat curves for PT1: (a) *Field* exposure; (b) *Extreme* exposure.

Table 9-2 Reduction in cumulative heat after exposure

Material	Unexposed Cumulative Heat	Minimum Reduction (%)	Maximum Reduction (%)
PT1	214	19	28
PT2	195	10	44
PT3	219	8	37
PT5	154	6	49
PT7	211	4	67

PT2 grout thermal power curves for both exposure conditions are shown in Figure 9-10. PT2 results also show a decrease in the intensity of the thermal power peak, which decreases to 1.3-1.5 mW/g for exposure times of 7 and 14 days. Peaks of the power curves for the unexposed and exposed samples occur at similar times, except for the 3-day exposure peak, which was delayed by 6 h-7 h. Different behavior among PT grouts was expected as each PT grout has unknown quantities of constituents.

Figure 9-11 shows cumulative heat of PT2 measured over the first 70 h of heat of hydration testing. The cumulative heat curves of the *Field* exposed samples showed a delay in the cumulative heat increase. The *Extreme* exposure cumulative heat profiles show similarly shaped cumulative heat curves, irrespective of the exposure time. The delay difference between *Field* and *Extreme* exposure curves can be attributed to the percent of cement present in PT2. Recall that during exposure, prehydrated cement forms a crust layer in the surface due to hydration products formed by the reaction of cement and moisture in the air. Therefore, during *Extreme* exposure, the prehydrated crust would be expected to form more rapidly due to higher moisture content and larger percentage of portland cement. If the crust layer in the surface is rapidly formed, it can then serve as protection for the cement particles under the layer; however, the crust layer will continue to react with the moisture in the air. Prehydration of the portland cement is expected to reduce the total amount of unreacted material, which would reduce the total heat generated during the 70-h test time. The reduction of total heat is expected to be greater in the *Extreme* exposure than the *Field* exposure because the higher level of moisture in the air will result in the formation of more hydration products during hydration. This resulted in a decrease of cement available to react during calorimetry test. The reductions in total heat ranged from 10% to 44%, depending on the exposure conditions (Table 9-2).

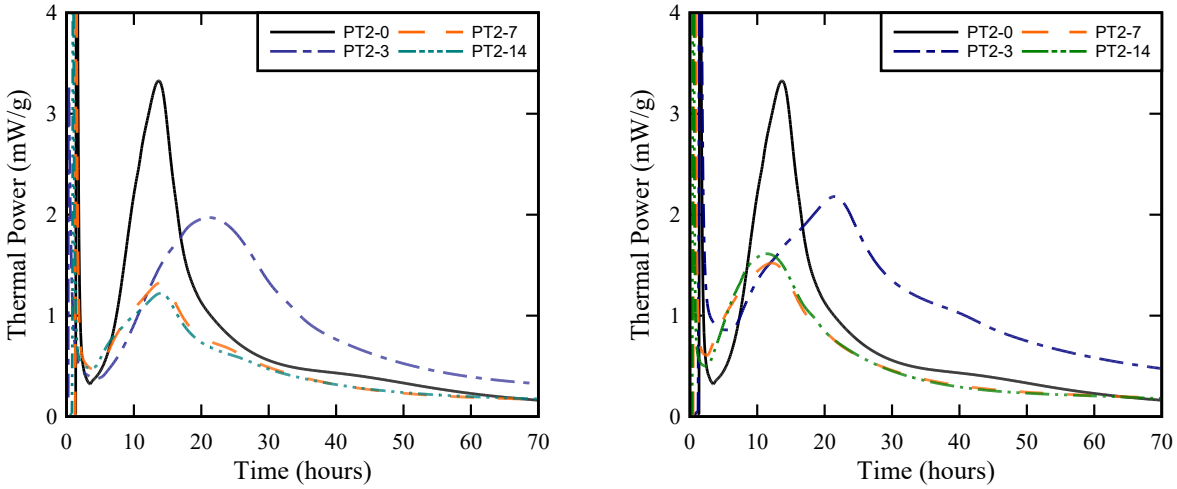

Figure 9-10 Heat flow curves for PT2: (a) *Field* exposure; (b) *Extreme* exposure.

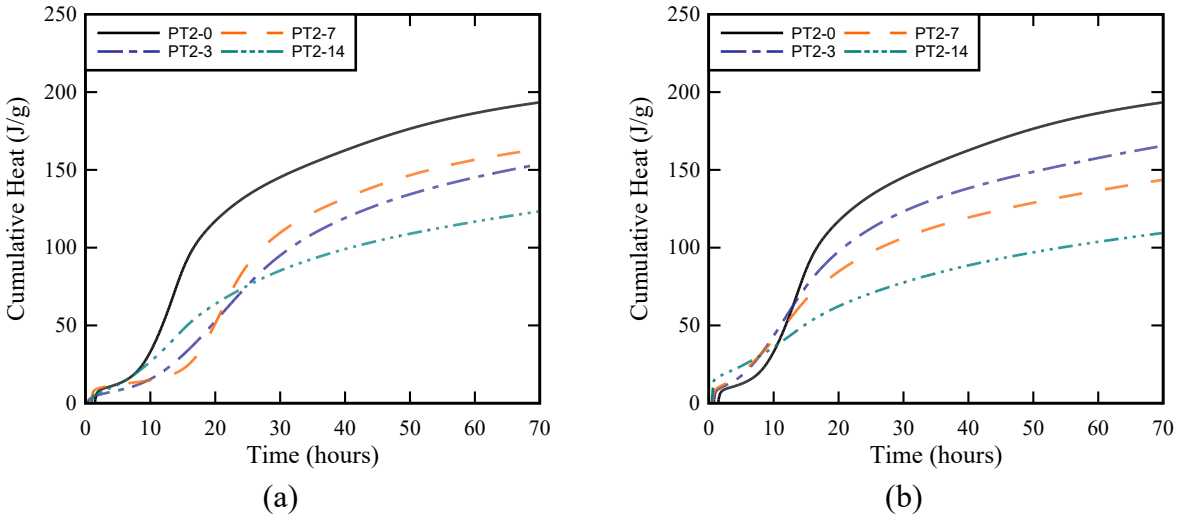

Figure 9-11 Cumulative heat curves for PT2: (a) *Field* exposure; (b) *Extreme* exposure.

PT3 grout thermal power curves for both exposure conditions are shown in Figure 9-12. It was found that PT2 and PT3 had similar results for the unexposed samples, which was expected considering that PT2 and PT3 are manufactured by the same manufacturer and likely had similar formulation and constituents. PT3 thermal power peaks occurred earlier for the *Extreme* exposed samples than the unexposed sample. Similar behavior was observed for PT2 samples, except for the 3-day exposure samples.

Figure 9-13 shows cumulative heat of PT3 measured over the first 70 h of heat of hydration testing. The reduction in heat for PT3 ranged from 8% to 37% depending on the exposure conditions (Table 9-2).

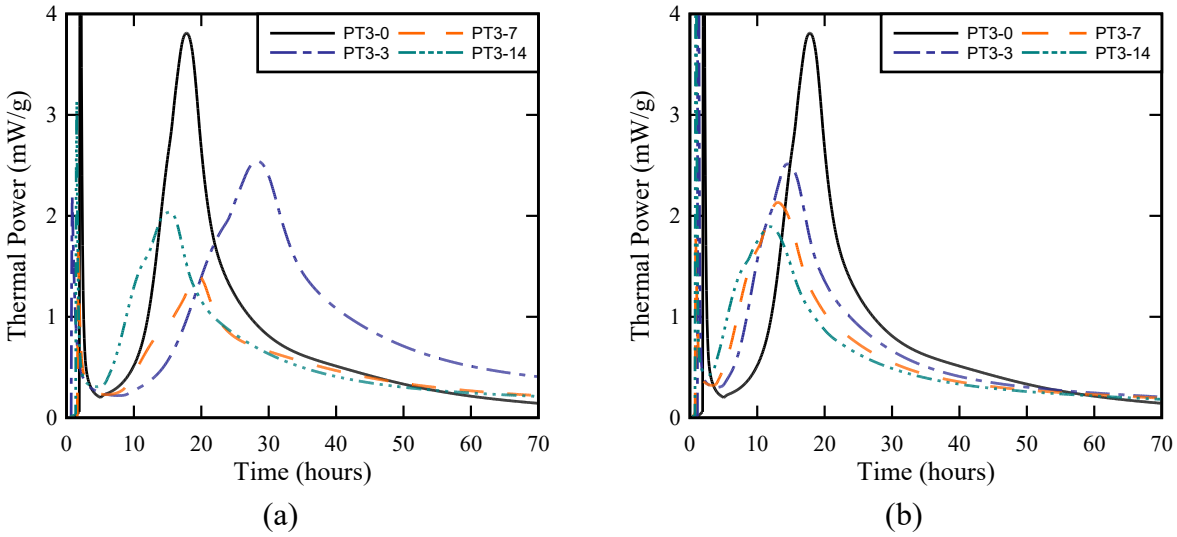

Figure 9-12 Heat flow curves for PT3: (a) *Field* exposure; (b) *Extreme* exposure.

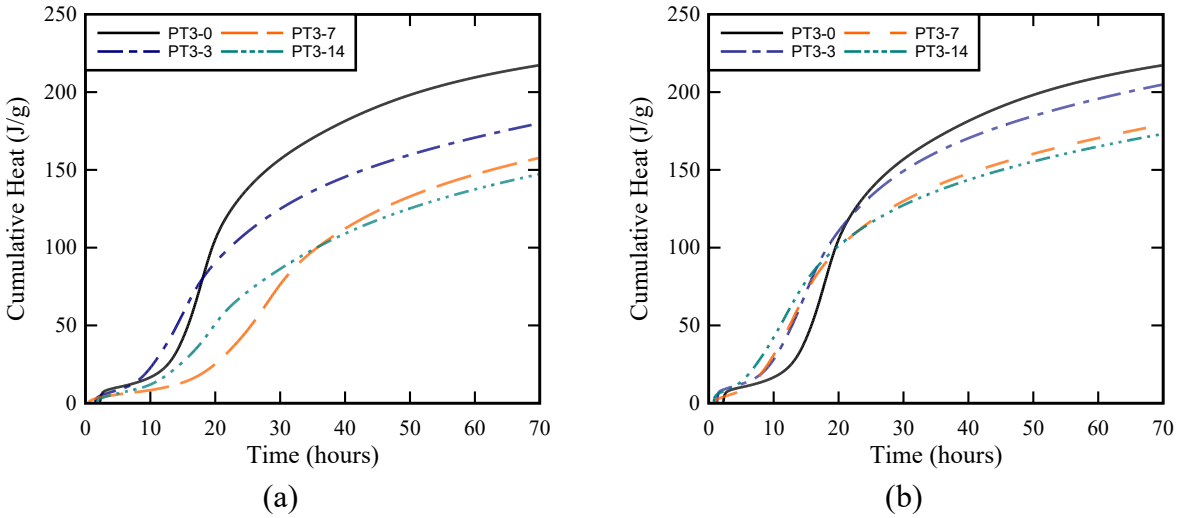

Figure 9-13 Cumulative heat curves for PT3: (a) *Field* exposure; (b) *Extreme* exposure.

PT5 results (Figure 9-14) also showed a marked decrease in peak thermal power for exposed samples compared to the unexposed sample. Also, in most cases the exposed samples exhibited long induction periods. The slope of the increasing-heat-flow leg of the main hydration peak was also considerably reduced as time of exposure increased. The deceleration period shows a lower slope, indicating a higher thermal power for the entire deceleration phase when compared to the unexposed material, as the cement in the unexposed grout has already reacted at that point.

Figure 9-15 shows cumulative heat of PT5 measured over the first 70 h of heat of hydration testing. PT5 shows similar results to PT2 and PT3 with higher reduction in total heat

during *Field* exposure than *Extreme* exposure. Similar to PT3, it is thought that the difference in total heat between *Field* and *Extreme* exposures was a result of the protective crust formed by the prehydrated cement. Exposure of PT5 grout resulted in an increase of the total amount of material that was unreacted, resulting in a reduction of total heat produced during the 70-h test time for *Field* Exposure. Alternatively, during *Extreme* exposure the 3-, 7-, and 14-day curves were very similar. This reduction in cumulative heat ranged from 6% to 49%, depending on the exposure conditions (Table 9-2).

PT7 results (Figure 9-16) showed a marked decrease in the rate of thermal power generation (peak height of power curve) for *Field* exposure samples compared to the unexposed sample. Conversely, for *Extreme* exposure samples, the decrease in the rate of thermal power generation was similar for all exposure times. Results from comparison of the *Field* and *Extreme* exposures were consistent with the formation of a crust layer at the surface that mitigated further penetration of moisture. Isothermal calorimetry results for 14-day *Field* exposure samples showed that the thermal power due to hydration was very low, indicating that the majority of the cement was prehydrated. PT7 grout is thought to have a high percentage of SCMs that may retain moisture and make it available for the portland cement to start prehydration. The cumulative heat curves (Figure 9-17) for the exposed samples show a delay of 5 -10 h compared to the unexposed samples. At 24 h of testing, the cumulative heats of *Field* exposure samples were considerably lower than the unexposed sample or even the *Extreme* exposure samples. The reduction in total heat ranged from 4% to 67%, depending on the exposure conditions (Table 9-2).

So far, the effect of prehydration on cementitious materials has been used to explain the experimental results. However, it is also possible that admixtures contribute to the retarding action observed in most PT grouts after exposure. This is discussed in Chapter 8, Grout Fluidity.

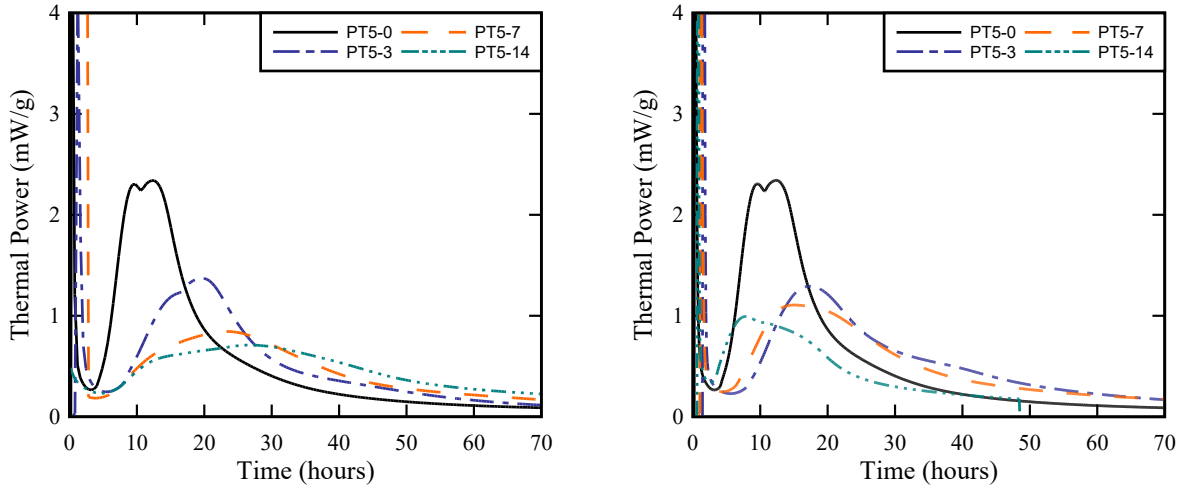

Figure 9-14 Heat flow curves for PT5: (a) *Field* exposure; (b) *Extreme* exposure.

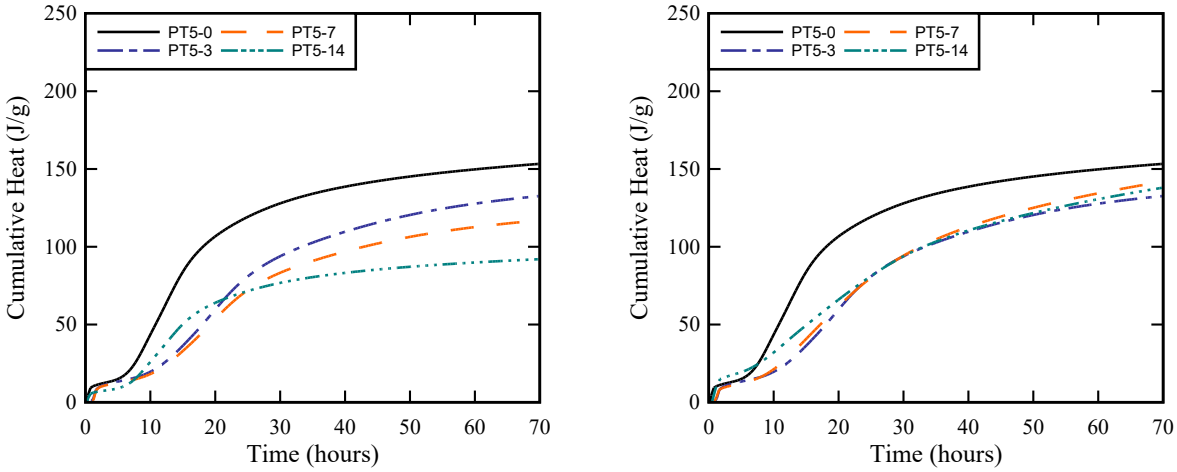

Figure 9-15 Cumulative heat curves for PT5: (a) Field exposure; (b) Extreme exposure.

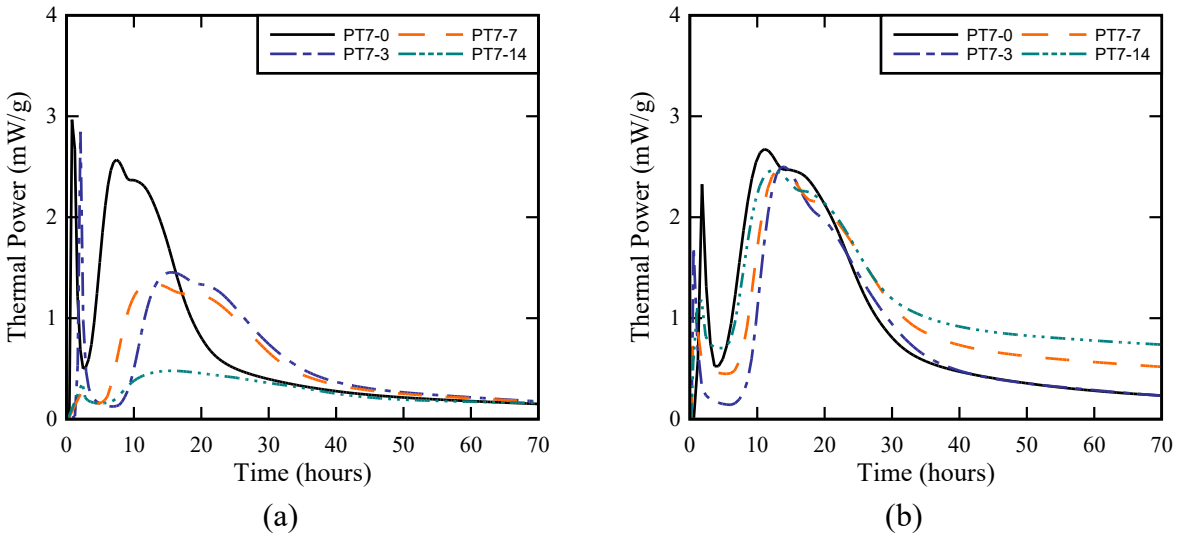

Figure 9-16 Heat flow curves for PT7: (a) *Field* exposure; (b) *Extreme* exposure.

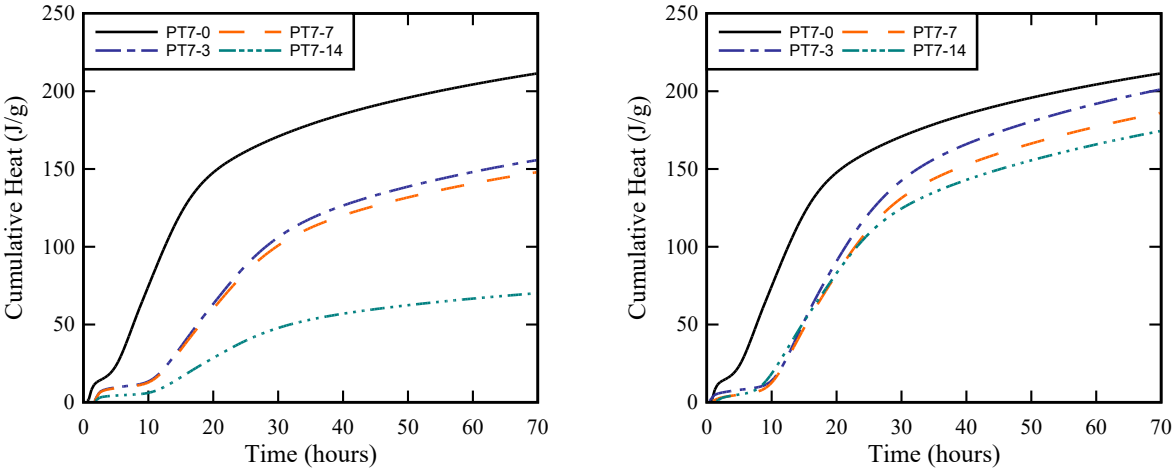

(a) (b)

Figure 9-17 Cumulative heat curves for PT7: (a) *Field* exposure; (b) *Extreme* exposure.

10 Mass Gain

10.1 Summary of Test Method

Mass gain measurement tests were performed in this study to determine the physical mass gain sensitivity of the various PT grouts and cements. Prepackaged PT grouts and portland cement samples were dry-blended using a V-blender prior to preparation of small-scale samples and exposure. Mass gain testing was performed on small-scale samples filled with either PT grout or cements, and were then subjected to a variety of environmental conditions for extended periods of time. For admixtures, the sample containers differed from those used for SCMs. Approximately 50 g of admixture were distributed over the surface of a 4-in. diameter cylinder lid. The mass gain measurements were recorded at intervals of 1, 3, 7, 13, and 14 days. Figure 10-1 shows the small-scale samples filled with PT grout or cement and exposed in an environmental chamber.

Figure 10-1 Small-scale mass gain samples

10.2 Results and Discussion

10.2.1 PT Grout and Cement

Figure 10-2 shows the mass gain from small-scale testing of PT grout exposed to both *Field* and *Extreme* exposures; each point represents the average results from three samples, with an average coefficient of variation of 9.2% and a maximum value of 15.8%. PT grouts exposed for 7 days had an average mass gain of 1.8% for *Field* and 5.7% for *Extreme* exposure, an increase by a factor of 3.2. These results show that more aggressive exposure with heat and humidity resulted in an increase in average mass gain.

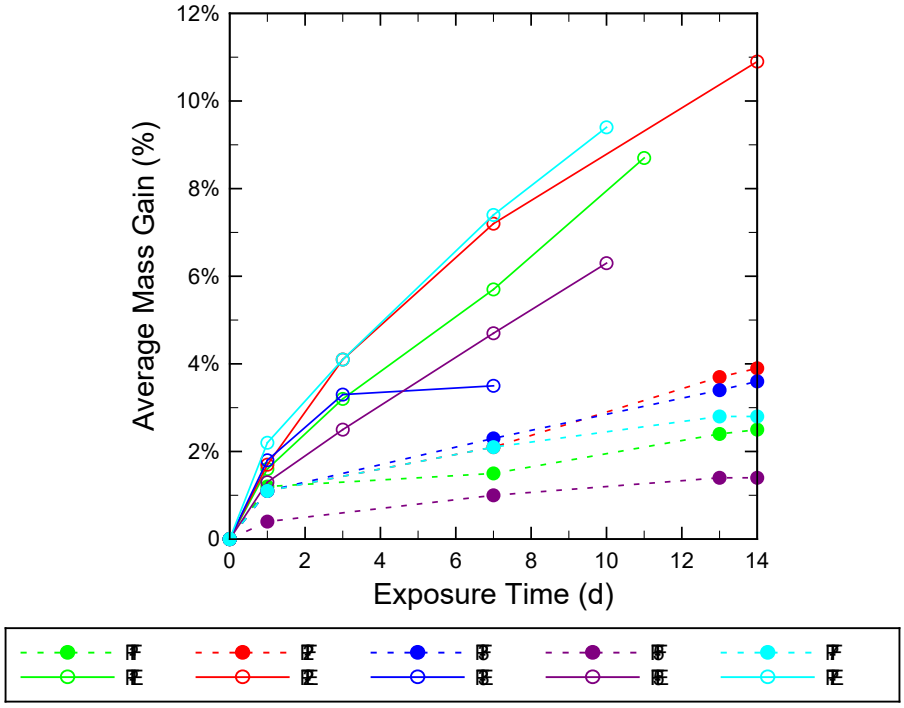

Figure 10-2 Average mass gain from small-scale grout samples in *Field* and *Extreme* exposures

Figure 10-3 shows the average mass gain from small-scale testing of portland cement subjected to the *Field* and *Extreme* exposures. Each point represents the average results from three samples, with an average coefficient of variation of 9.8% and a maximum value of 11.8%. Cements exposed for 7 days had an average mass gain of 1.0% for *Field* and 4.9% for *Extreme* exposures, an increase by a factor of 4.9. These results show that more aggressive exposure with heat and humidity resulted in an increase in average mass gain. Since portland cement is the chief constituent in grout, the trend of increased mass gain in the cement during the *Extreme* exposure suggests the trend in MITT testing in which the PT grouts produced an increased amount of soft grout in the *Extreme* condition may be connected.

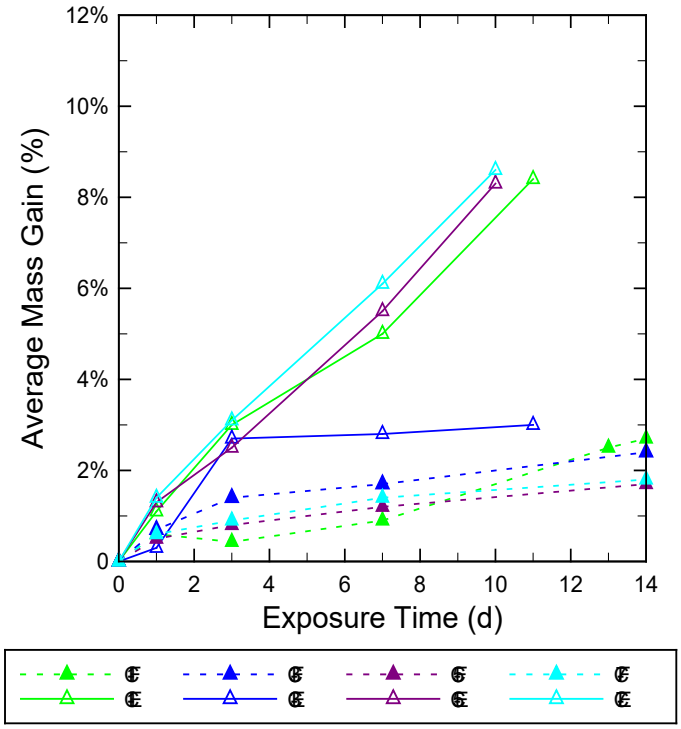

Figure 10-3 Average mass gain from small-scale portland cement samples in *Field* and *Extreme* exposures

Figure 10-4 through Figure 10-8 show the average mass gain, for all four exposures for each of the PT grouts and their corresponding portland cements, plotted separately for clarity. Figure 10-4 through Figure 10-8 show an overall trend, for both grout and cement, where the average mass gains in *Extreme* exposures are greater than those from *Field* exposures.

Figure 10-4 shows the average mass gain of PT1 grout and C1 portland cement during prolonged exposure in the four conditions, with an average coefficient of variation of 13.7%. For *Field* exposure, there were similar mass gains from 14-day exposures for PT1 and C1, with 2.5% and 2.7% respectively. For *Extreme* exposure, there were similar mass gains from 7-day exposures for PT1 and C1, 5.7% and 5.0%, respectively. The data for PT1 and C1 would suggest that most of the mass gain in the grout is driven by the portland cement, which is the chief constituent in the grout. Although, PT1 was not imposed to the *Control* or *Laboratory* exposures, it is the opinion of the researchers that PT1 would exhibit the same mass gain behavior as C1, which was conditioned to these levels. In the *Control* and *Laboratory* exposures, the mass gain sensitivity behavior for C1 was similar in both conditions for 14-day exposure, and showed an average mass gain of less than 0.8%.

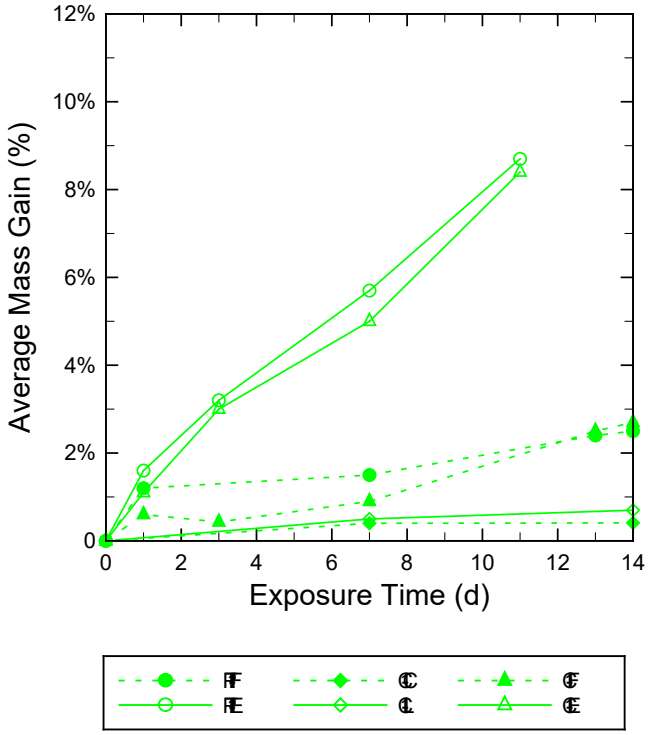

Figure 10-4 PT1 grout and C1 cement average mass gain from small-scale samples in all exposures

Figure 10-5 shows the average mass gain of PT2 grout during prolonged exposure in the *Field* and *Extreme* storage conditions, with an average coefficient of variation of 13.7%. In the *Field* and *Extreme* exposures, PT2 showed the greatest mass gain of any of the five PT grouts tested, with a mass gain peak of 10.9% from the 14-day *Extreme* exposure and 3.8% from the 14-day *Field* exposure.

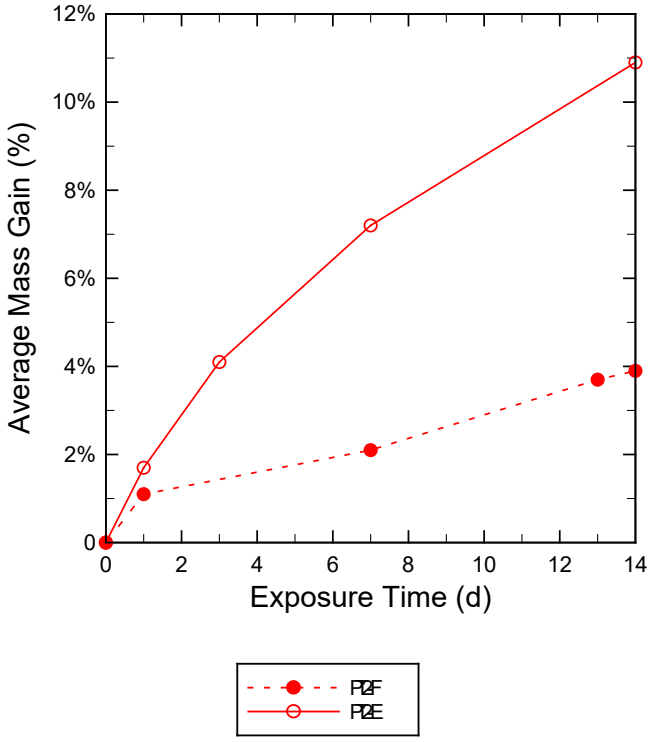

Figure 10-5 PT2 grout average mass gain from small-scale samples in all exposures

Figure 10-6 shows the average mass gain of PT3 grout and C3 portland cement during prolonged exposure in the four conditions, with an average coefficient of variation of 9.5%. For 7-day *Field* exposure, the grout had a greater mass gain than the cement, 2.3% for PT3 and 1.4% for C3. Likewise, for the 7-day *Extreme* exposure, the PT3 grout had a greater mass gain than its corresponding cement, 3.5% and 2.8%, respectively. Although the proportions of the constituents in the grout were unknown in this study, the cement may not be the only material affecting the grout's mass gain behavior. Other SCMs and admixtures in the grout may influence the grout's larger mass gain than that of the cement. These constituents may be adversely affected by the *Field* and *Extreme* exposures and, consequently, account for the mass gain difference.

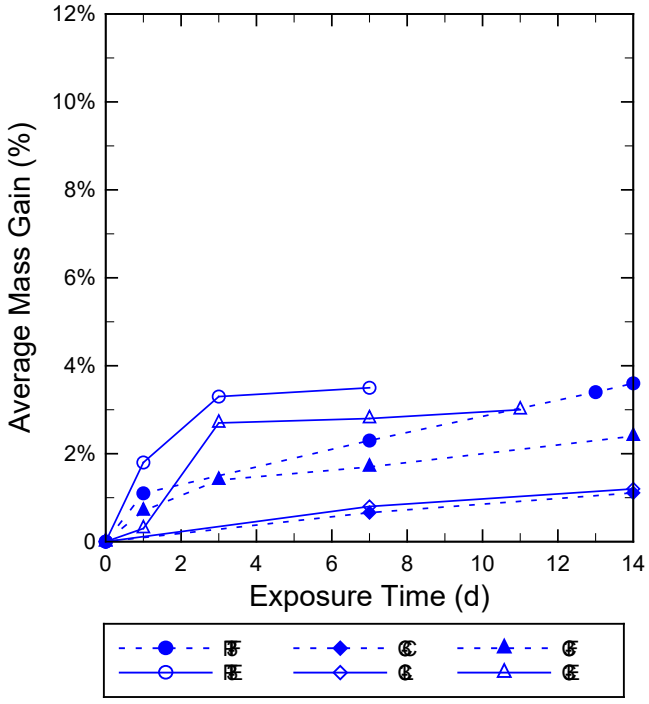

Figure 10-6 PT3 grout and C3 cement average mass gain from small-scale samples in all exposures

Figure 10-7 shows the average mass gain of PT5 grout and C5 portland cement during prolonged exposure in the four conditions, with an average coefficient of variation of 9.2%. For the 7-day *Field* exposure, the mass gains of the PT5 grout and its corresponding cement (C5) were similar, 1.0% and 0.8%, respectively. For the 7-day *Extreme* exposure, the mass gain of the PT5 grout was lower than its corresponding cement (C5), 4.7% and 5.5%, respectively. This occurs in contrast to PT1, PT5, and PT7 grouts, which have similar mass gains to their respective cements.

The general consensus thus far is that the portland cement may account for the bulk of the prehydration mass gain, but other constituent materials, such as SCMs and admixtures, may contribute to the PT grout's mass gain behavior at high temperature and humidity.

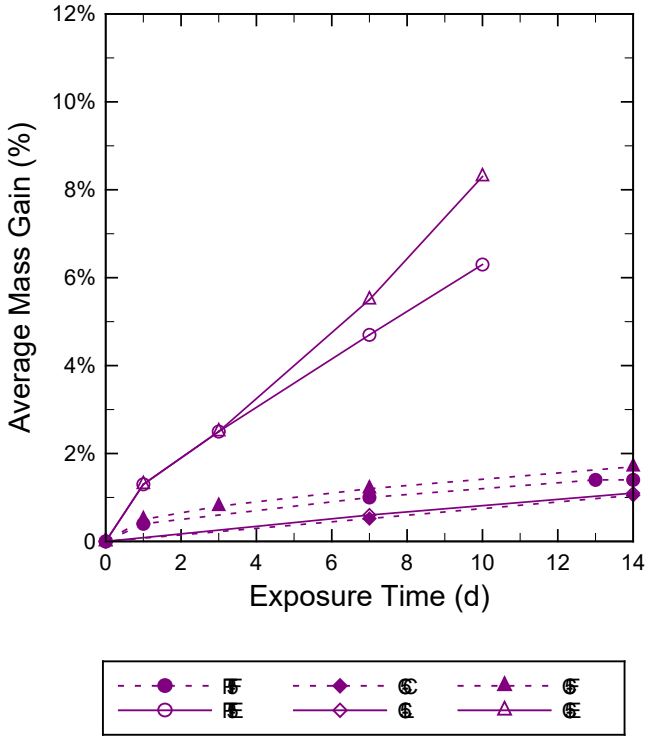

Figure 10-7 PT5 grout and C5 cement average mass gain from small-scale samples in all exposures

Figure 10-8 shows the average mass gain of the PT7 grout and its corresponding portland cement (C7) during prolonged exposure in the four conditions, with an average coefficient of variation of 9.9%. For the 7- day *Field* exposure, the mass gain of the PT7 grout was higher than the mass gain for its corresponding cement (C7), 2.1% and 0.9%, respectively. The mass gain for the 7-day *Extreme* exposure of the PT7 grout was also higher than the mass gain for the C7 cement, 7.4% and 6.1%, respectively.

The *Field* exposure results show that the average mass gains slopes for both the PT7 grout and the C7 cement were parallel between 1 and 14 days exposure. For the *Extreme* exposure results, the sensitivity behavior of PT7 and C7 showed some similarities that would suggest that most of the mass gain in the grout can be attributed to the cement. Overall, PT7 and C7 showed increased mass gain from increased exposure to high temperature and humidity.

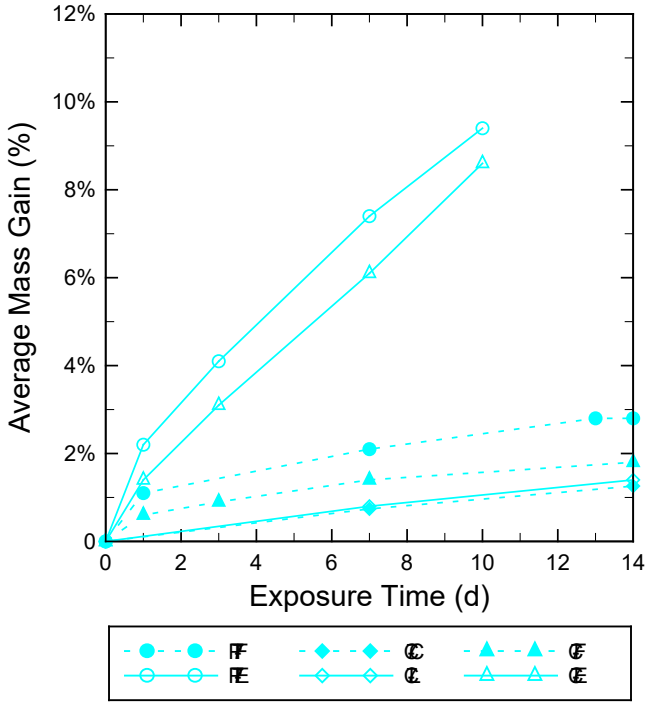

Figure 10-8 PT7 grout and C7 cement average mass gain from small-scale samples in all exposures

Although none of the PT grouts were tested for mass gain or MITT in the *Control* or *Laboratory* exposures, it is the opinion of the researchers that all PT grouts used in this study would generally exhibit similar mass gain behavior as their respective cements under these two conditions. In the *Control* and *Laboratory* exposures at 14-day exposure, the highest average mass gain sensitivities measured for all cements were 0.7% for C1, 1.2% for C3, 1.1% for C5, and 1.2% for C7. All cements showed similar mass gain behaviors below 1.3% in the *Control* and *Laboratory* exposures.

When comparing the *Control* or *Laboratory* to the *Field* and *Extreme* exposures, the mass gains from these exposures were below the *Field* and *Extreme* exposures, which would suggest no soft grout formation would be found from those exposures. This trend shows that the relatively higher temperature and humidity from *Field* and *Extreme* exposures did in fact increase the grouts' susceptibility to the formation of soft grout when compared to the *Control* or *Laboratory* exposures. This finding aligns with the claim that elevated temperature and humidity result in increased levels of mass gain, which indirectly indicated the degree of prehydration in the grout, and that these increased levels of prehydration facilitate the formation of soft grout during MITT.

Overall, the mass gain test method demonstrated that a direct comparison between grout and the portland cement used in the grout mix was not possible due to different mass gain rates between grouts mixes. Mass gain rates are dependent of the type and amount of SCMs and admixtures in the grout mix. Cements and grouts tested in the *Extreme* exposure had higher mass gains compared to the *Control, Laboratory* or *Field* exposures. The increased mass gains in the *Extreme* exposure may be associated with the prehydration of the different cement phases in the cement or SCM used in the grout. As described in the background chapter, the different

cement phases in the cements have known reaction sensitivities to high temperature and humidity, which would support the increased mass gain in the *Extreme* exposure compared to the *Field* exposure, and the reduced mass gain rates at the *Control* and *Laboratory* exposures.

10.2.2 SCMs

Figure 10-9 shows the mass gain from small-scale testing of SCMs subjected to both *Field* and *Extreme* exposures; each point represents the average results from three samples. These results show that the more aggressive exposure resulted in an increase in average mass gain for all SCMs. In general, the rate of mass gain of most SCMs reduces significantly after 3 days of exposure, indicating that the surfaces of these particles are approaching their equilibrium adsorption at the specific temperature and relative humidity. The extended higher rate of adsorption shown by the class C fly ash in the *Extreme* exposure condition is likely due to hydration of hydraulic cementitious phases present in the as-received material. The difference between *Field* and *Extreme* results was at least 0.5% after three days, and continued to increase substantially as exposure time increased. This is consistent with a higher equilibrium adsorption due to exposure to a higher temperature and relative humidity.

The reactivity of SCMs exposed only to moisture is known to be low, so mass gain will be primarily controlled by specific surface area of the loose material. For instance, silica fume (SF) has the highest specific surface area at approximately 17,000-17,500 m^2/kg (BET), which then results in the highest moisture adsorption compared to the other SCMs. The specific surface areas of class F fly ash (FAF) and slag (S) using Blaine Fineness have been reported to be about 200 m^2/kg and 300 m^2/kg, respectively. Based on the specific surface and mass gain data, the differences in mass gain between SF, FAF, and S were attributed to the higher surface area of SF. Finally, class C fly ash (FAC) had the highest mass gain among all SCMs and did not approach a stable state. This is attributed to the presence of hydraulic cementitious materials that hydrate in the presence of water.

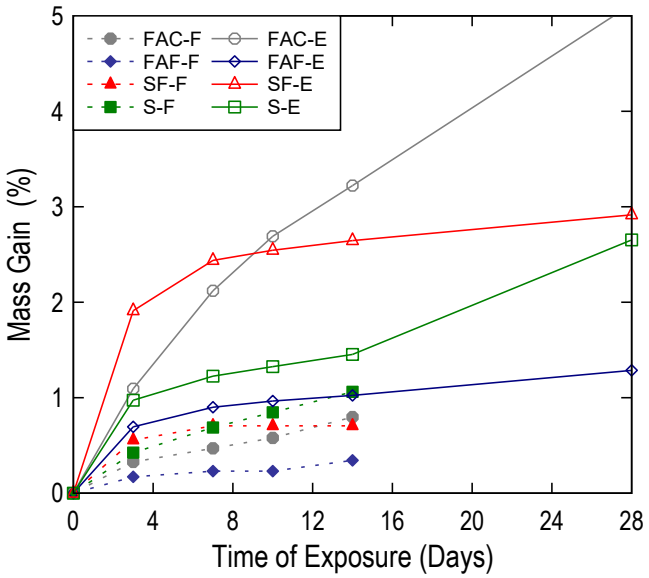

Figure 10-9 Mass gain results for all SCMs during both *Field* and *Extreme* exposures

10.2.3 Admixtures

Figure 10-10 shows the mass gain results for the admixtures. In general, all admixtures exhibited an increase in mass of approximately 20%-60% during the first three days of both *Field* and *Extreme* exposures, indicating extreme hydrophilic behavior relative to other PT grout constituents. After the initial seven days, however, the mass gain had become relatively constant. A1 and A2, which are HRWRs, showed the highest mass gain. Furthermore, A1 had a larger difference in mass gain between *Field* and *Extreme* exposures, which agrees with the physical changes that were visually observed in A1 during exposure. For instance, during *Field* exposure, A1 formed a layer on the surface, but the color and consistency remained the same (Figure 10-11a). During *Extreme* exposure, A1 formed a dark yellow solution on the surface of the sample; as exposure continued this solution hardened, which may have protected the underlying sample from further moisture penetration (Figure 10-11b).

A2 showed similar mass gain values for both *Field* and *Extreme* exposures. During the first hours of exposure, the powder started to dissolve with the adsorbed moisture until a transparent solution formed, as seen in Figure 10-12. As exposure continued, a gluey paste formed in the lower part of the container, but was still covered by the transparent solution.

A3 had a lower mass gain during exposure than A1 and A2. Also, this admixture did not exhibit visual signs of changes due to moisture adsorption during exposure.

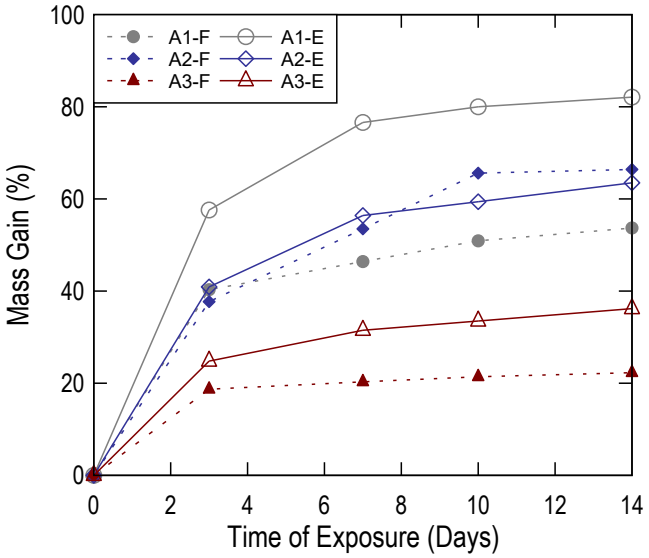

Figure 10-10 Mass gain results of all admixtures for both *Field* and *Extreme* exposures

(a)

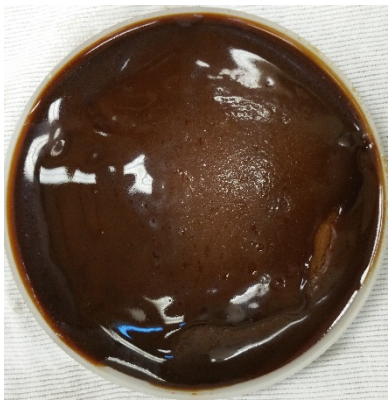

(b)

Figure 10-11 Admixture 1 during exposure: (a) *Field* exposure and (b) *Extreme* exposure

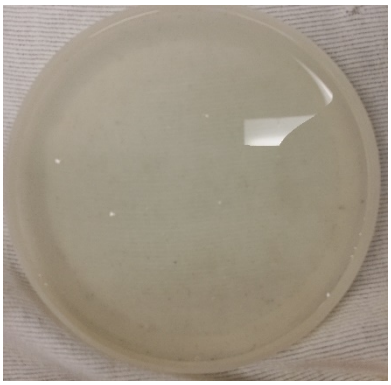

Figure 10-12 Admixture 2 during *Field* and *Extreme* exposures

11 Particle Size Analysis

11.1 Summary of Test Method

Particle size analysis (PSA) tests were performed in this study to determine the change in particle characteristics caused by prehydration of the portland cement and perhaps other SCM components. Particle size measurements were taken for the as-received materials and after exposure to different storage conditions for extended periods of time between zero and fourteen days. This particle size analysis was performed on the dry and wet grout material, portland cement, and SCMs. Testing was done with a Horiba LA-950V2 Laser Scattering Particle Size Distribution Analyzer Figure 11-1. For PT grout and the portland cement, it should be noted that due to severe clumping of the materials during exposure, a No.16 sieve was used to remove relatively large clumps prior to testing in PSA. Sieving was not needed before SCM testing. There was some question regarding the efficacy of sieving the material prior to testing since this action will greatly affect the absolute PSA results. Ultimately, since the absolute PSA results were less important than the change in readings, it was decided to maintain the sample in a relatively undisturbed condition for testing, but to remove agglomerations that would affect the results. In future research, PSA results after homogenization of the complete sample would be interesting and may prove to provide a better before-and-after contrast.

After exposure, an approximately 1-gram sample of the PT grout, cement, or SCM was collected and placed in the Horiba LA-950V2 analyzer along with ethanol as the dispersive solution. Then, the material was homogenized for 2 minutes using the ultrasonic homogenizer inside the analyzer. For densified silica fume, however, a procedure adopted from Gapinski and Scalon (2005) was utilized. Approximately 50 mg of silica fume was placed in a 200-ml beaker with ethanol and three drops of dish detergent to act as a surfactant during external homogenization. A 750-Watt external homogenizer was utilized to disperse agglomerated particles. Most of the agglomerates were soft, being held together by the binder used in the densification process. Some of the agglomerates persisted after homogenization because they were fused together during cooling. Silica fume was then homogenized for 20 minutes and tested in the HORIBA LA-950V2 analyzer.

Figure 11-1 Laser-scattering particle size distribution analyzer

As described in Brunner and Hamilton (2014), whenever light collides with a particle, the particle diffracts the light and scatters the light rays. Using light scattering theory, the scattered

light strength is determined by the particle's diameter and the particle's diffractive index. The HORIBA LA-950V2 first asks the user to input the refractive index of the material being test, then controls the wavelength of the incoming light, and finally, it measures the strength of the scattered light in various directions. With these three pieces of information: 1) refractive index, 2) wavelength of incoming light, and 3) strength of diffracted light in various directions, the computer uses light scattering theory to determine the particle size distribution. The refractive index and imaginary index used for SCM testing are shown in Table 11-1.

Table 11-1 Index values required for laser scattering particle size analysis (Arvaniti et al. 2015 and Ferraro et al. 2017)

SCM	Refractive Index	Imaginary Index
Ethanol	1.36	-
FAC	1.65	0.100
FAF	1.56	0.100
Slag	1.63	0.150
Silica Fume	1.53	0.100

For both MITT samples and small-scale samples, the mixed cementitious material within the container was used for particle size distribution testing in the HORIBA LA-950V2 PSA machine. In the previous study (Brunner and Hamilton 2014), PSA measurements with the Horiba LA-950V2 indicated that the average particle sizes of the grout increased with prolonged *Extreme* exposure. In addition, it was concluded that the particle size change could be tracked over time and may be a useful tool to identify and evaluate the susceptibility to soft grout formation. Figure 11-2 shows that the particle size change measured in this study is directly related to particle surface topochemical hydration, water absorption, and water interconnectivity, which will cause the particles to adhere to one another during hydration. In this study, PSA is further examined as a screening test for soft grout formation; however, the Horiba LA-950V2 Laser Scattering Particle Size Distribution Analyzer is an expensive and somewhat fragile machine that must be used in ideal laboratory conditions.

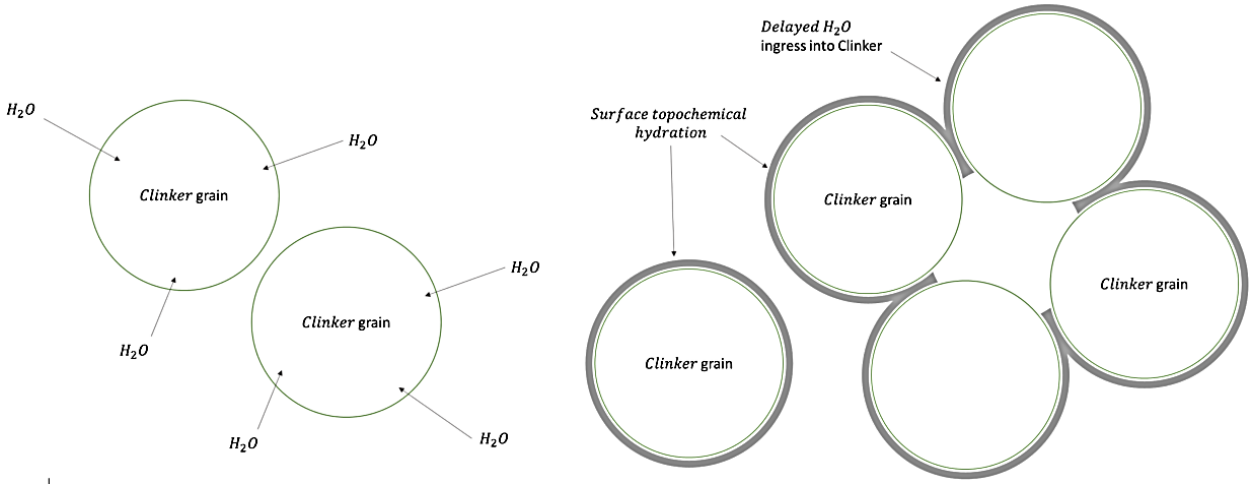

Figure 11-2 Particle size change due to prehydration and water absorption

11.2 Results and Discussion

This section presents the results of laser PSA testing of both cement and PT grout samples using dry and wet methods. Although the tests results provide a distribution of absolute particle size, the research was focused on the assumption that possible changes in particle size are directly related to particle surface topochemical hydration, water absorption, and water interconnectivity, which will cause the particles to agglomerate during hydration. To evaluate the relative particle size change, the mean values from the PSA distribution were normalized to the results obtained prior to initiating exposure (0-day MITT and 0-day small-scale).

11.2.1 Unconditioned Results

Figure 11-3 shows the mean particle size data for all five grouts and corresponding cements prior to exposure (0-day MITT). Figure 11-4 shows the standard deviation of the particle size data for all five grouts and corresponding cements prior to exposure (0-day MITT).

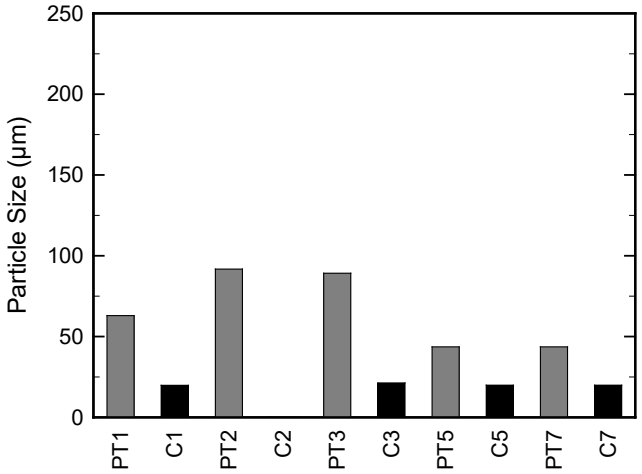

Figure 11-3 Mean particle size data

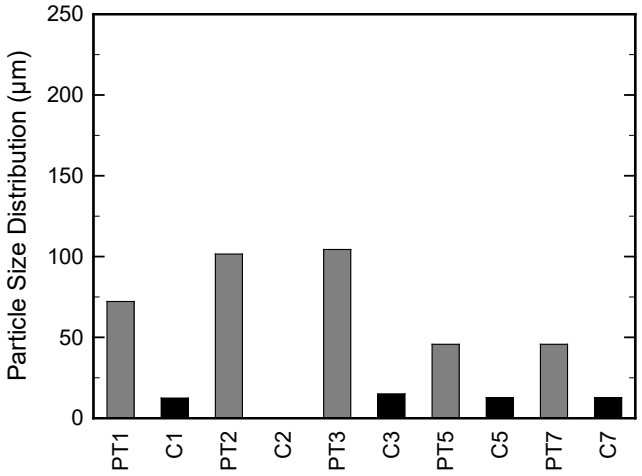

Figure 11-4 Standard deviation particle size data

11.2.2 Grout and Cement Dry Samples

Figure 11-5 and Figure 11-6 show the normalized mean particle size data for PT grout used in MITT, and small-scale samples tested using the dry method, with an average coefficient of variation of 13.6% and a maximum value of 22.7%. The data were normalized such that a value greater than one indicates that exposure caused an increase in mean particle size. *Extreme* exposure increased the normalized mean particle size for all PT grout except PT1. For MITT samples, the largest increase in particle size was 1.25 for PT3 in the *Extreme* exposure at 10 days and for the small-scale samples the largest increase was 2.8 in the *Extreme* exposure at 10 days PT7. Generally, particle size growth was larger under *Extreme* exposure when compared that of *Field* exposure, which supports the claim that particle growth is tied to topochemical hydration of the particle and the expansion associated with that behavior.

MITT samples taken from bags and small-scale samples were expected to exhibit similar particle size growth because the surface-area-to-volume ratios of their respective containers were similar. The small-scale samples, however, generally showed more growth than the MITT samples; the difference in growth may be influenced by the pre-packaged bags, which deter moisture penetration through the bag. Because the bag was not completely open during exposure, moisture penetration was deterred, unlike that of the small-scale sample, which was completely exposed. Also, MITT samples were taken following v-blending the entire bag after exposure, which may have masked the actual particle growth at the surface of the bag. Sensitivity behavior in small-scale PSA testing may provide a conservative approach compared to MITT PSA samples for screening cementitious material's particle size growth associated with prehydration during exposure. Thus, by using small-scale samples, the effects of various packaging techniques used by the manufacturers are removed, which allows a focus on PT grouts sensitivity behavior alone.

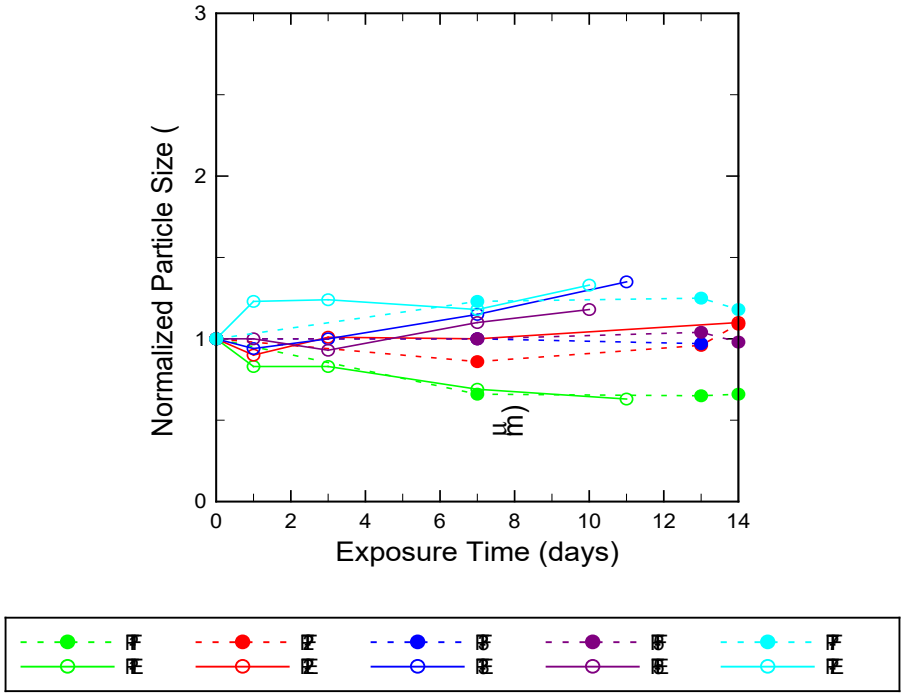

Figure 11-5 Normalized dry PSA mean particle sizes for MITT samples of grout exposed in *Field* and *Extreme* exposures

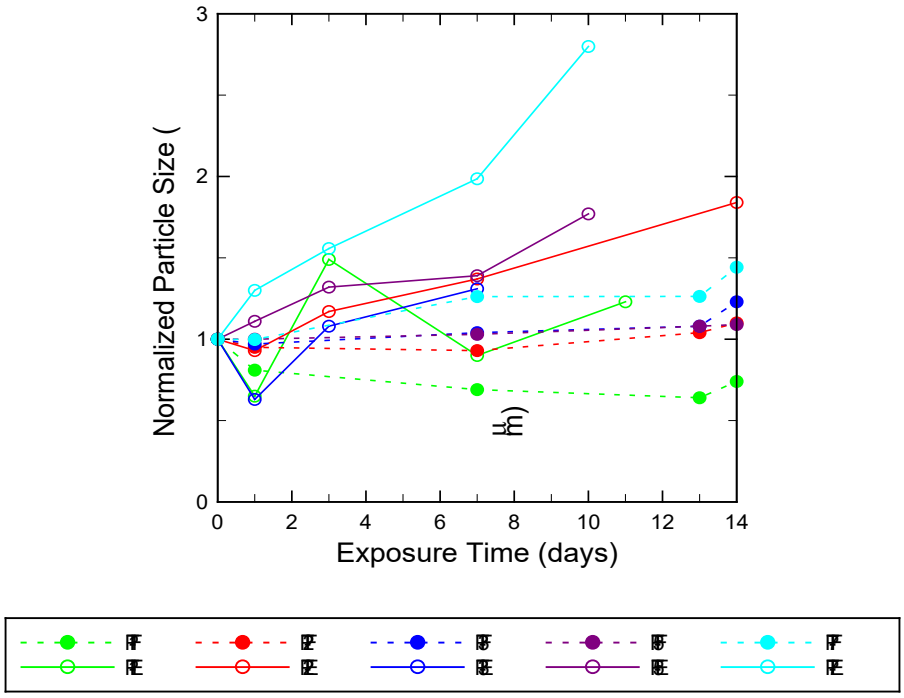

Figure 11-6 Normalized dry PSA mean particle sizes for grouts exposed in small-scale *Field* and *Extreme* exposures

Figure 11-7 shows the normalized mean particle size data of the small-scale portland cement samples under *Field* and *Extreme* exposures with an average coefficient of variation of 5.1% and a maximum value of 12.7%. As the *Field* and *Extreme* exposure period increased, the mean particle size for portland cement also increased. In *Field* exposure, the average normalized mean particle size was 1.09 at 7 days. In *Extreme* exposure, the average normalized mean particle size was 1.69 at 7 days. The largest increase was in C3, where the mean particle size increased by a factor of 2.7 after 7 days of *Extreme* exposure. The smallest increase was in C5, where the mean particle size increased by a factor of 1.04 after 7 days of *Field* exposure.

It is unclear why the change over time in mean particle size of portland cement did not better align with the trend for change over time in mean particle size for the PT grouts displayed in Figure 11-7.

Figure 11-8 shows the normalized mean particle size for portland cement under *Control* and *Laboratory* exposures with an average coefficient of variation of 4.9% and a maximum value of 6.5%. All cements tested had a particle size change below 1.07 at 14 days in both *Control* and *Laboratory* exposures. The reduced particle size growth in cements shown in Figure 11-8, compared to the cements conditioned in *Field* and *Extreme* shown in Figure 11-7, suggests that, as expected, lower temperature and humidity resulted in slower particle growth associated with topochemical prehydration.

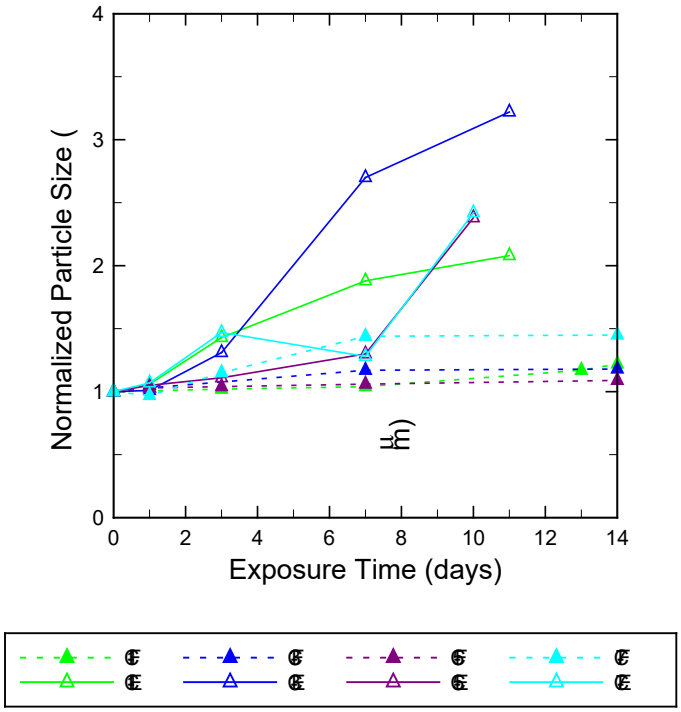

Figure 11-7 Normalized dry PSA mean particle sizes for small-scale portland cements in *Field* and *Extreme* exposures

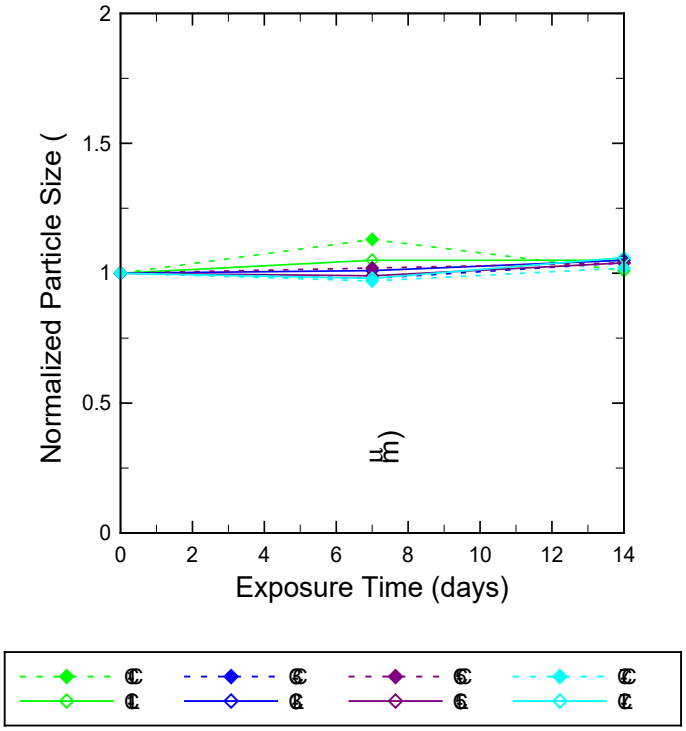

Figure 11-8 Normalized dry PSA mean particle sizes for small-scale portland cements in *Control* and *Laboratory* exposures

11.2.3 Grout and Cement Wet Samples

Figure 11-9 through Figure 11-11 show the wet-PSA, normalized mean particle size data of all PT grouts in MITT and small-scale PT grout and cement samples imposed to the *Field* and *Extreme* exposures at time intervals ranging from 0 to 14 days exposure, with an average coefficient of variation of 7.1% and a maximum value of 10.9%. PT7 showed the greatest normalized mean particle size increase of 4.4 in the 10 days of MITT *Extreme* exposure.

The small-scale PSA wet data from Figure 11-10 and Figure 11-11 did not continue the same upward trend in particle size that the study found in dry PSA. The wet-PSA, small-scale data were sporadic, and no conclusive trends or correlations could be made from the grouts or cements.

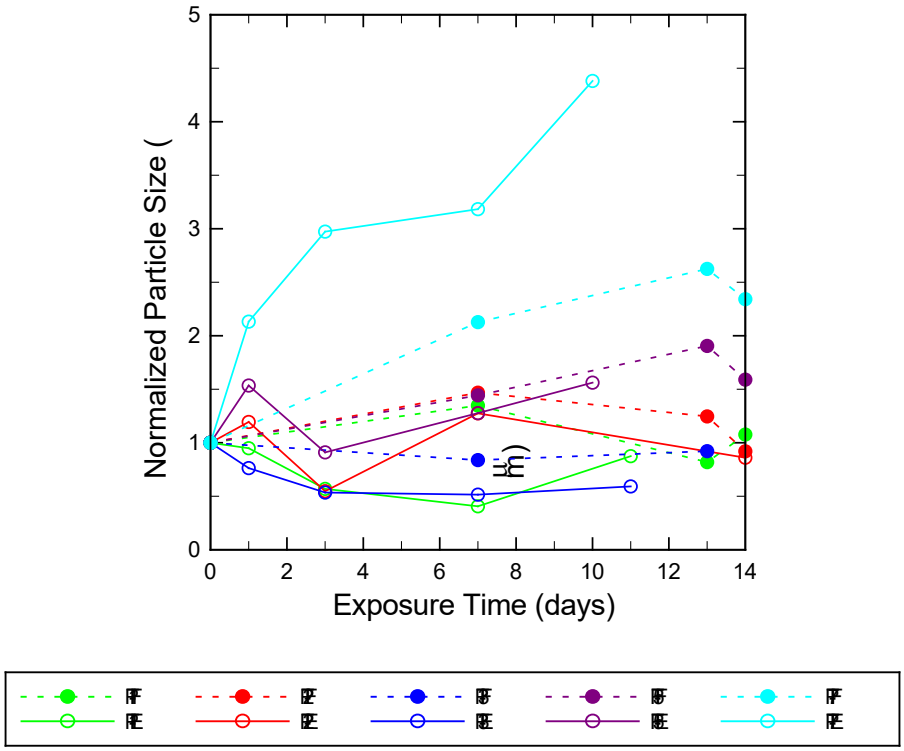

Figure 11-9 Normalized wet PSA mean particle sizes for MITT samples of grout in *Field* and *Extreme* exposures

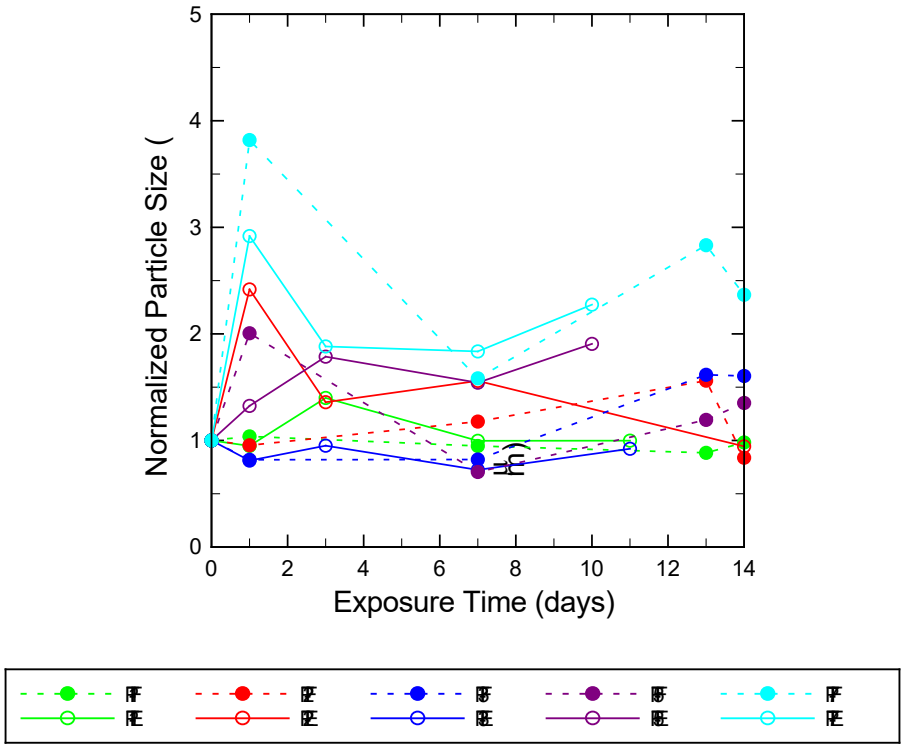

Figure 11-10 Normalized wet PSA mean particle sizes for small-scale grout in *Field* and *Extreme* exposures

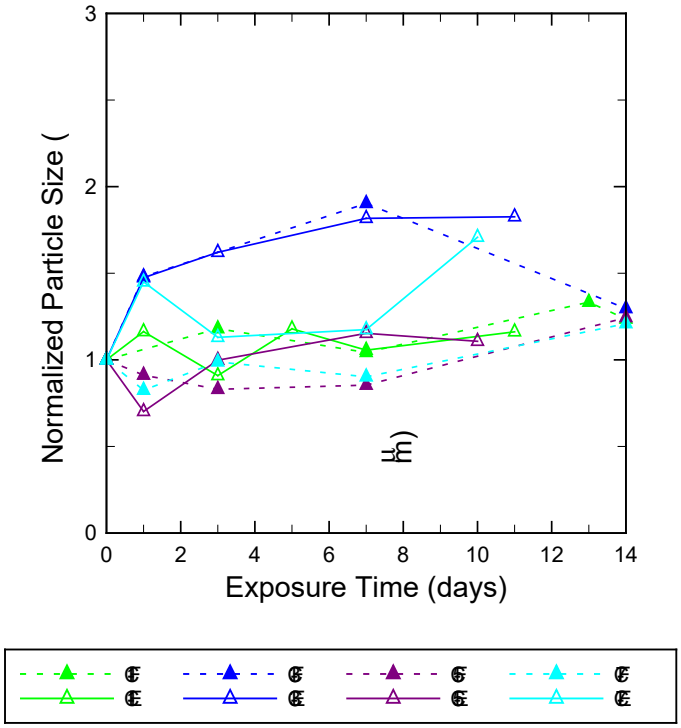

Figure 11-11 Normalized wet PSA mean particle sizes for small-scale portland cements in *Field* and *Extreme* exposures

11.2.4 SCM

Figure 11-12 through Figure 11-15 show the particle size distributions of all SCMs. Overall, SCMs show an increase in particle size with exposure time, with the largest increase for FAC. Increase of particle size occurred due to agglomeration from capillary forces generated by thin films of adsorbed water when particles come into contact with each other. Hydration of any hydraulic cementitious phases can bond contacting particles together, forming hard agglomerates that cannot be easily broken apart by ultrasonic homogenization. This was expected to occur as the chemical composition of slag and FAC have high contents of calcium oxide and silica. For instance, slag and FAC can develop low strengths when mixed with water, and can be used to replace high percentages of cement in concrete. However, the susceptibility of SCMs to increase particle size was lower than PT grout or cement; therefore, the results of SCMs are shown as the entire percent passing distribution curve rather than the normalized mean particle size.

FAC particle size distribution shows a notable increase of particle size at 90% passing (Figure 11-12). For instance, for the unexposed FAC, 10% of the particles were above 10 µm, but after exposure 40% of particles were above 10 µm. Also, the percent of particles under 10 µm decreased from 71% for the unexposed sample to 55% for *Field* exposure and 40% for *Extreme* exposure.

FAF particle size distribution also shows effects due to exposure (Figure 11-13), where it can be observed that the passing percent of particles above 10 µm increased by 8% for *Field* exposure and 5% for *Extreme* exposure. Also, for the unexposed sample 10% of particles were above 26 µm, but after exposure 27% of the particles were above 26 µm, which shows an increase in the number of bigger particles.

Slag (Figure 11-14) shows less variation of particle size due to either exposure. For *Extreme* exposure, results show an increase up to 5% in percent passing 10 µm, while the percent passing below 10 µm seemed to align with the unexposed sample result. Slag typically shows moderate reactivity when mixed with portland cement. Exposure to moisture without the presence of the high-alkaline environment, however, resulted in little particle size change, indicating almost no reaction.

Obtaining an accurate representation of SF particle distribution (Figure 11-15) is difficult due to agglomerations found in densified silica fume. For the unexposed SF, the first curve starts at 0.12 µm and the second curve starts at 3 µm. Recall that for SF an external homogenizer of higher intensity was used to break the agglomerations. The use of a stronger homogenizer can be helpful to obtain more accurate results; however, for this study, agitation affected the results by breaking apart the agglomerates formed during exposure. Silica fume results show a slight increase in particle size during *Extreme* exposure, and similar particle size between *Field* exposure and the unexposed sample. Nevertheless, SF needs an environment with calcium hydroxide CH and high pH levels to react, so no reaction was expected to occur during exposure.

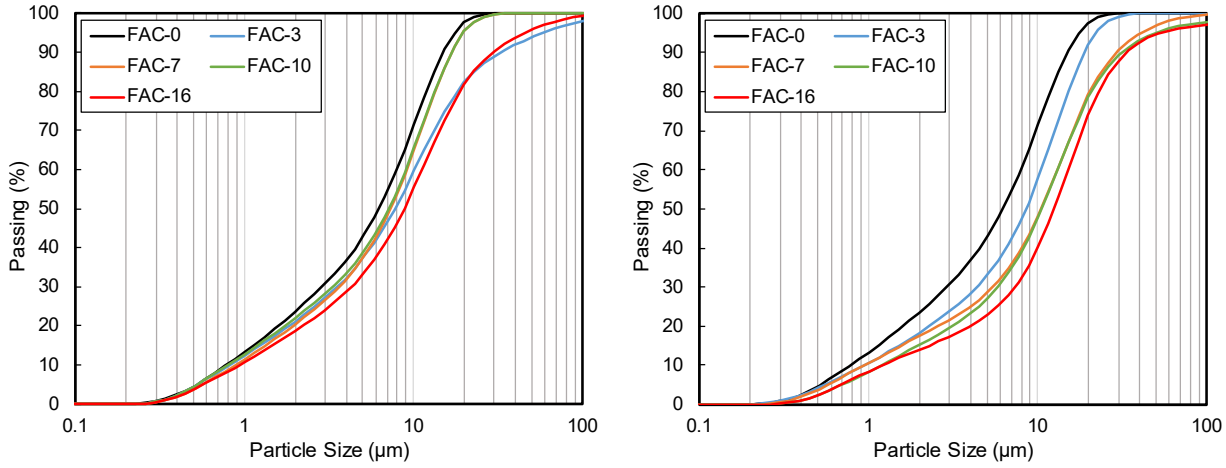

(a) (b)

Figure 11-12 Particle size distribution of Fly ash class C: (a) *Field* exposure and (b) *Extreme* exposure

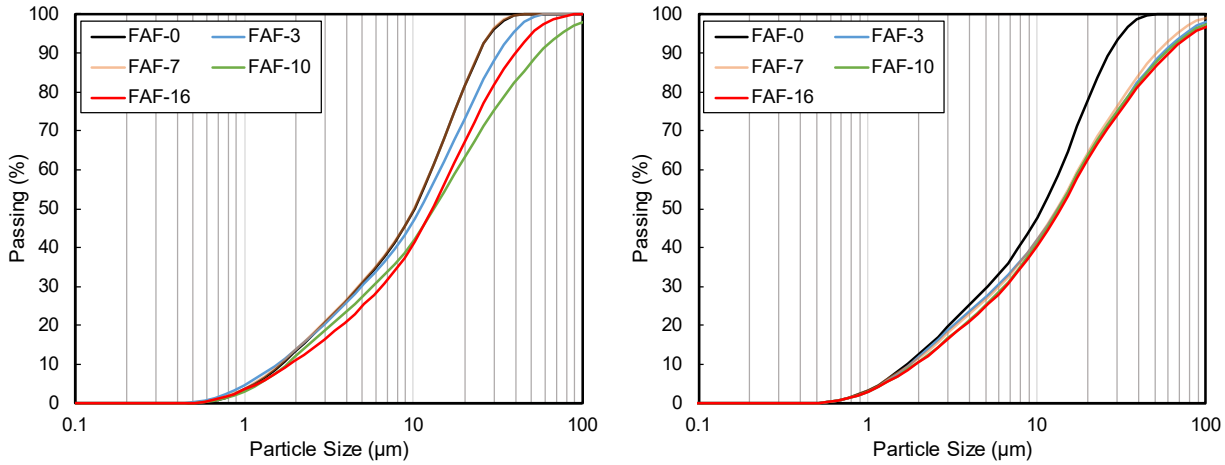

(a) (b)

Figure 11-13 Particle size distribution of Fly ash class F: (a) *Field* exposure and (b) *Extreme* exposure

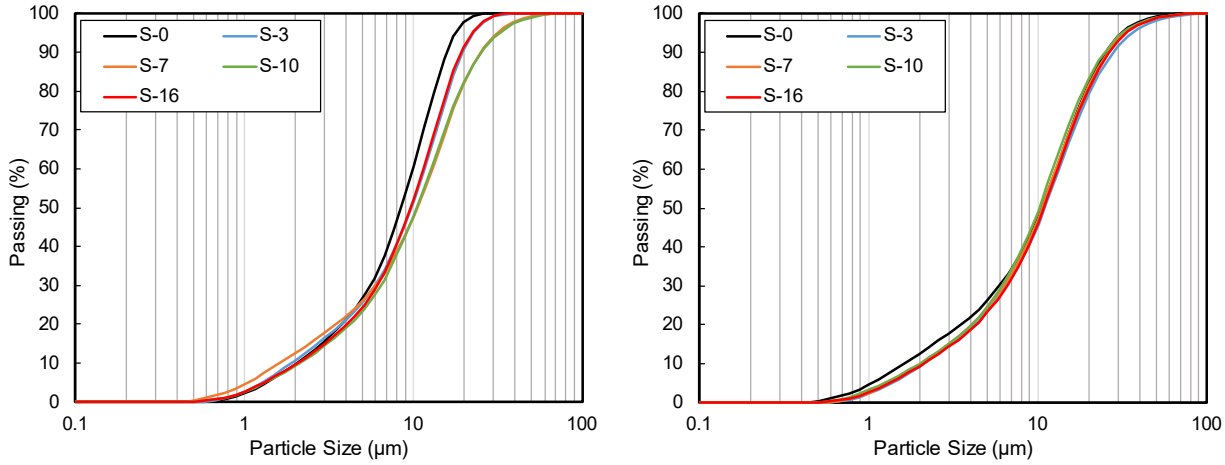

(a) (b)

Figure 11-14 Particle size distribution of slag: (a) *Field* exposure and (b) *Extreme* exposure

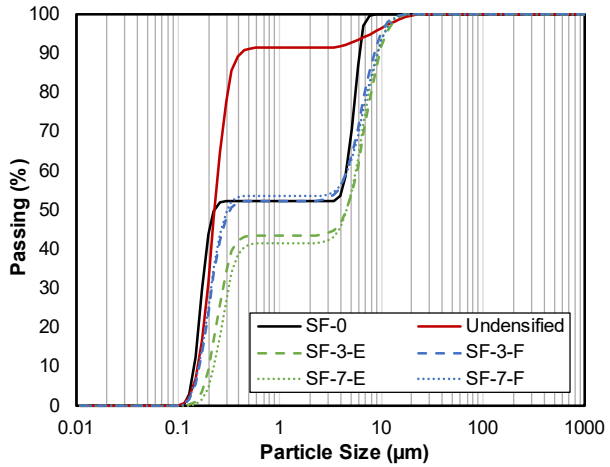

Figure 11-15 Particle size distribution of silica fume for both *Field* and *Extreme* exposures

An alternative *Field* test method to track the growth of particles in PT grout is given in ASTM C430 Standard Test Method for Fineness of Hydraulic Cement by the 45-µm (No. 325) Sieve. This test method determines the mass of particles retained on a 45-µm sieve. Based on the SCM particle size results shown in Table 11-2, most of the particles of the SCMs were smaller than 45 µm, even after exposure, which indicates that an increase in percent retained by the 45-µm sieve directly corresponds to an increase in size of the cement particles due to prehydration.

Table 11-2 Percent of particles below 45 µm

Material	Unexposed (%)	*Field* (%)				*Extreme* (%)			
		3	7	10	14	3	7	10	14
FAC	100	92	100	100	95	100	96	94	94
FAF	99.	97	100	85	92	86	87	85	84
S	99	97	98	98	98	100	100	98	100
SF	100	100	100	100	100	100	100	100	100

12 Blaine Fineness

12.1 Summary of Test Method

As concluded in the previous study Brunner and Hamilton (2014) the Blaine Fineness Test outlined in ASTM C204-11 was capable of capturing data of grout particle growth and has the advantage of being a test that could be performed on site. The Blaine Fineness test measured the surface area per volume of cementitious materials, and typically this ratio decreases as a particle's mean size increases. In this study, Blaine fineness is further examined as a potential test method for evaluating the susceptibility of PT grouts to form soft grout and to track the change in particle size as high temperature and humidity are imposed on grouts and portland cement. The Blaine Fineness test setup is shown below in Figure 12-1.

Figure 12-1 Blaine fineness test setup

The Blaine fineness test measures the surface area per unit volume of cementitious materials by drawing a known quantity of air through a known volume of space filled with a known mass of cementitious material. The machine is calibrated using a standard material for which the surface area per volume is already known, which allows the user to obtain an approximate surface area per volume values. However, in this study, the actual surface area to volume values are of little concern because each PT grout uses different constituents and various amounts of those constituents in their blend; every PT grout begins its shelf life with a different mean particle size based on the constituents that are present. This proprietary nature of PT grout means that a standard reference or baseline particle size does not exist across all different types of PT grout manufacturers. Therefore, of primary concern in this study is the relative change in grout and portland cement particle size of any particular manufacturer over time. The level of

relative growth in a cementitious material's mean particle size seems to indicate the relative level of prehydration of the portland cement and perhaps other SCM components present in the mix.

It was determined that Blaine fineness tests would be conducted on every small-scale sample of grout alongside every MITT sample as described in the previous chapters, these side-by-side tests were done to investigate the relationship between any changes in relative fineness values to the production of soft grout in the MITT test. The Blaine Fineness Air-Permeability Apparatus was calibrated in accordance with ASTM C204-11 using the ASTM standard reference material and a couple preliminary Blaine fineness trial tests were done to ensure the apparatus was working properly. In these preliminary tests, it was discovered that the densities of the PT grouts and cements varied so much between manufacturers that the standard testing mass (which was determined in the calibration process) was unable to be compacted into the volume of the Blaine cell for three of the five PT grouts being investigated. To address this issue, the standard testing mass was held constant across all five PT grouts, but new volumes were specified for each particular PT grout and cement number to be used in a modified version of the Blaine Fineness test. These volumes were determined by compacting the PT grout material to a level of pressure that seemed roughly equal to that of pure portland cement. The plunger was then marked using a fine tipped pencil, as shown below in Figure 12-2 and Figure 12-3, to ensure the exact same volume could be achieved in the packing of those materials for subsequent tests.

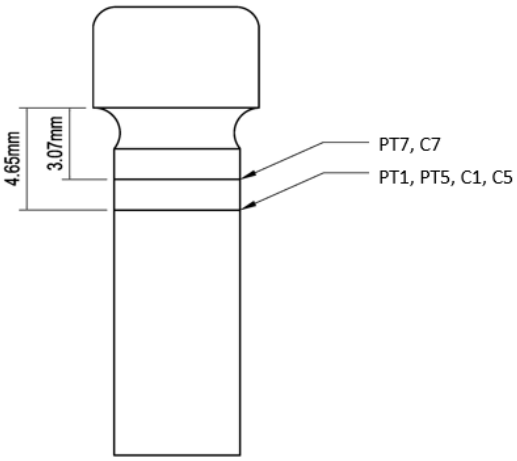

Figure 12-2 Markings on plunger and corresponding grout manufacturers and cement

Figure 12-3 Actual markings on plunger used for testing

These marks denoting the standard test volumes for every PT manufacturer made it possible for the exact same volume to be used for every ensuing fineness test for that particular PT grout. The plunger was simply returned to the same position every time a Blaine fineness test was conducted on that particular PT grout, thus compacting the standard mass of PT grout to the same volume for every test. PT2, PT3, and C3 were all compacted to the level of the standard reference material by inserting the plunger all the way into the Blaine cell and seating the ridge of the plunger against the top of the Blaine cell. These modified procedures for the Blaine fineness test prevent absolute fineness values from being obtained and are, therefore, not within the specifications outlined in ASTM C204-11; however, they do provide relative fineness values for a particular PT grout and cement over time, which is the intent of this particular study on the shelf life sensitivity of PT grout and its respective portland cement. The fineness of the various PT grouts and cements was converted to a fineness ratio. This fineness ratio is defined as follows:

$$BF_{ratio} = 1.0 - \frac{blaine\ time\ (no\ exposure) - blaine\ time\ (with\ exposure)}{blaine\ time\ (no\ exposure)} \quad \text{Equation 2}$$

Note that the 0-day fineness value is used as the standard for this ratio, the measurement was taken upon delivery of the material to the lab, thus every PT grout starts with a BF_{ratio} equal to 1.0 before being exposed to the various imposed exposure levels. As previously discussed by Brunner and Hamilton (2014), a decrease in Blaine time, which usually accompanies an increase in particle size, will result in a decrease in the BF_{ratio}. It was believed that extended exposure to the *Extreme* condition would result in prehydration of the portland cement, thus increasing the mean particle size, decreasing the Blaine time, and ultimately reducing the BF_{ratio} to values progressively lower than 1.0. Other than the modification to the compaction volume previously discussed in this chapter, all the procedures outlined in ASTM C204-11 were followed in obtaining the Blaine times for the tests conducted in this study.

12.2 Results and Discussion

12.2.1 PT Grout

The Blaine Fineness test provides an indirect measure of the surface-area-to-volume ratio of cementitious materials. The fineness of the various PT grouts and cements was converted to a fineness ratio defined as (BF_{ratio}), the ratio equation is show in the testing procedures chapter. Note that the 0-day fineness value is used as the standard for this ratio, the measurement was taken at (0-day MITT), thus every PT grout and cement starts with a BF_{ratio} equal to 1.0 before being subjected to the four exposure levels. All of the data in this chapter is presented as BF_{ratio}.

Figure 12-4 shows results from MITT samples in both the *Field* and *Extreme* exposures; at 7 days exposure, the average BF_{ratio} for all PT grouts was 0.73 for *Field* and 0.58 for *Extreme.* Significantly greater decreases in BF_{ratio} occurred in the *Extreme* exposures compared to the *Field* exposures. The differences in BF_{ratio} from *Field* and *Extreme* were likely due to the increased temperature and humidity. The cement phases each have a specific sensitivity to prehydration, moisture absorption, and degradation as a function of the temperature and humidity. Specifically, the increased susceptibility of topochemical hydration on the surface of the cementitious material is magnified at elevated temperatures and humidities for prolonged periods of time.

Whenever the particles of a particular material experience growth, the surface area-to-volume ratio for that material decreases, which allows the known quantity of air to pass through the bed of material more quickly during the Blaine Fineness test. Therefore, the decreases in BF_{ratio}, shown in Figure 12-4 through Figure 12-6, indicate growth in the mean particle sizes of the grouts and cements tested.

Figure 12-5 shows the BF_{ratio} results from the grout small-scale samples in both the *Field* and *Extreme* exposures. Significantly greater decreases in BF_{ratio} occurred in the *Extreme* exposures compared to the *Field* exposures.

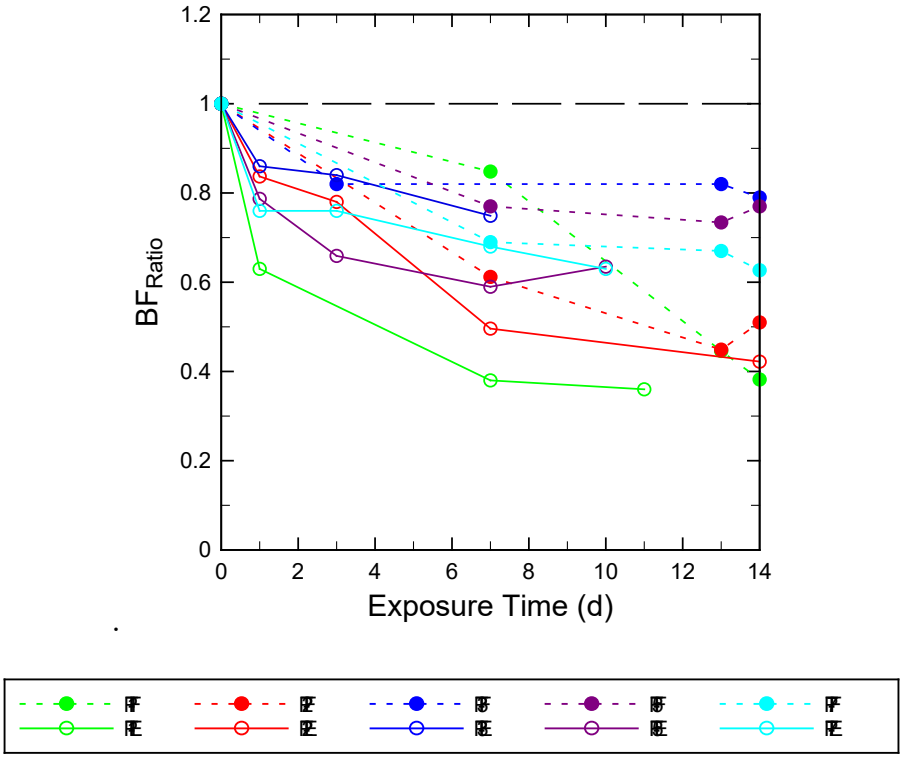

Figure 12-4 BF_{ratio} for MITT samples grouts exposed in *Field* and *Extreme* exposures

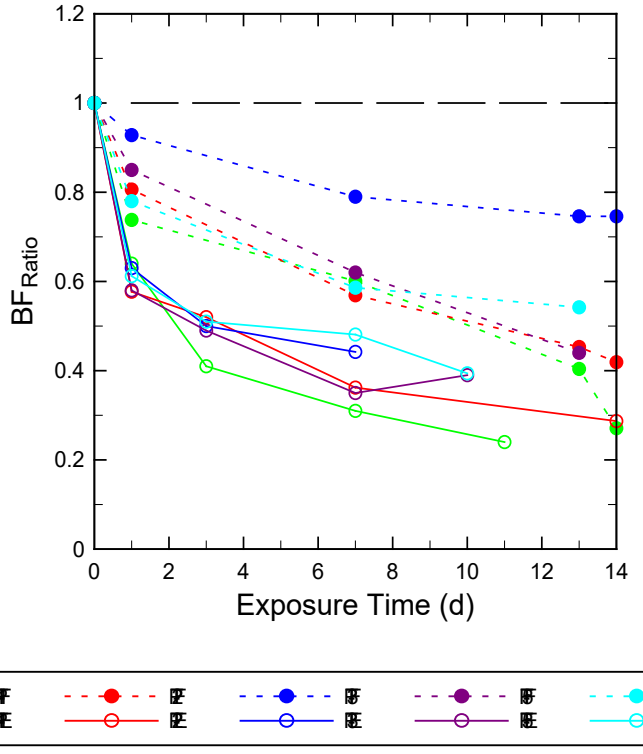

Figure 12-5 BF_{ratio} for small-scale grout samples in *Field* and *Extreme* exposures

12.2.2 Cement

Figure 12-6 shows the BF_{ratio} results from the grout small-scale samples in both the *Field* and *Extreme* exposures. Comparison of test results for the small-scale grout to the cement at 7 days of *Field* exposure shows that PT1 had a BF_{ratio} of 0.60 and C1 had a BF_{ratio} of 0.55. Meanwhile, at 7 days *Extreme* exposure, PT1 had a BF_{ratio} of 0.38 and C1 had a BF_{ratio} of 0.37. Both PT grout and cement exhibited close to the same BF_{ratio} decreases in small- scale samples, which suggests that cement is responsible for most, if not all, of the reduced BF_{ratio} as exposure occurred.

Contrary to the results for PT1 and C1, PT5 and C5 had 7-day *Field* exposure BF_{ratios} of 0.62 and 0.65, respectively, and 7-day *Extreme* exposure BF_{ratios} of 0.35 and 0.56, respectively, which would suggest the cement is not the only material responsible for particle size growth. The difference in particle size growth of PT grouts compared to their cements may be influenced by the particular SCMs and admixtures used, or by the proportions of cement used in the grout. It should be noted that this same PT grout behavior was seen in PSA results.

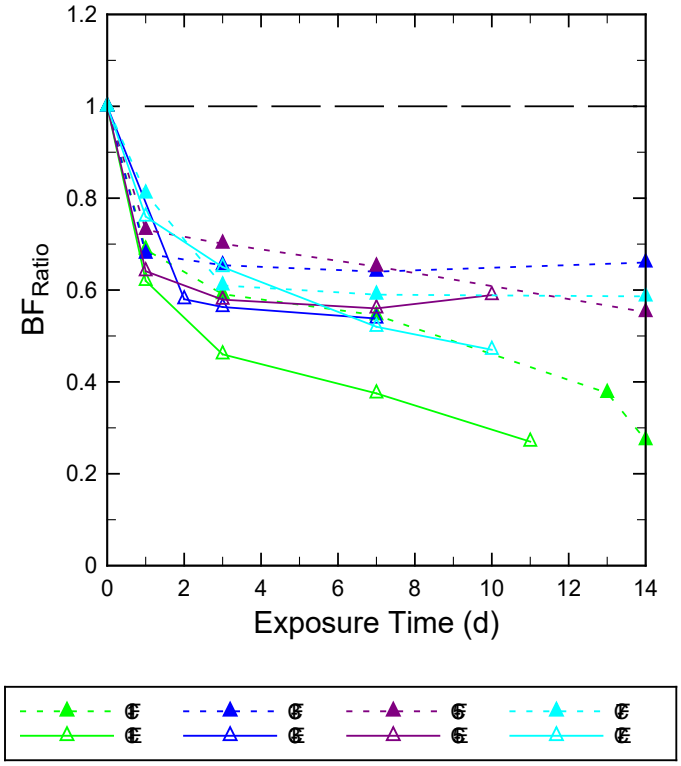

Figure 12-6 BF_{ratio} for small-scale portland cement samples in *Field* and *Extreme* exposures

13 Loss on Ignition

13.1 Summary of Test Method

Loss on Ignition (LOI) testing was performed to determine the mass changes caused by *Field* and *Extreme* exposures of PT grout, cement, and SCMs. As described in ASTM D7348-13 Standard Test Method for Loss on Ignition (LOI) of Solid Combustion Residues (2013), the test method is used to determine the loss in mass of the test specimens when heated under controlled temperature, time, atmosphere, specimen mass, and equipment specifications.

The LOI test method requires a furnace with a sustained heating capacity above 1000°C and an interior volume large enough to simultaneously run multiple crucible samples. Figure 13-1 illustrates one of the laboratory-grade LOI heating furnace used in this study.

Figure 13-1 Loss on Ignition testing furnace

Small-scale, layered (0.5 in. thick) containers were used (Figure 13-2) for PT grout and portland cement LOI testing. LOI measurements were taken from each of the three layers to determine the variation in mass gain between inner and outer portions of bagged material. Each layer of the container was sampled after exposure was completed, as described in Appendix D.

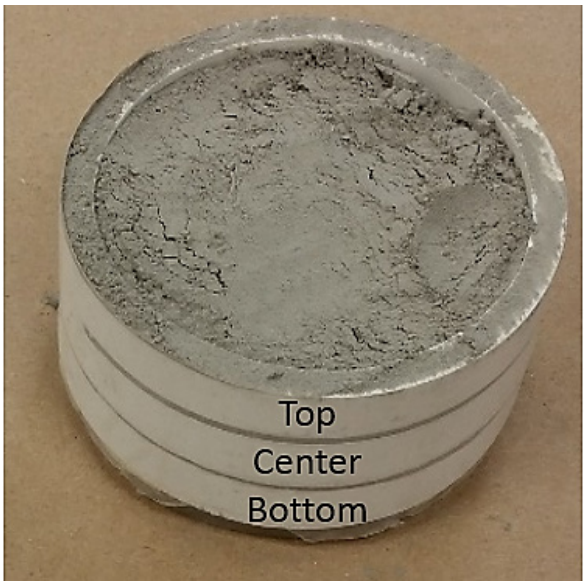

Figure 13-2 LOI small-scale depth-layered container

13.2 Results and Discussion

13.2.1 PT Grout

Figure 13-3 shows LOI results from MITT grout samples in *Field* and *Extreme* exposures. One plot shows the LOI mass loss for each test day. The other plot shows the LOI mass loss results normalized to the initial test result, which shows a relative change in mass loss with exposure time. PT grouts had an initial (0 day) mass loss between 2.5% and 4.2% except PT7, which had an initial mass loss of 7.2%. The high LOI value of PT7 suggests that this PT grout may have experienced prehydration before arriving to the laboratory for testing.

After normalizing the LOI data for all five PT grouts, the LOI results for *Field* exposure were generally less than for *Extreme* exposure. For example, at 7 days of *Field* exposure, PT5 had a normalized mass loss of 1.12, and for *Extreme* exposure, PT5 had a normalized mass loss of 1.26, which suggests that the increased mass gain is affected by elevated temperature and humidity.

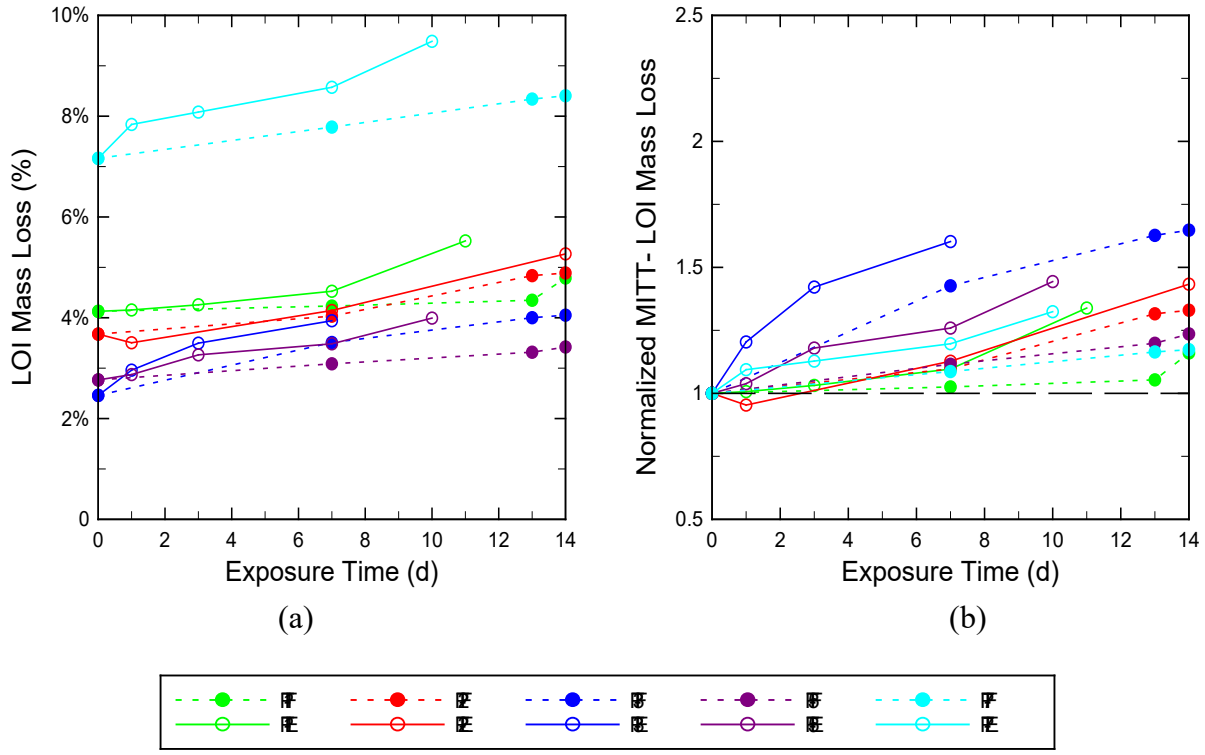

Figure 13-3 PT grouts LOI mass loss from MITT samples in *Field* and *Extreme* exposures

Figure 13-4 through Figure 13-8 show the LOI results for small-scale samples of grout. LOI samples were taken from each of three layers to evaluate the diffusion of moisture through the sample. Absolute and relative LOI results are presented for each material.

When comparing the PT grout LOI data for the Top layer compared to the Center and Bottom layer, the Top layer experienced the highest level of mass change. When dissecting the small-scale layered samples, the Top layer was the hardest layer to remove because heavy deposits of hardened grout covered the top of the container. The hardened layer was likely caused by hydration of the cementitious materials, which had absorbed moisture. The Center and Bottom layers did have some clumping and minor hardened particles, but not at the level of the Top layer.

It is expected that after the Top layer had begun to gain mass and interact with the water vapor during exposure, it acted as a barrier layer to moisture movement and diminished the amount of prehydration that occurred at the Center and Bottom layer. This effect was also seen in the prepackaged bags of grout after exposure, where the corners of the bags and grout surface area along the bag closest to the exposure cuts showed clumping and hardened cementitious compounds.

Furthermore, clumping was present at the surface of the samples after exposure because a low water-to-solid ratio environment makes the hydration reaction predominantly topochemical. In topochemical hydration, immediately after the first contact of the cement with water, a calcium-rich, siliceous cement phase liberates Ca^{++} ions. This is accompanied by swelling of the hydration products relative to the original volume of the anhydrous cement (van Breugel, 1992).

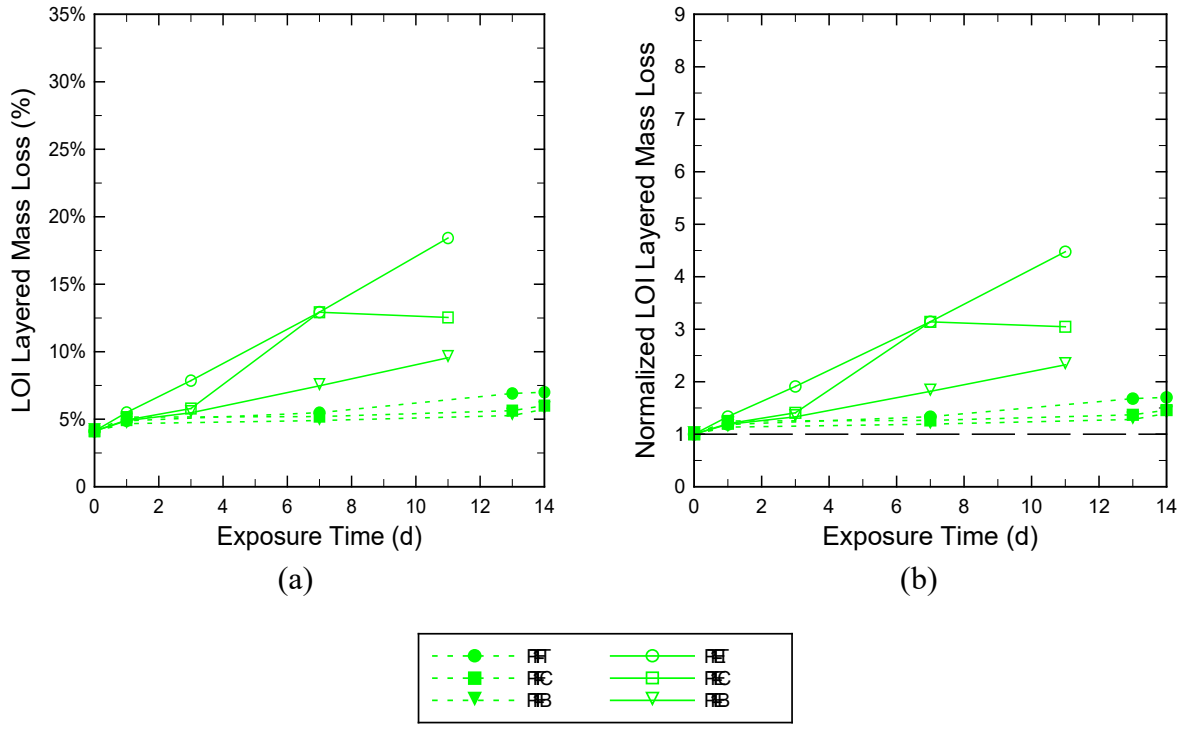

Figure 13-4 PT1 grout LOI layered mass loss from small-scale samples in *Field* and *Extreme* exposures

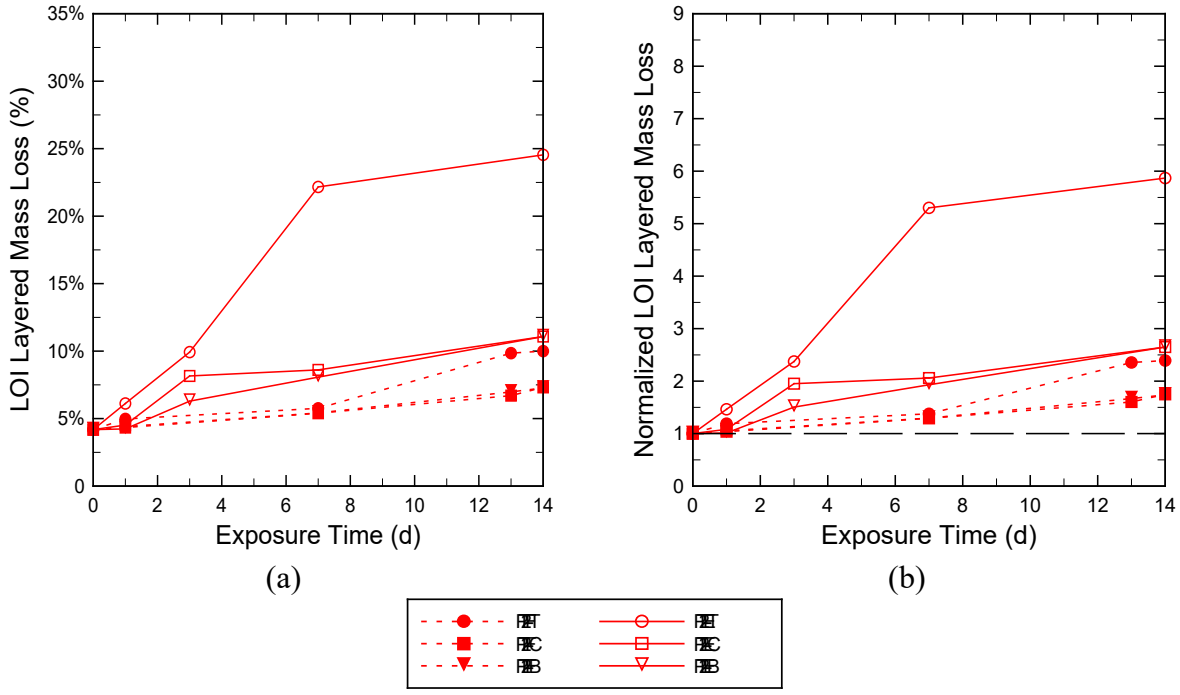

Figure 13-5 PT2 grout LOI layered mass loss small-scale samples in *Field* and *Extreme* exposures

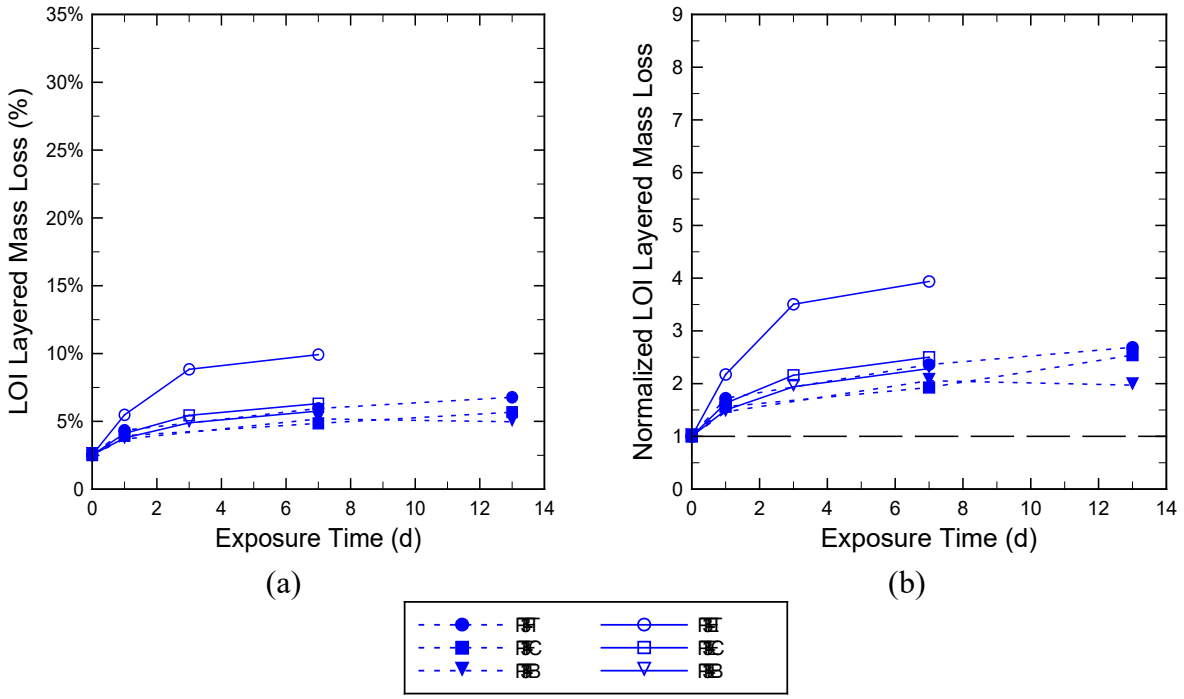

Figure 13-6 PT3 grout LOI layered mass loss from small-scale samples in *Field* and *Extreme* exposures

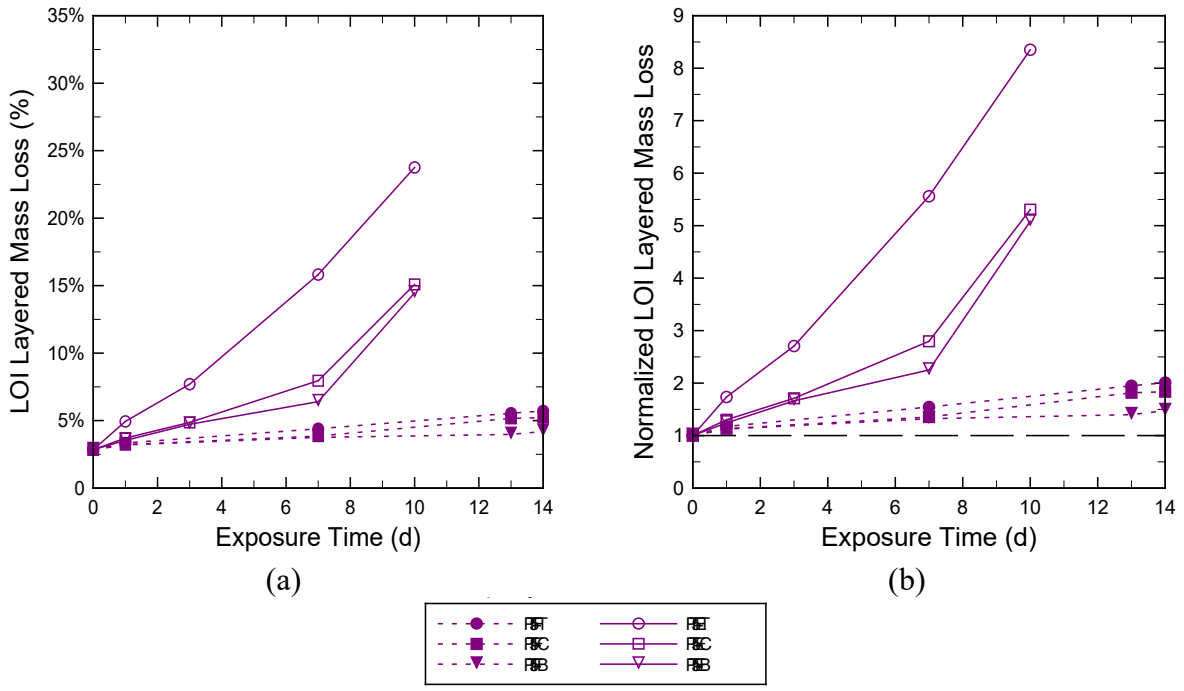

Figure 13-7 PT5 grout LOI layered mass loss from small-scale samples in *Field* and *Extreme* exposures

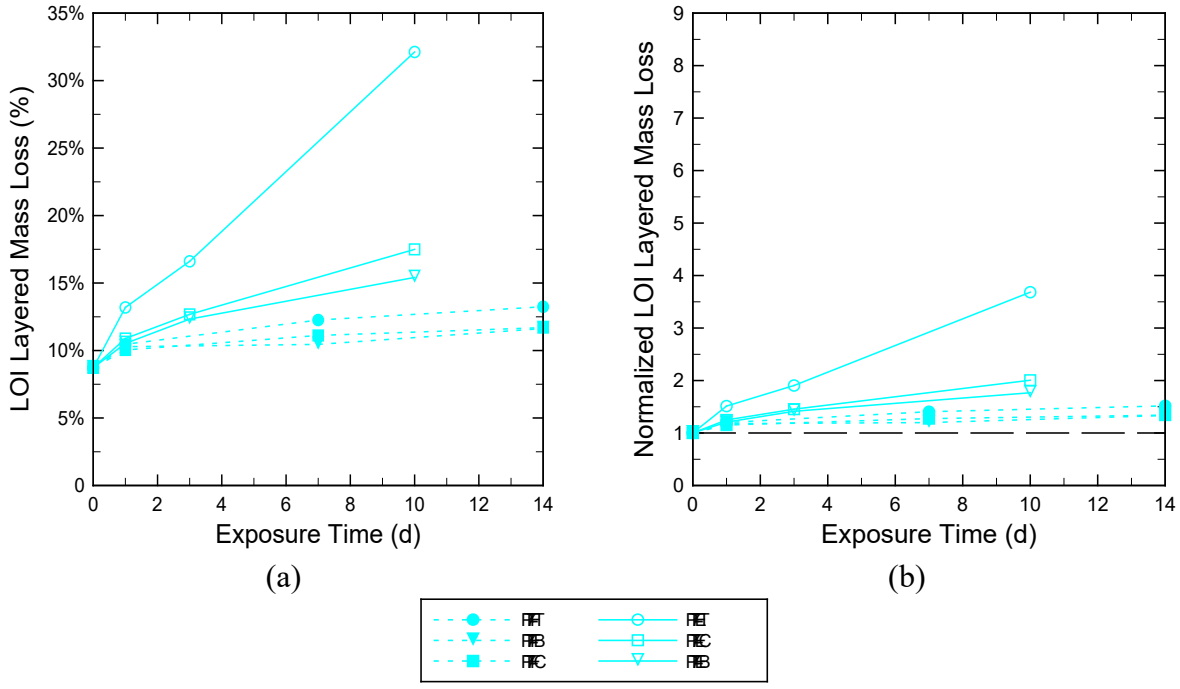

Figure 13-8 PT7 grout LOI layered mass loss small-scale samples in *Field* and *Extreme* exposures

13.2.2 Cement

Figure 13-9 through Figure 13-12 show the LOI data for layered samples of the portland cements used in the various manufactured grouts. In general, the results for cements showed the same mass change behavior as the grout, the top layer experienced the highest level of mass change of the three layers followed by the Center and Bottom layers. The Top layer was the most difficult layer to remove because heavy deposits of hardened cement covered the top of the container.

Overall, PT grout and cement LOI results support the claim that cement drives the mass change behavior in grout during exposure. The grout and cements share the same trend that the Top layer had the highest mass loss, followed by the middle and bottom layers in LOI layered-sample testing. For example, for the 7-day *Field* exposure of layered samples, PT1 had a 5.5% mass loss for the Top layer, 4.9% for the Center layer, and 4.9% for the Bottom layer; while C1 had a 5.5% mass loss for the Top layer, 5.1% for the Center layer, and 4.9% for the Bottom layer.

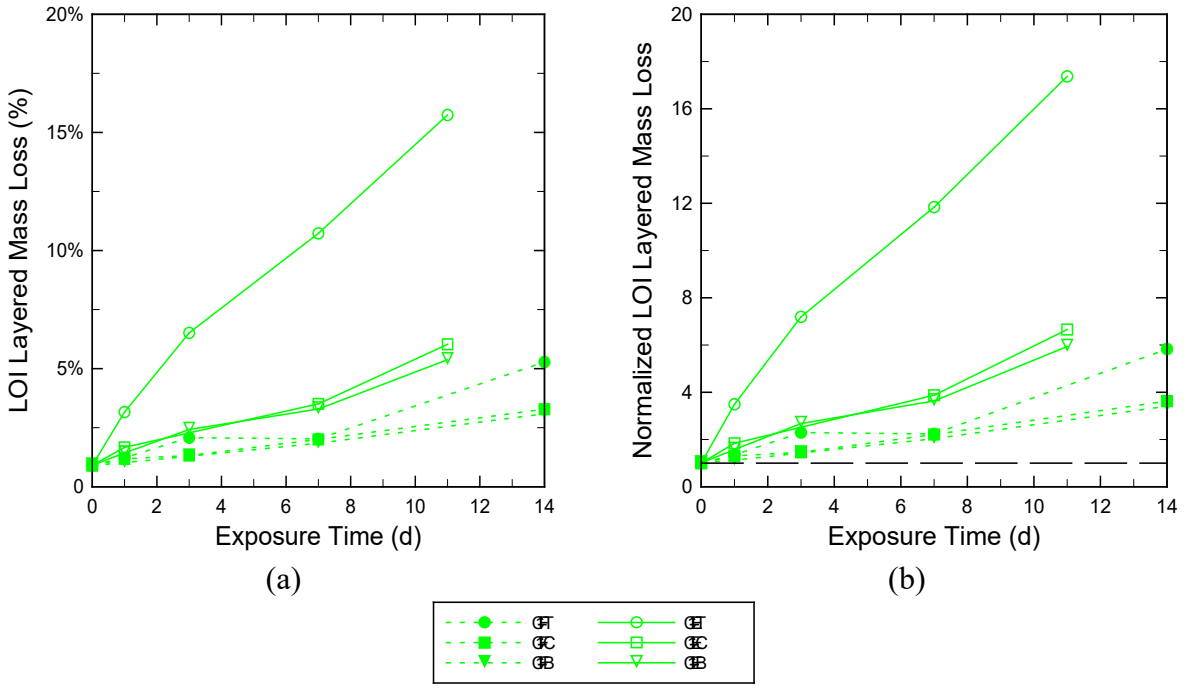

Figure 13-9 C1 portland cement LOI layered mass loss from small-scale samples in *Field* and *Extreme* exposures

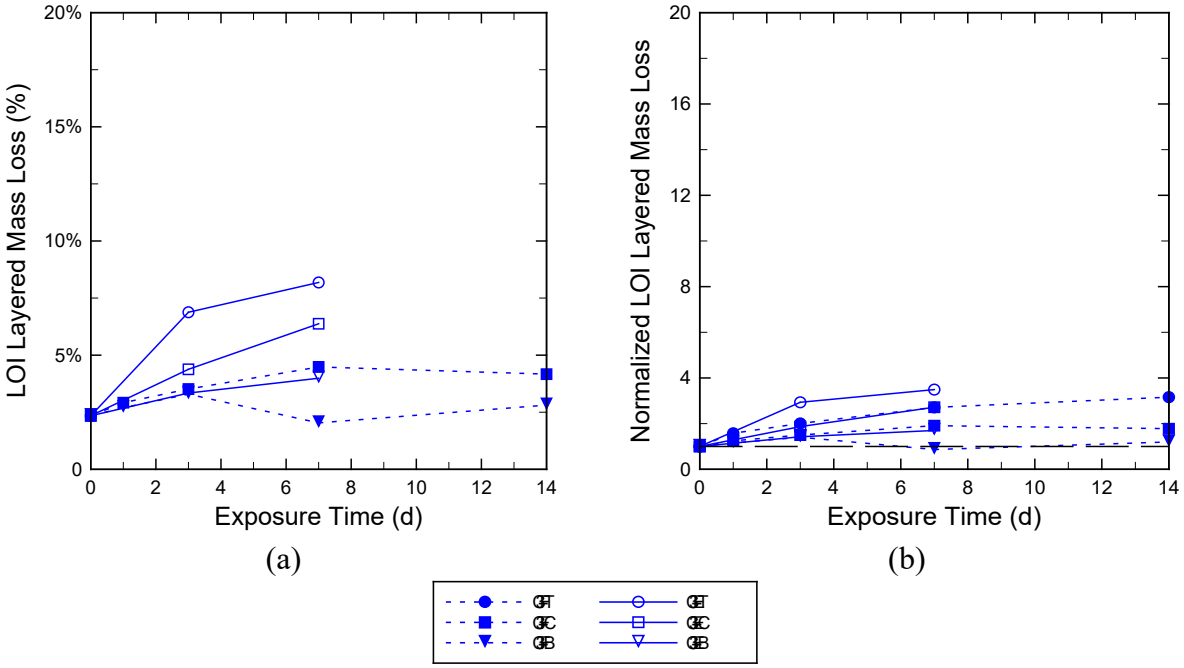

Figure 13-10 C3 portland cement LOI layered mass loss from small-scale samples in *Field* and *Extreme* exposures

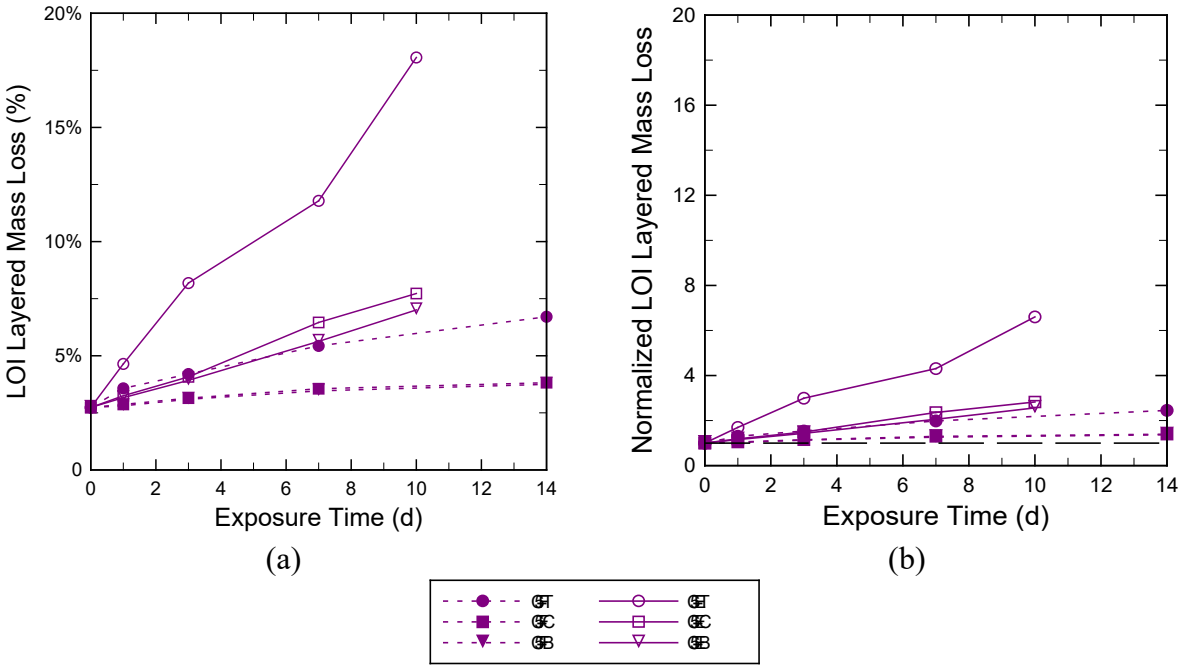

Figure 13-11 C5 portland cement LOI layered mass loss from small-scale samples in *Field* and *Extreme* exposures

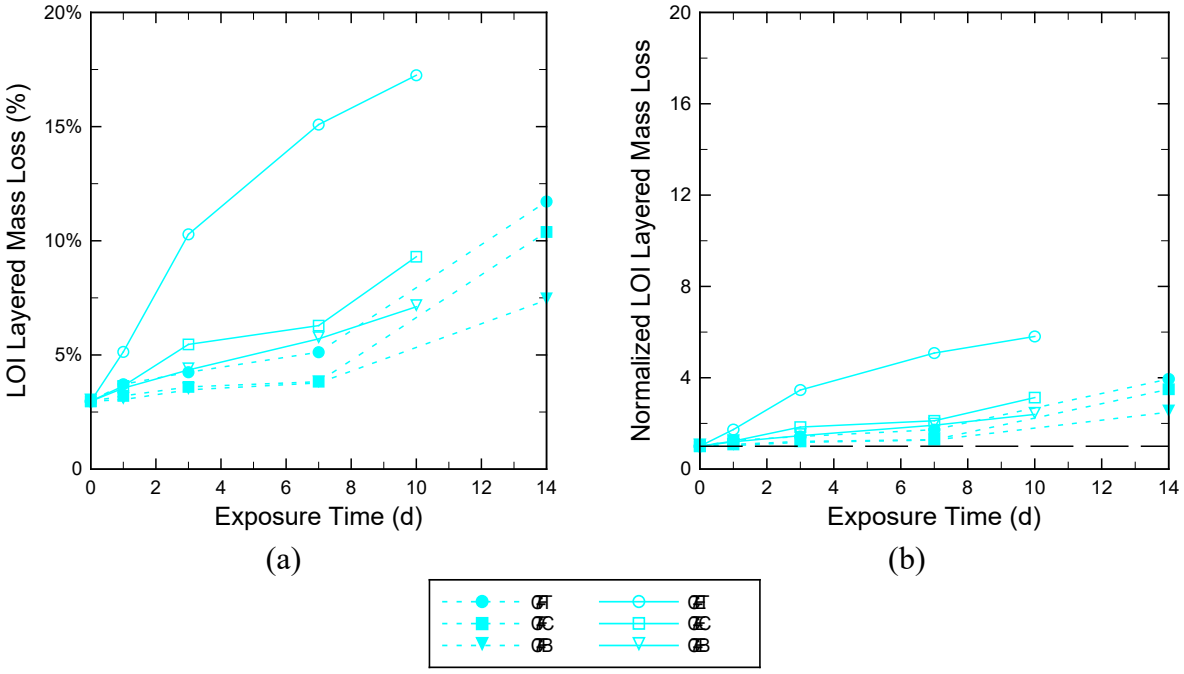

Figure 13-12 C7 portland cement LOI layered mass loss from small-scale samples in *Field* and *Extreme* exposures

The general trend observed was that LOI results of all small-scale, layered samples were higher than for the MITT samples in all exposures. This trend suggests that the small-scale samples experienced more mass loss than the MITT samples exposed to the same conditions.

The LOI testing results support the claim that the PT grouts and cements have an increased sensitivity to elevated temperature and elevated humidity, as reflected by mass gain, moisture uptake, and any other mechanisms associated with prehydration.

Furthermore, the small-scale LOI results on layered samples show that all three layers were exposed to different relative humidities but the same temperature. These results suggest that humidity alone may drive mass change in the grout and cement. Each of the phases in the cement have a specific sensitivity to humidity and their proportions in the cement may drive the mass change. The inert fillers are known to prehydrate during exposure, but to what degree is still unknown.

13.2.3 SCMs

Figure 13-13 through Figure 13-16 show the LOI results for small-scale samples of SCMs. Each figure provides the LOI mass loss and the normalized LOI value. Similar to PT grout and portland cement, the results represent the average of at least three samples of each layer. For identification, the letters T, C, and B are used for the top, center, and bottom layers, respectively. Also, *Field* and *Extreme* exposures are identified with the letters F and E in the legend.

No significant differences were observed in the LOI values determined for each layer. In some cases, the bottom layer had a higher LOI mass loss; this was expected to some extent because the bottom layer usually was more compacted, giving the appearance of having more moisture between particles. This occurred because the container was closed at the bottom so the moisture penetrates and gathers in the bottom layer or condenses at the powder-container interfaces. One possibility for this effect is that the lack of reactivity prevented the formation of a protective top layer or crust, which subsequently would have prevented penetration of moisture into the deeper layers.

The difference in temperature and humidity levels between *Field* and *Extreme* conditions only had a significant effect for FAC (Figure 13-13). The difference in LOI mass loss of FAC between exposures is approximately 2.5%, while for the other SCMs the values of both exposures were within 0.2%-0.5% of each other during exposure time.

The mass loss for all SCMs approached an equilibrium value at 3-7 days of exposure. For example, FAF (Figure 13-14) and SF (Figure 13-15), which showed no signs of reaction as discussed in the previous test methods, had mass loss changes of under 0.2% beyond 3 days of exposure. FAC (Figure 13-13) and Slag (Figure 13-16) had changes of at least 0.60% after 3 days of exposure, indicating more interaction with free moisture.

Normalized LOI values are another indicator of the moisture adsorbed by the SCMs during exposure. SF and FAC normalized LOI values were only 1.5 times their initial value, indicating that these SCMs do not adsorb much moisture regardless of the exposure conditions. These results are positive in terms of the effect of these SCMs in prepackaged PT grout bags. It can be concluded that FAF and SF do not react with the moisture in the environment, and do not accumulate water that can prolong prehydration of the portland cement present in the prepackaged bags.

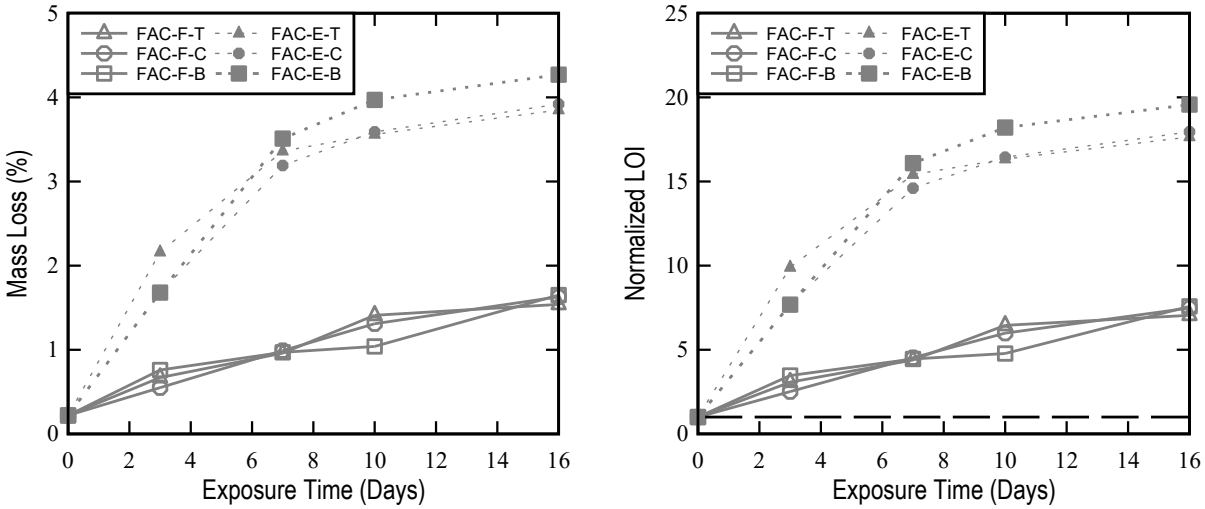

Figure 13-13 LOI results of FAC during both *Field* and *Extreme* exposure: (a) Percent mass loss and (b) Normalized LOI

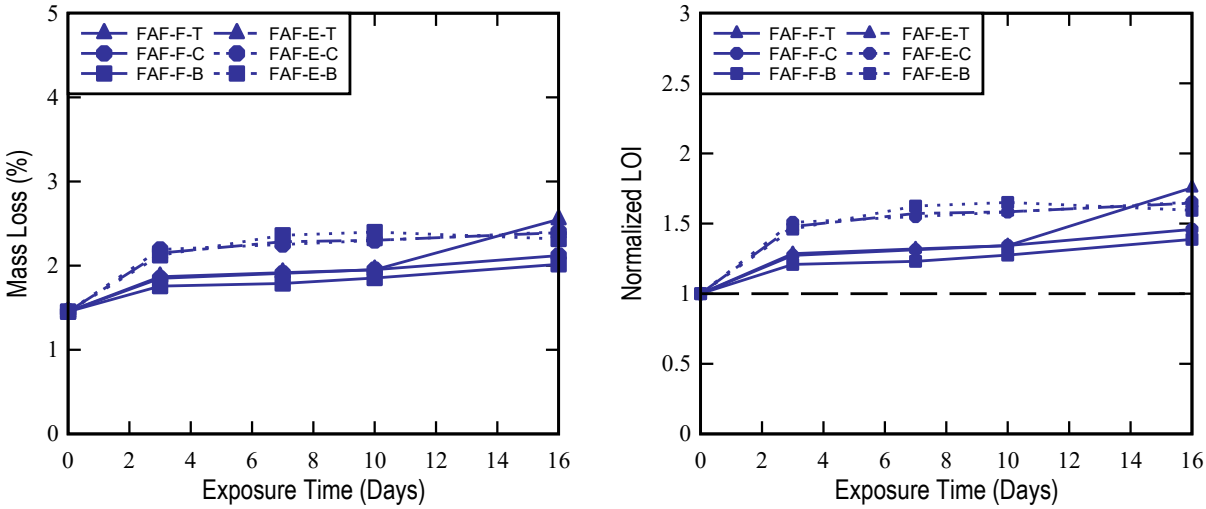

Figure 13-14 LOI results of FAF during both *Field* and *Extreme* exposure: (a) Percent mass loss and (b) Normalized LOI

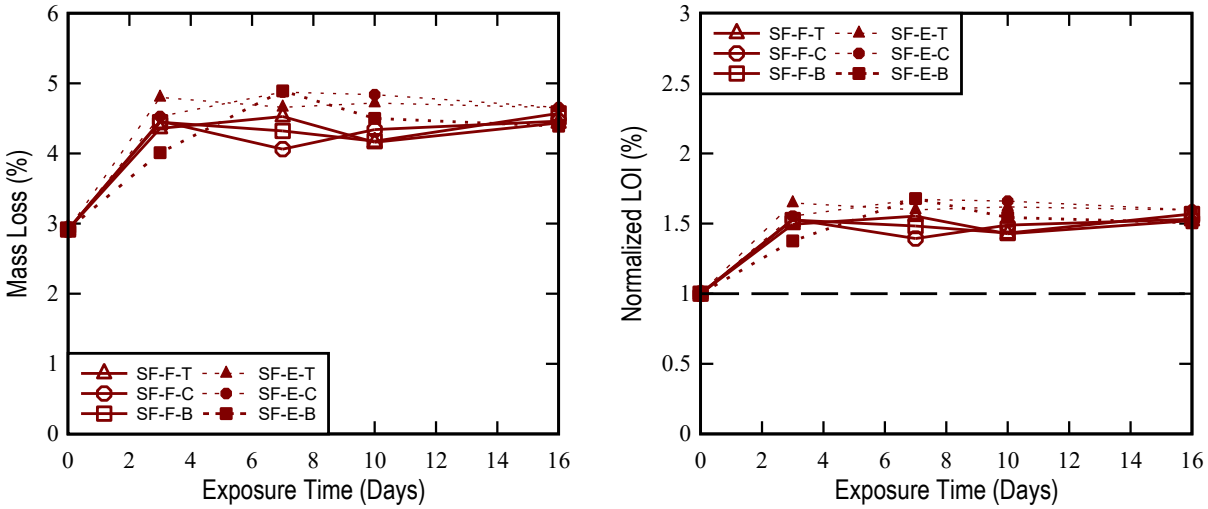

Figure 13-15 LOI results of SF during both *Field* and *Extreme* exposure: (a) Percent mass loss and (b) Normalized LOI

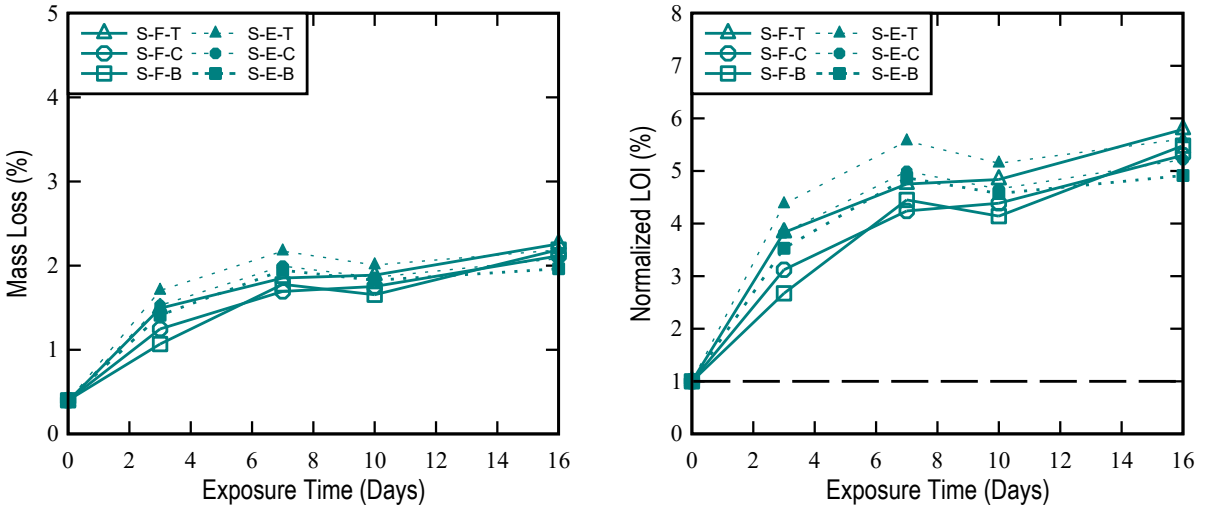

Figure 13-16 LOI results of S during both *Field* and *Extreme* exposure: (a) Percent mass loss and (b) Normalized LOI

14 Thermogravimetric Analysis

14.1 Summary of Test Method

In addition to mass change measurements using LOI testing, the cementitious materials' response to differential heating temperature was investigated in this study. As previously discussed in the background chapter, Jensen et al. (1999) explored the prehydration of the clinker components in portland cement and found that each particle structure had a unique sensitivity to prehydration. When a cement specimen is heated from 32°F (0°C) to 1742°F (950°C) five reactions are known to occur at different temperature ranges as specified by Alarcon-Ruiz et.al. (2004): 1) 86°F -221°F water physically bonded in the surface is completely evaporated, 2) 230°F -338°F the decomposition of gypsum, ettringite and loss of water from carboaluminate hydrates occurs, 3) 356°F -572°F loss of water from decomposition of C-S-H and carboaluminate hydrates takes place, 4) 450°F -550°F dehydroxylation of portlandite undergoes, and 5) 1292°F -1652°F decarbonation of calcium carbonate. In an effort to track the weight-loss mechanisms, our study evaluated the grouts and cements after *Field* and *Extreme* exposures using Thermogravimetric Analysis (TGA). The ASTM E2105-10 Standard Practice for Thermogravimetric Analysis (2010) was followed. TGA measures weight changes in a material as a function of temperature and time under a controlled atmosphere. Its primary use includes measurements of a material's thermal stability. TGA was performed on PT grouts, corresponding cements, and SCMs that were exposed to the *Field* and *Extreme* conditions, with samples taken from MITT and small-scale containers. The cementitious materials were analyzed in a temperature range from ambient to 1830°F (999°C); weight change was recorded once the microbalance sensed a stabilized weight at the given temperature, and then continued to increase in temperature at a rate of 36°F/min (20°C/min) until 1830°F (999°C).The TGA test was performed with an atmosphere of nitrogen at a flow rate of 100 ml/min.

Figure 14-1 below shows the Mettler-Toledo TGA/SDTAA851 model, which was one of the instruments used for TGA testing. The TGA instrument is capable of analyzing material in a range from ambient temperature to 2912°F (1600°C), and is equipped with a microbalance, which allowed for sample mass to be continuously recorded over the total temperature range. In addition, the TGA instrument utilized an auto sampler for multiple testing runs. The TGA test is a laboratory test that can output results in a matter of hours.

Figure 14-1 Mettler-Toledo TGA/SDTAA851 model used for TGA testing

14.2 Results and Discussion

14.2.1 PT Grouts

Figure 14-2 through Figure 14-6 show the TGA results for MITT samples exposed to the *Field* and *Extreme* conditions. All figures in this chapter plot the unexposed sample data with a solid black line to use as the reference point for TGA testing.

All grouts showed a decrease in mass percentage as exposure time progressed. In addition, a reduced percent of mass was found in the *Extreme* exposure compared to the *Field* exposure for the same amount of exposure time with the exception of PT1-F14 and PT3-E-3. These findings would suggest that prolonged exposure to high temperature and humidity adversely affected the initial properties of the cementitious material and residual mass percentage.

The TGA mass percent is important because it can correlate the prehydration physical and chemical reaction behavior of the cementitious material as exposure continues. The MITT samples show reduced slopes for mass change before 1022°F (550°C) compared to the majority of the mass change that occurred after 1112°F (600°C). This trend would suggest that although bound water, decomposition of the gypsum and ettringite, and decomposition of the calcium silicate hydrate occurred mainly prior to 1022°F (550°C), the majority of the mass change occurred above 1112°F (600°C), which is associated with the decarbonation of calcium carbonate, which is a product of cement hydration.

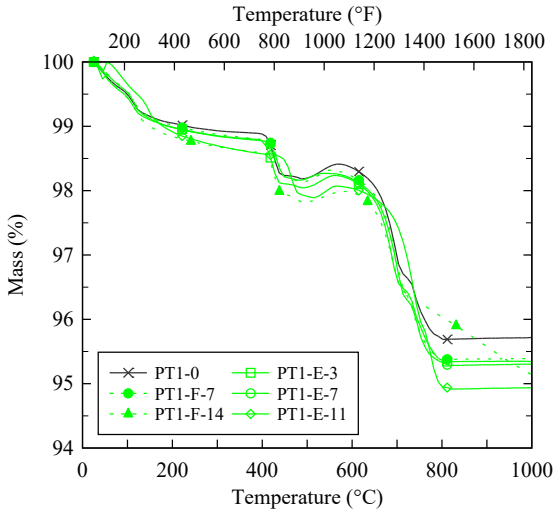

Figure 14-2 TGA results of PT1 MITT samples after *Field* and *Extreme* exposures

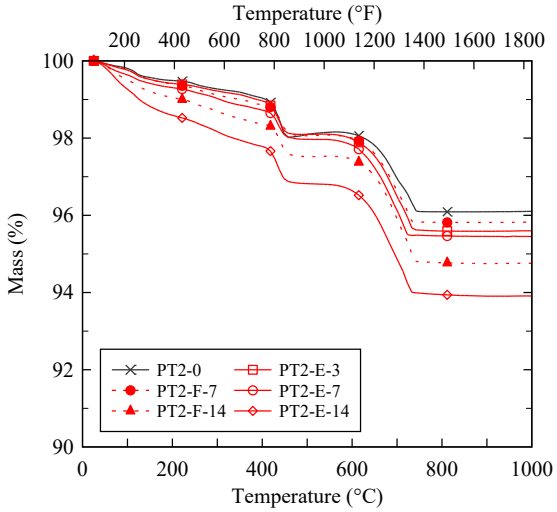

Figure 14-3 TGA results of PT2 MITT samples after *Field* and *Extreme* exposures

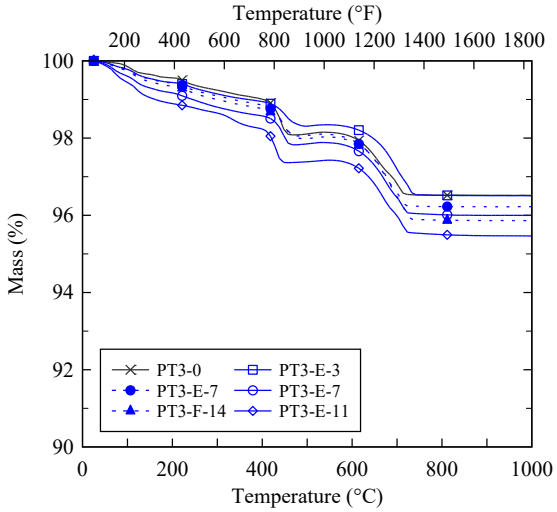

Figure 14-4 TGA results of PT3 MITT samples after *Field* and *Extreme* exposures

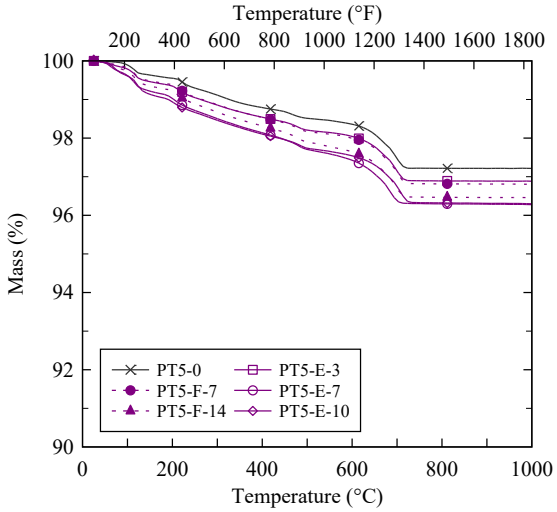

Figure 14-5 TGA results of PT5 MITT samples after *Field* and *Extreme* exposures

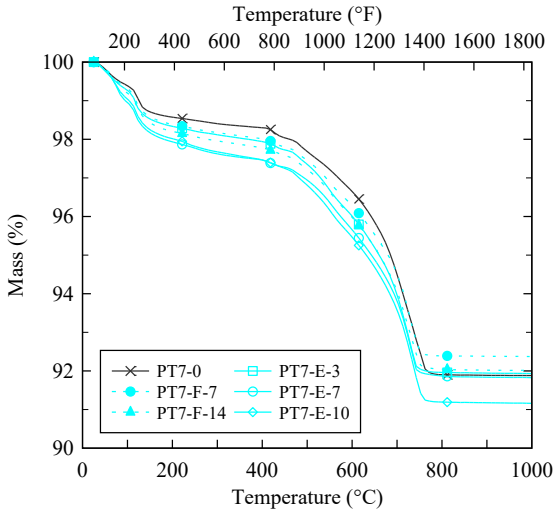

Figure 14-6 TGA results of PT7 MITT samples after *Field* and *Extreme* exposures

Figure 14-7 through Figure 14-11 show the TGA testing mass percent data for all grouts and cements from small-scale samples to both the *Field* and *Extreme* conditions. Also, the solid black line in each plot refers to the initial sample taken prior to exposure. As both the *Field* and *Extreme* exposures continued, the mass change occurring before 1022°F (550°C) showed reduced slope changes compared to the majority of the mass change that occurred after 1112°F (600°C). The mass gain during exposure associated with prehydration may likely be the source for the large mass loss between the data collected prior to 1022°F (550°C) and after 1112°F (600°C). Specifically, hydration on the surfaces of the particles due to topochemical hydration, which is favored in conditions of low water-to-solid ratios.

The small-scale grout TGA measurements up to 1830°F (999°C) show that the total initial mass percent for grouts PT1 through PT5 was between 95.7% and 97.2%, while PT7 had a mass of 90.2%. It is speculated that the higher mass loss in PT7 was attributed to the type of

SCMs or admixtures used in the mix. All of the compounds added to the grout mix may affect the prehydration sensitivity of the grout and affect the TGA mass percent results after exposure.

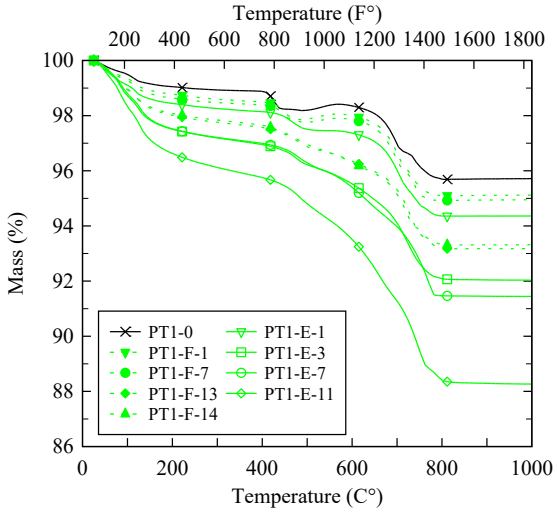

Figure 14-7 TGA results of PT1 small-scale samples after *Field* and *Extreme* exposures

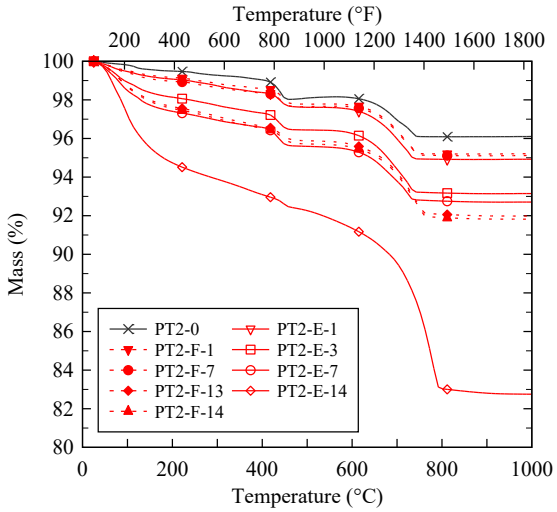

Figure 14-8 TGA results of PT2 small-scale samples after *Field* and *Extreme* exposures

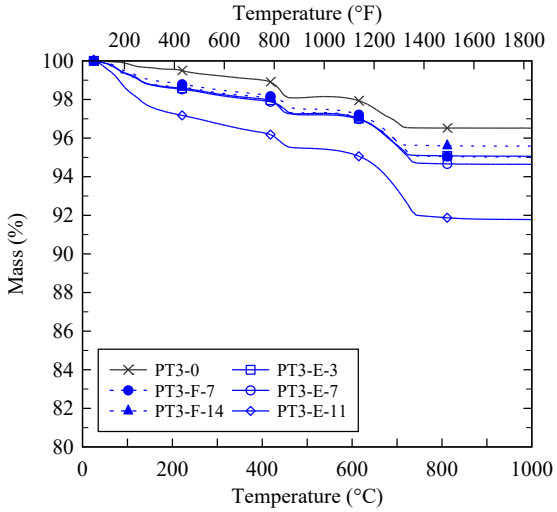

Figure 14-9 TGA results of PT3 small-scale samples after *Field* and *Extreme* exposures

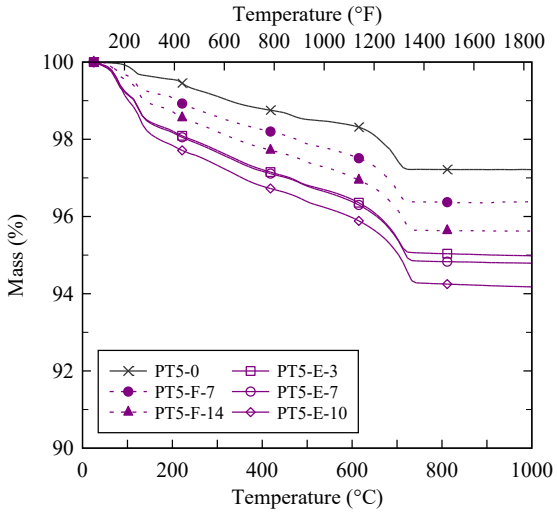

Figure 14-10 TGA results of PT5 small-scale samples after *Field* and *Extreme* exposures

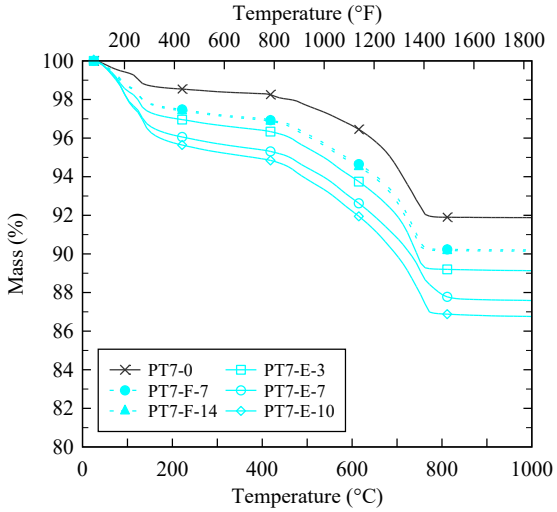

Figure 14-11 TGA results of PT7 small-scale samples after *Field* and *Extreme* exposures

14.2.2 Cements

Figure 14-12 through Figure 14-15 show the TGA data for cements from small-scale samples exposed to both the *Field* and *Extreme* conditions. The same general trend observed for MITT samples was found for small-scale samples. All small-scale samples of portland cement, except C5, showed a reduced loss in the percent of mass for all exposures compared to their respective PT grout, which means that the PT grout may have hydrated and gained more mass than its cement under the same exposure.

Although the proportions of the cement phases in the cements was unknown, it is known that the cement used in the PT grouts conforms to ASTM C150/C150M requirements. The TGA results for all initial samples of cements showed an average mass of 97.2% at 1830°F (999°C), with the least mass of 96.8% from C7. The TGA results for the initial cements showed a uniform mass change slope throughout. As exposure time increased, each cement showed some variation in mass, for example, C7 at 14 days of *Extreme* exposure showed a mass percent of 92.2% after the TGA test.

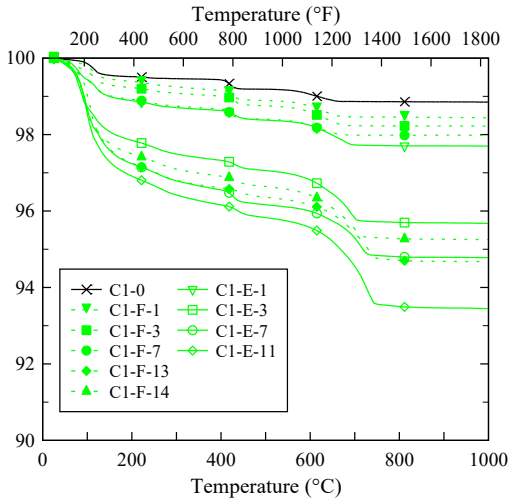

Figure 14-12 TGA results of C1 small-scale samples after *Field* and *Extreme* exposures

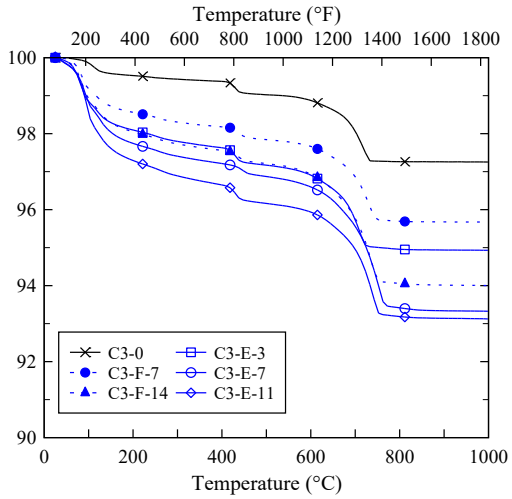

Figure 14-13 TGA results of C3 small-scale samples after *Field* and *Extreme* exposures

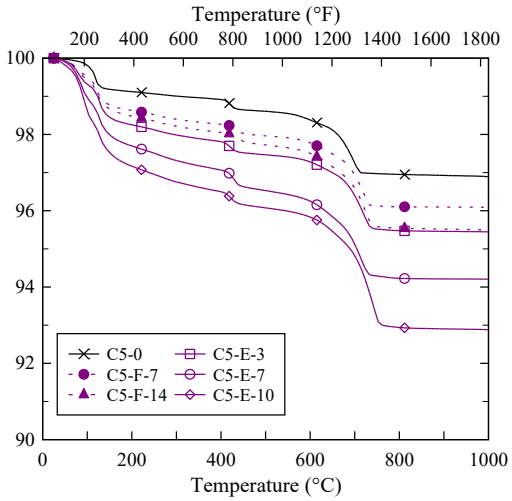

Figure 14-14 TGA results of C5 small-scale samples after *Field* and *Extreme* exposures

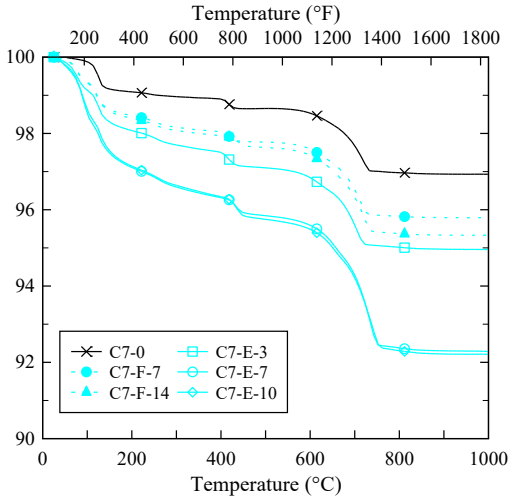

Figure 14-15 TGA results of C7 small-scale samples after *Field* and *Extreme* exposures

All small-scale TGA mass loss measurements were higher than the MITT samples in all exposure levels. This trend would suggest that the small-scale samples experienced more mass gain than the MITT samples exposed alongside. The TGA testing results supports the claim that the PT grouts and cements have an increased sensitivity to elevated temperature and elevated humidity, affecting mass gain, moisture uptake, and any other mechanisms associated with prehydration.

14.2.3 SCMs

Figure 14-16 through Figure 14-19 show the TGA results for SCMs; each figure indicates the type and time of exposure. All SCMs showed a decrease in mass with time. In addition, a higher mass loss was found for the *Extreme* exposure compared to the *Field* exposure for the

same exposure interval. All SCMs showed mass loss due to dehydration and decarbonation, usually occurring before 392°F (200 °C) and after 932°F (500 °C), respectively.

FAC (Figure 14-16) samples showed significant mass losses, especially due to dehydration of the *Extreme* exposure samples. The difference in mass loss between *Field* and *Extreme* conditions increased with time of exposure to approximately 3%.

FAF (Figure 14-17) continued the trend observed for the previous SCMs by showing minimal mass loss due to exposure. Interestingly, the largest change in mass was in the decarbonation region, which differed from other SCMs by having the largest change in mass occur in the dehydration region of temperature. Carbon can be present in fly ash, depending on the combustion process, but is often less than the LOI limit of 6%.

Silica fume (Figure 14-18) showed mass loss due to the evaporation of adsorbed water. Silica fume does not exhibit other sudden changes in mass loss, as it is almost entirely composed of inert silicon dioxide, although some mass loss can be attributed to free carbon from the manufacturing process.

Slag (Figure 14-19) exhibited a behavior similar to that observed for the PT grouts and their corresponding portland cements, as discussed earlier in this section. Slag can react with moisture resulting in hydration products such as C-S-H and hydrotalcite. Mass losses due to the decomposition of C-S-H occur before 572°F (300°C). According to Rey et al. (1992), hydrotalcite loses pore water up to about 212°F (100°C) and interlayer water up to about 482°F (250°C); dehydroxylation occurs in range of about 257°F to 977°F (125°C to 525°C), and decarbonation occurs in a range of about 572°F to 1527°F (300°C to 825°C). Also, Lopez-Arce et al. (2011) reported that $Ca(OH)_2$ at high RH levels (75%–90% RH) gives rise to amorphous calcium carbonate and monohydrocalcite, faster carbonation, and larger particles sizes with higher crystallinity compared to lower RH (33%–54% RH) conditions. This agrees with the TGA curves for FAC, slag, and FAF that showed mass losses in the decarbonation region 932°F to 1292°F (500°C to 700°C).

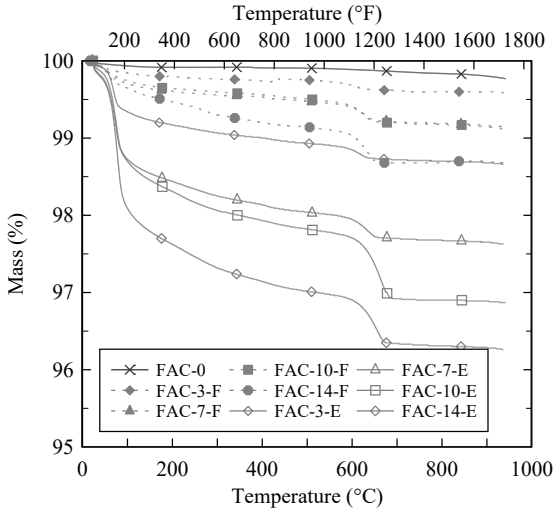

Figure 14-16 TGA results of FAC after both *Field* and *Extreme* exposures

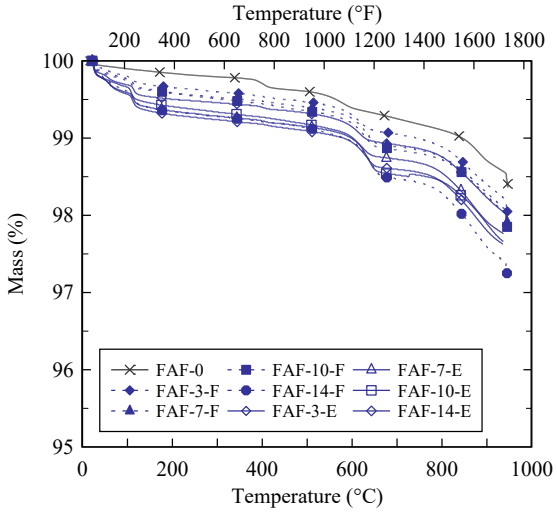

Figure 14-17 TGA results of FAF after both *Field* and *Extreme* exposures

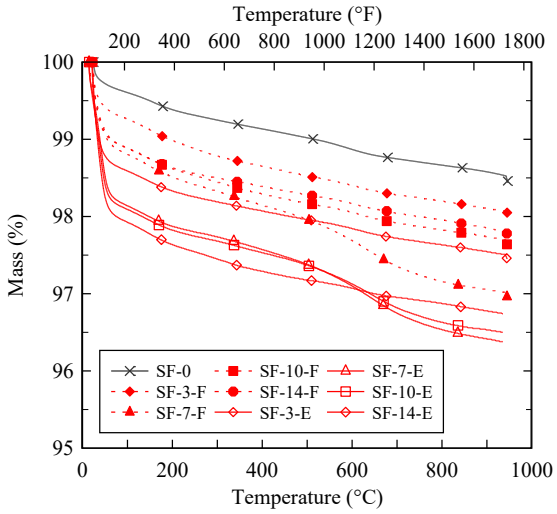

Figure 14-18 TGA results of SF after both *Field* and *Extreme* exposures

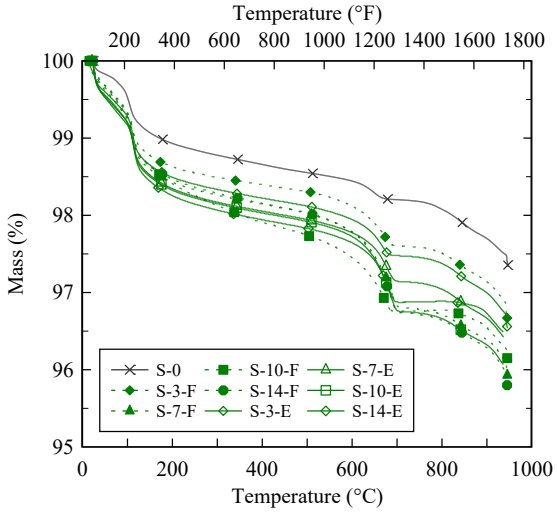

Figure 14-19 TGA results of S after both *Field* and *Extreme* exposures

15 Microwave Moisture Content

15.1 Summary of Test Method

Besides the development of methods to evaluate the amount of prehydration (mass change) experienced by PT grouts that can be employed in the laboratory, using LOI and TGA, an additional test method was desired for determining mass change at a jobsite. ASTM D4643-08 (2008) Standard Test Method for Determination of Water (Moisture) Content of Soil by Microwave Oven Heating was modified to measure the amount of prehydration that has occurred in a cementitious sample. This method has the potential to obtain results in a matter of minutes. The Microwave moisture content (MMC) method was used on PT grouts, their corresponding cements, and SCMs after various exposures.

MMC testing was done on MITT samples and small-scale samples. The basic approach was to heat a known mass of material in a typical home-use microwave for intervals not exceeding three minutes, and then measure the mass. This heating process was repeated until less than 0.01% mass change was achieved, at which point a total mass loss was determined.

The MMC test was used to track the amount of prehydration that had occurred in PT, cement, and SCM samples. Figure 15-1 shows a microwave with a 700-watt capacity that is readily available in stores. A low-end microwave, with a minimum capacity of 700 watts and a cost of less than fifty dollars, was used to ensure that any type of microwave of higher grade could conduct the MMC test. It was believed that any microwave with a capacity above 700 watts would perform the MMC test in less time due to the increased heating capacity. The MMC test data is user-dependent and, with experience, the user can modify its procedures for a known cementitious material.

Figure 15-1 Microwave Moisture Content Test

15.2 Results and Discussion

15.2.1 PT Grout

Figure 15-2 shows the MMC mass change measurements for all five PT grouts from MITT samples after imposed *Field* and *Extreme* exposures from 0 to 14 days. The MITT sample

results ranged from 0.1% to 0.9% at 7 days in both the *Field* and *Extreme* exposures. A trend similar to the other test methods was found in MMC testing, an increased mass change occurred as exposure increased. From the grout MITT samples, PT7 had the greatest mass change considering all exposure levels. PT7 was also the first grout which produced soft grout in *Field* and *Extreme* exposures. The MMC results may be an indicator of prehydration of the material prior to MITT testing.

The MMC mass results suggested that the MMC test method cannot heat the sample to the point where all of the bound water described by Whittaker (2013) is driven off at 1022˚F (550˚C). The MMC test method reached a max temperature of 421˚F (216˚C), the limitation in heating temperature may not capture all of the mass change associated with the prehydration of the cementitious material during exposure, but its relative mass change can still be used to indicate the material's prehydration change from the 0-day sample to when the material is mixed with water. The MMC test method may be a viable test method to determine mass change, of a grout or cement due to prehydration, as a preliminary field test prior to any laboratory testing.

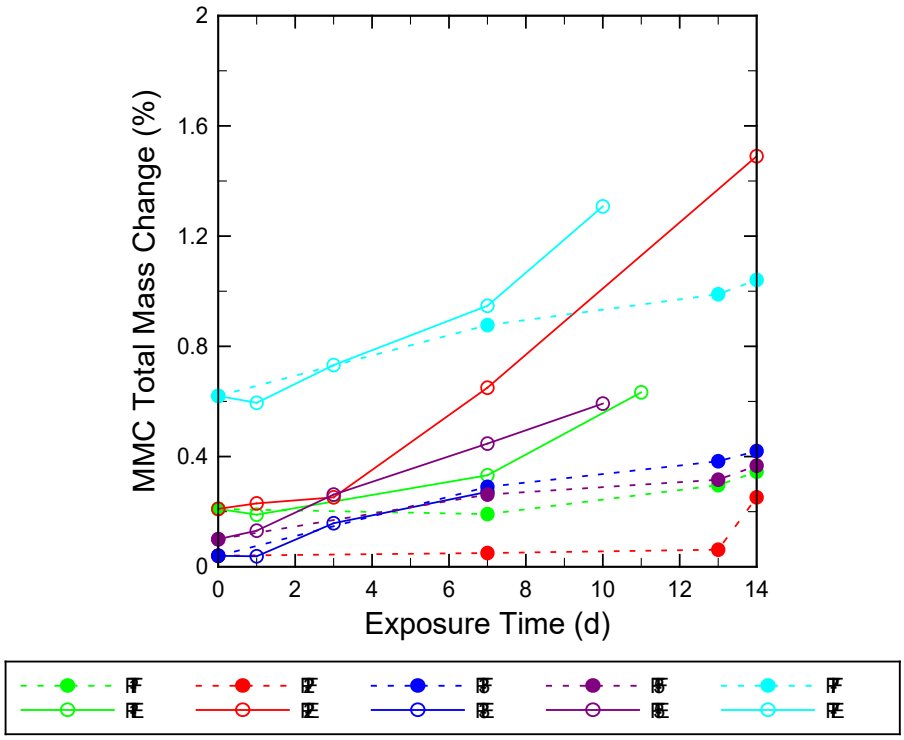

Figure 15-2 MMC testing total mass loss on MITT samples from *Field* and *Extreme* exposures

Figure 15-3 shows the MMC mass change measurements for all five PT grouts from small-scale samples after imposed *Field* and *Extreme* exposures from 0 to 14 days. The MMC results for the grout small-scale samples showed the same trends as the MITT samples. The MMC results for small-scale grouts indicate PT7 as the grout with the greatest MMC mass change increase in both the *Field* and *Extreme* exposures.

When comparing the MMC mass change from MITT samples in Figure 15-2 to small-scale samples results, for example at 7 days in the *Extreme* exposure, PT7-MITT had a mass

change of 0.9%, while in the small-scale sample the mass change was 2.8%. The MMC data suggests more mass change occurred in the small-scale samples compared to the MITT samples. As described in Chapter 11, the difference in mass gain between the small-scale and MITT samples may be due to v-blending the entire bag after exposure, which may have masked the actual particle growth at the surface of the bag.

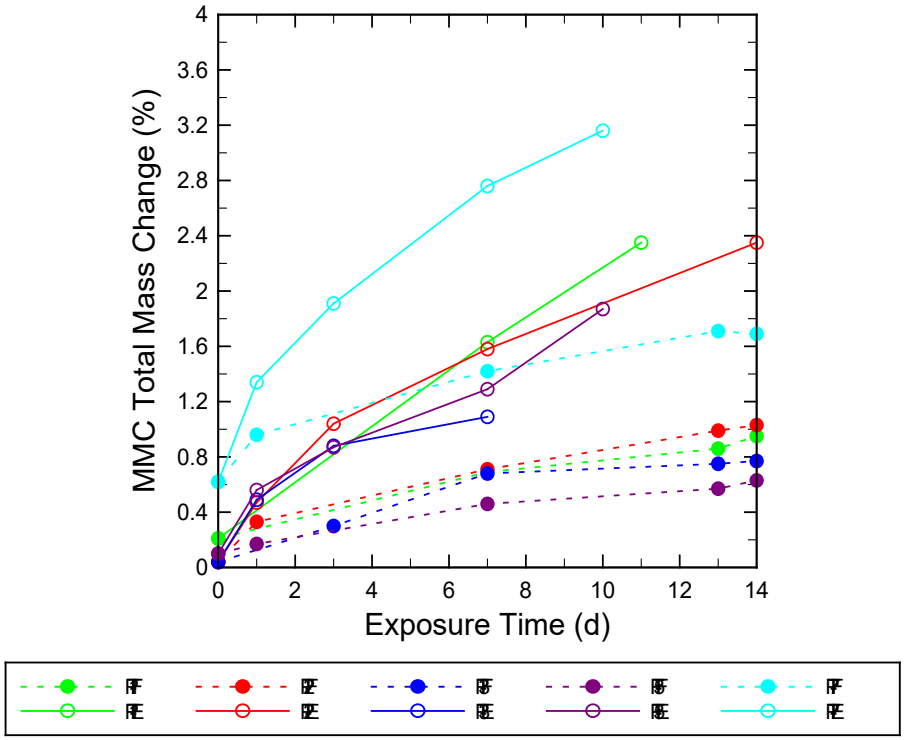

Figure 15-3 MMC testing total mass change for grouts after small-scale *Field* and *Extreme* exposures

15.2.2 Cement

Figure 15-4 shows the MMC measurements of the portland cements in the *Field* and *Extreme* exposures. All of the cements except C3 exhibited less mass loss than their respective grout. For example, at 7 days in the *Extreme* exposure, C7 had a mass loss of 1.74% while PT7 had a 2.8% mass loss. This correlation between the cements and grouts would suggest other constituents (SCMs) in the grouts are adding to the mass change behavior in addition to the portland cement during exposure.

Figure 15-5 shows the cements exposed to the *Control* and *Laboratory* conditions from 0 to 28 days. Overall, no cement exhibited a mass change above 0.25% after 28 days in either the *Control* or *Laboratory* exposures, which was below all mass change for both grouts and cements beyond 7 days of *Field* exposure, and beyond 3 days in the *Extreme* exposure. The MMC mass change results support the idea that the mass change sensitivity behavior of the cement is reduced as temperatures and humidity decrease.

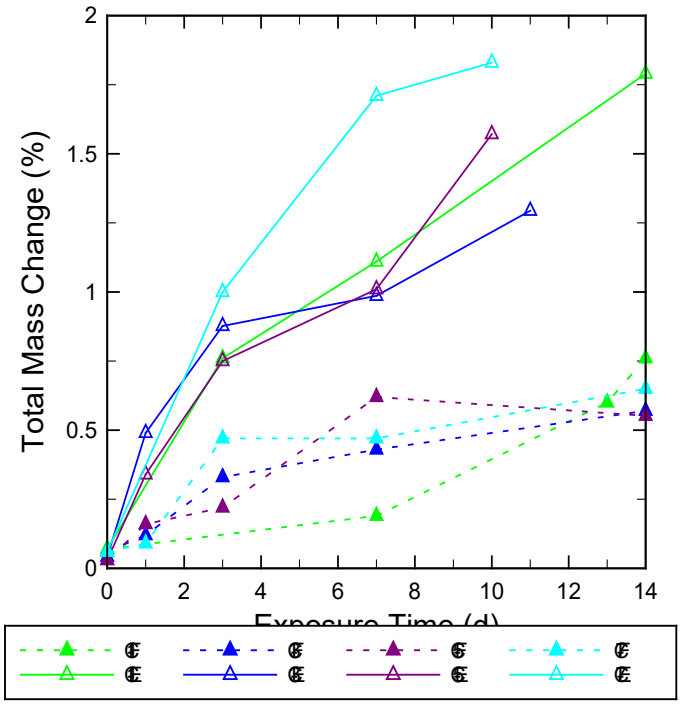

Figure 15-4 MMC testing total mass change of portland cements after small-scale *Field* and *Extreme* exposures

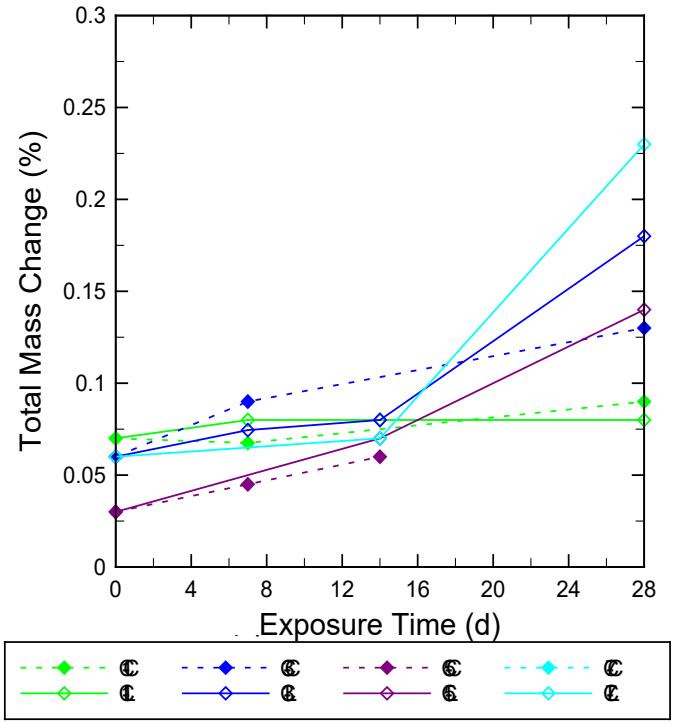

Figure 15-5 MMC Testing total mass change of portland cements after small-scale *Control* and *Laboratory* exposures

A direct comparison between LOI measurements and MMC testing is not possible due to the difference in heating temperatures and times of both test methods. In LOI, the samples were heated to 1742°F (950°C), while in MMC testing, the sample was heated to temperatures between 284°F and 420°F (140°C-216°C). As described by Alarcon-Ruiz et al. (2004), the first mass loss that occurred between 212°F and 392°F (100°C-200°C) was the evaporation of water, which was completely removed by 248°F (120°C), and was described as a rapid mass change. A second mass loss occurs between 230°F and 338°F (110°C–170°C) and corresponds to the dehydroxylation of gypsum (with a double endothermal reaction), the decomposition of ettringite, and the partial dehydroxylation of the carboaluminate hydrates. The last mass loss captured began at about 356°F (180°C), corresponding to the beginning of the loss of bound water from the decomposition of the CSH and continued dehydroxylation of the carboaluminate hydrates. Although it is known that some of these phases occur beyond the range of the heating capacity of MMC test, it can measure the mass change due to dehydration.

General trends from all MMC testing showed that increased exposure time resulted in an increase of sample heating cycles, and total mass change. All of the MMC testing trends may be associated with the mass change, which accounts for prehydration, moisture uptake, and any other hydration mechanisms at work during exposure.

15.2.3 SCM

Figure 15-6 shows the MMC mass loss measurements for all SCMs after *Field* and *Extreme* exposures. Results show that the SCMs with higher surface area had more mass loss. This does not agree with results of previous test methods, where FAC exhibited higher mass loss among all SCMs. Also, the slag samples showed very little change in mass during either *Field* or *Extreme* exposure. These results can be explained by the difference in specific surface area of each material and that the low-temperature heating cycles most likely removed adsorbed water present on the surface of the particles and not chemically bound water. This agrees well with the results, where FAC and SF showed more mass loss through exposure time and type. This finding indicates that the MMC values of PT grouts can be highly influenced by the type and quantity of SCMs present in their blend, resulting in high variability of measurements.

MMC mass losses were compared to TGA results to determine what mass losses are incurred during MMC testing. It was found that the mass loss from MMC testing of each SCM corresponded to a specific temperature range of TGA mass loss. For example, FAC mass losses from MMC testing corresponded to the TGA mass losses that occurred in a temperature range of 377°F to 831°F (192°C to 444°C), which represent losses due adsorbed water, C-S-H, and possibly $Ca(OH)_2$. FAF mass losses were found to be within 768°F to 1164°F (409°C to 629°C) of the TGA results; however, exposed samples had mass losses in the temperature range of 1122°F to 1164°F (606°C and 629°C) when compared to TGA results. This implies that for both FAC and FAF, the mass losses do not account for decarbonation, as the mass loss due to decarbonation was beyond these temperatures as discussed in the TGA results section. In the case of slag, the mass loss during MMC only represents the mass loss from 291°F to 345°F (144°C to 174°C) in the TGA test. This agrees with the previous results as the MMC test only accounts for adsorbed water and C-S-H. Finally, SF mass losses were inconsistent in terms of temperature range during TGA, as the range varied from 115°F to 1718°F (239°C to 937°C). The variation in results can be attributed to the high surface area of the SF particles and the low reactivity that SF had with moisture.

These results can be explained by the difference in specific surface area of each material and that the low-temperature heating cycles most likely removed adsorbed water present on the surface of the particles and not chemically bound water. This agrees well with the results as FAC and SF show more mass loss through exposure time and type. This finding indicates that the MMC values of PT grouts can be highly influenced by the type and quantity of SCMs present in their blend, resulting in high variability of measurements.

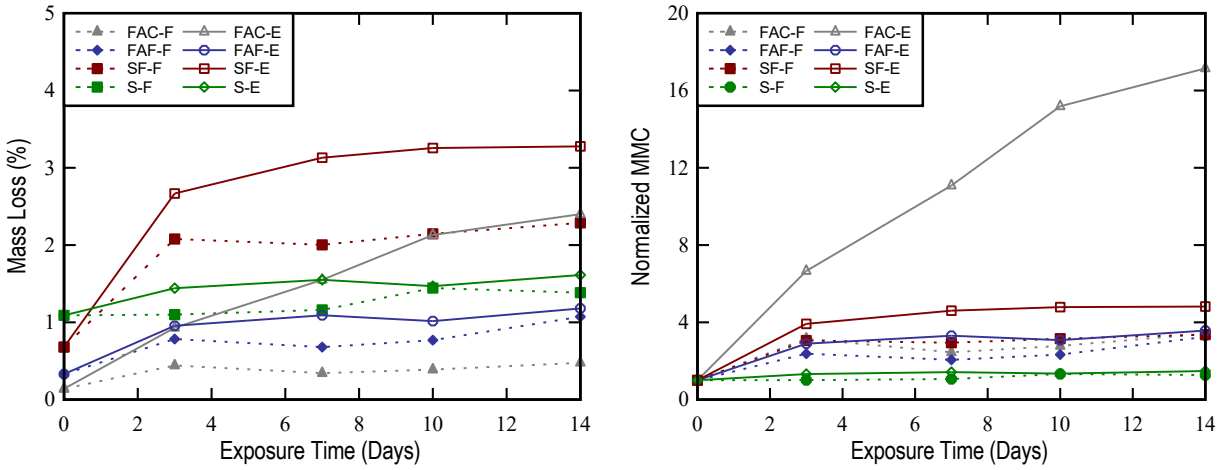

(a) (b)

Figure 15-6 Microwave moisture content results: (a) Percent mass loss and (b) Normalized MMC results

16 Deterioration Mechanisms

Several commercially-available, prepackaged PT grouts were exposed to elevated temperature and humidity to investigate their susceptibility to deterioration in such conditions. It was found that all PT grouts tested were prone to the formation of soft grout after exposure. The time required to form soft grout and the amount of soft grout itself varied among manufacturers' products, which indicates that the composition of constituents in the prepackaged bags affects the overall deterioration mechanism that results in soft grout formation.

As part of this research project, PT grout and the individual constituents were investigated to assess the susceptibility of each material to deteriorate and form soft grout. It was found that all constituents adsorbed and retained moisture during exposure. In addition, when exposed to moisture, portland cement showed signs of prehydration through changes in particle characteristics and the measurement of mass change. From the overall results, the following theories are thought to explain the deterioration of PT grouts during exposure:

1. Prehydration of portland cement is the primary cause of the formation of soft grout. It is suspected, however, that there are a number of possible synergistic effects from the deterioration of other PT grout constituents that may amplify the tendency to form soft grout.
2. Crust effect: In bagged material containing primarily portland cement, the material close to the surface of the bag tends to prehydrate more than the material deeper in the bag, forming a crust layer that follows the contour of the bag. This crust may protect inner material from moisture and prevent/slow prehydration.
3. SCMs show low reactivity, compared with portland cement, when exposed to heat and humidity. The surface-area-to-volume ratios of SCMs are proportional to the respective amounts of moisture adsorbed during exposure.
4. Dissolution of powder admixtures in the bag caused by moisture and temperature can lead to poor fresh properties, and potentially bleeding and segregation.

Potential synergistic effect (speculation)

1. Portland cement prehydration may reduce or delay the reaction rate of pozzolanic SCMs due to the reduced volume of calcium hydroxide.

16.1 Prehydration of Portland Cement

Cement prehydration was found to be most significant after exposure to high relative humidity and is presumed to be one of the main causes of soft grout formation. This conclusion regarding prehydration of portland cement was deduced during mass gain tests. The mass gain test was used to track the increase in weight of PT grout and individual grout constituents during exposure. Figure 16-1 shows mass gain results during *Extreme* exposure for PT1 and individual grout cementitious materials. This figure shows that the increase in mass gain for PT1 and C1 are almost identical, suggesting that mass gain occurs mainly due to moisture consumed as a result of prehydration reactions of the portland cement.

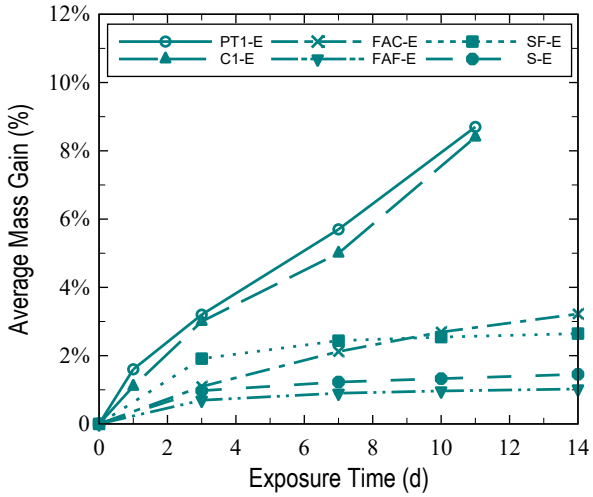

Figure 16-1 Mass gain comparison of PT grout cementitious constituents

Prehydration of portland cement results in effects that are likely related to soft grout formation as illustrated in Figure 16-2. For example, during heat of hydration testing it was observed that most PT grouts underwent a retardation of the hydration reactions compared to the unexposed material, which can be attributed to the prehydration of portland cement and admixture deterioration. Retardation of hydration reactions result in a delay of setting time, which can prolong the movement of lower-density, partially hydrated cement particles, particle size, and unreactive fillers to the top of the post-tensioning duct prior to set. Such delays in set time could increase the volume of soft grout that accumulates due to segregation. This implies that with retardation, the time for the segregation mechanism to occur increases, resulting in higher probability of bleeding and soft grout formation in the upper section of the tube. Although it is thought that prehydration is the primary cause, further work is needed to investigate the deterioration of admixtures and its effect on setting time.

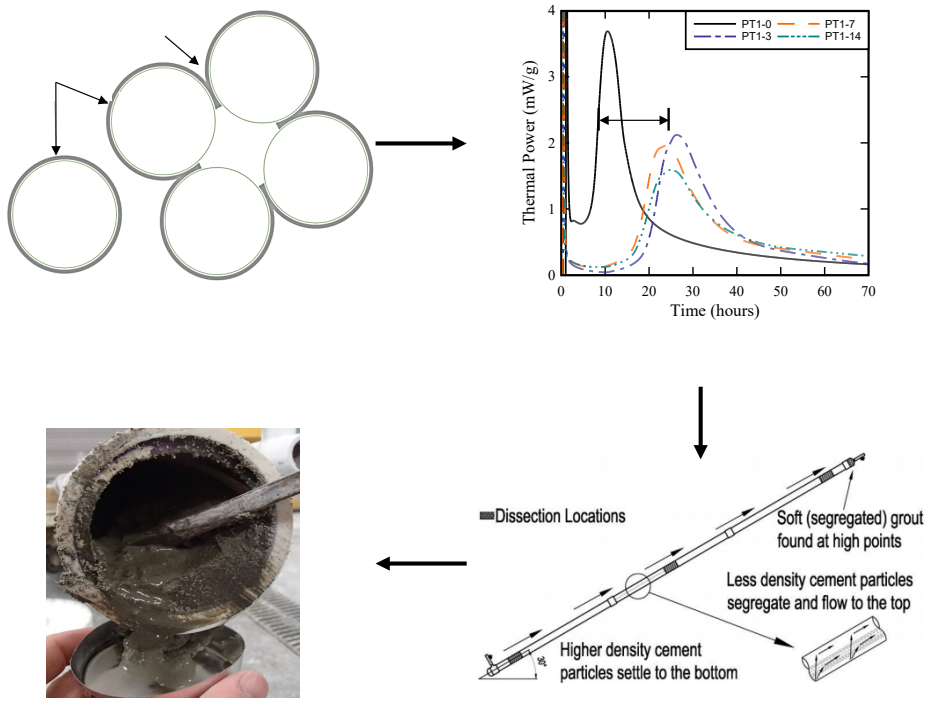

Figure 16-2 Suggested mechanism for soft grout formation

16.2 Crust Effect

PT grout bags have printed information that specifies the recommended storage conditions and shelf life of the grout. In the present study, PT grout bags were placed in environmental chambers and exposed to elevated temperature and humidity levels. Normally, bags are lined to limit moisture penetration, but there are no requirements regarding their effectiveness in protecting the contents from moisture. The arrangement and level of protection provided by the bag varies among manufacturers, resulting in different protection levels. To avoid the effect of this variation and ensure consistency of exposure during testing, bagged samples were exposed by making three 18-in. incisions in the bag before exposure.

As a result of the exposure, the dry portland cement reacted with the excessive moisture to form hydration products such as the cementing phase calcium-silicate-hydrate (C-S-H) and calcium hydroxide (CH). These hydration products form a semi-hardened crust layer near the bag surface. If sufficient hydration occurs, then the crust will slow or prevent further moisture penetration to the dry material underneath. This behavior was verified during layered LOI testing, where the top layer had higher mass gain (from moisture adsorbed and reacted) than the remaining layers. Also, it is assumed that the level of protection provided by the crust depends on the amount of portland cement and type of SCM used. For instance, if the amount of cement in the prepackaged bag is low due to the presence of an SCM, the crust may not be as thick and would allow moisture to penetrate further into the bag. The mechanism of formation of the crust in PT grout bags and grout samples used in this study is shown in Figure 16-3.

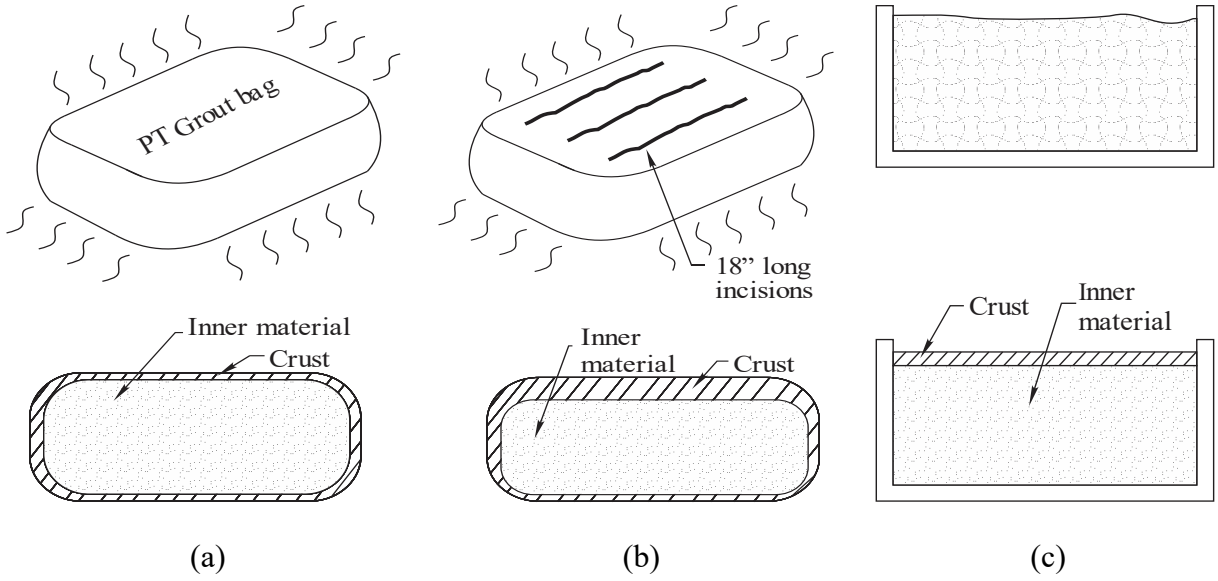

Figure 16-3 Locations of crust formation during exposure: (a) Normal PT grout bag, (b) MITT PT grout bag, and (c) Small-scale container

16.3 Effect of SCM

Supplementary cementitious materials are typically used in prepackaged PT grout, but specific types and quantities are proprietary. SCMs are blended with the cement to improve fresh properties, reduce bleeding, and reduce cost. The addition of these materials does not contribute to soft grout formation if storage conditions are adequate; however, it is possible that under adverse exposures, the presence of SCMs can contribute to soft grout formation or faster deterioration as shown in Figure 16-4. The specimen having only portland cement would form the crust faster and slow down moisture penetration into the material. On the other hand, the specimen with SCMs would allow further penetration of moisture, which on a volume basis, a greater penetration would always result in higher percentage of portland cement prehydration. SCMs do not have the same level of reaction with moisture, but can store water in the particles surface, and allow more penetration of the moisture until a crust of hydration products forms to protect the material underneath.

One example of the effect of SCM is shown in Figure 16-5 and Figure 16-6, where both PT2 and PT3 are from the same manufacturer and utilize the same portland cement, but had different results in the LOI layered test. PT2 is recommended for injection in vertical tendons, as it is capable of providing bleed resistance under this configuration. One of the reasons to include an SCM in the prepackaged blend is to decrease bleeding due to the smaller particle size compared to portland cement particles i.e., silica fume. PT3 is designed to be pumped over long distances or tight openings and provides higher compressive strength than PT2, suggesting that it has a higher cementitious material content. PT2 and C2 LOI data had a 12.5% greater mass loss for the top layer after *Extreme* exposure (Figure 16-5). This difference in LOI suggests that PT2 has a high SCM content, which agrees well with the application of PT2, which is manufactured to be bleed resistant and fill vertical tendons. PT3 had 1.5% greater LOI mass loss after *Extreme* exposure compared to the respective portland cement used in its blend. The comparison of both

PT2 and PT3 support the hypothesis that an increase in the percent replacement of portland cement would result in more moisture absorption due to deeper moisture penetration, resulting in a thicker crust formation. Further investigation with several PT grout mixtures having different proportions and types of SCM is recommended to evaluate the effects of moisture penetration and the crust effect. Knowledge about the prehydration rate on each PT grout mixture can then be related to particle size growth or mass gain changes from prehydration for further development of a test method to determine the shelf life.

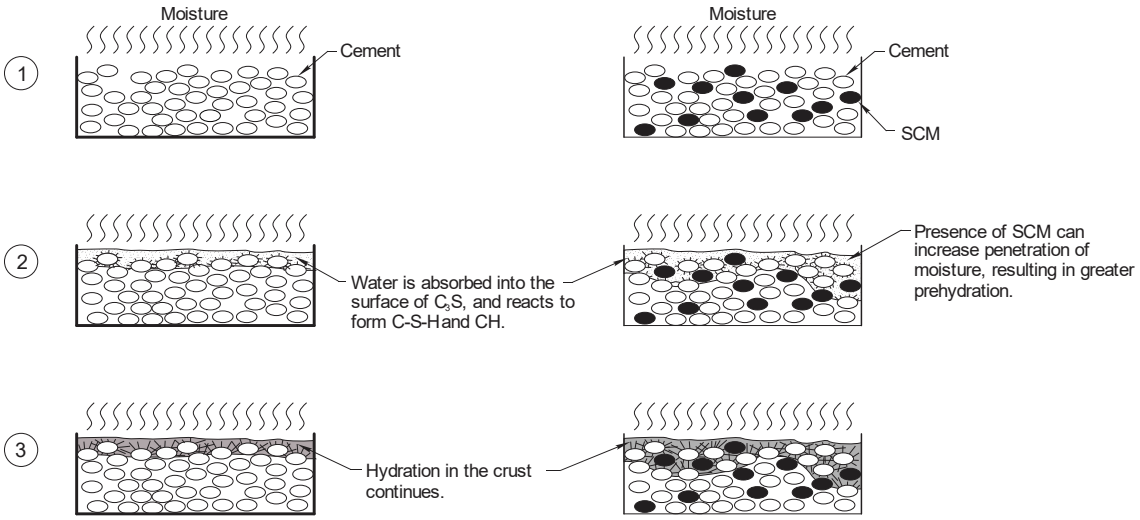

Figure 16-4 Effect of SCM during exposure of small-scale samples

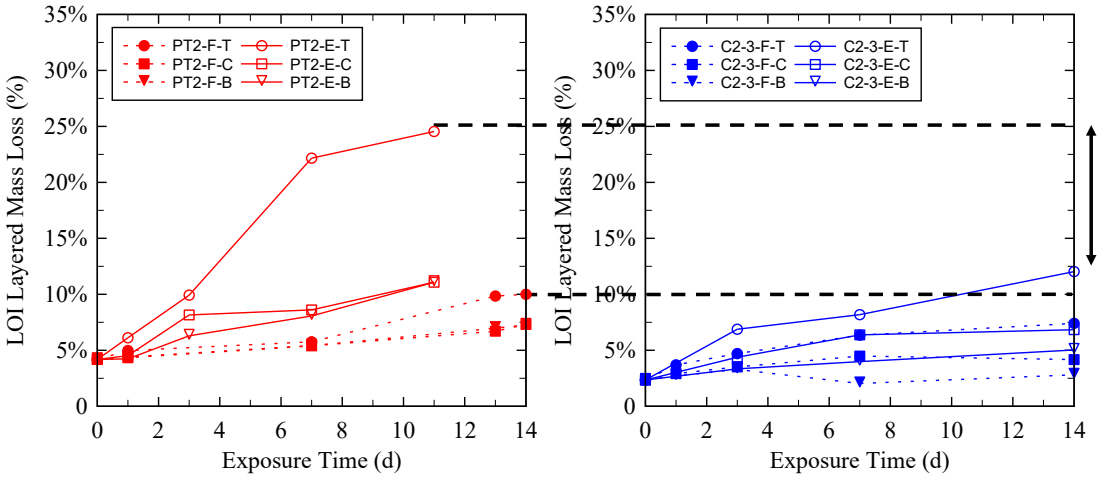

Figure 16-5 LOI mass loss results of PT Grout PT2 and its corresponding cement C2

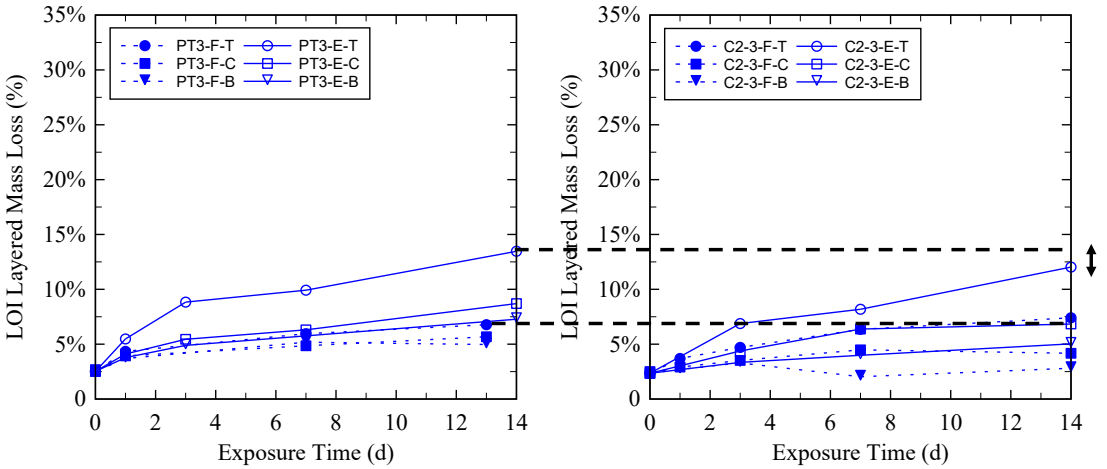

Figure 16-6 LOI mass loss results of PT Grout PT3 and its corresponding cement C2

16.4 Dissolution of Admixtures

Admixtures were found to be very sensitive to elevated temperature and humidity. In this study, the deterioration of the admixtures was investigated by dynamic shear rheometer testing and bleed testing. Nominal shear rate (NSR) results were used to evaluate the effect of exposure on the admixture performance by analyzing changes in the viscosity between fresh and exposed material. During exposure, admixtures exhibit physical changes and their effect on performance was unknown prior to testing. NSR viscosity showed that the cement paste prepared with the exposed admixture was still able to maintain some level of fluidity after mixing with water. That part of the study, however, was performed by exposing the dry-powder admixtures alone, and not when blended with the portland cement and SCM. During exposure, it was observed that the admixtures absorbed sufficient moisture to dissolve and form a pasty liquid. Considering that the admixture particles dissolve during exposure, this would be likely to occur inside the prepackaged bag as well. After the admixture dissolves, the moisture may be readily available to hydrate the cement if it sufficiently wets the cement particles

Figure 16-7 shows an illustration of an admixture particle dissolving between cement and SCM particles. This would result in agglomerations and possibly more prehydration of the cement particles due to higher moisture available from the saturated admixture. Also, the reaction products that would form from the prehydration of the cement and the admixture dissolution are unknown and further testing such as XRD or SEM is recommended to investigate the interface of this reaction.

Finally, it can be concluded that admixture performance diminishes due to exposure, but can also contribute to further agglomerations, which delay setting and foster segregation.

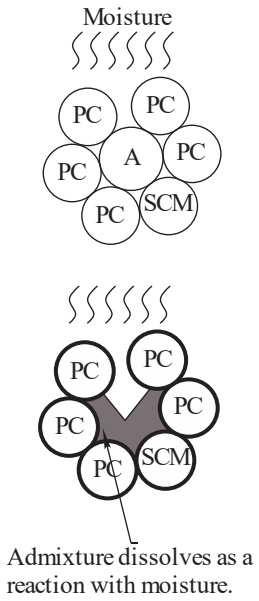

Figure 16-7 Dissolution of admixtures resulting in agglomeration of portland cement during exposure

16.5 Possible Synergistic Effect

In addition to the direct prehydration of the portland cement, deterioration of other PT grout constituents can cause synergistic effects that can result in soft grout formation. Soft grout is defined as an unhydrated material of putty consistency. A material of similar characteristics was found by Randell et al. (2015) during MITT when incorporating powdered limestone to replace portland cement. The amount of soft grout increased with the increase of limestone dosage due to the low-reactivity nature of the powdered limestone. A similar effect can occur with SCMs that need specific conditions for the pozzolanic reaction to occur. During exposure, portland cement reacts with the moisture to form C-S-H and CH. The formation of these compounds prior to mixing and the reduced surface area available for reaction due to formation of agglomerates can result in less available CH in the solution during mixing and injection in the tendon. This suggests that during the initial hours after injection, SCMs such as silica fume may move to the upper section of the tube due to the mass transport mechanism occurring in the inclined tube. This effect is supported by the MITT research by Lau et al. (2016), which found soft grout accompanied with deposits of unreacted silica fume. The combination of unhardened material and bleeding, due to segregation of particles, would result in soft grout formation in the upper section of the tendon. Consequently, it is recommended to investigate the chemical and physical composition of the bleeding in the upper section and the hydration phases formed in the first 24 hours for both unexposed and exposed grout.

17 MITT and Screening Test Calibration

This section presents an analysis of the MITT results along with the results from selected shelf-life screening tests. Screening included the small-scale mass gain (MG) test, particle size analysis (PSA), Blaine fineness test (BF), loss on ignition (LOI), thermogravimetric analysis (TGA), and microwave moisture content (MMC), all of which were used to determine cementitious mass change sensitivity effects from *Field* and *Extreme* exposures. The raw data of the screening tests is listed in Appendix K.

MITT soft grout results (see Figure 17-1) were used to calibrate the limits for the screening test methods. This approach allows the potential for soft grout formation to be easily and quickly evaluated using screening tests without conducting the expensive and time-consuming MITT. As an example of the procedure, Figure 17-2 shows the process used to calibrate mass gain results to the MITT soft grout results. Under *Field* exposure, soft grout was found during MITT at 13 days of exposure. The next shorter exposure time that did not produce soft grout during MITT was then conservatively selected as the limit on exposure time under the *Field* conditions (7 days). This selected exposure time was then used to determine a mass gain for the same exposure time. In this particular example, if the bagged PT grout was protected such that the mass gain was prevented from exceeding 2.1%, then soft grout would not be expected to form by that same grout in MITT. Notice that in some cases soft grout was found at an earlier age during *Extreme* exposure; for example, at 4 days the mass gain value was 4.1%, which was above the value found at 7 days of *Field* exposure (2.1%). As a result, the lowest mass gain value before soft grout was found for any exposure was designated as the limit.

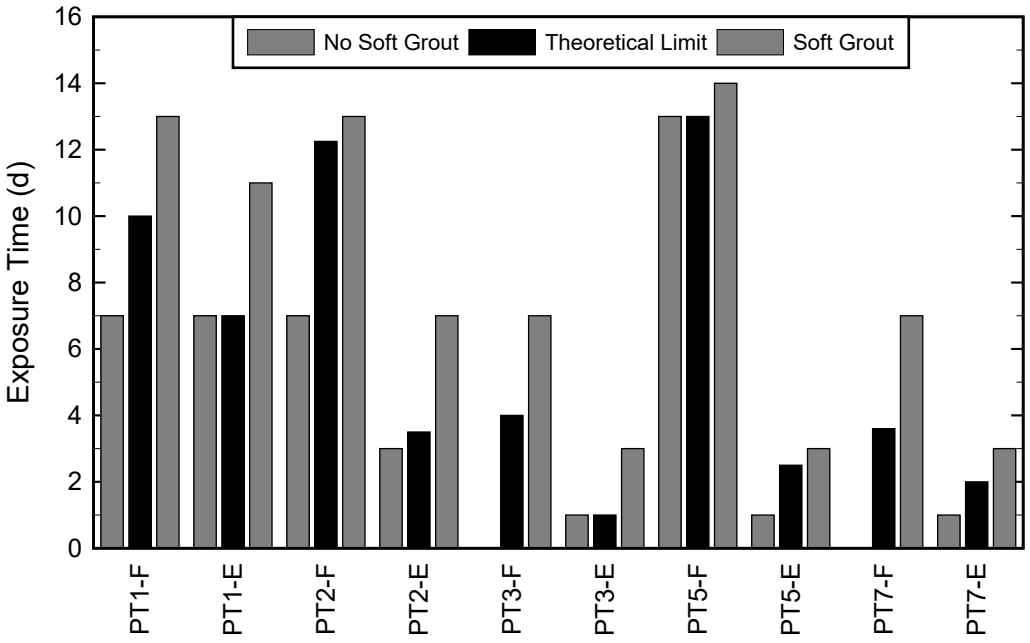

Figure 17-1 Exposure times resulting in MITT soft grout formation, and the estimated exposure time, estimated from linear regression, needed to initiate soft grout formation

The limits provide a range of screening test values that signal the possibility of soft grout formation for field-tested PT grouts. Or, more simply, that the grout was beyond its shelf life. It

is expected, however, that there was a specific mass gain associated with the formation of soft grout, which was independent of the exposure time. Soft grout should be formed at a consistent level of moisture uptake for a particular PT grout. Practical testing limitations, however, dictated that MITT could not be conducted daily. Insufficient data were available to generate a trend that could then be used to interpolate the exposure time to the nearest day. Accordingly, the actual exposure time will vary between the selected limit and the first MITT to produce soft grout. Nevertheless, the limits selected here should be less than the actual exposure time based on the process used. Furthermore, in applying this process to a single PT grout, one could envision conducting MITT daily until soft grout is formed, thus providing a more accurate measure of the exposure time. The results presented here can assist with estimating the total amount of time required to form soft grout.

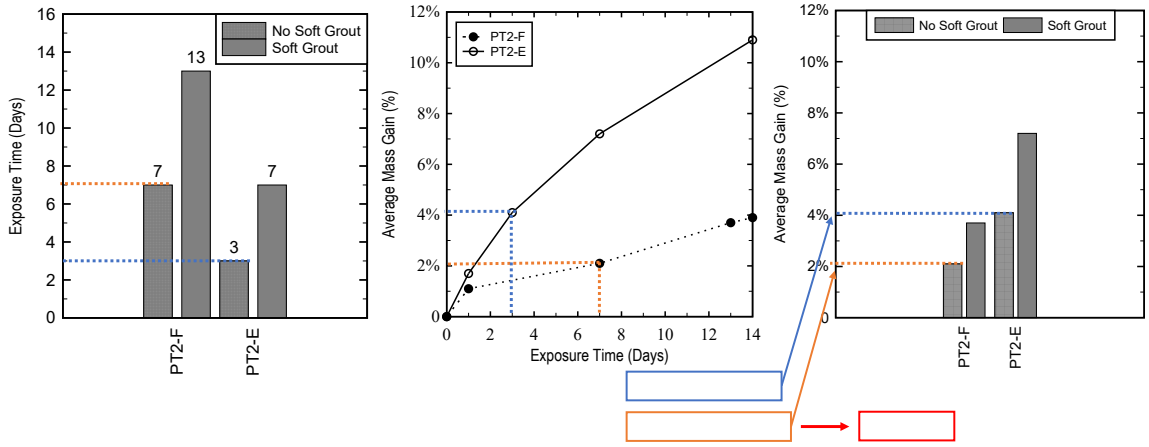

Figure 17-2 PT2 MITT results and shelf life correlation process using percent mass gain results.

17.1 Mass Gain

Mass gain measurement tests were performed to determine the physical mass gain sensitivity of PT grouts. The mass gain measurements were recorded on intervals of 1, 3, 7, 13, and 14 days. Mass gain measurements relate to the time of exposure that produced soft grout for each PT grout. Figure 17-3 shows the small-scale samples of grout in average mass gain testing with individual grout limits. The mass gain data showed an increase of at least 1.4% before any PT grout in the *Field* exposure would have formed soft grout. However, the mass gain of 1.4% cannot be simply used as the limit against which all grouts are measured because many of the *Extreme* exposures that produced mass gains above 1.4% did not produce soft grout. It appears that the relative change in small-scale mass gain that would indicate the formation of soft grout during MITT varies by manufacturer; therefore, each grout has its individual limits. As previously explained, the shelf life screening tests would set an overall limit of 1.1% small-scale mass gain in all PT grout tested, which would theoretically not produce soft grout during MITT. The study supports the claim that the average mass gain testing, in conjunction with various screening tests, can be used to evaluate the susceptibility of soft-grout formation in PT grouts.

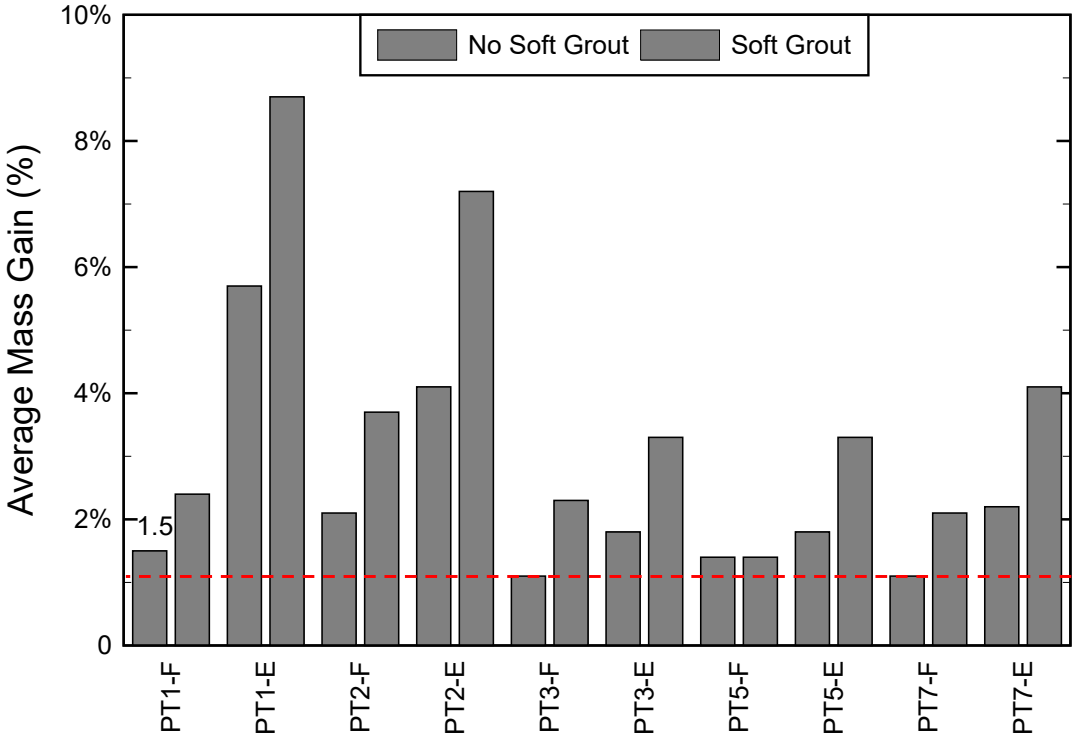

Figure 17-3 Average mass gain percent from small-scale samples after *Field* and *Extreme* exposures

17.2 Particle Size

Particle size measurements were taken for the as-received materials, and after exposure of the materials to different storage conditions for periods of time between zero and fourteen days. Particle size analysis was performed on the dry and wet grout materials and portland cements; testing was done with a Horiba LA-950V2 Laser Scattering Particle Size Distribution Analyzer. Figure 17-4 shows the normalized, dry-PSA mean particle size data, with individual grout limits, collected for MITT samples after *Field* and *Extreme* exposures. Figure 17-5 shows the dry-PSA, mean particle size data collected from the small-scale containers subjected to *Field* and *Extreme* exposures. From the current PSA data collected in this study, the overall limits were not established for MITT samples or small-scale samples. Dry-PSA results did not exhibit a clear trend when comparing mean values of samples that formed soft grout to those that did not. For instance, for the MITT samples (Figure 17-4) after *Field* exposure, the normalized mean values for PT1-F were 0.7 and 0.6, respectively, for with and without soft grout. These values differed from the normalized mean values of PT7-F, which were 1 and 1.2 for with and without soft grout, respectively. In addition, the conditions for soft grout formation differed among PT grouts. For example, for the small-scale samples (Figure 17-5) after *Field* exposure, PT1-F exhibited a decrease in mean particle size of 0.1, PT5-F showed no difference, and PT7-F showed an increase of 0.2.

Figure 17-4 Normalized dry PSA mean particle sizes for MITT samples of grout after *Field* and *Extreme* exposures

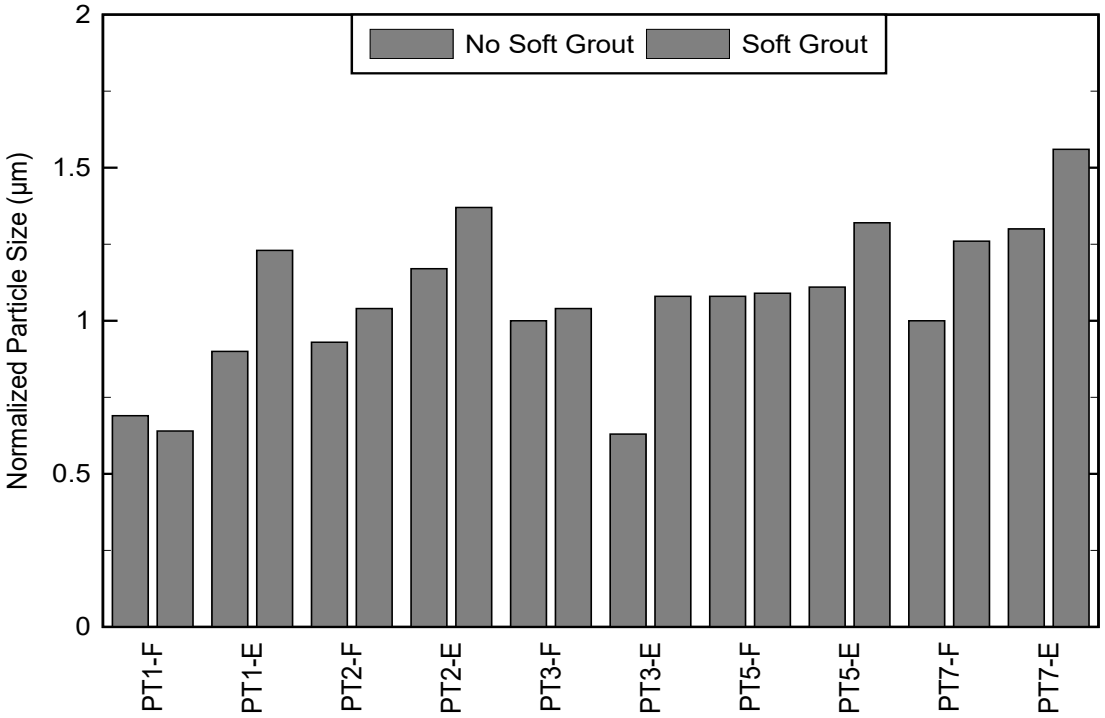

Figure 17-5 Normalized dry PSA mean particle sizes for small-scale samples of grouts after *Field* and *Extreme* exposures

Selection of an overall limit for wet PSA was not possible, because in some cases, such as PT3-E, soft grout formation occurred at a lower mean value than the samples with no soft grout. Figure 17-6 shows the normalized, wet-PSA mean particle size data, with individual grout limits, collected for MITT samples after *Field* and *Extreme* exposures. Figure 17-7 shows the dry-PSA mean particle size of the small-scale samples collected after *Field* and *Extreme* exposure . Similar to MITT samples, the formation of soft grout was not correlated to an increase or decrease of particle size from the PSA measurements, which did not allow establishment of a limit. The inconsistency of the results could have been a result of the ultrasonic homogenizer capacity to separate agglomerations formed during prehydration. The degree of hydration of the cement particles affects the ultrasonic homogenizer power setting needed to break apart the agglomerates.

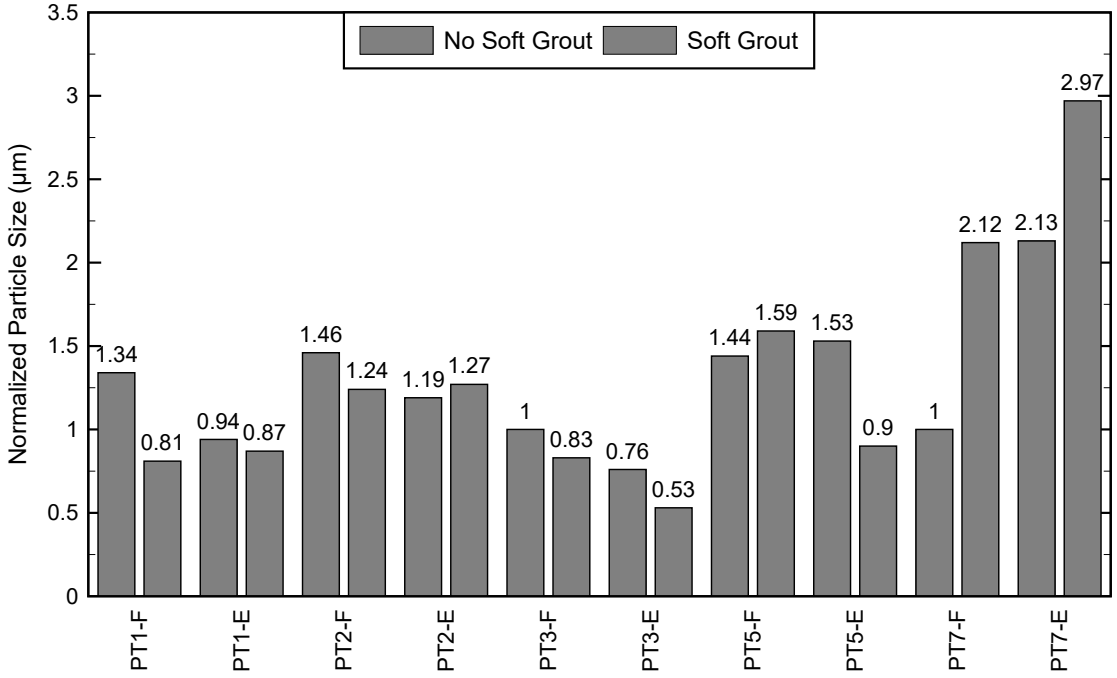

Figure 17-6 Normalized wet-PSA mean particle sizes for MITT samples of grout after *Field* and *Extreme* exposures

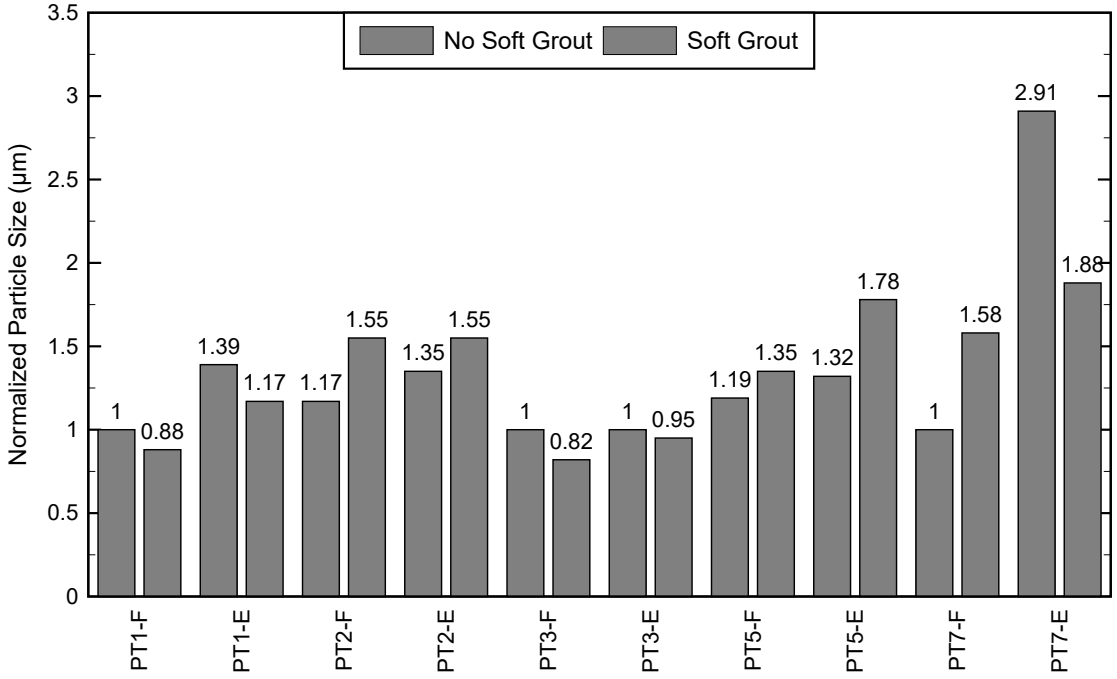

Figure 17-7 Normalized wet PSA mean particle sizes for small-scale samples of grouts after *Field* and *Extreme* exposures

17.3 Blaine Fineness Ratio

The Blaine fineness test measures the surface area per unit volume of cementitious materials. For this study, the Blaine time of unexposed and exposed samples was used to calculate the BF_{ratio} (Equation 1).

Figure 17-8 shows the BF_{ratio}, with individual grout limits, of MITT grouts exposed in *Field* and *Extreme* conditions. The soft-grout screening limits for the BF_{ratio} data of MITT sampleswere as follows. The overall limit of 0.85 for the BF_{ratio} would suggest that grout used to make MITT samples with a ratio above 0.85 will not produce soft grout. If a PT grout fails a screening test, the PT grout may be tested using MITT.

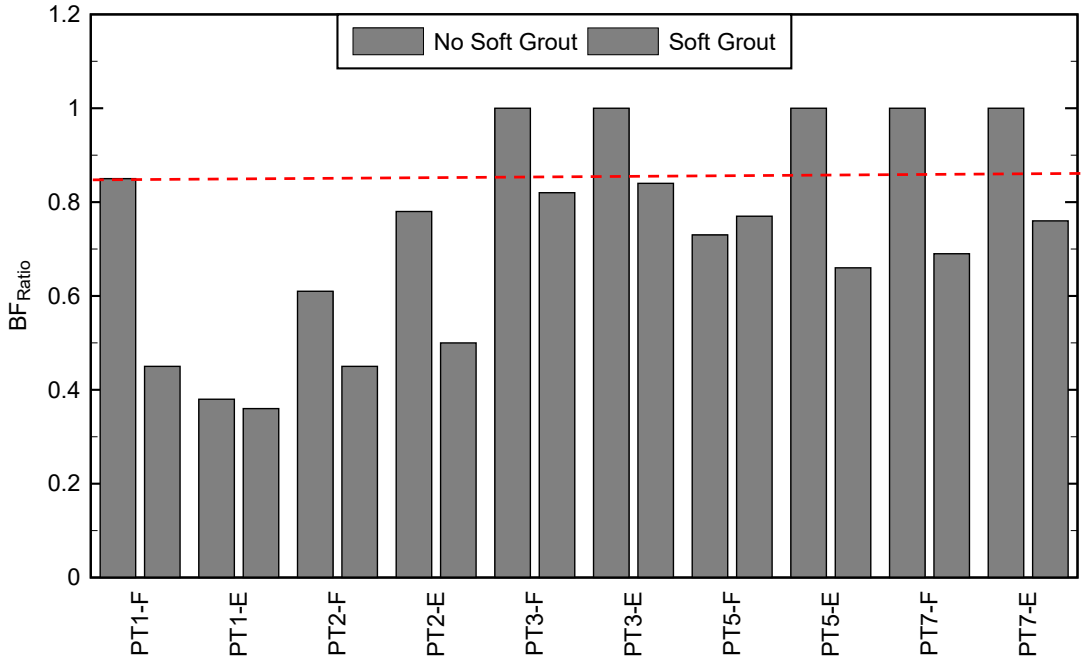

Figure 17-8 BF_{ratio} for MITT samples of grout after *Field* and *Extreme* exposures

Figure 17-9 shows the BF_{ratio} of small-scale grouts exposed to *Field* and *Extreme* exposures. The same trend of decrease in Blaine fineness for MITT samples was also seen in small-scale testing. Estimating shelf life using small-scale BF_{ratio} limits was done as follows. The overall limit of 0.93 BF_{ratio} suggests small-scale samples with a ratio above 0.93 would not be expected to produce soft grout. If a PT grout fails the BF_{ratio} screening test, it can be tested using MITT.

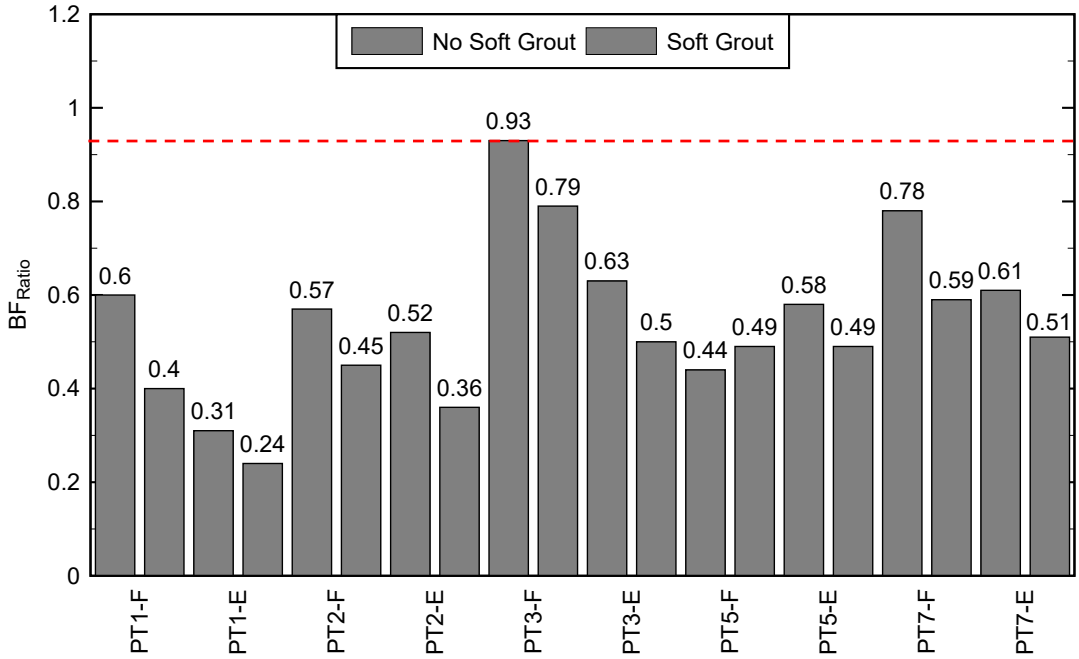

Figure 17-9 BF_{ratio} for small-scale samples of grout after *Field* and *Extreme* exposures

17.4 Loss on Ignition

Loss on Ignition (LOI) measures the mass gain caused by prehydration of the grout by heating the specimen to a sustained temperature of 1832°F (1000°C). The mass loss resulting from heating the specimen is related to the prehydration of the PT grout.

Figure 17-10 shows the PT grouts' normalized mass changes from MITT samples after *Field* and *Extreme* exposures. The shelf-life test method limits for MITT samples' normalized LOI data were as follows. The overall limit of 1.03 suggests MITT samples would not be expected to produce soft grout if the normalized LOI data is below 1.03. Additional screening tests, used in parallel with the LOI test method, would help evaluate the potential for soft grout formation.

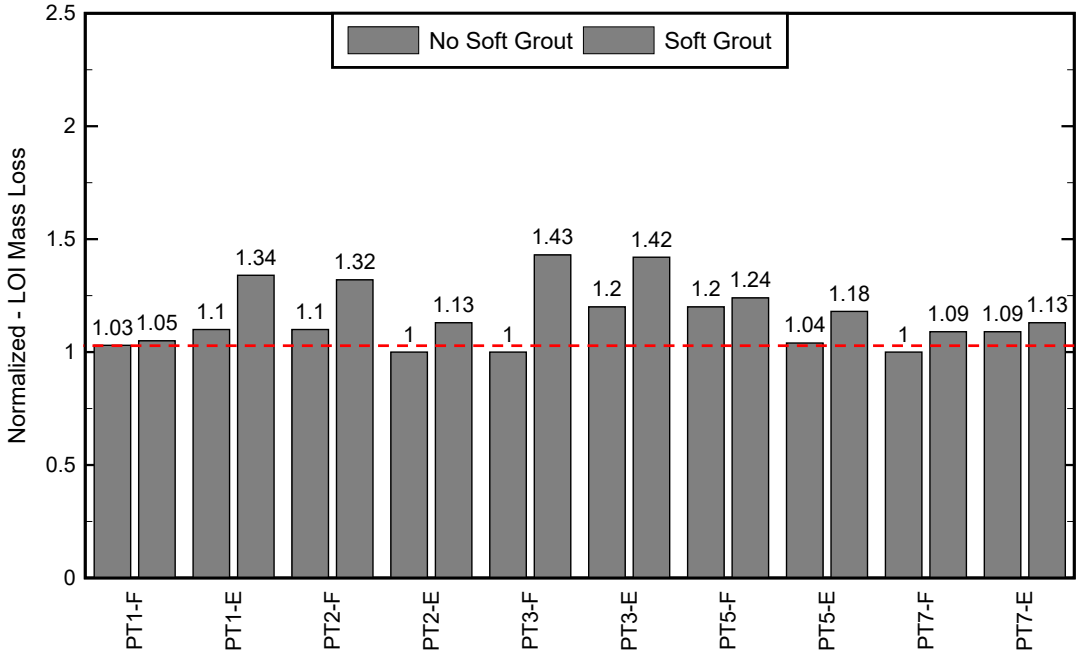

Figure 17-10 Normalized LOI mass loss from MITT grout samples after *Field* and *Extreme* exposures

Figure 17-11 shows the normalized average of LOI values, with individual grout limits, for small-scale grout samples from *Field* and *Extreme* exposures. The overall shelf-life screening limit determined from small-scale, normalized LOI data was established as the first value, for which no soft grout was formed, that was below the lowest value for which soft grout was formed. The limit of 1.26 indicates small-scale samples will not produce soft grout if the normalized LOI is below 1.26.

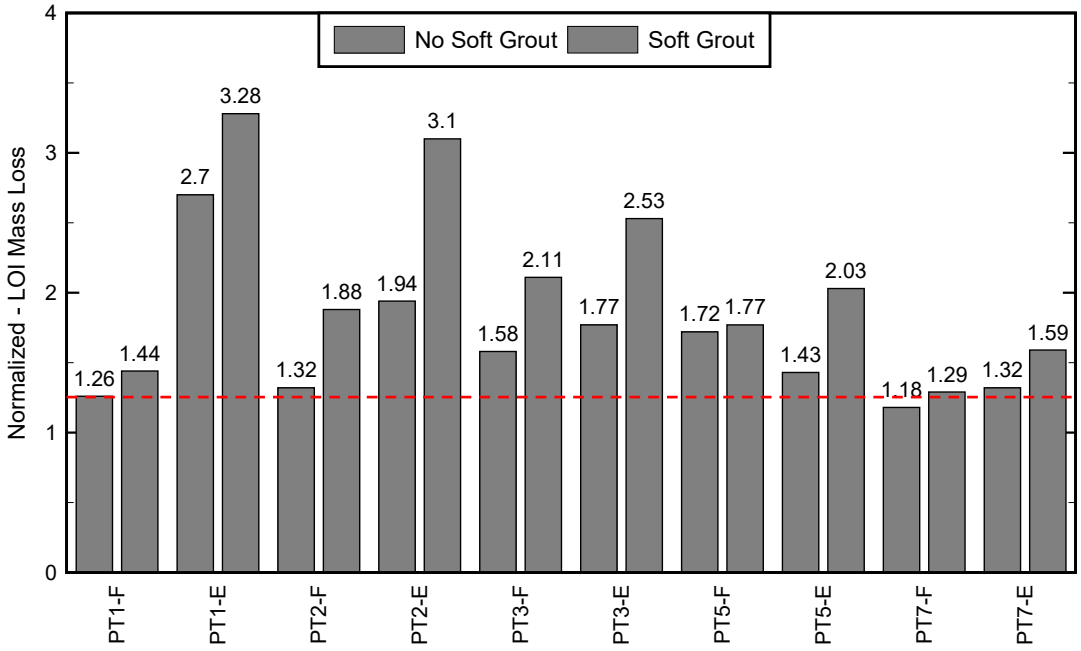

Figure 17-11 Normalized average LOI mass loss from small-scale grout samples after *Field* and *Extreme* exposures

17.5 Thermogravimetric Analysis

TGA measures weight changes in a material as a function of temperature and time under a controlled atmosphere. The TGA procedure involved heating a grout sample at a controlled rate in a laboratory furnace from ambient temperature to 1832°F (1000°C), while continuously recording the sample mass. The intention was to use the TGA data to establish a mass loss limit to determine shelf life (service life of grout without soft grout formation).

TGA testing was conducted on PT grouts that were exposed to *Field* and *Extreme* conditions. Figure 17-12 shows the MITT grout samples tested in a thermogravimetric analyzer (TGA) after *Field* and *Extreme* exposures.

The results show that soft grout first appeared in PT5 at a mass loss of 3.1% for *Extreme* exposure. This mass loss was below the mass losses for *Field* exposure samples for which soft grout was found. For MITT samples, the limit was chosen as the highest value of mass loss before soft grout was found after either *Field* or *Extreme* exposures. Thus, the selected limit was 2.7% mass loss. This limit indicates that any grout (from the tested grouts) with mass loss below 2.7% would not result in soft grout formation.

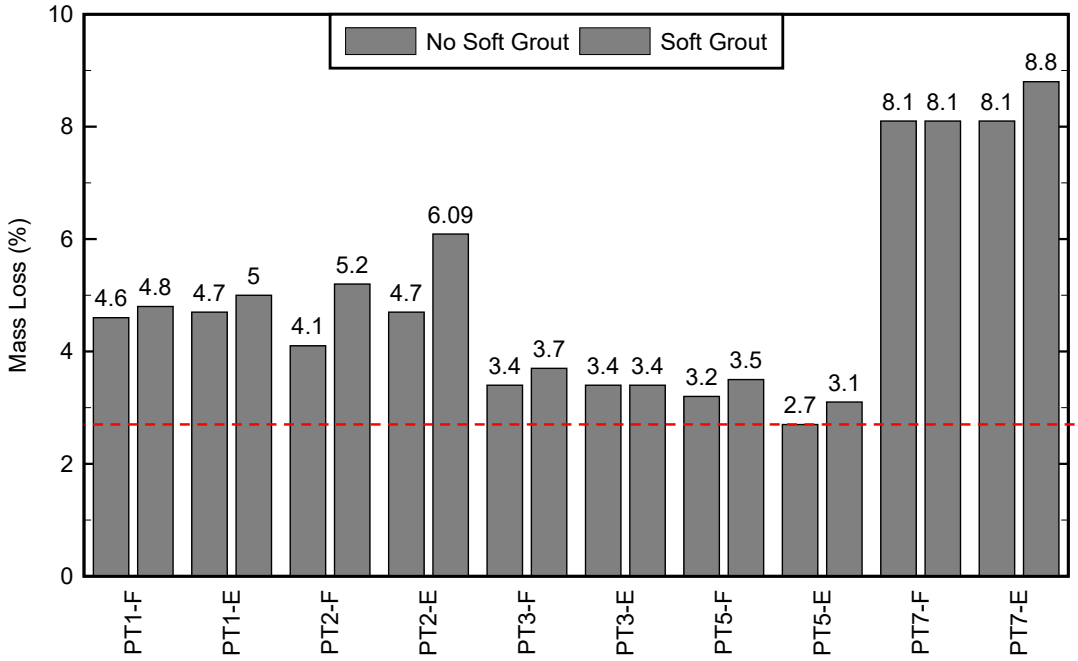

Figure 17-12 TGA percent of mass loss from MITT samples after *Field* and *Extreme* exposures at 1832°F (1000°C)

Figure 17-13 shows the TGA mass loss from small-scale grout samples after *Field* and *Extreme* exposures. As with the MITT samples, PT7 was the grout with the greatest percent mass loss, and no limit could be established when PT7 was considered. The small-scale grout data for TGA, with the exception of PT7, established an overall limit of maximum mass loss at 3.6%. If the grout tested in TGA followed the limit as developed from the test data, then the grout would not be expected produce soft grout. It should be noted that there are instances where a higher TGA percent mass loss did not produce soft grout. In those cases, further testing may help decide if the grout is acceptable for commercial use. As discussed previously, when the shelf life test results are outside the limit, then it can either be screen-tested using another method and/or MITT-tested to ensure that it will not produce soft grout.

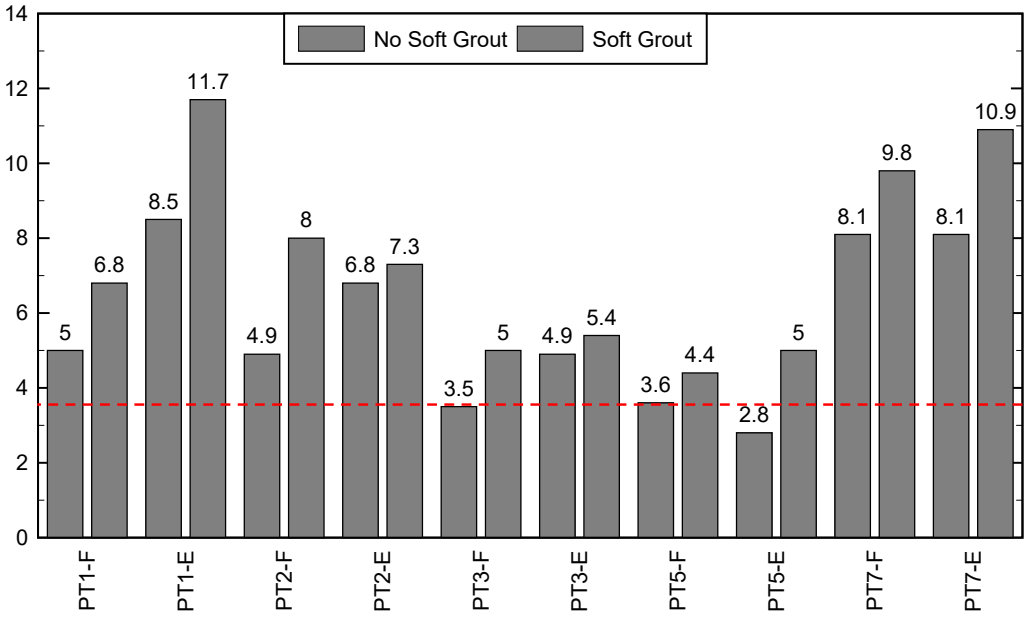

Figure 17-13 TGA mass loss from small-scale grout samples after *Field* and *Extreme* exposures at 1000°C

17.6 Microwave Moisture Content

MMC testing consisted of heating a known mass of material in a typical home-use microwave for intervals for a maximum of 3 minutes, and then measuring the mass. This heating process continued until less than 0.01% mass change was achieved, at which point a total mass loss was determined. Figure 17-14 shows the MMC total mass loss percent, with an overall limit, for MITT samples after *Field* and *Extreme* exposures. The screening test limit for MITT samples after MMC testing was found as follows. When an MMC mass loss percentage was below 0.13, no soft grout was found in MITT testing, with the exception of the PT2 13-day *Field* sample that produced soft grout at 0.06; therefore, an overall limit of 0.13 was selected. PT1, PT5, and PT7 grouts had mass loss percentages above 0.13 and did not produce soft grout. Therefore, these three grouts would have been improperly categorized as failing the test. Further analysis using values normalized to the initial mass loss was conducted. Relative change, rather than absolute change, however, was ineffective at establishing the limit. This result shows the importance of developing individual MMC testing limits for each PT grout.

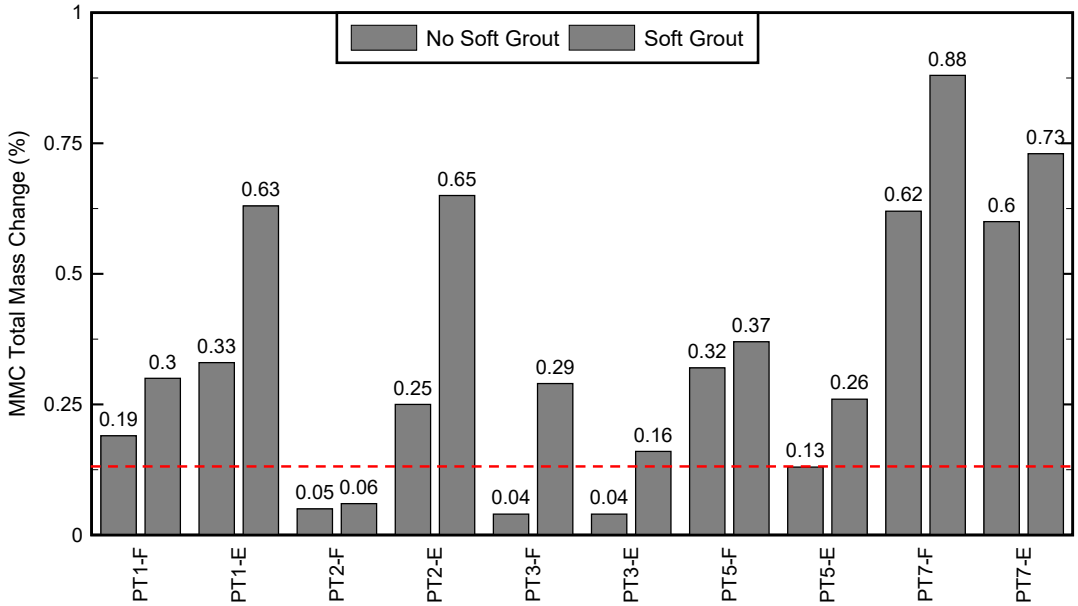

Figure 17-14 MMC total mass loss percent for MITT grout samples after *Field* and *Extreme* exposures

Figure 17-15 shows the total mass loss percent, with individual grout limits, for MMC testing of small-scale samples after *Field* and *Extreme* exposures. The overall screening test limit determined from small-scale MMC testing was a total mass loss percent of 0.62, because no soft grout was found in the corresponding MITT samples.

Percent mass loss values from MMC testing were 2% to 10% below values obtained with either TGA or LOI tests. Lower mass loss values are attributed to the lower temperature to which the samples were subjected in the microwave used for this testing.

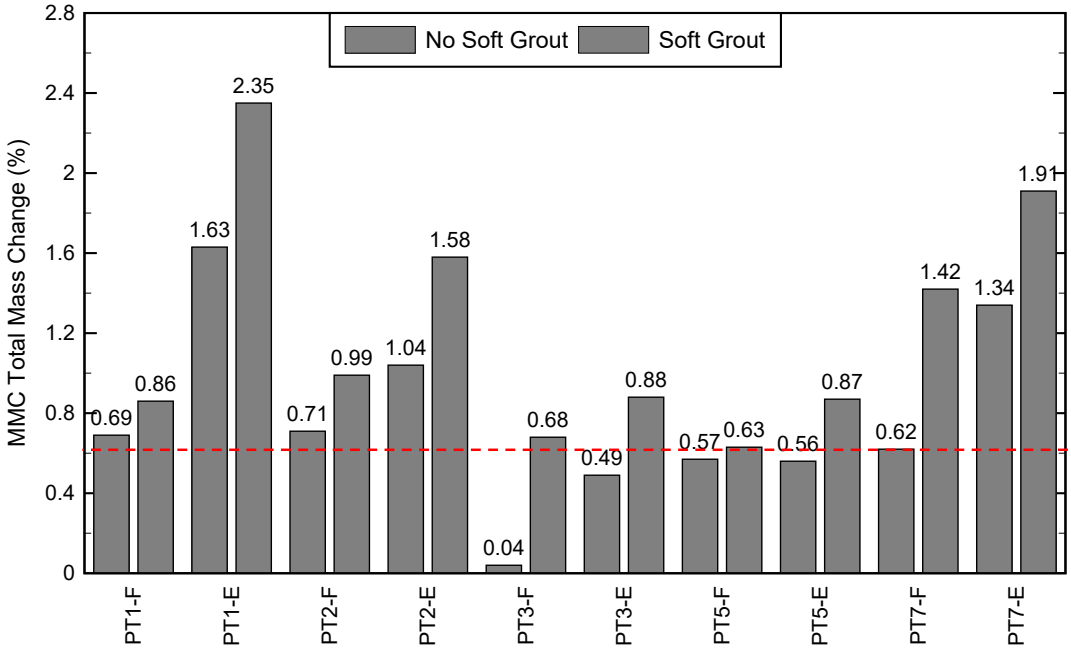

Figure 17-15 MMC total mass loss percent for small-scale grout samples after *Field* and *Extreme* exposures

17.7 Summary

A summary of the overall limits computed in the previous sections is shown in Table 17-1 and Table 17-2. The limits shown in Table 17-1 and Table 17-2 are for MITT full-bag samples and small-scale samples, respectively. These are an average of the limits determined for PT grouts that were tested during this study, and they should not be used to deem if a grout is acceptable for use. Note that no limits were established for PSA. As mentioned in the PSA and MMC sections in this chapter, limits were not selected when the relationship to soft grout did not have a clear trend. This occurred when the individual limits for a PT grout were below 1 for the normalized value, and above 1 for another PT grout. Also, for PSA testing, the difference in results for the presence or absence of soft grout was positive for one PT grout and negative for another PT grout.

Table 17-1 Average limits for MITT full-bag samples for the tested PT grouts

Test Method	Limit
PSA (dry)	N/A
PSA (wet)	N/A
BF_{ratio}	≥ 0.85
Normalized LOI	≤ 1.03
TGA (%)	≤ 2.7
MMC (%)	≤ 0.13

N/A indicates that no limit was determined from the results of the respective test method

Table 17-2 Average limits for small-scale samples for the tested PT grouts

Test Method	Limit
Mass Gain (%)	≤1.1
PSA (dry)	N/A
PSA (wet)	N/A
BF_{ratio}	≥0.93
Normalized LOI	≤1.26
TGA (%)	≤3.6
MMC (%)	≤0.62

N/A indicates that no limit was determined from the results of the respective test method

18 Proposed Screening Method for Grout Viability

Based on the results of the tests using the various methods, the sensitivity of individual test methods can be estimated by computing the change in the screening test method metric for each grout over the time period from initiation of exposure (0 days) to soft-grout formation. Table 18-1 shows the average of change between Control (0 days) and day of soft-grout formation for all test methods. Also, the table indicates the average of the percent difference for each PT grout between control (0 days) and time of soft-grout formation for both *Field* and *Extreme* conditions. The percent-difference results indicate that the Blaine Fineness test and the MMC test are the most sensitive test methods to track particle changes due to adverse exposure. Blaine Fineness is considered the most practical test among all the test methods in this project. As discussed in Chapter 12, this test method only requires a properly calibrated Blaine device, which facilitates field testing and allows the possibility of performing several tests in a matter of minutes. However, accuracy of results is highly dependent on the operator performing the test.

MMC appears to be the most sensitive test with a percent difference of 206 and 440 for *Field* and *Extreme* exposures, respectively. This test is also practical for field application because it only requires a conventional microwave and a balance with 0.1g precision. In Chapter 15, however, it was discussed that MMC temperatures are not sufficient to account for complete dehydroxylation and decarbonation, meaning that the test results may not represent the entire exposure history of the PT grout. This may amplify the apparent sensitivity of the test. Individual PT grout values used to compute Table 18-1 are shown in Appendix L.

Table 18-1 Sensitivity of screening test methods used in this study

Test Methods		*Field*		*Extreme*	
Name	Metric (units)	Average metric change over soft grout period	Average of Percent Change (%)	Average metric change over soft grout period	Average of Percent Change (%)
Normalized Dry PSA	Mean particle size (μm)	0.13	13	0.14	14
Normalized Wet PSA		0.16	16	0.14	14
BF	BF_{ratio}*	0.36	36	0.38	38
Normalized LOI	Mass loss (%)	0.21	21	0.14	14
TGA		0.57	16	0.80	19
MMC		0.18	206	0.28	440
* Blaine fineness ratio: non-dimensional ratio of Blaine fineness results from Equation 2					

Implementation of a screening test method for grout viability would require testing for both product qualification and product quality assurance during construction. Qualification would consist of exposing PT grout to the *Extreme* exposure conditions and conducting MITT daily for each PT grout, along with the selected screening test method until soft grout is found. Several samples should be obtained from different PT grout bags to obtain the desired repeatability of results. Then, a limit of the screening test methods should be determined for the respective PT grout.

Quality assurance may then be implemented by conducting the screening test immediately after production. The results of the screening test should then be documented as part of the certification of the grout lot. Then, the PT grout should be tested in the field, and if the product exceeds the specified limit (determined during qualification), then the PT grout may not be suitable for use. At that point, either MITT can be used to verify the adequacy of the product, or new grout should be requested for grouting.

19 Summary and Conclusions

The objective of this research project was to explore the cause of bleeding, soft grout formation, and segregation of commercially available, prepackaged, post-tensioning grouts. This study focused on two goals. The primary goal was aimed at developing test methods that indirectly tracked particle agglomeration or other indicators of prehydration so that the viability (suitability for use) of PT grout could be verified. The secondary goal was to explore the sensitivity to elevated temperature and humidity of various PT grouts and their corresponding cements and SCMs. For the purposes of this research, the grout is considered to be unfit for use when the constituents have deteriorated such that soft grout is produced when tested according to the modified inclined tube test (MITT).

Prior to testing, the various PT grouts and individual constituents were exposed to a selected temperature and humidity in their original packaging and also in small-scale containers. *Extreme* exposure was at 95˚F and 95% RH. *Field* exposure was at 85˚F and 85% RH. *Laboratory* exposure was at 65˚F and 50%-70% RH. *Control* exposure was at 65˚F and 45%-65% RH.

Following exposure of bagged material at the selected condition, the grouts were subjected to MITT to evaluate the susceptibility to soft grout formation. Nominal shear rate (NSR) viscosity testing was conducted using a dynamic shear rheometer in parallel with MITT to determine if a correlation could be established between the rheology of the fresh mixed grout and its affinity for producing soft grout. These tests established the exposure time and conditions necessary to generate soft grout in MITT. Small-scale samples of the same grout were then tested for mass gain (MG), particle size analysis (PSA), Blaine fineness (BF), loss on ignition (LOI), thermogravimetric analysis (TGA), and microwave moisture content (MMC). The portland cements from the same grouts were also tested using these methods to determine the overall contribution that the portland cement had to the deterioration.

Individual PT grout constituents were also investigated to determine their sensitivity to elevated temperature and moisture. These materials included portland cement, supplemental cementitious materials, and powdered admixtures. Each of these materials exhibited physical changes, chemical changes, or both during exposure. While these materials were affected by exposure, the primary cause of the soft grout formation appears to be the prehydration of portland cement. There appears to be some potential for synergistic effects that amplify the deleterious effect of moisture on the PT grout. More work is needed to identify these effects.

Specific conclusions are highlighted below:

1. Modified inclined tube testing of samples exposed to 95°F and 95% RH (*Extreme* exposure) produced soft grout 5 days earlier than samples exposed to 85˚F and 85% RH (*Field* exposure).
2. Modified inclined tube testing of samples exposed to 95°F and 95% RH produced 35.5% more soft grout than samples exposed to 85˚F and 85% RH.
3. Prolonged exposure to elevated temperatures and relative humidities of PT grouts and portland cements resulted in significant mass gains, increased particle sizes, and decreased surface areas.
4. LOI and TGA showed that the SCMs typically adsorbed less than 4% mass in exposures up to 14 days. Class C fly ash (FAC) had the highest absorption due to the usual presence of free lime and C_3A.

5. FAC had the largest increase in particle size among all SCMs during exposure, with a 30% increase in the amount of particles above 10 μm. In general, the fraction of particles above 10 μm increased for all SCMs.
6. All admixtures exhibited changes in physical properties during exposure. In particular, all admixtures had at least 20% of their mass gain during the first three days of exposure.
7. Exposure resulted in changes in viscosity for all admixtures. The mechanism responsible for the decrease in viscosity remains unknown and its further study is recommended for future work. Also, exposure of some admixtures resulted in a decrease of workability, which eventually caused untestable mixtures.
8. Exposure of admixtures prior to use resulted in increased bleeding for all mixtures; a high-range water-reducer had the highest bleed of 3.2 ml, or 10% of the total cement paste.
9. Exposure of PT grout to adverse temperature and humidity resulted in a delay of setting time, which allowed more time for segregation to occur, and may have contributed to the process of soft grout formation.
10. The effects of prehydration were evident, based on reductions of up to 67% in the cumulative heat of hydration measured by isothermal calorimetry. Also, it was observed that the induction period of hydration increased by 2 to 11 hours for several PT grouts, resulting in a delay of set time.
11. The delay of setting is thought to have occurred due to changes that occurred during prehydration of the portland cement in the PT grout. Possible factors could include coating of the cement particle surfaces with reaction product (C-S-H), which would greatly impede the transport of adsorbed water to the unreacted cement beneath the coating.
12. The microwave moisture content (MMC) and Blaine fineness test methods were the most sensitive to changes in particle size and surface area. However, both tests have limitations that should be considered when selecting a screening test method.
13. An implementation procedure was recommended to incorporate a screening test method for qualification of a specific PT grout and for quality control before grouting operations in the field.

20 Future Research

This study covered the PT grouts and respective constituent sensitivity under various exposure levels. Several test methods were used to track the sensitivity of PT grout particles in terms of particle size and mass change. Limits were recommended for each test method to indicate the likelihood to form soft grout. These limits are for all the PT grouts tested in this study; however, the authors recommend additional testing to develop limits for individual manufacturers, to achieve higher repeatability confidence. The authors consider that percent of mass loss data obtained from LOI and TGA tests are promising screening methods that can be used by manufacturers and contractors. These test methods would require the manufacturer to label each bag of PT grout with LOI or TGA values obtained during quality control of recently manufactured grout. PT grouts would then be tested prior to grouting to estimate prehydration that occurred during transportation or storage prior application.

PSA and Blaine fineness were capable of tracking the increase in particle size during exposure, although inconsistency and lack of repeatability were noticed during testing. The authors suggest the exploration of other techniques such as ASTM C 430 Standard Test Method for Fineness of Hydraulic Cement by the 45-μm (No. 325) Sieve.

When conducting PSA testing of PT grout and portland cement, it was decided to sieve the material prior to testing to remove the agglomerations. There was some question regarding the efficacy of sieving the material prior to testing since this action will greatly affect the absolute PSA results. Ultimately, since the absolute PSA results were less important than the change in readings, it was decided to maintain the sample in a relatively undisturbed condition for testing, but to remove agglomerations that would affect the results. In future research, PSA results after homogenization of the complete sample would be interesting and may prove to provide a better before-and-after contrast. One approach would be to start at a low homogenizer power and increase until an optimal proper power setting is found that produces the most consistent results. The particle size measured should decrease until all the loose agglomerates are dispersed, after which the particle size would not appreciably change until the power was high enough to start breaking up the hard agglomerates formed by the C-S-H formed from prehydration. The plateau region (soft agglomerates dispersed, but bonded agglomerates are intact) should be found for each sample and exposure condition.

The proportions of the constituents in the grout or cement have not been studied. Therefore, future research should be continued on the chemical constituents contained in each of the grouts, before and after exposure. In particular, the following areas should be investigated:

1) Continue exploring the prehydration that occurs in PT grouts and cements using TGA to determine the hydration phases (formation of C-S-H and CH at early hydration times) that form during exposure and relate these changes to shelf life.
2) Employ scanning electronic microscopy (SEM) and x-ray diffraction analysis (XRDA) to determine the physical and chemical compositions of fresh grout, conditioned grout, and soft grout vs hardened grout.
3) Various proportions of cements, SCMs, and admixtures should be studied with consideration of the effects of age and adverse exposure.
4) Characterize the bleed solution by means of pH, zeta potential, and FTIR to identify changes in composition that can lead to conditions favorable to soft grout formation.
5) Investigate the effects of various admixtures commonly used in PT grout, such as HRWRs, VMAs, anti-bleeding agents, and retardants on the PT grout properties

before and after deterioration due to exposure. Employ isothermal calorimetry to monitor delays of setting time, and NSR viscosity for fluidity changes.

21 References

AASHTO T 260-97 (2011). Standard Method of Test for Sampling and Testing for Chloride Ion in Concrete and Concrete Raw Materials, American Association of State and Highway Transportation Officials. Washington, DC.

Alarcon-Ruiz, L., Platret, G. Massieu, E., and Ehrlacher, A. (2005). The use of thermal analysis in assessing the effect of temperature on cement paste. *Cement and Concrete Research,* 35(3), 609-613.

Arvaniti, M., Juenger C.G., Bernal, S., Duchesne, J., Courard, L., Leroy, S., Provis, J., Klemm, A., & Belie, N. (2015). Determination of Particle Size, Surface Area, and Shape of Supplementary Cementitious Materials by Different Techniques. *Journal of Materials and Structures*, 48(11): 3687–3701.

ASTM C33-17 (2017). Standard Specification for Concrete Aggregates. ASTM International, West Conshohocken. ASTM International, West Conshohocken, PA.

ASTM C150-17, 2017. Standard Specification for Portland Cement. ASTM International, West Conshohocken. ASTM International, West Conshohocken, PA.

ASTM C204-17, 2017. Standard Test Methods for Fineness of Hydraulic Cement by Air-Permeability Apparatus. ASTM International, West Conshohocken, PA.

ASTM C430, 2017. Standard Test Method for Fineness of Hydraulic Cement by the 45-µm (No. 325) Sieve. ASTM International, West Conshohocken, PA.

ASTM C618-17, 2017. Standard Specification for Coal Fly Ash and Raw or Calcined Natural Pozzolan for Use in Concrete. ASTM International, West Conshohocken, PA.

ASTM C989-17, 2017. Standard Specification for Slag Cement for Use in Concrete and Mortars. ASTM International, West Conshohocken, PA.

ASTM C1240-15, 2015. Standard Specification for Silica Fume Used in Cementitious Mixtures. ASTM International, West Conshohocken, PA.

ASTM C1602-17, 2017. Standard Specification for Mixing Water Used in the Production of Hydraulic Cement Concrete. ASTM International, West Conshohocken, PA.

ASTM C1738-14, 2014. Standard Practice of High-Shear Mixing of Hydraulic Cement Pastes. ASTM International, West Conshohocken, PA.

ASTM D4643-08, 2008. Standard Test Method for Determination of Water (Moisture) Content of Soil by Microwave Oven Heating. ASTM International, West Conshohocken, PA.

ASTM D7348-13, 2013. Standard Test Method for Loss on Ignition (LOI) of Solid Combustion Residues. ASTM International, West Conshohocken, PA.

ASTM E1269-14, 2014. Standard Test Method for Determining Specific Heat Capacity by Differential Scanning Calorimetry. ASTM International, West Conshohocken, PA.

ASTM E2105-10, 2010. Standard Practice for Thermogravimetric Analysis (TGA). ASTM International, West Conshohocken, PA.

Bazzoni, A. (2014). *Study of Early Hydration Mechanisms of Cement by Means of Electron Microscopy* (Doctoral Dissertation). École Polytechnique Fédérale de Lausanne, Lausanne, Switzerland.

Bentz, D. P., Barrett, T., Varga, I., & Weiss, J. (2012). Relating Compressive Strength to Heat Release in Mortars. *Advances in Civil Engineering Materials*, 1(1), 1–16. doi: 10.1520/ACEM20120002.

Bertolini, L., & Carsana, M. (2011). High pH Corrosion of Prestressing Steel in Segregated Grout. *In: Andrade C., Mancini G. (eds) Modelling of Corroding Concrete Structures. RILEM Bookseries, 5*, 147-158.

Berodier, E., & Scrivener, K.L. (2014). Understanding the filler effect on the nucleation and growth of C–S–H. *J Am Ceram Soc,* 97(12), 3764–3773.

Brunner B., & Hamilton H.R. (2014). *Shelf Life and the Effects of Storage Conditions on Post-Tensioned Grouts* (Masters Thesis). University of Florida, Gainesville, FL.

Bullard, J.W., Jennings, H.M., Livingston, R.A., Nonat, A., Scherer, G.W., Schweitzer, J.S., Scrivener, K.L., & Thomas J.J. (2011). Mechanisms of cement hydration. *Cem. Concr. Res*. 41, 1208–1223.

Carsana, M., & Bertolini, L. (2016). Characterization of Segregated Grout Promoting Corrosion of Posttensioning Tendons. *J. Mater. Civ. Eng.,* 28(6).

Dubina, E., Sieber, R., Plank, J., & Black, L. (2008). *Effects of Prehydration on Hydraulic Properties of Portland Cement and Synthetic Clinker Phases*. Paper presented at the 28th Cement and Concrete Science Conference.

Dubina, E., Black, L., Sieber, R., & Plank J. (2010). Interaction of water vapour with anhydrous cement minerals. *Adv. Appl. Ceram*, 109, 260–268.

Dubina, E., Wadsö, I., & Plank, J. (2011). A sorption balance study of water vapour sorption on anhydrous cement minerals and cement constituents. *Cem. Concr. Res*, 41, 1196–1204.

Dubina, E., and Plank, J. (2012). Influence of Moisture- and CO2-Induced Ageing in Cement on the Performance of Admixtures Used in Construction Chemistry. *ZKG International*, 65 (10), 60-68.

Dubina, E., Plank, J., & Black, L. (2015). Impact of water vapour and carbon dioxide on surface composition of C3A polymorphs studied by X-ray photoelectron spectroscopy. *Cem. Concr. Res*, 73, 36–41.

European Committee for Standardization, (2007). EN 445 Grout for Prestressing Tendons Test Methods.

FDOT. (2002). Grouting of Bridge Post-Tensioning Tendons-Training Manual.

FDOT. (2018). Standard Specification for Road and Bridge Construction. Florida Department of Transportation.

Ferraro, C.C., Paris, J.M., Townsend, T.G., & Tia, M. (2017). Evaluation of Alternative Pozzolanic Materials for Partial Replacement of Portland Cement in Concrete. FDOT Contract Number: BDV31-977-06. Tallahassee, FL.

FHWA. (2013). Post-Tensioning Tendon Installation and Grouting Manual. Washington, DC

Gapinski, G. M. & Scanlon, J. (2005). Silica fume. *Norchem*. doi: 10.1016/S0008-8846(97)00191-9.

Goldsberry, B. (2013). Post-Tensioning Best Practice Update and New Directions for Post-Tensioned Structures. Florida Department of Transportation.

Ghorbanpoor, A., & Madathanapalli, S.C. (1993). Performance of Grouts for Post-Tensioned Bridge Structures, Report No. FHWA-RD-92-095, National Technical Information Service, Springfield, VA.

Hunt, C.M., Dantzler, V., Tomes, L.A., & Blaine, R.L. (1958). Reaction of portland cement with carbon dioxide. *Journal of Research of the National Bureau of Standards Section A: Physics and Chemistry*, 66A(6), 441-446.

Khayat, K.H., Yahia, A., & Sayed, M. (2008). Effect of supplementary cementitious materials on rheological properties, bleeding, and strength of structural grout. *ACI Mater J.*,105(6), 585–93.

Lau, K., Permeh, S., and Vigneshwaran, K. (2016). Corrosion of Post-Tensioned Tendons with Deficient Grout. FDOT Project BDV29-977-04. Tallahassee, FL.

Lee, S., & Zielske, J. (2014). An FHWA Special Study: Post-Tensioning Tendon Grout Chloride Thresholds. Rutgers University.

López-Arce, P., Gómez-Villalba, L. S., Martínez-Ramírez, S., Álvarez de Buergo, M., & Fort, R. (2011). Influence of relative humidity on the carbonation of calcium hydroxide nanoparticles and the formation of calcium carbonate polymorphs. *Powder Technology*, 205(1–3), 263–269.

Lowke, D., & Gehlen, C. (2017). The zeta potential of cement and additions in cementitious suspensions with high solid fraction. *Cem. Concr. Res*, 95, 195–204.

Mehta, P., & Monteiro, P. (2006). *Concrete: Microstructure, Properties, and Materials*. Fourth Edition.

Meier, M. R., Napharatsamee, T., & Plank, J. (2017). Dispersing performance of superplasticizers admixed to aged cement. *Construction and Building Materials*, *139*, 232–240.

Jensen, O. M., Jensen, P. Freiesleben Hansen., Lachowski, E.E., & Glasser, F.P. (1999). Clinker mineral hydration at reduced relative humidities. *Cement and Concrete Research*, 29, 1505-1512.

Mindess, S., Young, F., & Darwin, D. (2003). *Concrete*. Prentice-Hall, Inc, Upper Saddle River, NJ.

Paper, C., Ramge, P., Bundesanstalt, W. S., & Schmidt, W. (2013). *Effect of the storage of cement on early properties of cementitious systems*. International Conference on Advances in Cement and Concrete Technology in Africa, Johannesburg, South Africa.

Piper A., Hamilton, H. R., Ferraris, C., Schokker, A. &. Dave, V. (2014). Development of Laboratory Test Methods to Replace the Simulated High-Temperature Grout Fluidity Test. FDOT Contract Number: BDK75-977-39. Tallahassee, FL.

Piper, A., Randell, A., Brunner, B., & Hamilton, H.R. (2014). Simulation of Prepackaged Grout Bleed under Field Conditions. FDOT Contract Number: BDK75 977-59, Tallahassee FL.

PTI M55.1-12. (2012). Specification for Grouting of Post Tensioned Structures. Post-Tensioning Institute, Farmington Hills, MI.

Powers, R., Sagues, A., & Virmani., Y. (2016). Corrosion of Post-tensioned Tendons in Florida Bridges. FDOT Contract Number: BDK29-977-04. Tallahassee, FL.

Rafols, J., Lau, K., Lasa, I., Paredes, M., & Elsafty, A. (2013). Approach to Determine Corrosion Propensity in Post-Tensioned Tendons with Deficient Grout. *OJCE*, 3, 182-187.

Randell A., & Hamilton H.R. (2013). Improved Test Methods for Evaluating Fresh and Hardened Properties of High Performance Post-Tensioning Grout (Master Thesis). Gainesville: University of Florida.

Randell, A., Aguirre, M., & Hamilton, H.R., 2015. Effects of Low Reactivity Fillers on the Performance of Post-Tensioning Grouts. *PTI Journal* August, 11, 17-28.

Rey, F., Fornes, V., & Rojo, J. (1992). Thermal Decomposition of Hydrotalcites: An Infrared and Nuclear Magnetic Resonance Spectroscopic Study. *Section Title: Catalysis, Reaction*

Kinetics, and Inorganic Reaction Mechanisms 88 (15): 2233–38. doi:10.1039/ft9928802233.

Schokker, A.J., Koester, B.D., Breen, J.E., & Kreger, M.E. (1999). Development of High Performance Grouts for Bonded Post-Tensioned Structures. Texas Department of Transportation. Research Report 1405-2.

Scrivener, K.L., & Nonat, A. (2011). Hydration of cementitious materials, present and future. *Cem. Concr. Res*, 41, 651–665.

Scrivener, K. L., Lothenbach, B., De Belie, N., Gruyaert, E., Skibsted, J., Snellings, R., & Vollpracht, A. (2015). TC 238-SCM: hydration and microstructure of concrete with SCMs: State of the art on methods to determine degree of reaction of SCMs. *Materials and Structures/Materiaux et Constructions*, 48(4), 835–862.

Sidney, M., Young, J.F., & Darwin, D. (2003). Concrete 2nd Edition. Upper Saddle River, NJ: Prentice Hall.

Starinieri, V., Hughes, D.C., Gosselin, C., Wilk, D., & Bayer, K. (2013). Prehydration as a technique for the retardation of Roman cement mortars. *Cem. Concr. Res*., 41, 1–13.

Stoian, J., Oey, T., Bullard, J. W., Huang, J., Kumar, A., Balonis, M., & Sant, G. (2015). New insights into the prehydration of cement and its mitigation. *Cement and Concrete Research*, 70, 94–103.

Theryo, T., Hartt, W., & Paczkowski, P. (2013). Guidelines for Sampling, Assessing and Restoring Defective Grout in Prestressed Concrete Bridge Post-Tensioning Ducts. FHWA -HRT-13-028.

van Breugel, K. (1992). Numerical Simulation of Hydration and Microstructural Development in Hardened Cement-Based Materials. *Cement and Concrete Research*, 25(2), 319-331.

VSL. (2002). *Grouting of Post - Tensioning Tendons*. VSL International Ltd. Lyssach, Switzerland

Wang, Kejin., Grove, J.; Ge, Z., Ruiz, M.J., & Rasmussen, R. (2006). Developing a Simple and Rapid Test for Monitoring the Heat Evolution of Concrete Mixtures for Both Laboratory and Field Applications. Center for Transportation Research and Education Iowa State University. FHWA DTF61-01-00042.

Winnefeld, F., Zingg, A., Holzer, L., Pakusch, J., & Becker, S. (2009). *The ettringite – superplasticizer interaction and its impact on the ettringite distribution in cement suspensions*. Paper presented in the 9th ACI International Conference on Superplasticizers and Other Chemical Admixtures in Concrete, Sevilla, Spain,

Whittaker, M, Dubina, E, Al-Mutawa, F, Arkless, L, Plank, J & Black, L. (2013). The effect of prehydration on the engineering properties of CEM I Portland. *Advances in Cement Research*, 25 (1), 12 - 20. ISSN 0951-7197

Appendix A—V-Blender Procedures

To ensure a uniformly blended powder sample for the small-scale tests, it was necessary to blend materials obtained from the entire bag in a V-blender. Both prepackaged PT grout and bagged portland cement were blended prior to sample preparation. Figure A-1 shows the Ross V-Blender series tumbler blender with an intensifier bar that was used to blend the bagged material.

Figure A-1 Ross V-Blender Model VCB-1 SN#110960 – 2-HP driving motor and 1-HP Intensifier motor

Grout V-Blending Procedure		
Procedure	Description	Figure
1	A total of two bags of grout up to 125 lb. per cu. ft. are to be loaded into the v-blender hollow holder. Add one bag of grout at a time. Add grout over a period of 20-30 seconds per bag	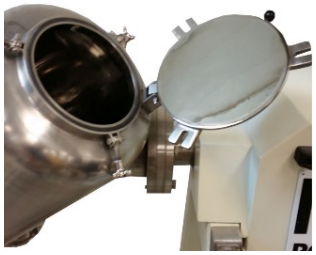
2	Close and tighten the V-Blender loading lids and discharge valve to ensure a closed seal.	
3	Turn on the machine and start a ten-minute tumble cycle with an intensifier speed of 700 rpm and a tumbling speed of 30 rpm.	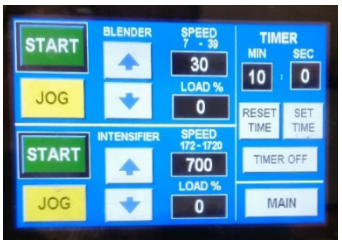
4	When the dry tumbling cycle is complete open the discharge valve and pour the blended grout into buckets.	

Appendix B—Container Sample Preparation

The following procedures were used to make the small-scale containers used to measure the total amount of prehydration that occurred in the PT grout and cement samples, which were subjected to a variety of environmental conditions for extended periods of time

B.1 Sample Preparation

Figure B-1 shows the grey original small-scale containers used to evaluate the mass gain due to prehydration and moisture absorption. The small-scale containers were made by cutting a six-inch height by three-inch diameter cylinder concrete molds into four symmetric parts using a band saw. The actual container size is one and a half inches in height and three inches in diameter. A plastic cap and water proof glue was used to seal the bottom of the containers prior to testing.

Figure B-1 Small-scale containers used to in mass gain testing

B.2 Layered Sample Preparation and Collection

Figure B-2 shows the white small-scale LOI depth layering container that was dissected to evaluate the total prehydration as depth changed. The container was cut from a three-inch diameter PVC pipe, the bottom of the container was sealed using a plastic cap and water proof glue. The actual container size is one and a half inches in height and three inches in diameter. Two intermediate slits were added at half an inch from the top and at one inch from the top using a band saw. The container was then labeled layer one through three from top to bottom.

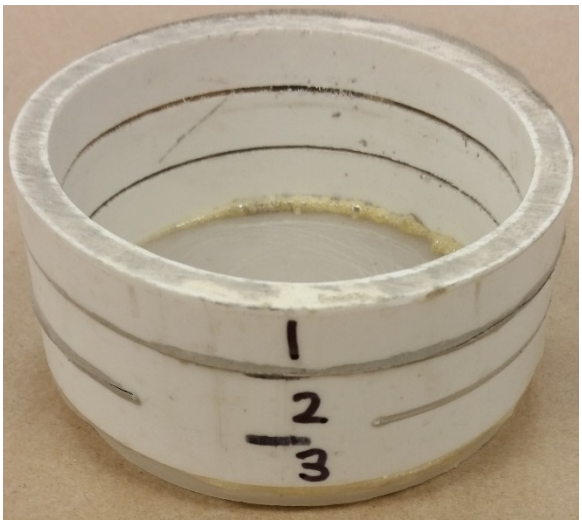

Figure B-2 Small-scale container used for LOI depth-layered testing

LOI container dissection		
Procedure	Description	Figure
1	Obtain three sample containers and number them one through three to represent each depth layer	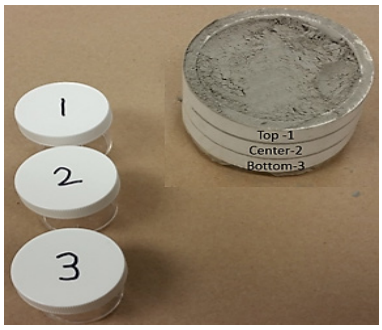
2	Insert dividing strip into layer one and ensure the strip has completely divided the material	
3	Mix the material with a glass rod for 30 seconds	
4	Remove the material from layer 1 and place it in a testing container labeled layer one, ensure all of the material has been removed before continuing.	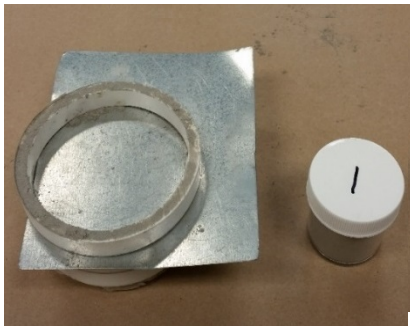

LOI container dissection		
Procedure	Description	Figure
5	Insert a dividing strip into layer two and ensure the strip has completely divided the material.	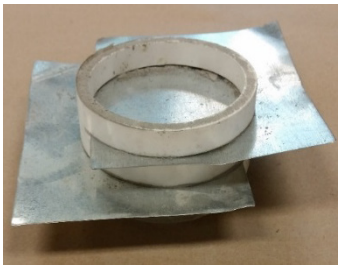
6	Remove the dividing strip from layer one and mix the material with a glass rod for 30 seconds	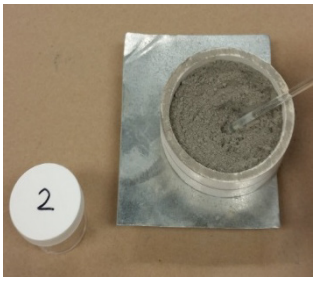
7	Remove the material from layer two and place it in a testing container labeled layer two, ensure all of the material has been removed before continuing.	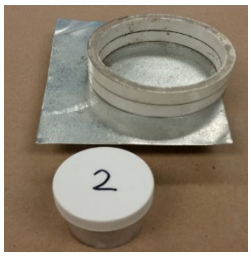
8	Remove the dividing strip from layer two and mix the material with a glass rod for 30 seconds.	

LOI container dissection		
Procedure	Description	Figure
9	Remove the material from layer three and place it in a testing container labeled layer three, ensure all of the material has been removed.	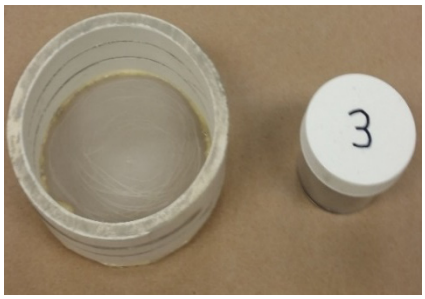
10	Follow the standard LOI testing procedure for the containers labeled layer one through three	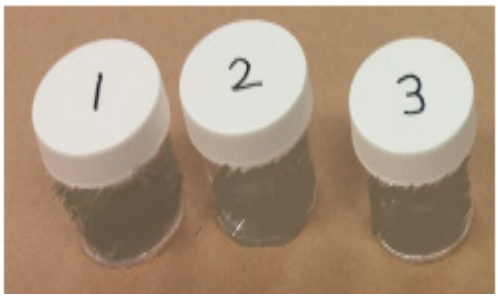

Appendix C—Mass Gain Test Procedures

The following procedure was done after the initial PT grout and corresponding cement were V-blending as detailed in Appendix A.

1. Label container one through four with material testing ID code
2. Weigh each empty clean container and record its initial mass (Mc)
3. Add the cementitious material to each container without compacting the material. Leave a slight lip without filling about 1/16" from the top of the container.
4. Weigh each container and record its total initial mass (M1)
5. Place the containers in the appropriate environmental chamber for prehydration testing Note: When placing the containers in the exposure condition place them in a centralized location away from any water preferably on a stand or table top.
6. After the exposure time is complete take out the containers and immediately weigh them and record the final total mass (M2)
7. Use Equation 3 to determine the percent of prehydration (w) that has occurred in the sample container.

w = Prehydration gain, %,
M1 = Initial mass of container and cementitious specimen, g,
M2 = Final mass of container and cementitious specimen after exposure, g,
Mc = Initial mass of container, g,

$$w = \left(\frac{M2 - M1}{M2 - Mc}\right) x100\% \qquad \text{Equation 3}$$

Appendix D—Loss on Ignition Test Procedures

The modified (ASTM D7348-13 Standard Test Method for Loss on Ignition (LOI) of Solid Combustion Residues, 2013) test method B was used to measure the amount of prehydration that occurred in the PT grout and cement samples, which were subjected to a variety of environmental conditions for extended periods of time. This test uses a furnace with a sustained heating capacity above 1000°C and a volume cavity large enough to run multiple crucible samples. Additional tools include a timer, desiccator for cooling the samples after heating and scale to measure the change in mass. The LOI test was conducted on all grouts and their respective cements that were exposure using both small-scale containers and exposed grout bags subjected to a variety of environmental conditions for extended periods of time.

D.1 Test Equipment

Figure D-1 shows crucibles containing grout samples in a furnace during LOI testing using Modified ASTM D7346-13 “Loss on Ignition” test method B.

Figure D-1 Modified ASTM D7346-13 Loss on Ignition test method B

D.2 Test Procedures

A modified version of ASTM D7346 Method B procedures was used to test either PT grout or portland cement following exposure.

1. Weigh each empty crucible and record its initial mass (Mc). See Figure D-2
2. Zero the scale. See Figure D-3
3. Add approximately 1 gram of the cementitious material to each crucible and record its total initial mass (M1). See Figure D-4.
4. Place the crucible with the cementitious material in the furnace at 550°C for 1 hour. See Figure D-5.
5. Increase the furnace temperature setting from 550°C to 950°C, temperature increase will take about 1 hour
6. Maintain a temperature of 950°C for an additional 3 h

7. Remove crucible from the furnace and place in a desiccator. See Figure D-6 and Figure D-7
8. Allow for crucible gradually cool to a temperature below 32°C
9. Remove the crucible from the desiccator and immediately weigh record the final total mass (M2). See Figure D-8.
10. Use Equation 4 to determine the percent of prehydration (w) that has occurred in the sample container.

LOI = Prehydration gain, %,
M1 = Initial mass of container and cementitious specimen, g,
M2 = Final mass of container and cementitious specimen after exposure, g,
Mc = Initial mass of container, g,

$$LOI = \left[\frac{M2 - M1}{M2 - Mc}\right] \times 100\% \qquad \text{Equation 4}$$

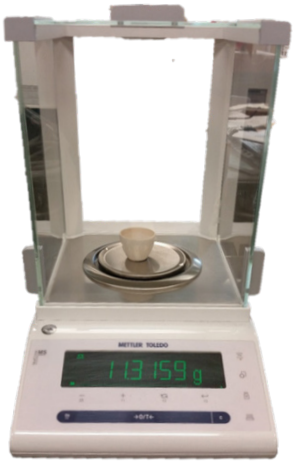

Figure D-2 Weigh and record initial crucible mass.

Figure D-3 Zero the scale.

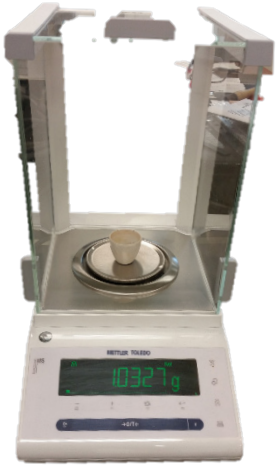

Figure D-4 Add 1 gram of material to crucible, and record the total mass.

Figure D-5 Add crucible to furnace at 550°C.

Figure D-6 Remove crucible from the furnace after 3 h at 950°C.

Figure D-7 Place crucible in desiccator, and gradually cool to 32°C.

Figure D-8 Remove crucible from the desiccator, and record the final mass.

Appendix E—Microwave Moisture Content Test Procedures

The Microwave Moisture Content (MMC) test method is an adaptation of the (ASTM D4643-08 Standard Test Method for Determination of Water (Moisture) Content of Soil by Microwave Oven Heating 2008), which was used for cementitious material moisture content. A microwave oven, with a vented chamber, variable power controls and input power rating of 700 Watts. A microwave safe specimen container and stirring apparatus as described in ASTM C1607 ceramic products that can be used in a microwave oven without any degradation, such as by deformation, fracturing, crazing, or heating up to excessive temperatures. A heat resistant handling apparatus such as a glove or holder, suitable for removing hot containers from an oven was used. A mass balance with a capacity ranging from 0.01 g to 2000 g, with adjustable supports for leveling on a surface and heat resistance for testing specimens was used. The MMC test was conducted on all grouts and their respective cements that were exposure using both small-scale containers and exposed grout bags subjected to a variety of environmental conditions for extended periods of time.

E.1 Test Equipment

Figure E-1 below shows the Microwave Moisture Content for cementitious material, Both PT grouts and their corresponding cements were tested using MMC after they were conditioned in varies environmental chamber conditions.

Figure E-1 Microwave used for Moisture Content of cementitious material

E.2 Test Procedures

The following procedure was done after the initial PT grout and corresponding cement were exposed in environmental chambers for a given time.

1. Setup balance on a level surface clear of any obstructions in a well-ventilated environment. See Figure E-2.
2. Measure the initial microwave safe container mass and record on data sheet. See Figure E-3.
3. Measure the initial cementitious material mass and record on data sheet. See Figure E-4.
4. Place the sample and container in the center of the microwave then set a heating time of 3 minutes. See Figure E-5. Note: Ensure the microwave oven is clear of any impurities

before commencing heating cycles. Use a thermometer to ensure overheating doesn't occur, overheating will be described as a temperature in excess of 400°C.

5. Using a heat resistance apparatus remove the sample container from the microwave oven once the heating cycle is complete. See Figure E-6.
6. Place container and sample on the balance measure total mass calculate mass change percent and report. See Figure E-7.
7. Using a stirring apparatus mix the sample carefully without any loss of material for about ten seconds. See Figure E-8
8. Repeat Steps 3 through 7 until two consecutive samples have a total mass change below 0.01% at which point additional testing will subside.
9. Calculate the moisture content using Eq. 5, and record.
10. Allow for sample container to cool down.
11. Discard the cementitious sample once MMC testing is complete. Note: Sample specimen should not be used to perform any other testing.
12. An MMC test data sheet is provided for data recording, note taking and modifications to the test and moisture content calculations as needed by the user.

As described in ASTM D4643. Calculate the water content of the cementitious material as follows:

M1 = mass of container and moist specimen, g,
M2 = mass of container and oven dried specimen, g,
Mc = mass of container, g,

$$\text{(Cycle) Mass Loss \%} = 1 - \left(\frac{(M2-Mc)-(M1-Mc)}{(M1-Mc)}\right) \times 100 \qquad \text{Equation 5}$$

Figure E-2 Set balance on a level surface.

Figure E-3 Measure container mass.

Figure E-4 Measure initial cementitious material mass.

Figure E-5 Place container with sample in the microwave, and begin heating cycle.

Figure E-6 Remove specimen from microwave with heat-resistant apparatus.

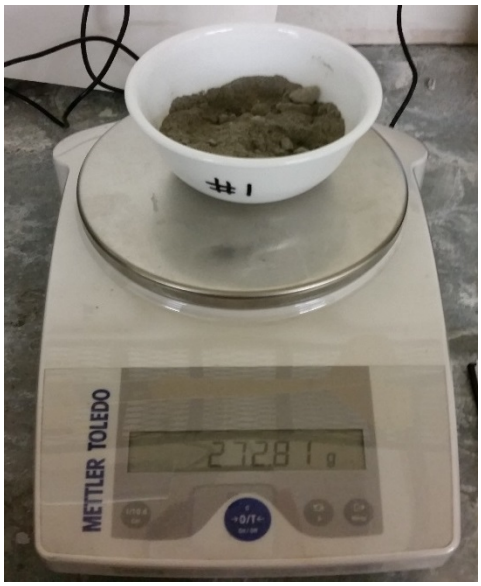

Figure E-7 Set container on the balance, and measure the final total mass.

Figure E-8 Stir sample for about ten seconds.

Post Tensioning Grout Microwave Oven Moisture Content (MCC) Test Inspection Form

[Name and Address of Laboratory]

Client: _____	Report NO:_____ Page ____ of ____
Project:_____	Project NO:_____
Material Source (Manufacture):_____	Date Material Sampled:_____
Material Type:_____	Date Material Received:_____

Material Delivery Initial Conditions

Is the material approved by PTI M55.1-12: YES NO	Date Manufactured:_____
Material Class Type (PTI M55.1-12 Table 3.1):_____	Expiration Date:_____
Initial Moisture Context (Given): _____%	Initial Age Ratio (Days): _____
	Initial Blaine Fineness (Given):

"Age ratio is (Current Age/ Expiration Date)
"Current age is defined as total days between produced date to current day

Material Storage Conditions Statement:

The cement or other prepackaged material can be delivered in bags but shall be stored in a building, bin, or other location that is both weather proof and located convenient to the work to be performed. General storage conditions shall be a maintained temperature ō5 ºF and relative humidity of ō5% to reduce pre-hydration of the material. Store material in accordance to manufactures recommendations. (PTI M55.1)

I _____ certify the material has been stored in accordance to the material storage conditions statement.

Lab Testing Conditions

Weather:_____
Air Temp: AM_____ (ºF)(ºC) PM____ (ºF)(ºC)
Relative Humidity: _____ %
Date at testing:_____
Age Ratio at Testing (Days):_____

Initial Sample Conditions

Crucible Initial Mass (g):	120
Material Initial Mass (g):	201
Total Initial Mass (g):	321

MCC Test #1 [Testing Coding Number] "Example calculations"

Cycle	Initial			Final			Cumulative	Notes
	Heating Time (min)	Initial Temp (ºF)	Total Mass (g)	Temp after heating (ºF)	Total Mass (g)	Mass Loss (%)	Mass Loss (%)	
1	15	80	321	210	315.3	0.018	1.78%	*"Initial heating for a minimum of 15 minutes*
2	10	190	315.3	270	298.2	0.054	5.42%	
3	10	210	298.2	320	294	0.014	1.41%	
4	5	240	294	380	293.7	0.001	0.10%	* *Test stopped when mass loss change is belong 0.1%*
Sum	40				293.7		8.71%	

"Use MCC testing procedures in conjunction with MCC test Inspection Form
"An average from three MCC tests can be used to compare to Manufactures age ratio moisture limit.

Sample Mass Loss % Calculation

$$(Cycle)\ Mass\ Loss\ \% = 1 - \left(\frac{Final\ Total\ Mass - Initial\ Total\ Mass}{Initial\ Total\ Mass}\right) x100$$

Material Robustness Limits

Manufactures Mass Loss Limit (%) "given": _____
Cumulative Mass Loss %:_____
Is the MCC test mass loss less than the manufactures limit: (YES) (NO)
If you answered NO, please refer to PTI M551.12 for further testing procedures

Remarks:

_____ _____
Inspector - Level/ Certification No. DATE Reviewer - Level/ Certification No. DATE

Appendix F—Shear Blender Procedure

The apparent viscosity of the PT grouts and their corresponding cements exposed using the small-scale exposure containers followed the (ASTM C1738-14 Standard Practice of High-Shear Mixing of Hydraulic Cement Pastes, 2014) in an attempt to correlate prehydration change with rheology behavior. A high shear mixer was used to mix the cementitious material with a 1.15 water to powder ratio above the manufacturer's recommendation. The small-scale high shear mixer was used to mimic the mixing power of the full colloidal mixer. After mixing was complete each mixture was then tested using the dynamic shear rheometer (DSR), further information on DSR test method can be found in Appendix G.

F.1 Test Equipment

Figure F-1 Small-scale high shear mixer below shows the small-scale high shear mixer that was used to mix PT grouts and their corresponding cements.

Figure F-1 Small-scale high shear mixer

F.2 Test Procedures

The following procedure was done after the initial PT grout and corresponding cement were exposed in environmental chambers for a given time.

13. Connect the temperature control pipes to the sides of the blender and set the temperature control panel to 21°C ±0.5°C. See Figure F-2 and Figure F-3.
14. Turn on the fume hood. See Figure F-4.

15. Pour a 1.15 ratio of water above the manufactures recommended dosage for the grout in the blender. See Figure F-5.
16. Set the blender agitation speed to 4,000 rpm and start cycle.
17. As cycle begins, pour the dry cementitious powder over a time of 60 seconds. See Figure F-6. Note: If needed use a scrapping paddle to remove excess material from blender sides.
18. Set the blender agitation speed to 10,000 rpm and start cycle for 30 seconds. See Figure F-7.
19. Turn off the blender agitation and allow the sample to rest for 2 minutes. See Figure F-8.
20. Set the blender agitation speed to 10,000 rpm and start cycle for 90 seconds.
21. Turn off the blender and pour the sample into the DSR testing cup. See Figure F-9. Follow the DSR testing procedure given in Appendix G

Figure F-2 Connect the temperature control pipes to blender.

Figure F-3 Set the temperature control panel to 21°C.

Figure F-4 Turn on fume hood.

Figure F-5 Pour water into blender, and start cycle.

Figure F-6 Pour cementitious material over a 60-second period.

Figure F-7 Set blender agitation speed to 10,000 rpm, and start cycle for 30 seconds.

Figure F-8 Turn off blender, and allow sample to rest for 2 minutes.

Figure F-9 Pour sample into DSR testing cup.

Appendix G—NSR Viscosity

G.1 Test Equipment

Figure G-1 shows the AR2000EX DSR used to test PT grout and the corresponding cements.

Figure G-1 AR2000EX DSR

G.2 Test Procedures

Pre-mix DSR Preparation

1. Fully open oven doors on DSR by undoing front latch, separating doors and carefully pushing them fully to the rear until they stop. The oven doors must be completely to the rear in the "fully open" position for machine to work. See Figure G-2 and Figure G-3.

2. Remove both the Smart Swap protective cover on DSR base plate and the threaded protective spindle cover on the DSR head. See Figure G-4.

3. Locate both the Stainless Steel Helical Rotor and the Peltier Concentric Cylinder with removable Cup insert. See Figure G-5 & Figure G-6.

4. Prepare to install Peltier Concentric Cup by removing the protective cover on the bottom of the assembly. Attach the assembly onto the DSR by indexing the metal tab on the cup base with the slot on the DSR base plate. The assembly will lock into the magnetic base when properly aligned and placed flat. See Figure G-7 & Figure G-8.

5. Connect the Peltier cup assembly Smart Swap cable to the DSR on the right side by indexing the red dots and pushing straight in. Ensure the cable is properly aligned before inserting and that it is fully seated after installation. See Figure G-9.

6. Connect the Peltier cup heating/cooling lines into the ports on the left by pushing the fittings straight in until the lines lock in with a positive click. The port selection of the lines is arbitrary. See Figure G-10.

7. Attach the Stainless Steel Helical Rotor to the spindle by threading the rotor onto the drawbar. ONLY FINGER TIGHTEN! See Figure G-11.

8. Check all connections and turn on power to DSR Tower by flipping switch on rear of the tower.

9. The DSR will run through its power up processes and display its status on the front LCD panel. You must wait until live data readouts are showing before proceeding. See Figure G-12 & Figure G-13.

10. Open the Rheology Advantage program found on the desktop. See Figure G-14.

11. When the program loads it will default to the main screen showing the DSR and instrument status. The oven door position is also displayed. It will either read "fully open" or "partially open". Adjust doors until "fully open" is shown. See Figure G-15.

12. Check the pre-loaded Geometry and Procedure programs on the main screen to ensure they are correct for the given test. If these are incorrect a different pre-installed program can be loaded by selecting "Open" under the dropdown menu of either the "Geometry" or "Procedure" tabs at the top. Information for the loaded geometry and procedure can be found by clicking the respective tabs from the main screen. For the purposes of this research the Helical Geometry program and the NSR Viscosity Continuous program were used. See Figure G-16 through Figure G-21.

13. Calibrate the DSR instrument by performing a precision rotational mapping of the geometry. Select "Rotational mapping" from the dropdown menu under the "Instrument" tab. Click "Perform mapping" on the dialog box that opens. The mapping process will take approximately five minutes and can be monitored by the progress bar within the dialog box. See Figure G-22 through Figure G-24.

14. Zero and set the instrument gap by selecting "Zero gap" under the "Gap" dropdown menu found under the "Instrument" dropdown menu. A dialog box will open instructing the user to lower the geometry to within 5mm of the lower plate. Do this by clicking and holding on the down arrow. The DSR head will start to lower and continue until it is partially in the cup. When the head stops, release the mouse and re-click and hold the down arrow again until the head stops. At this point the geometry should be contacting the base of the cup. Next click and hold the up arrow briefly (1-2 sec) until you notice the slightest movement of the head. This removes the geometry from directly contacting

the cup and keeps it within the 5mm requirement. Select the continue button. The DSR will now automatically lower the head slowly until it finds the bottom of the cup and will then set the minimal zero gap. This is the position within the cup where the geometry will shear the sample. When finished a dialog box will open asking to "raise the head to the back off distance", before selecting yes, check the gap at this zero point on the main screen showing instrument readouts. The gap typically reads 17 micrometers. If the value is drastically different it is recommended to re-zero the gap. If the value matches select yes and the head will return to its original top position. See Figure G-25 through Figure G-29.

15. The DSR is now ready to test a sample.

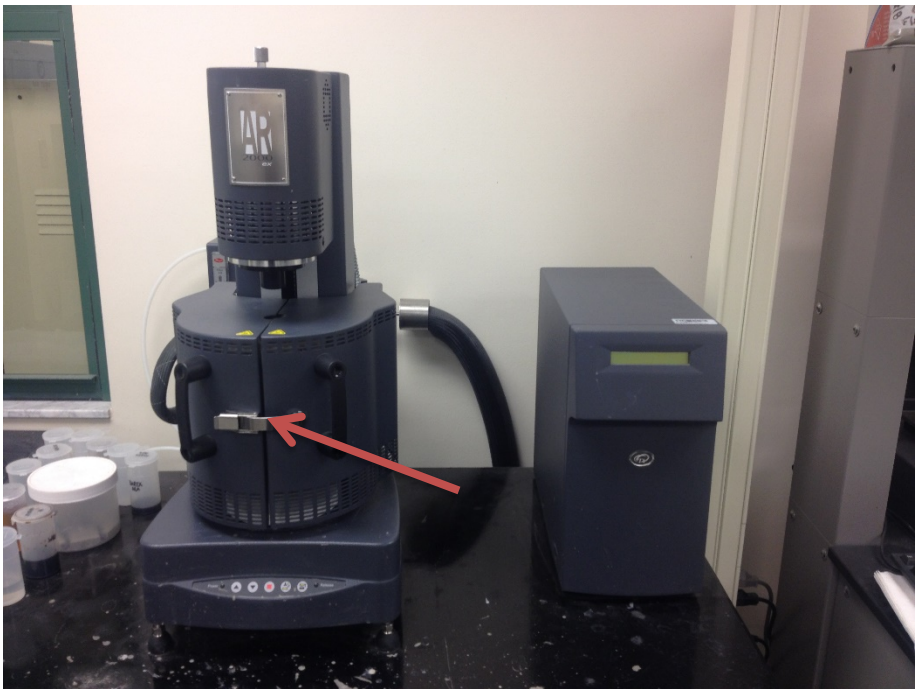

Figure G-2 DSR (left) and DSR tower (right) with latch indicated

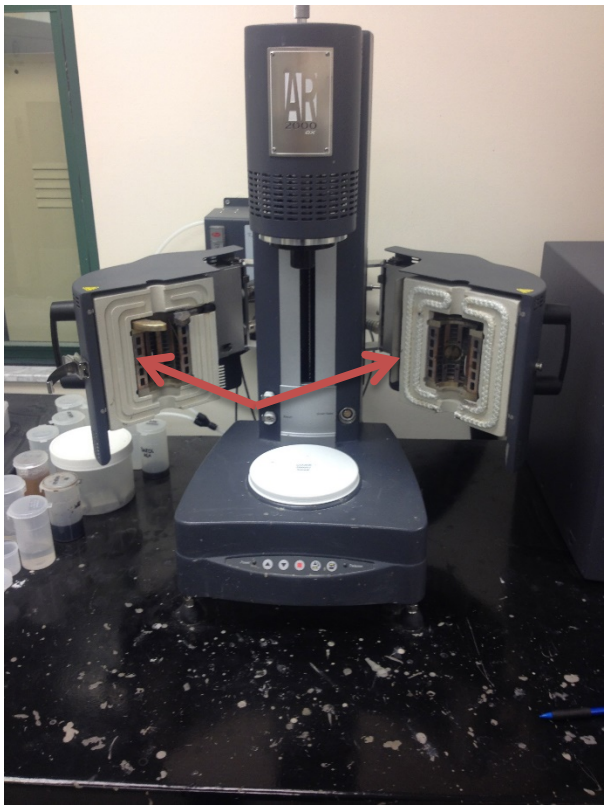

Figure G-3 DSR with doors fully open

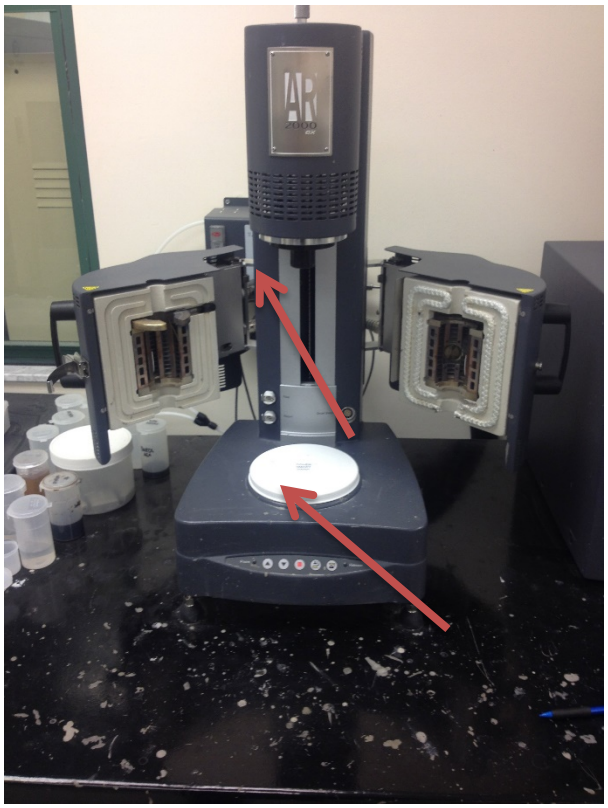

Figure G-4 Protective cover locations

Figure G-5 Stainless steel helical rotor

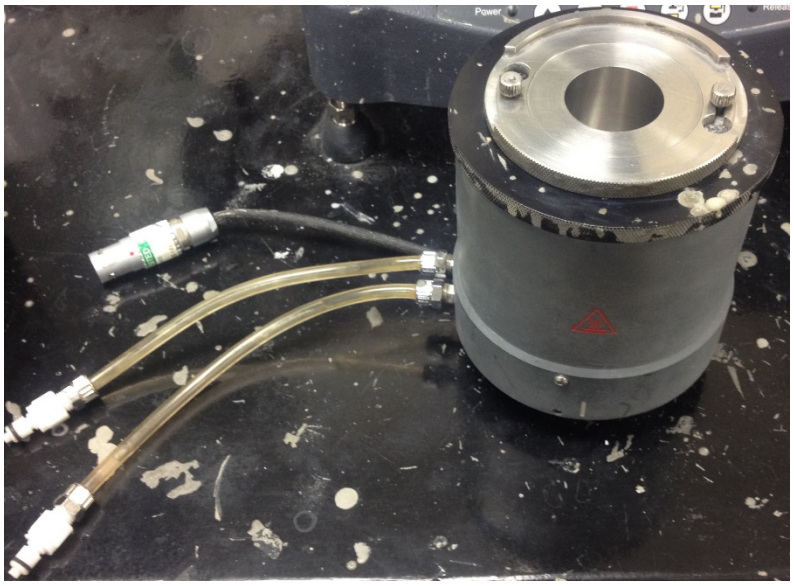

Figure G-6 Peltier concentric cup with stainless steel cup insert

Figure G-7 Protective cover

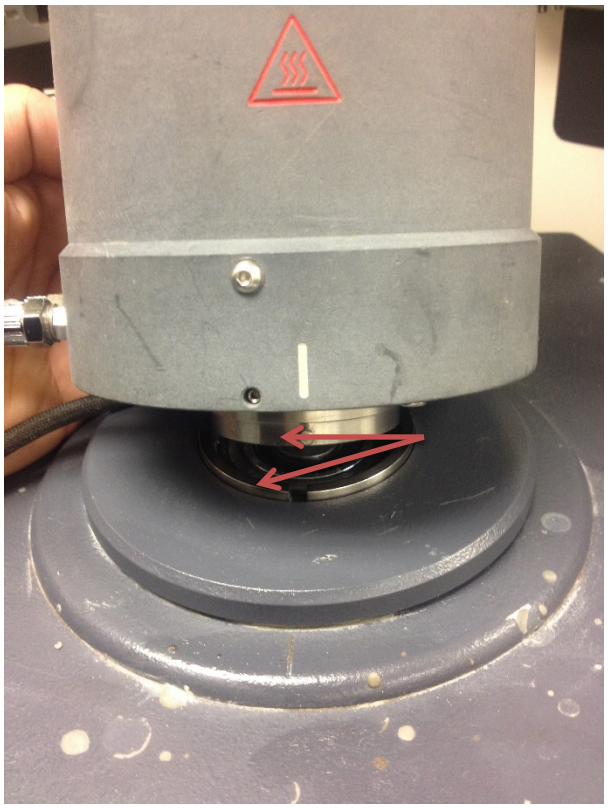

Figure G-8 Peltier assembly installation

Figure G-9 Smart swap connection

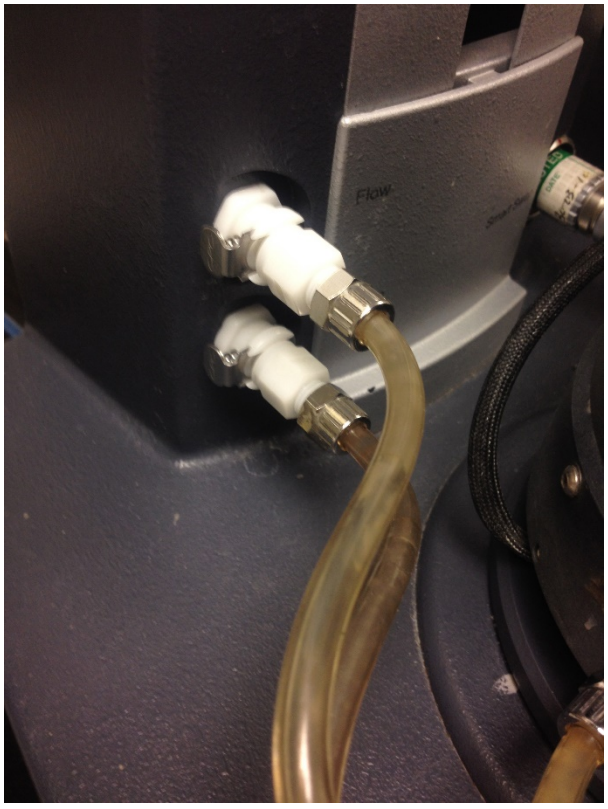

Figure G-10 Heating/cooling line connections

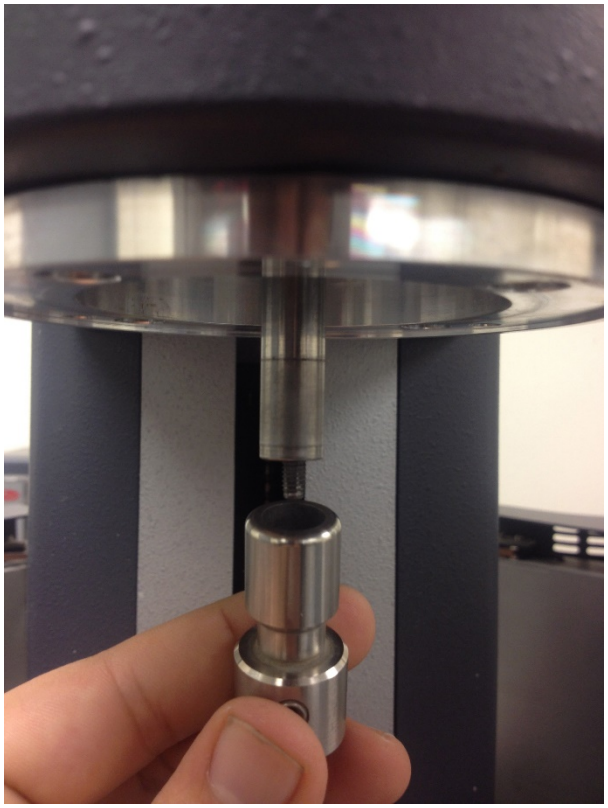

Figure G-11 Installing helical rotor onto spindle

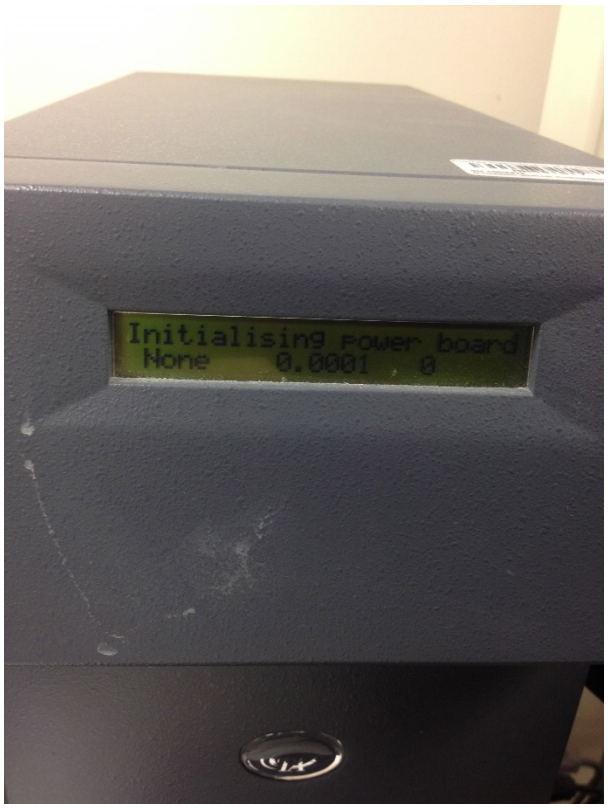

Figure G-12 DSR startup sequence

Figure G-13 Live data readout after startup sequence

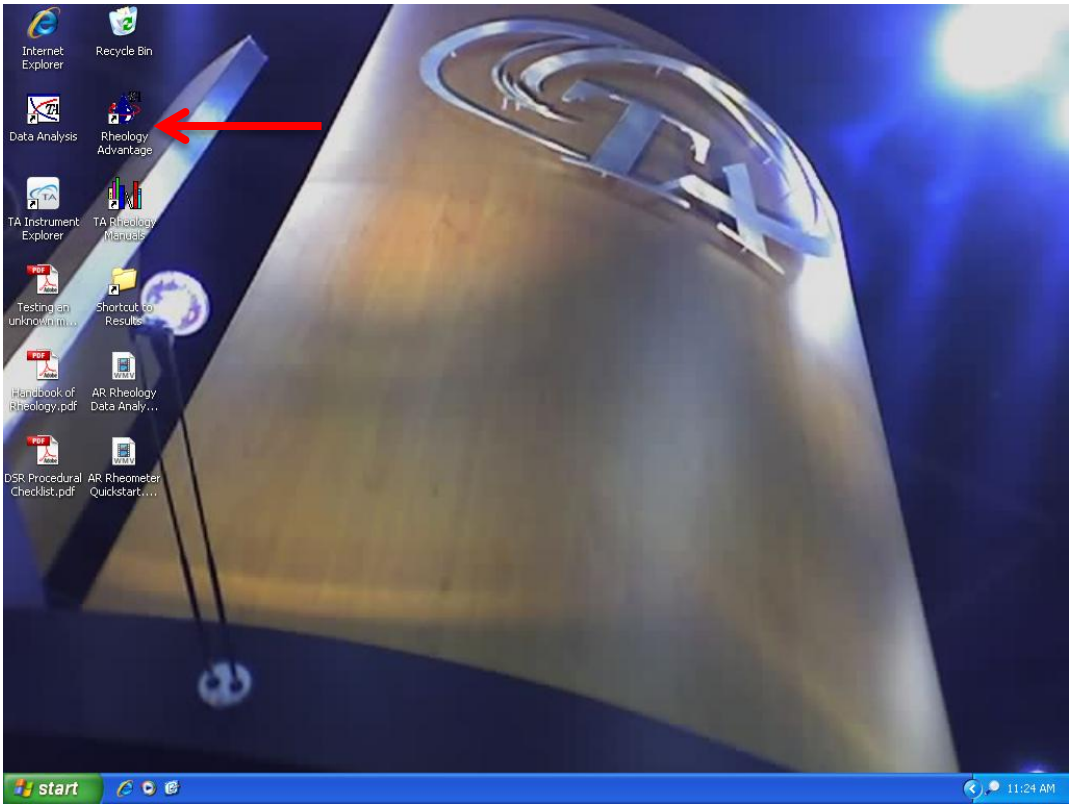

Figure G-14 Open “Rheology Advantage Software”.

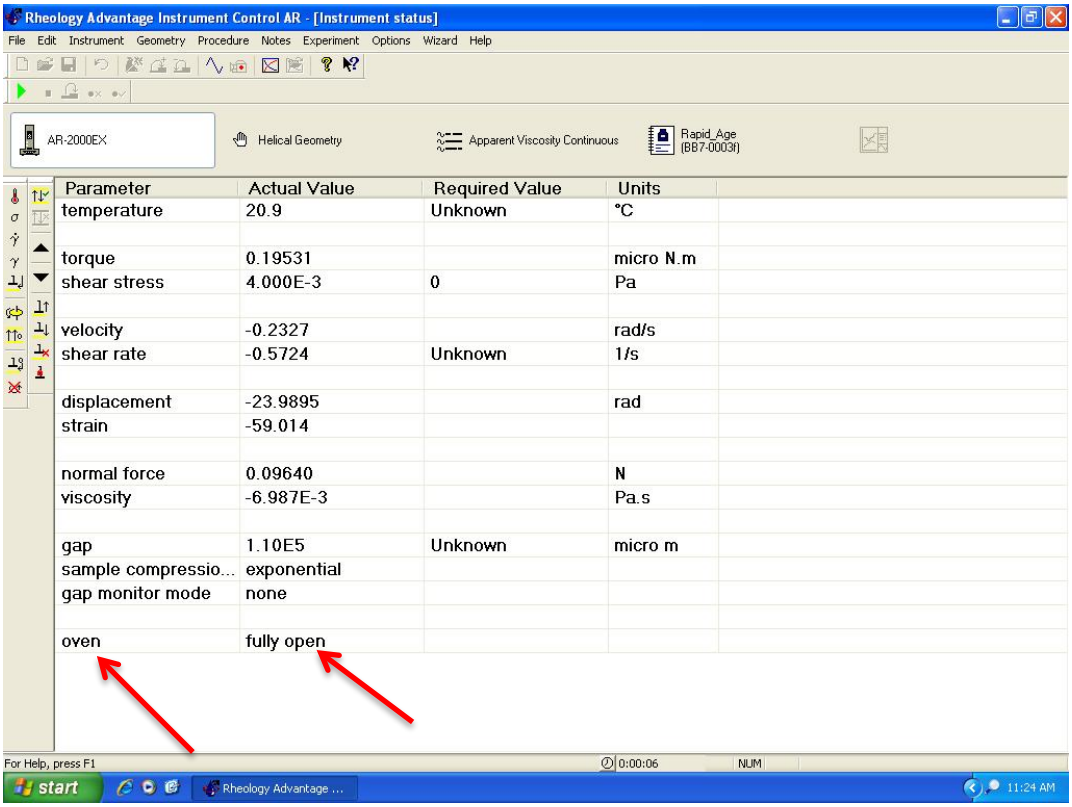

Figure G-15 Rheology Advantage default main screen and oven status

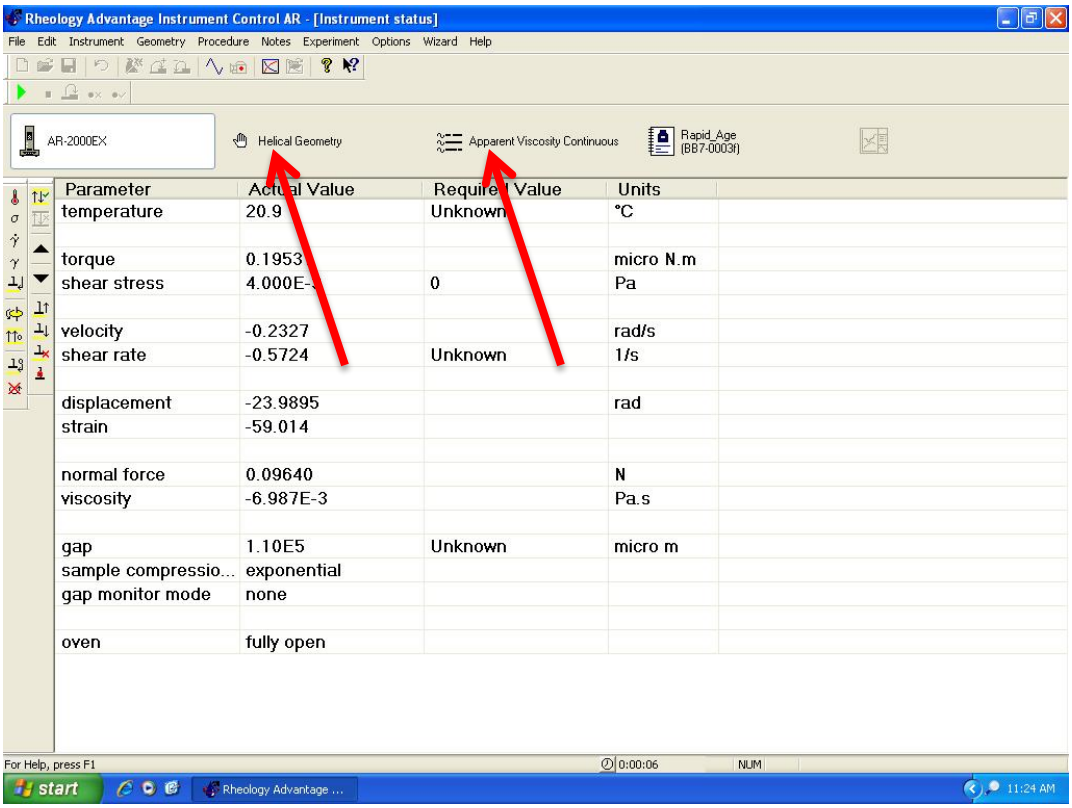

Figure G-16 Geometry and procedure tabs

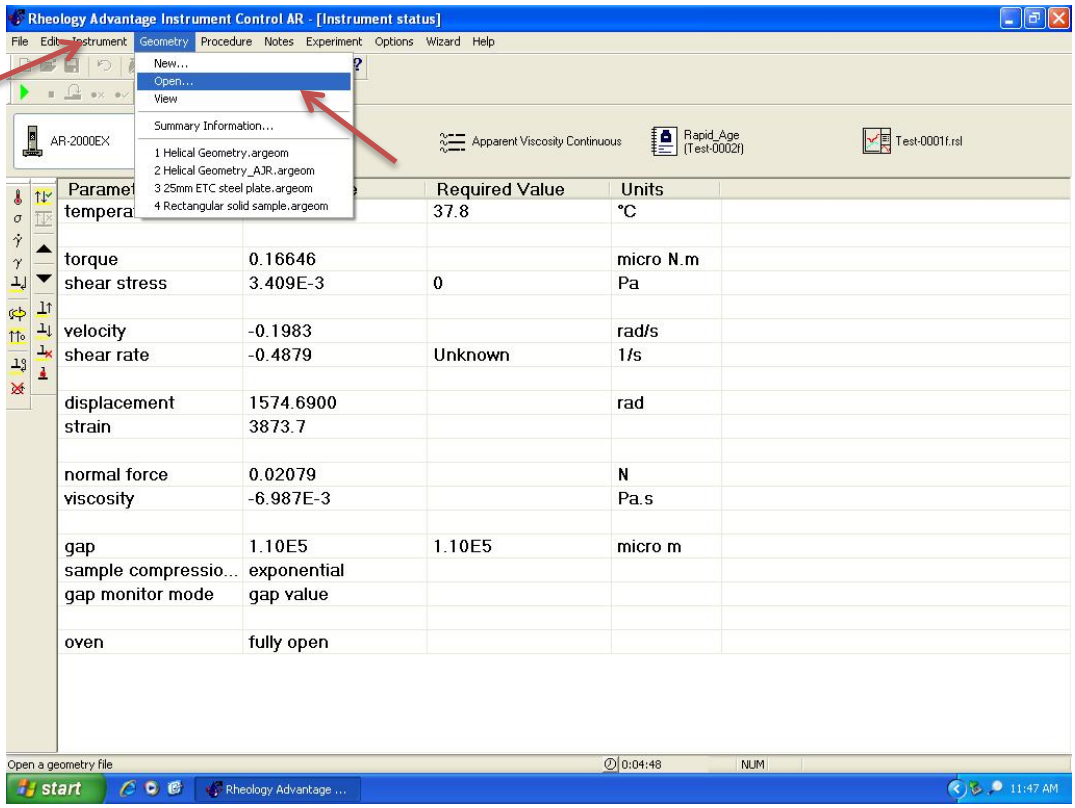

Figure G-17 Opening geometry selection

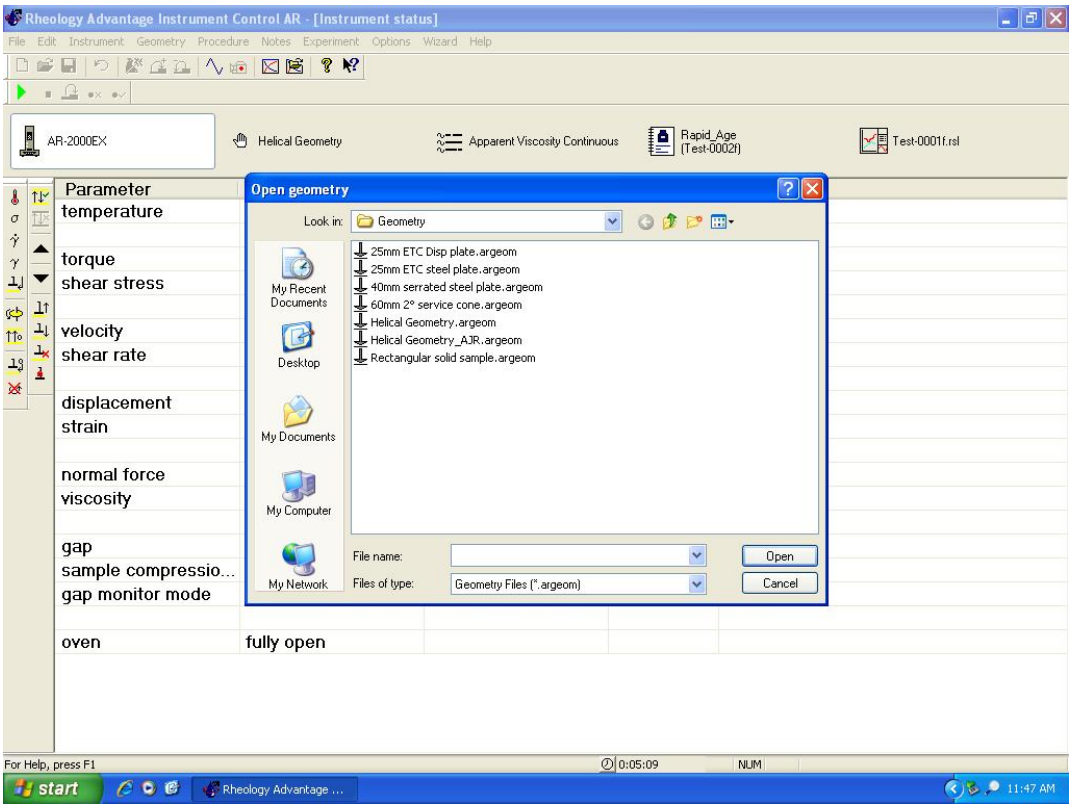

Figure G-18 Preloaded geometry selection menu

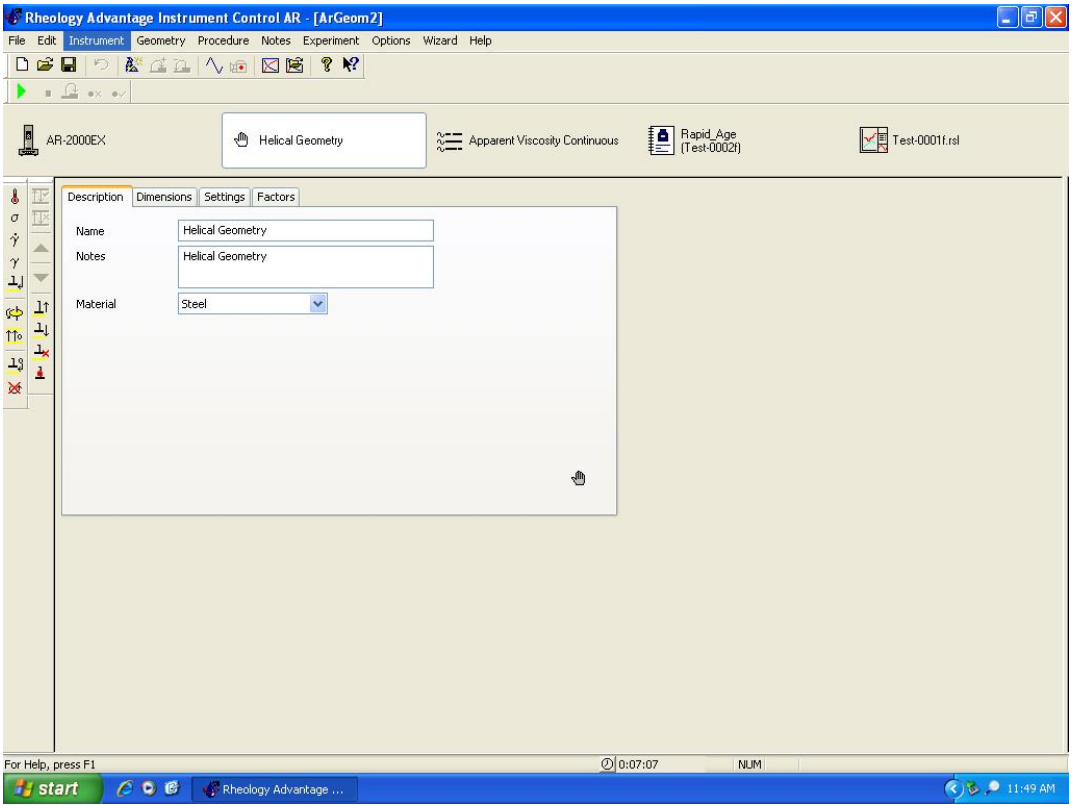

Figure G-19 Preloaded geometry details

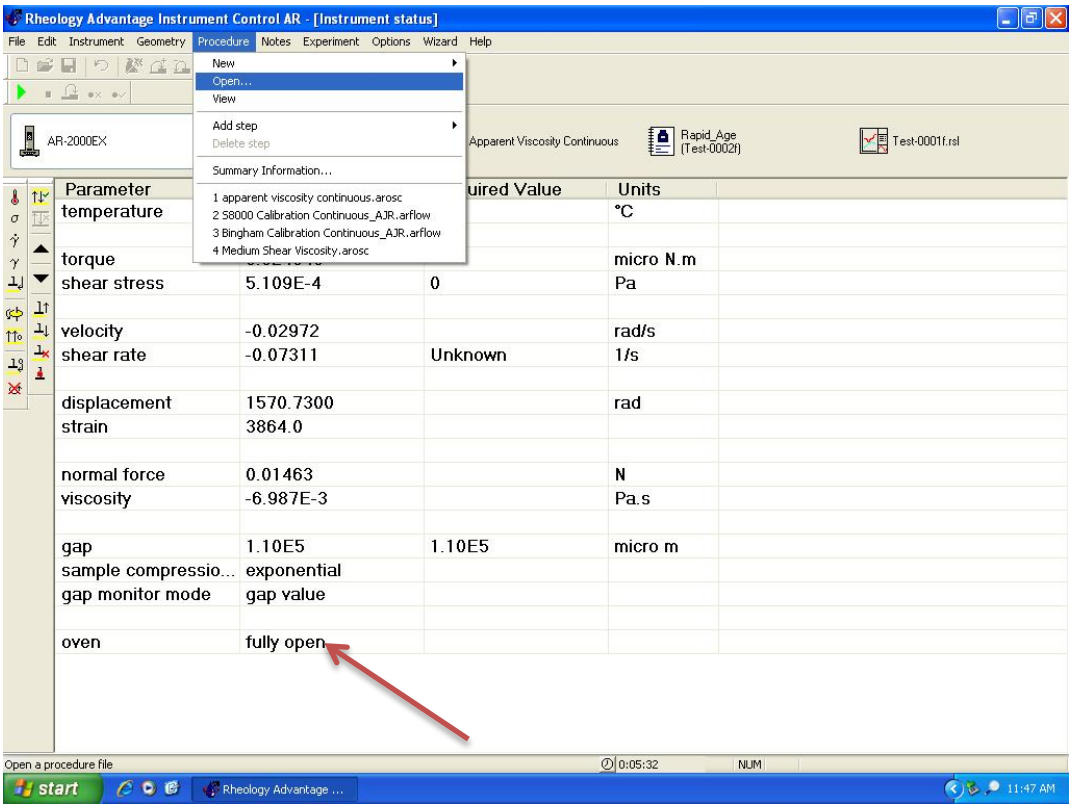

Figure G-20 Opening procedure selection

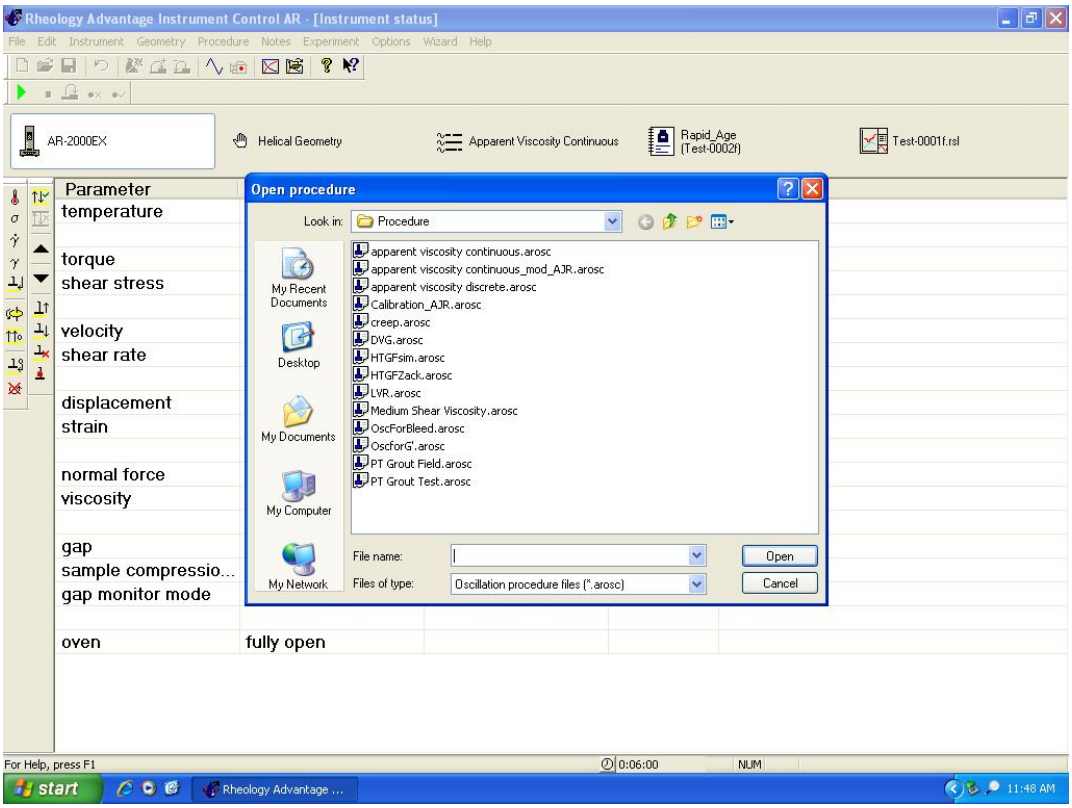

Figure G-21 Preloaded procedure selection menu

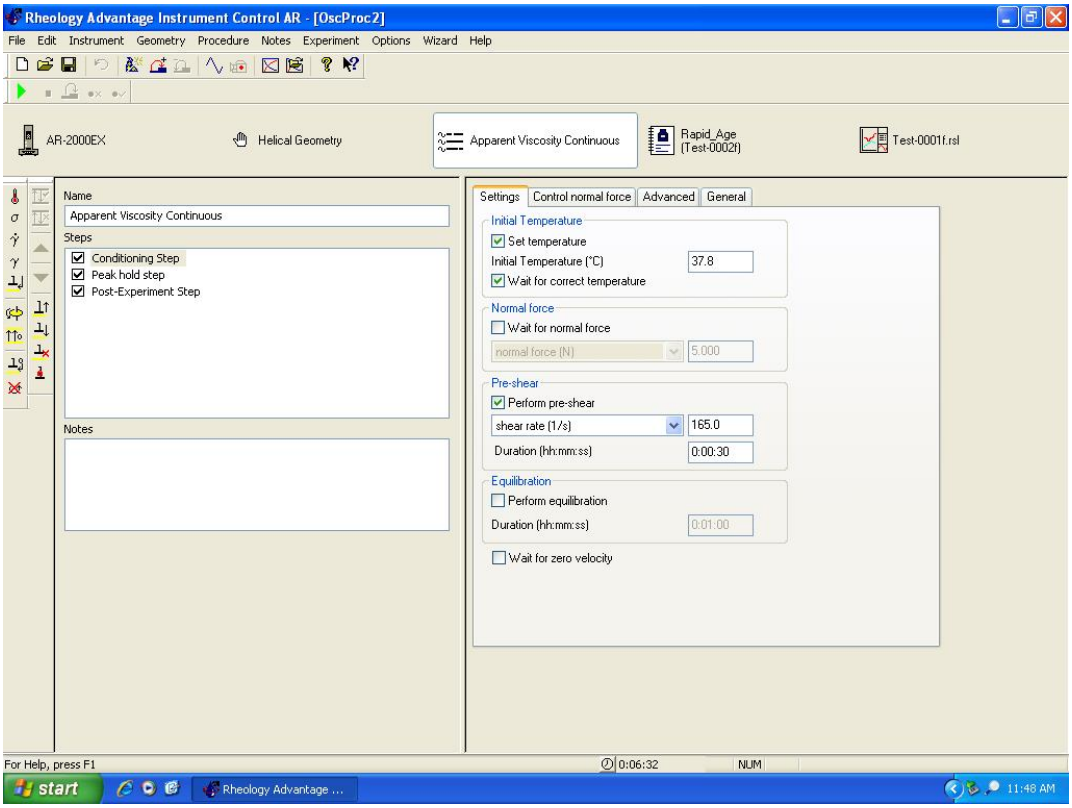

Figure G-22 Preloaded procedure details

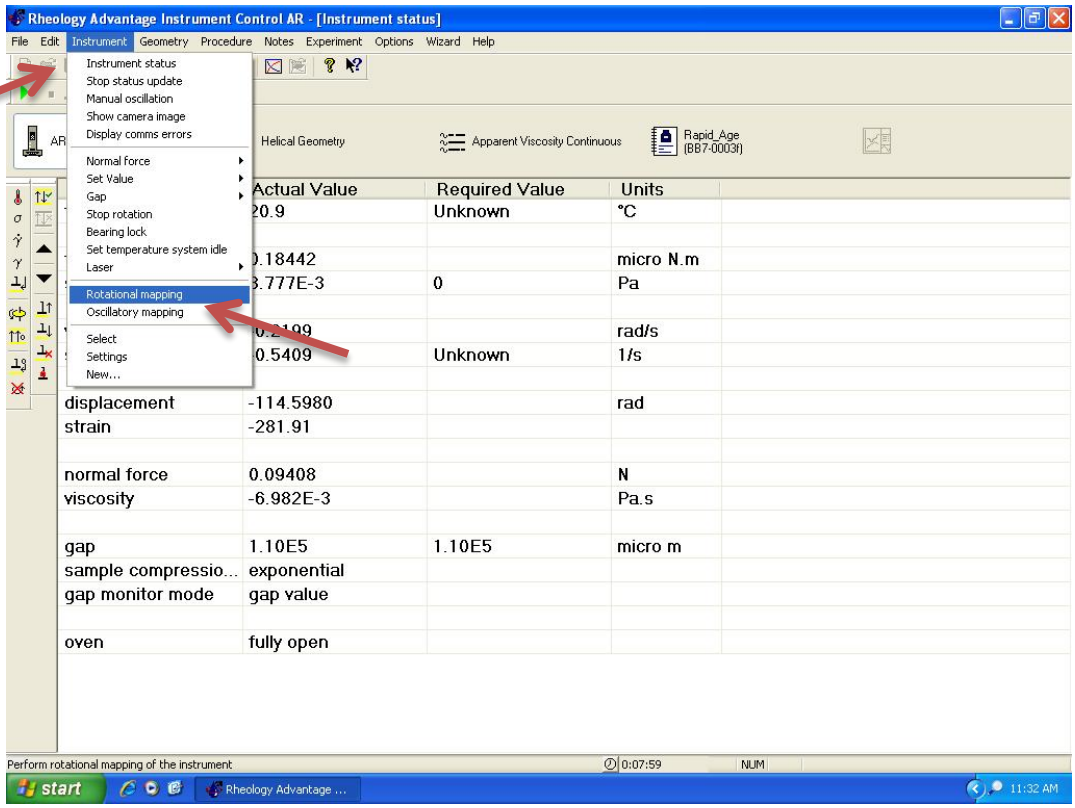

Figure G-23 Open “Rotational mapping”.

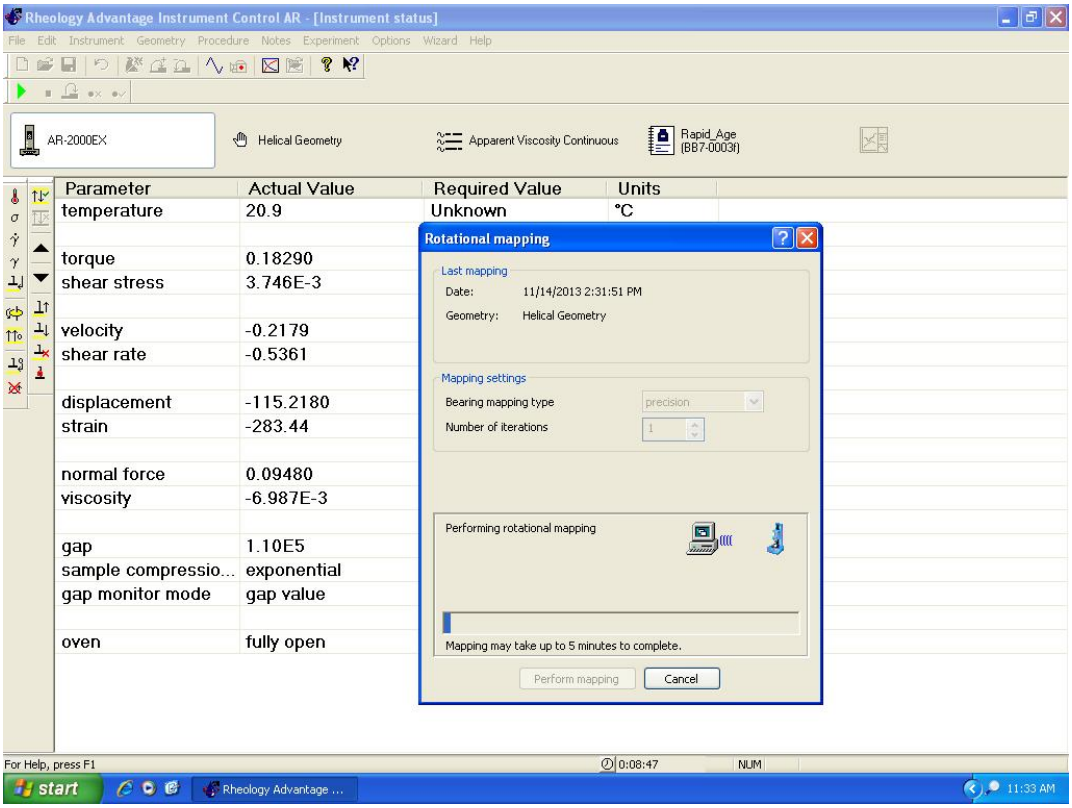

Figure G-24 Rotational mapping process

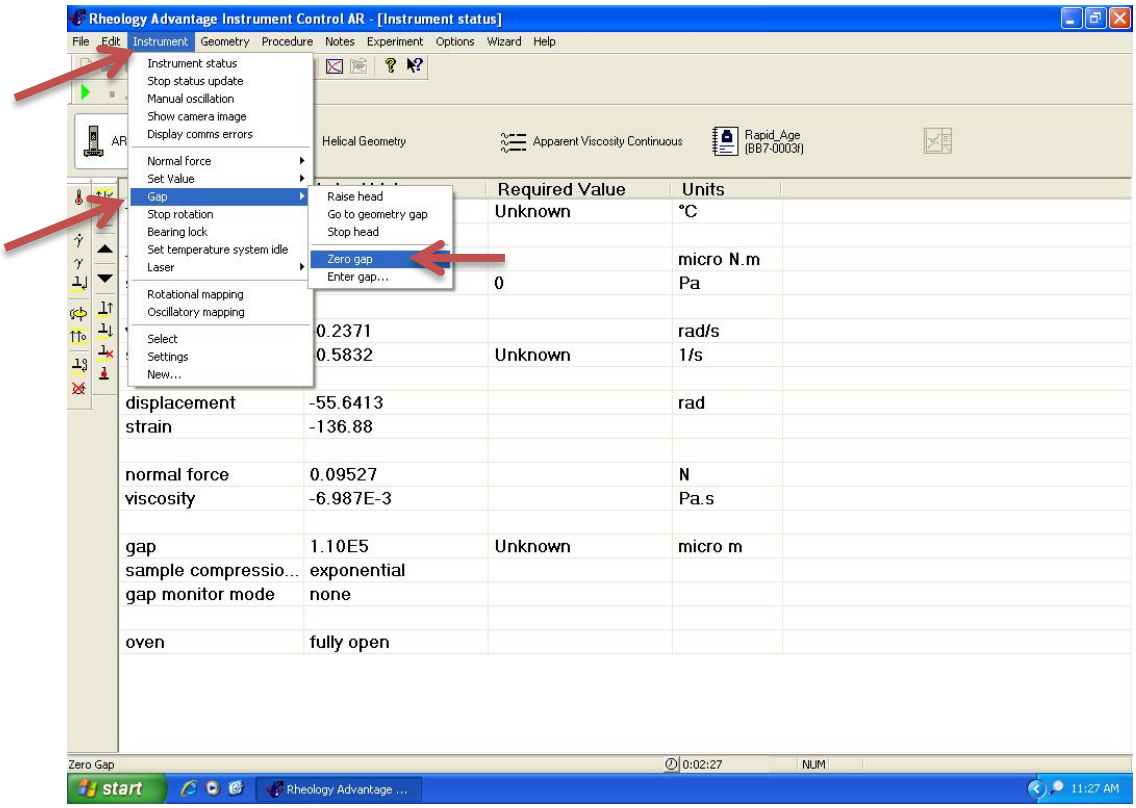

Figure G-25 Open “Zero gap”.

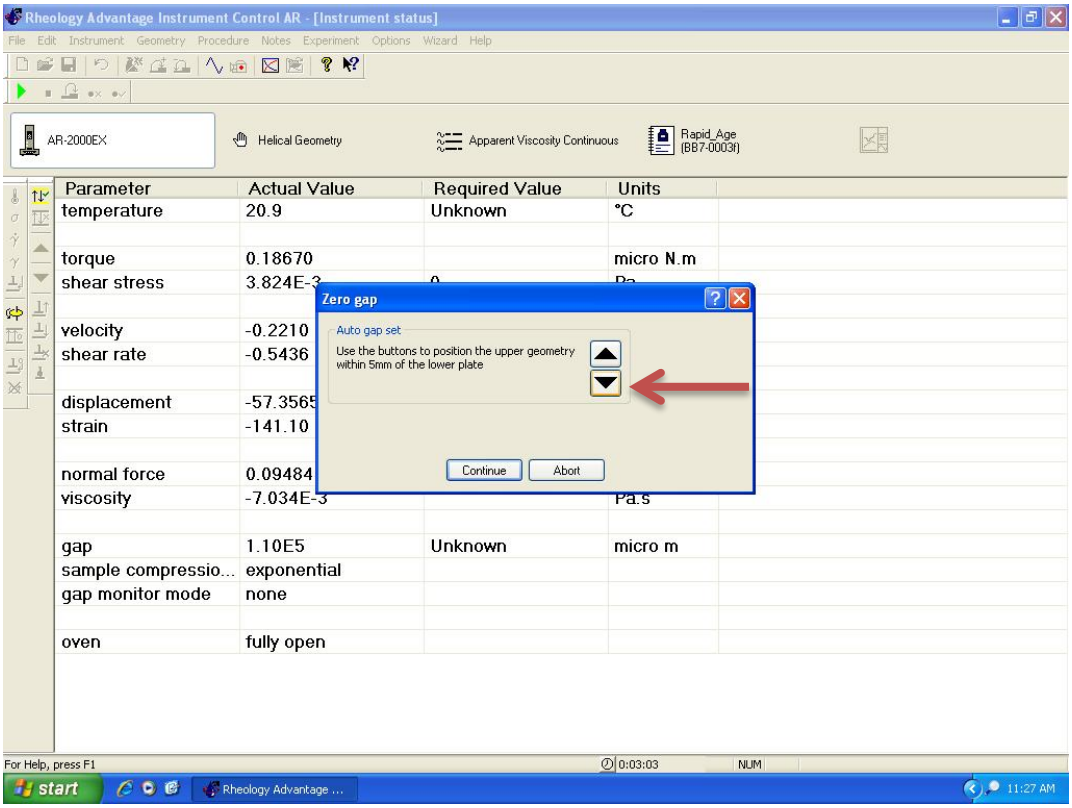

Figure G-26 Zero gap.

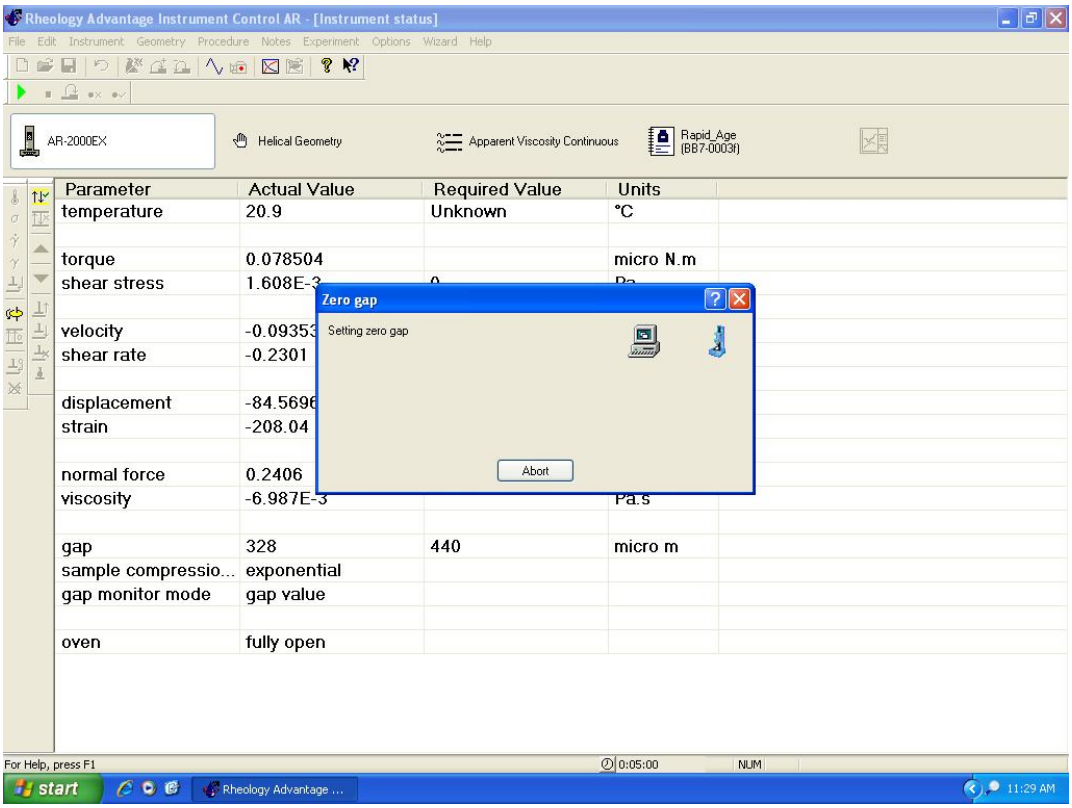

Figure G-27 Automatic setting of zero gap

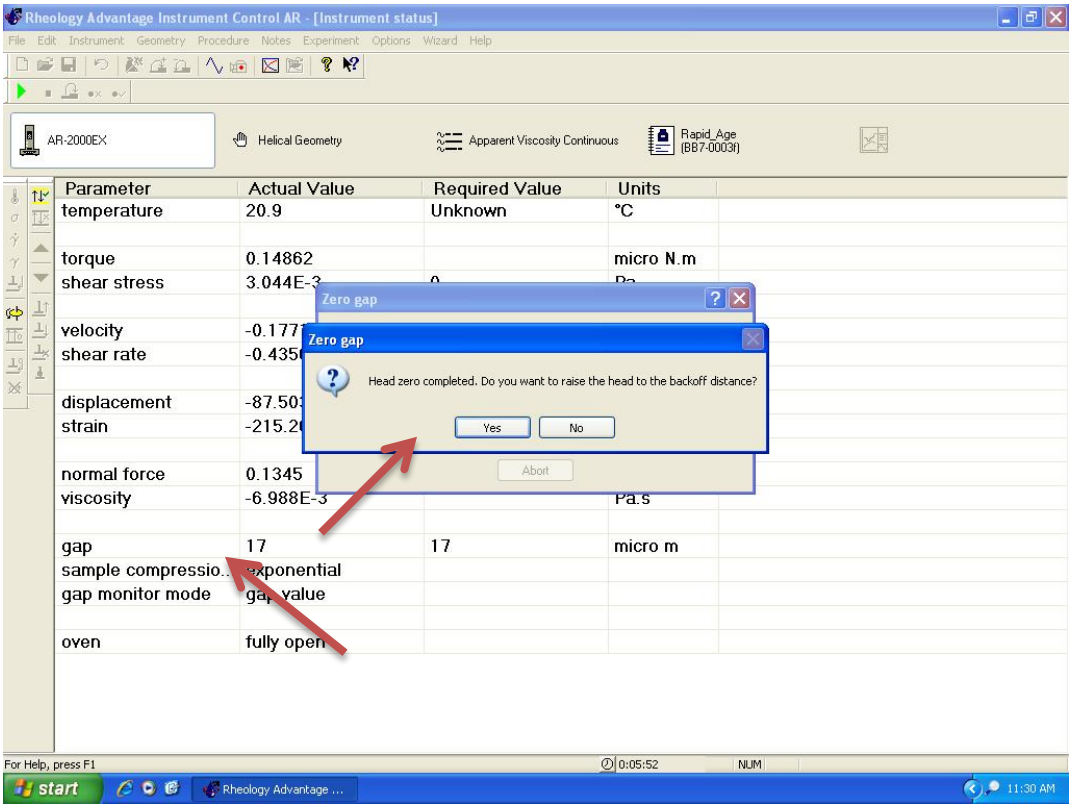

Figure G-28 Raise to back off distance dialog box and gap check

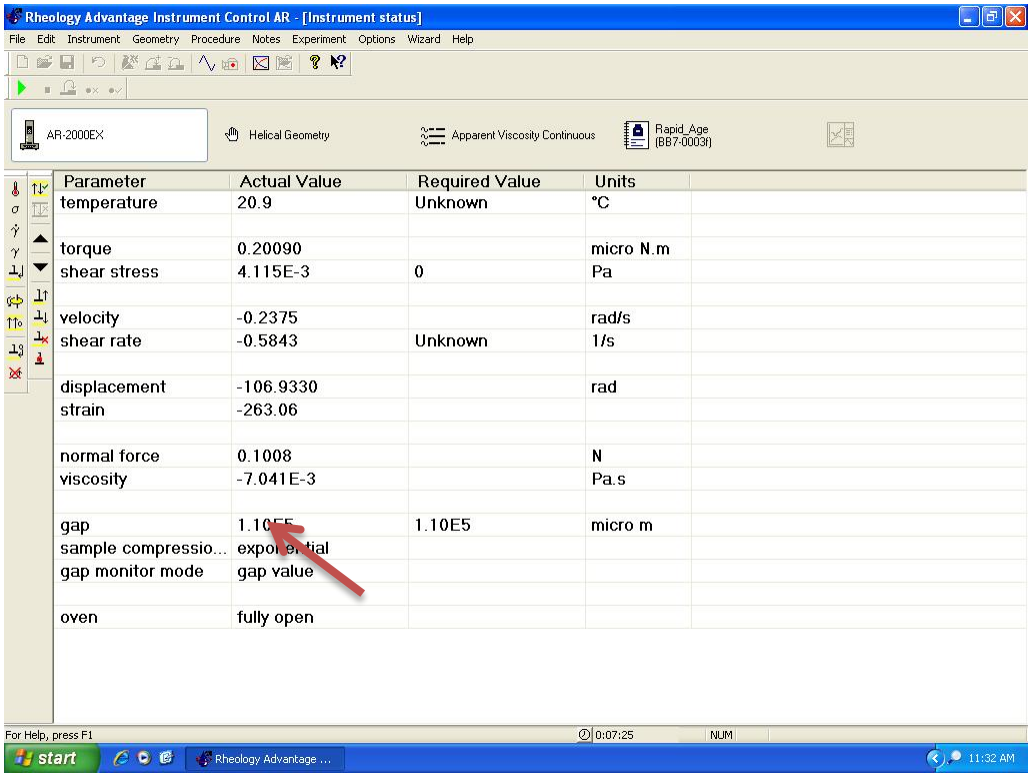

Figure G-29 Zeroing gap completed

Testing a Sample

1. Transport fresh grout sample to DSR in appropriate container. A thermos is recommended to maintain temperature and a sample volume of about one cup will be sufficient to run a test. While transporting, try to continuously and gently agitate the sample to prevent set or segregation.
2. Pour the sample into the Stainless Steel insert cup and fill level with the brim of the cup. Clean up any spills immediately.
3. Immediately start the test by clicking the green "Run experiment" arrow on the main screen. See Figure G-30.

4. A dialog box will open where the sample name and output file location can be altered. Change names and location if necessary and select "OK". See Figure G-31.

5. A dialog box will open asking to "Set the correct gap before proceeding?" Select "Yes". The head will now return to the zero position established earlier. The test screen will display the position readout, which will decrease until it matches the required value. See Figure G-32 &Figure G-33.

6. When the gap is set, the window will change to "Waiting for temperature". In this process the sample temperature is matched to the required temperature. This step can be

skipped by clicking the arrow in the window. BE SURE TO ONLY CLICK ONCE. See Figure G-34.

7. Next the window will change to “Performing pre-shear”. This step shears the sample at a specified rate for 30 seconds to thoroughly mix the sample. DO NOT SKIP THIS STEP. See Figure G-35.

8. When the pre-shear ends, the instrument will switch to the shear rate and test parameters designated in the procedure and will start recording and displaying data. Live data is displayed on the right side while viscosity data points are collected every second and graphed in the main window. See Figure G-36.

9. When sufficient data is collected, the test can be aborted by clicking the square “Abort experiment” button. Doing this stops the test and saves all data to the file and location specified. A plot of the data is shown by default. See Figure G-37 & Figure G-38

10. The DSR must be cleaned as soon as possible to prevent grout hardening. Return to the main screen by clicking the “Instrument status” tab. Click the “Raise head” button to bring the DSR head back to starting top position. Carefully remove the helical rotor by unscrewing from spindle and gently clean and rinse in separate bucket of water. Remove the stainless steel cup from the Peltier assembly by loosening the setscrews and rotating the cup out. Clean and rinse the cup in the same separate buckets of water. A small brush or toothbrush is useful for cleaning. Be sure all grout is removed and washed off before drying the rotor and cup. If another sample is to be tested, return the rotor and cup to the DSR and repeat from step 13 of the DSR preparation and follow the same testing procedure. See Figure G-39 & Figure G-40.

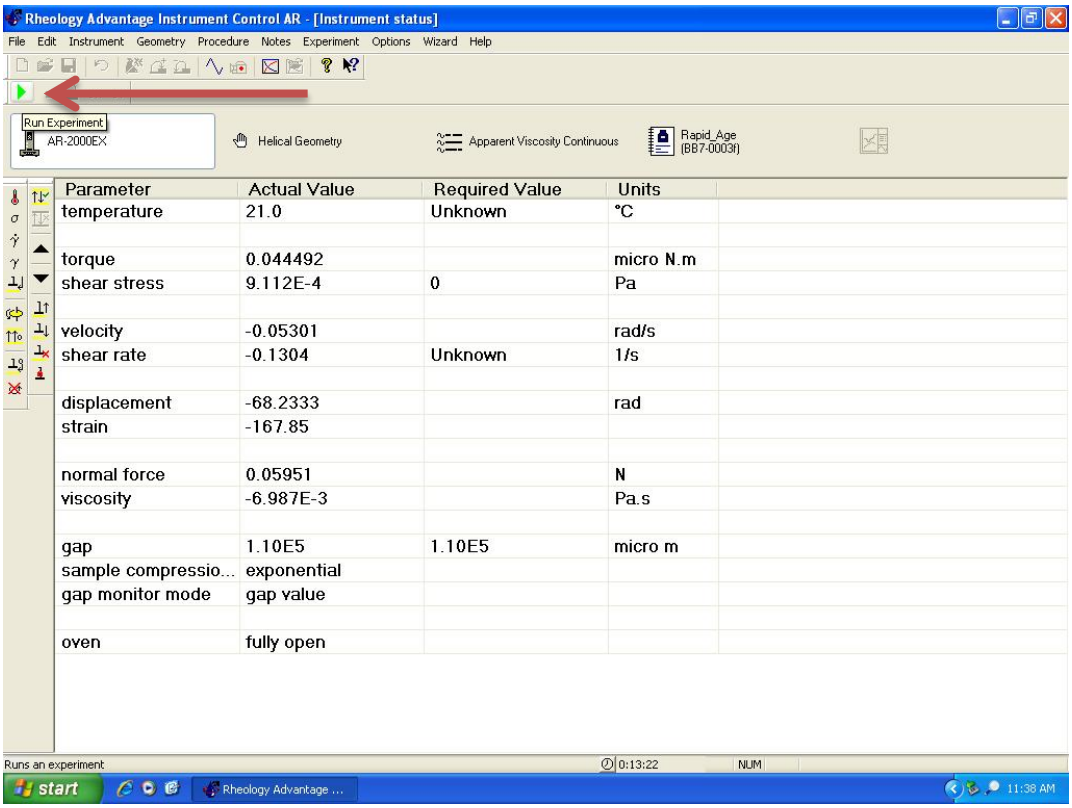

Figure G-30 "Run experiment" button

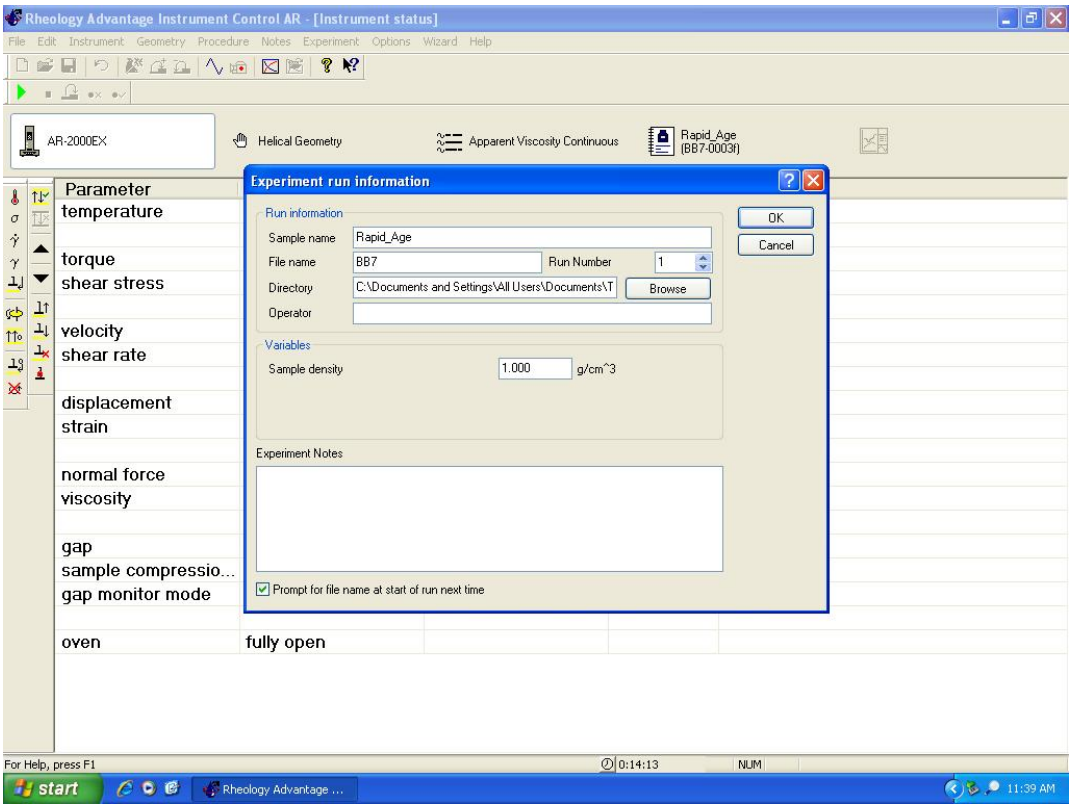

Figure G-31 Start screen with file and location selection

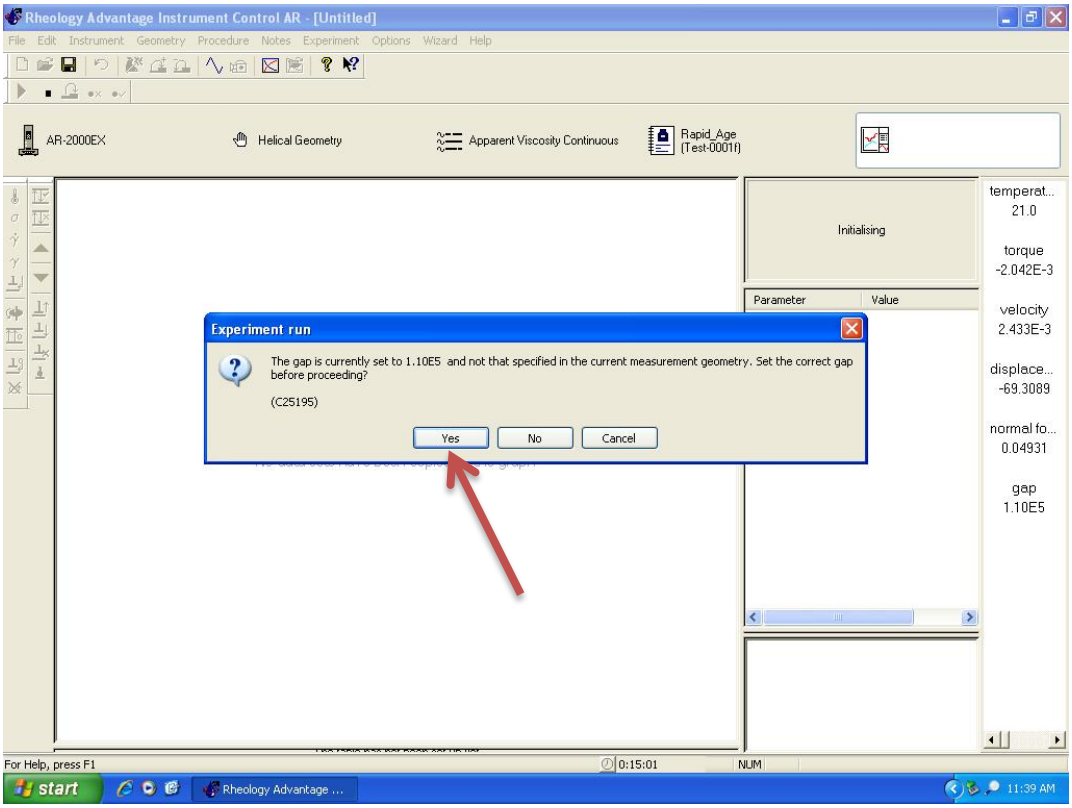

Figure G-32 "Set the correct gap" dialog box

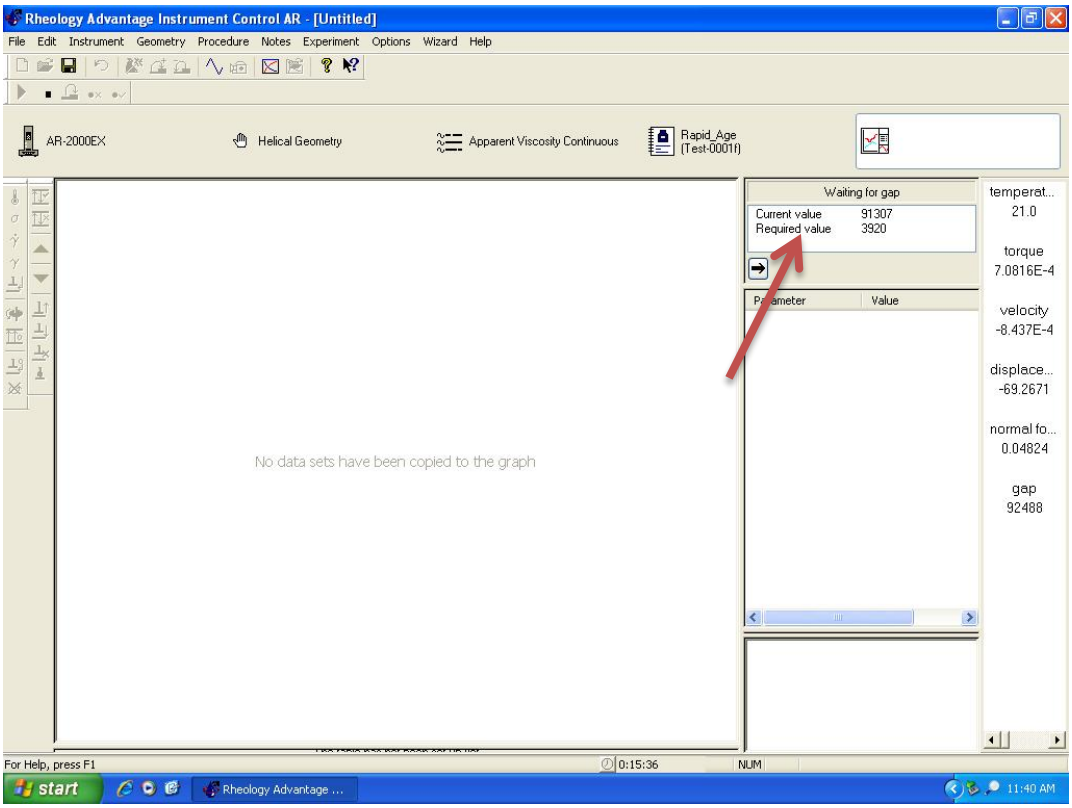

Figure G-33 Gap correction process showing position information

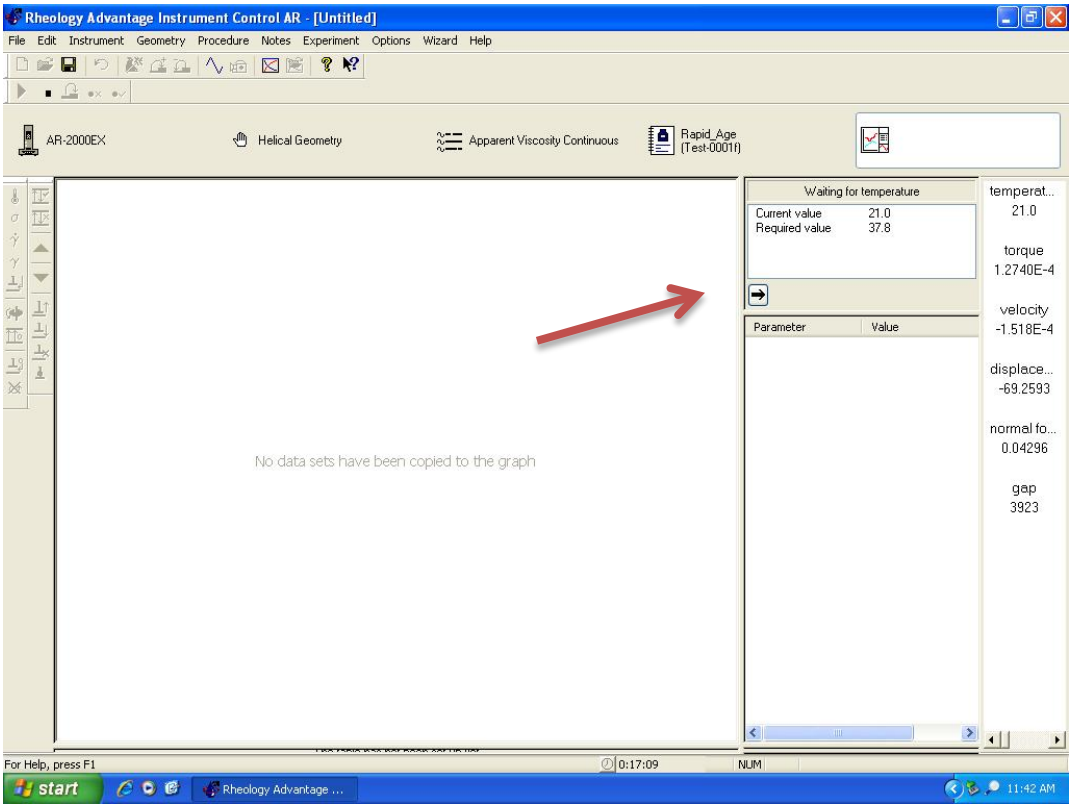

Figure G-34 Temperature matching indicating “Skip” arrow

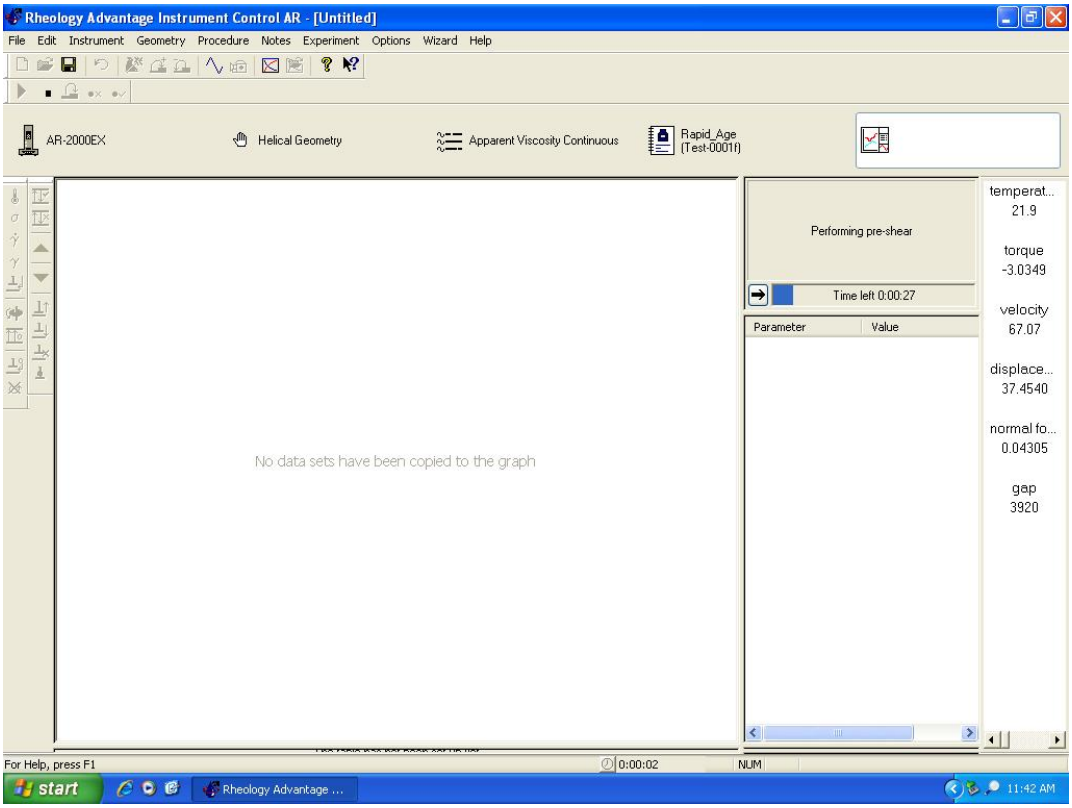

Figure G-35 Pre-shear process

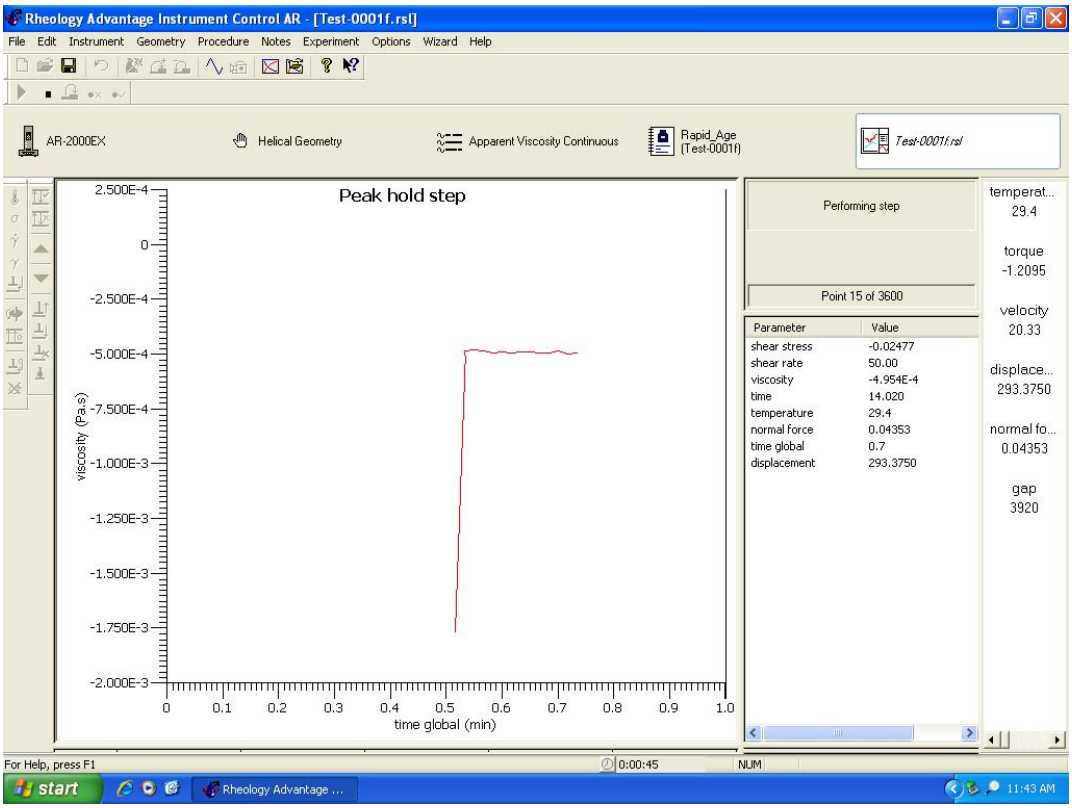

Figure G-36 Live data displayed during testing

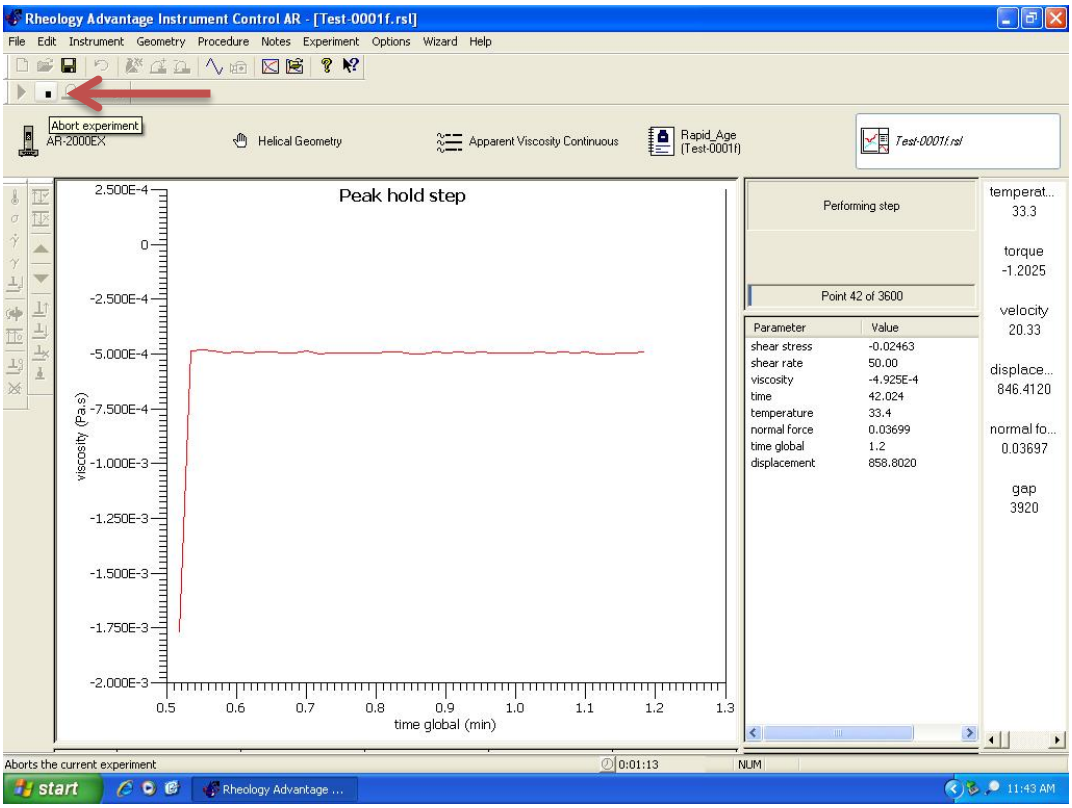

Figure G-37 Button to abort experiment

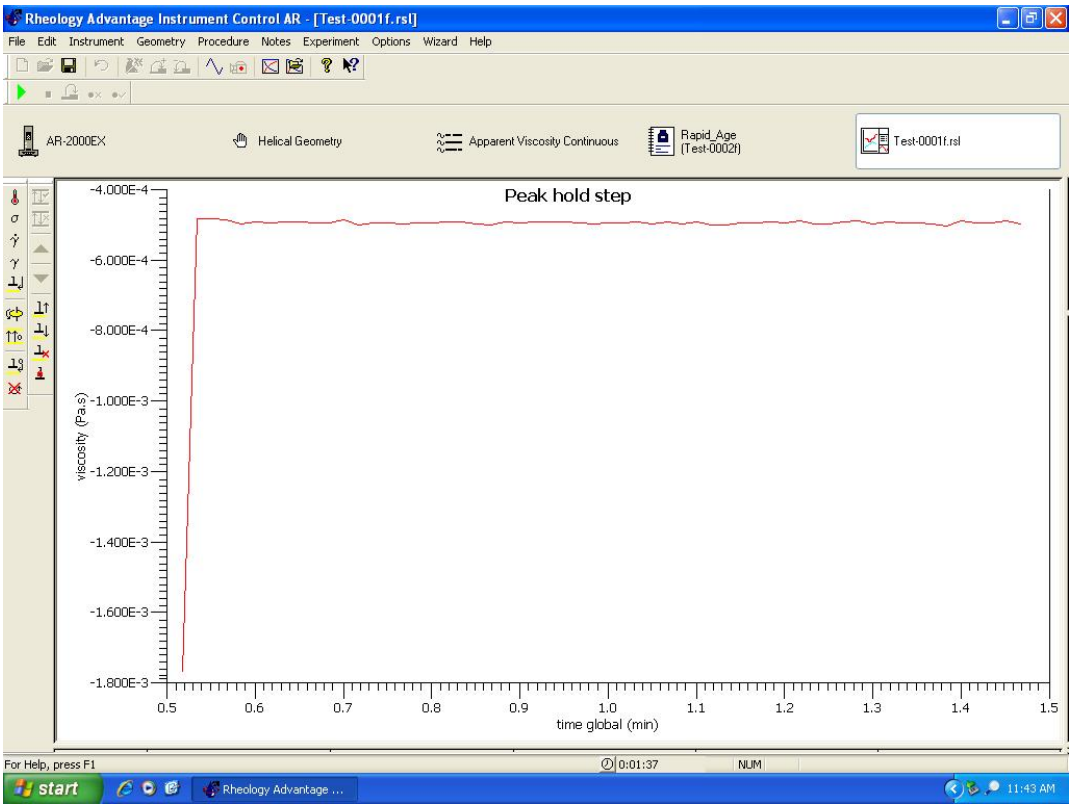

Figure G-38 Results shown after aborting experiment

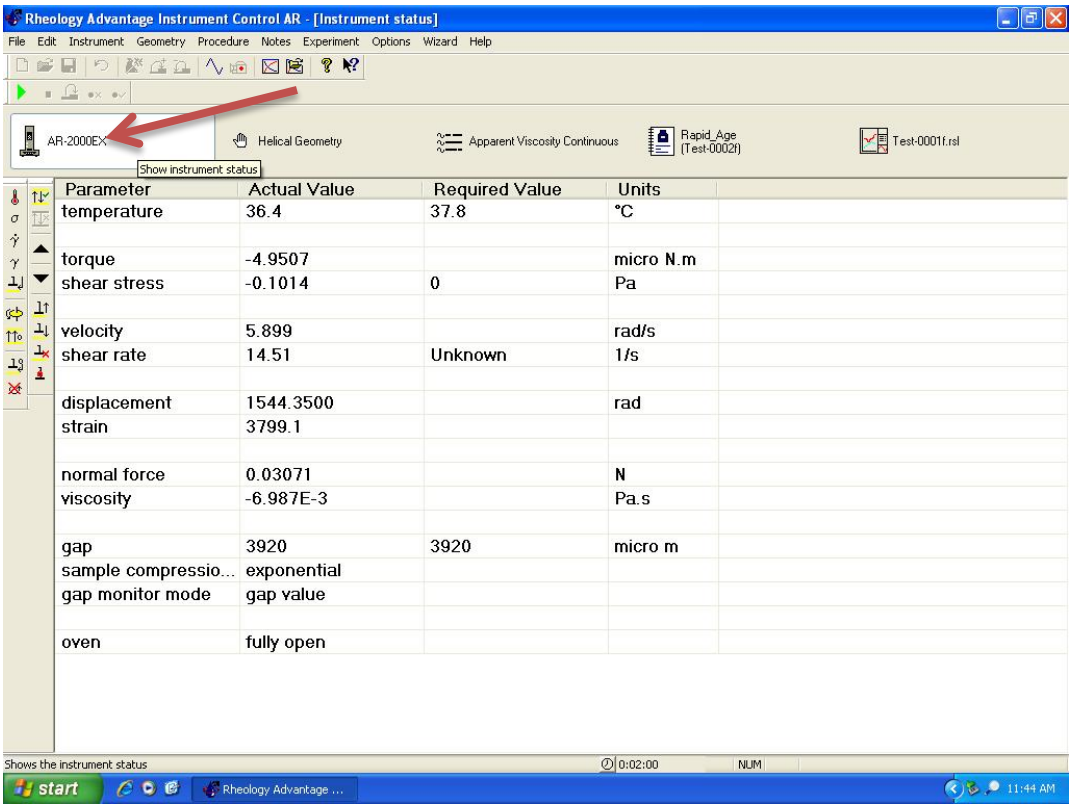

Figure G-39 Return to main screen by clicking “Instrument status”.

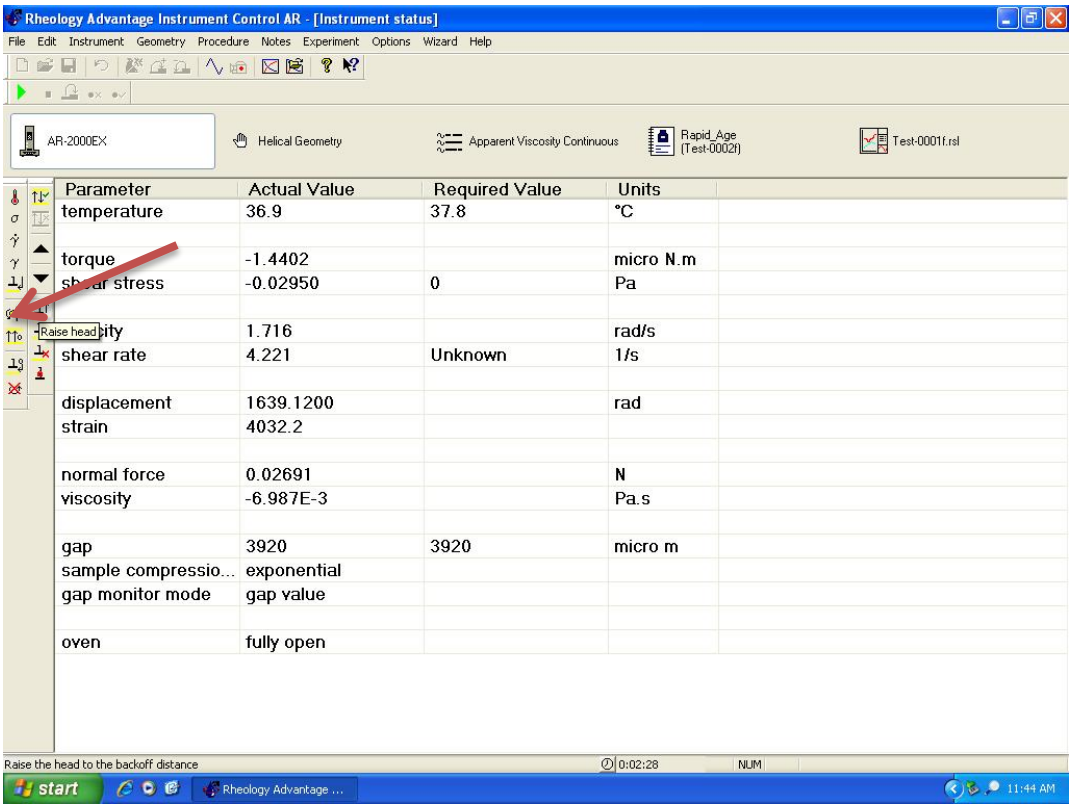

Figure G-40 Raise head to begin cleaning.

Disassembly and Shutdown

1. After all testing and cleaning is complete. Close the Rheology Advantage program.

2. Turnoff DSR power by flipping switch on rear of tower.

3. If helical rotor is still attached to spindle carefully unscrew it and return to storage box. Replace black protective spindle cover by threading onto spindle.

4. Unplug the Peltier assembly by pushing the silver heating/cooling line release buttons on the left side. Unplug the Smart Swap cable by pulling straight out on the release collar on the cable. Pull assembly off DSR base and replace the white protective covers to the DSR base and the assembly base. BE SURE DSR IS POWERED DOWN BEFORE REMOVING SMART SWAP CABLE OR PELTIER ASSEMBLY.

5. Return helical rotor and Peltier assembly to safe storage location.

6. Close oven doors and secure latch.

Data Analysis

1. Locate and open output file. By default the file will open in the "Rheology Advantage Data Analysis" program. See Figure G-41.

2. After file loads click the "grid" button to view a chart of collected data. To view data in graphical from, select "send data to graph" from the dropdown menu under the "View" tab. By default the graph plots viscosity vs. time. To change what variables and data are plotted, right click on either axis and select "change variables" from the popup menu. A selection screen will open allowing the user to make custom plots. See Figure G-42 - Figure G-46.

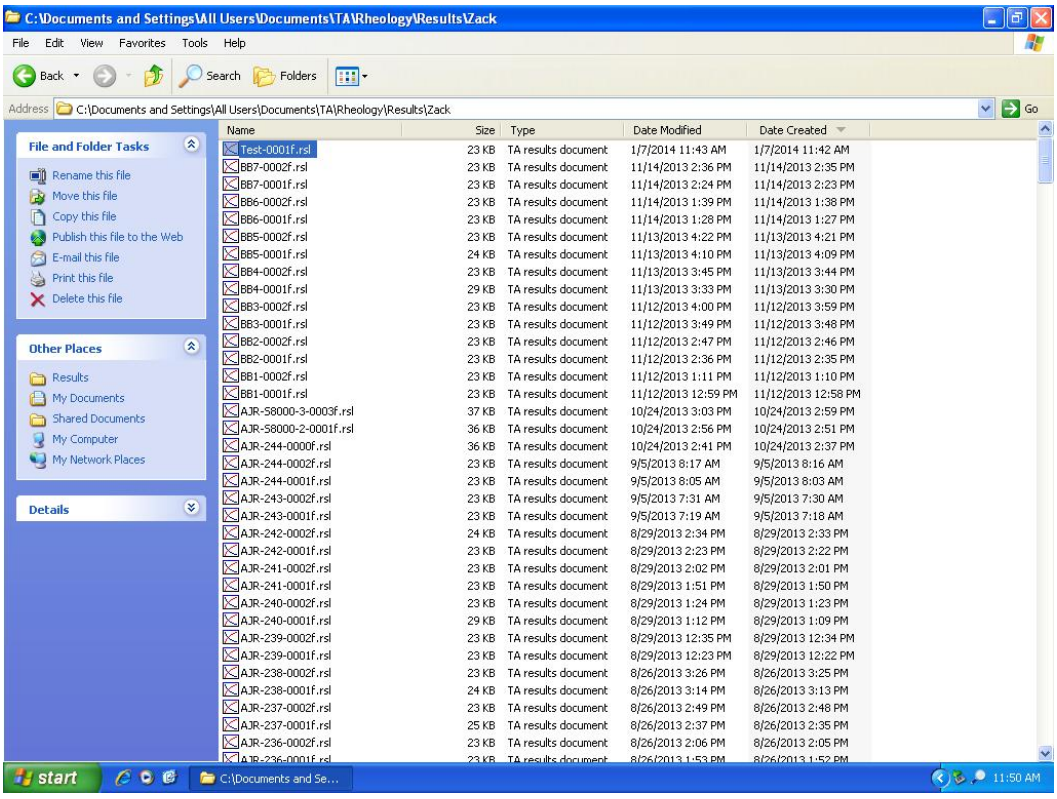

Figure G-41 Locate and open output file.

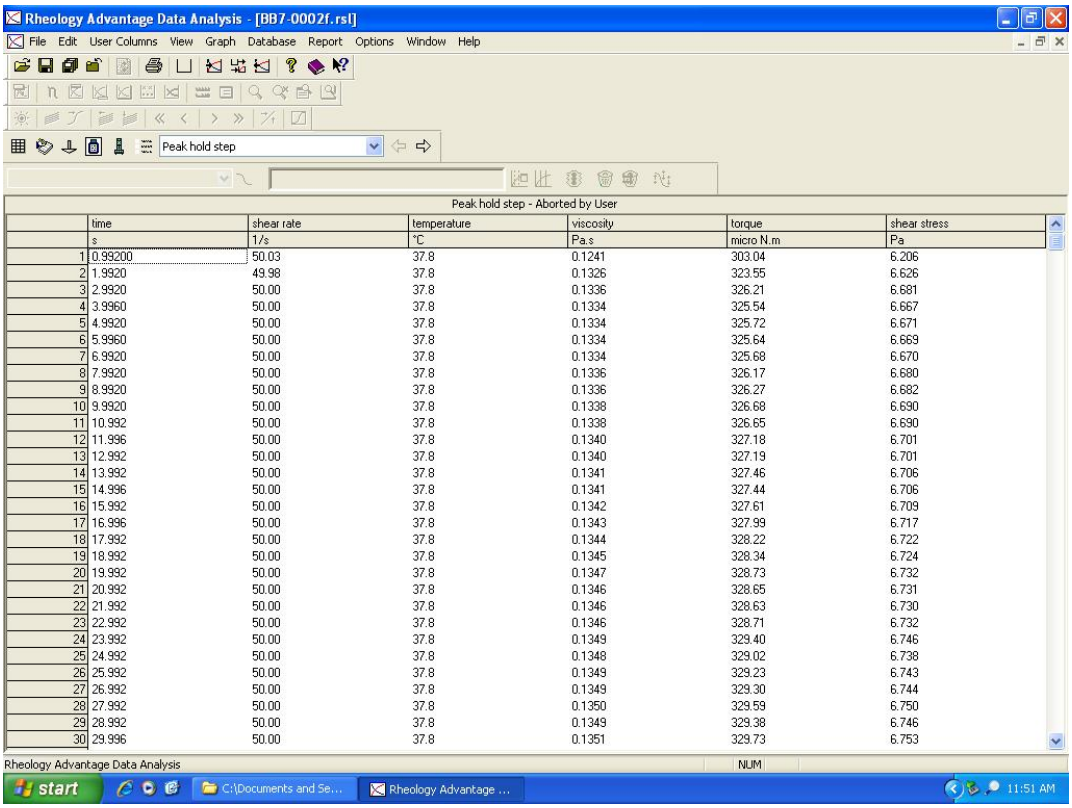

Figure G-42 Chart display of data

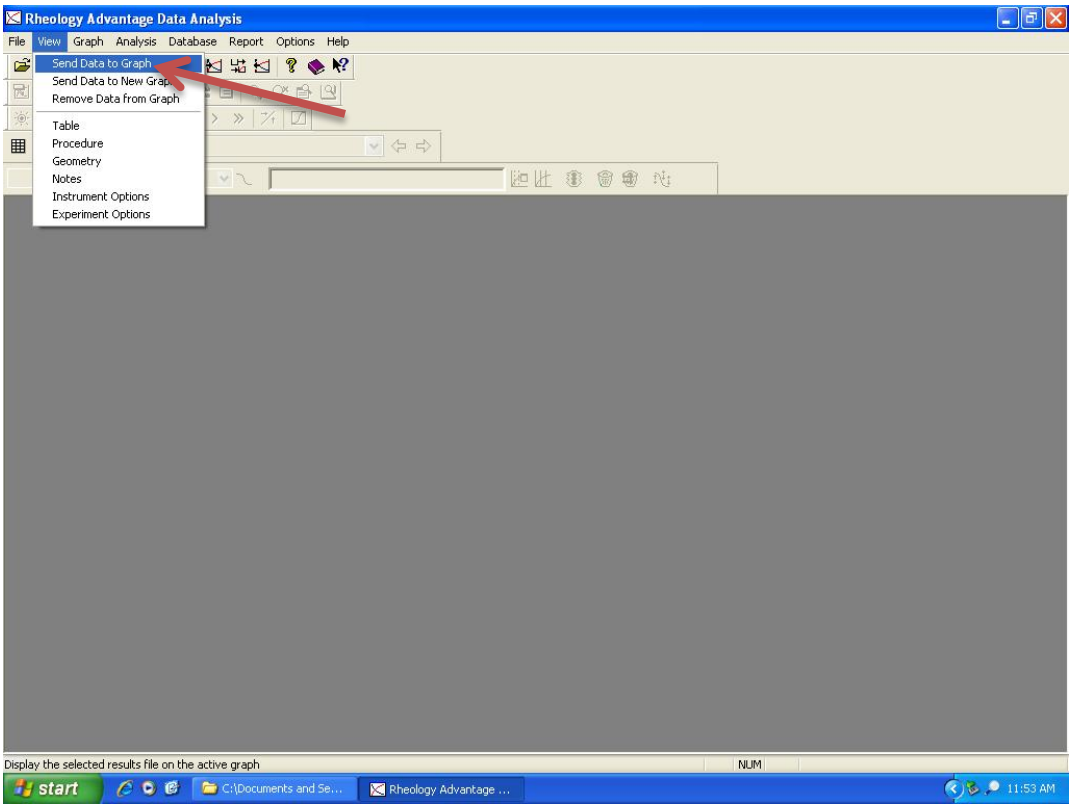

Figure G-43 Send data to graph.

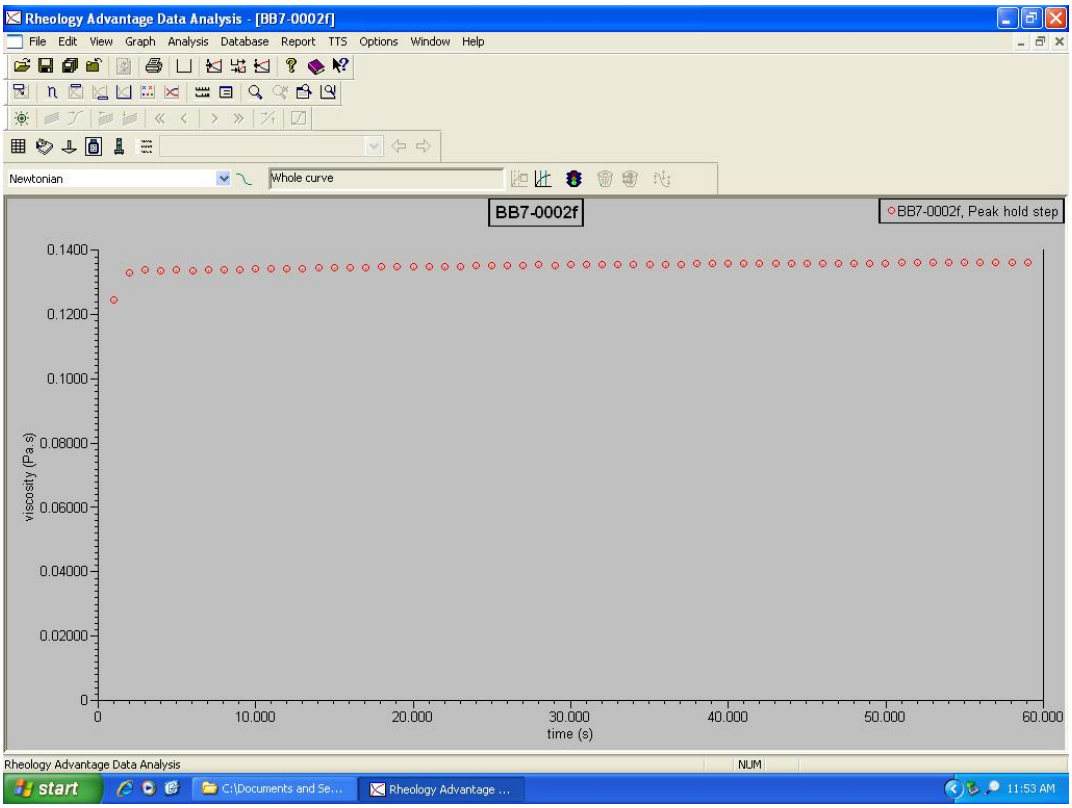

Figure G-44 Default viscosity vs. time plot

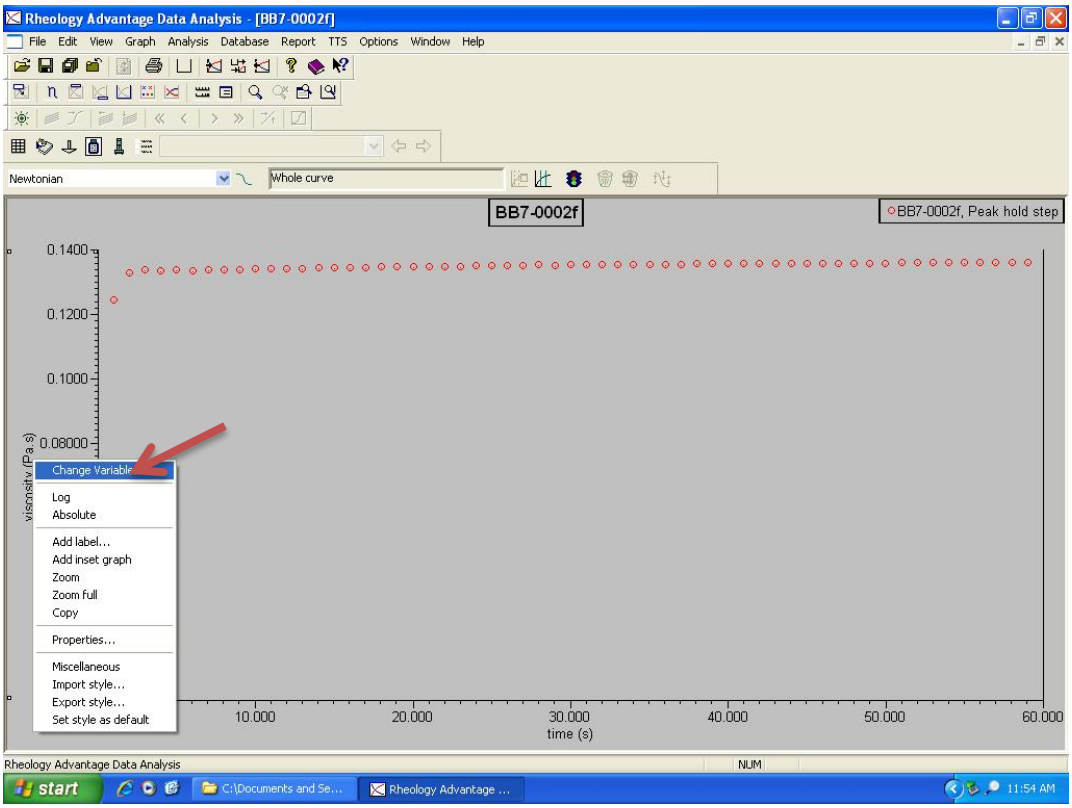

Figure G-45 Select “Change Variables” after right clicking on an axis.

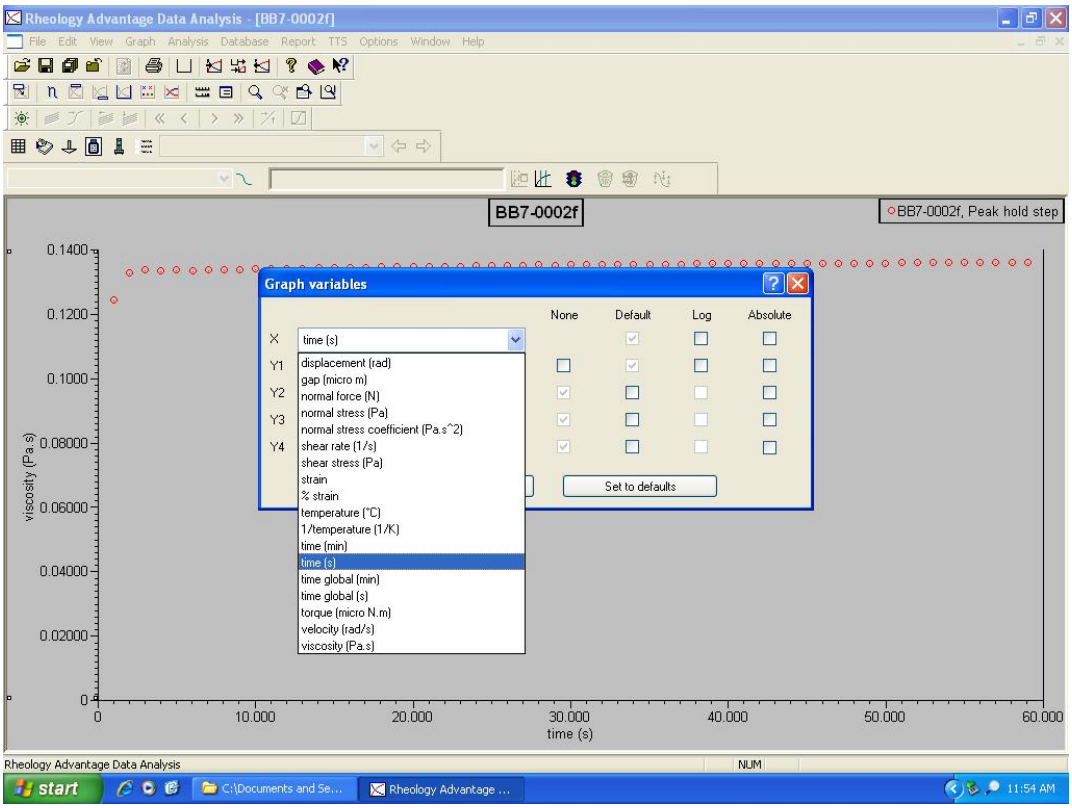

Figure G-46 Select custom plot outputs.

Appendix H—HORIBA LA-950V2 Particle Size Analysis Procedures

The following procedure was used to measure the mean particle size and particle size distribution of the six grouts tested in the first series of MITT testing:

1.) Remove appropriate grout samples from incubator (unless they are the initial control grout samples)
2.) Turn on the HORIBA LA-950V2 Laser Scattering Particle Size Distribution Analyzer. See Figure H-2
3.) Turn on the Dry Feeder Unit. See Figure H-3.
4.) Turn on the Particle Size Distribution Analyzer's attached computer.
5.) Open the LA-950V2 program on the attached computer.
6.) Insert 5 to 10 g of the V-blended grout into the hopper at the top of the HORIBA LA-950V2 Laser Scattering Particle Size Distribution Analyzer. See Figure H-4
7.) Select the proper setting for a dry sample test.
8.) Select the proper settings for the refractive index.
9.) Click the "Start" button to conduct measurement test.
10.) Conduct the test a minimum of 5 times per grout sample, but as many times as is required to get consistent outputs.
11.) After consistent outputs have been obtained, remove the hopper from the LA-950V2 and clean the hopper with compressed air to remove all the remaining grout from that particular sample. See Figure H-5
12.) Put the hopper back in the LA-950V2. See Figure H-6 Perform steps 7 through 12 on the remaining samples of grout.
13.) After all samples have been measured in the LA-950V2, remove hopper and clean using compressed air to ensure no grout remains in the hopper.
14.) Exit the LA-950V2 software.
15.) Shutdown the LA-950V2 and the attached computer.
16.) At the appropriate times (1 day, 3 days, 7 days, and 14 days) perform the measurement analysis outlined in steps 4 through 17 on all the grout types to be tested.

Figure H-1 HORIBA LA-950V2 Laser-Scattering Particle Size Distribution Analyzer

Figure H-2 On/Off switch for particle size distribution analyzer

Figure H-3 On/Off switch for dry feeder unit

Figure H-4 Place 5 to 10 grams of grout into the hopper.

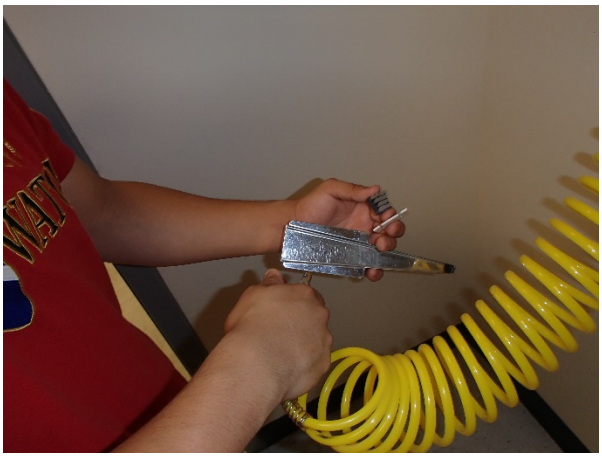

Figure H-5 Cleaning the hopper with compressed air

Figure H-6 Hopper in the LA-950V2

Appendix I—Mixing Equipment and Procedures

This section describes the equipment that was used to mix and inject both prepackaged PT grouts and plain grouts into the inclined test tube. Furthermore, the mixing procedures used for both plain grout mixtures and prepackaged PT grout mixtures are described in detail.

I.1 Colloidal Grout Plant

Figure I-1 Chemgrout CG600 E/H – 3CL6 Progressive cavity pump below shows the Chemgrout CG600 colloidal grout mixing plant that was used for these experiments.

Figure I-1 Chemgrout CG600 E/H – 3CL6 Progressive cavity pump

I.2 PT Grout Mixing Procedure

The following procedure was used to mix the PT grouts using the CG600 colloidal grout mixer.

1. Add water to mixing basin and turn on colloidal mixer and agitator paddle. See Figure I-2 below.
2. Add one bag of grout at a time. Add grout over a period of 20-30 seconds per bag. See Figure I-3 below.
3. Continue running colloidal mixer and agitator paddle for 30 seconds after adding last bag of grout.
4. Turn off entire machine and scrape any powder caked onto the inside of the mixing tank walls back into the grout.
5. Turn on the colloidal and continue mixing for 2 minutes
6. Record the temperature of the grout while it is in the mixing basin.
7. Transfer the grout to the agitation tank and start the paddle in the agitation tank. See Figure I-4 below.
8. Begin pumping grout after as quickly as possible. See Figure I-5 below.

Figure I-2 Add water to mixing basin.

Figure I-3 Add one bag of grout at a time

Figure I-4 Transfer the grout to the agitation tank

Figure I-5 Pump grout to target.

Appendix J—MITT Test Methods

The tests outlined in this appendix were conducted each time the grout was mixed and injected into the inclined tube. They consisted of tests on both fluid and hardened properties. The modified flow cone, unit weight, mud balance, Schupack, and apparent viscosity tests were conducted on the fluid grout immediately following mixing. After injection, visual observations were made on the tube to detect bleed water at the top of the incline. After 24 h, the tube was then dissected and inspected for soft grout. Finally, samples of grout were taken during dissection and measured for moisture content. The following sections describe the details of these test procedures.

J.1 Inclined Bleed Test

A modification of the Euronorm EN445 2007 (EN 445 Grout for pestressing tendons - Test methods, 2007) has been used to simulate grout bleed and segregation under *Field* conditions. The test was conducted by injecting grout into a 15-ft. long x 3-in. diameter transparent PVC pipe filled with twelve 0.6-in. diameter post-tensioning strands. The strand was cut to 14.5’ to leave a void where accurate measurements of any segregated soft grout can be obtained. The grout was mixed in the mixing basin using the colloidal, and pumped into the duct using the progressive cavity pump. Bleed and soft grout measurements and sampling took place 24 h after injection. Figure J-1 shows a schematic of the inclined bleed duct configuration. Figure J-2 shows a photograph of the actual inclined bleed ducts used for testing.

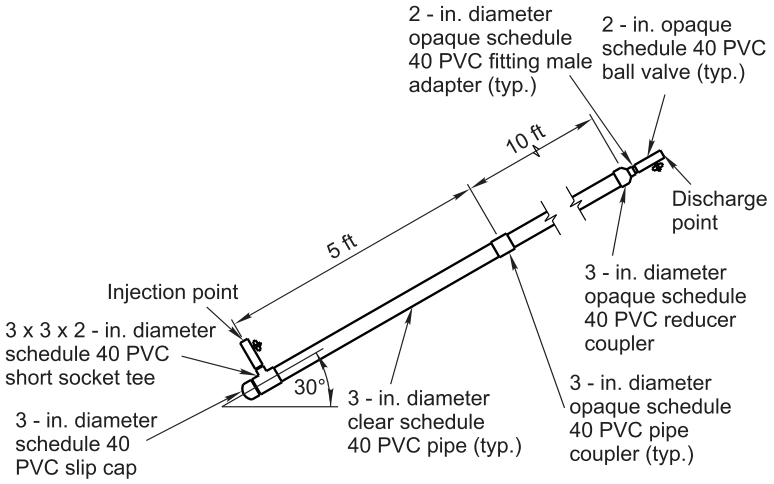

Figure J-1 MITT schematic

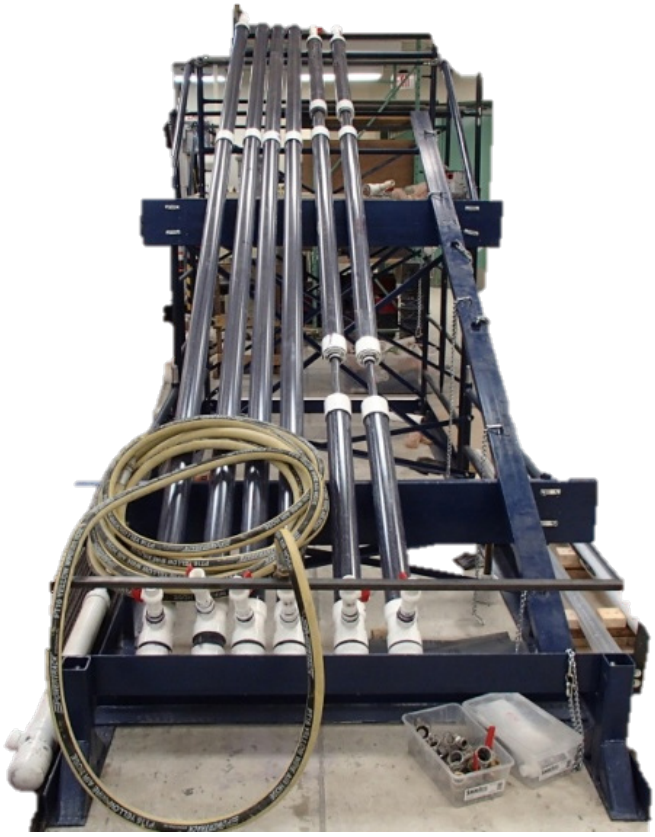

Figure J-2 MITT inclined stand

The procedure for mixing and injecting grout for the inclined bleed test is as follows:

1. Mix grout in colloidal grout plant according to mix procedure.
2. Transfer grout to agitation tank and start agitator paddle.
3. Pump grout from agitation tank through 50 ft. of 1” grout hose. Discharge approximately 2 gallons and conduct the following tests: apparent viscosity, flow cone, mud balance, unit weight and Schupack pressure bleed test.
4. Attach grout hose to duct.
5. Inject grout into duct over a period of approximately 1 minute. Discharge approximately 2 gallons out of the top of the duct. Record the following during injection: inlet and pump pressure, fill time, discharge temperature.
6. Conduct the following tests on the 2 gallons of grout discharged from the top of the duct: flow cone, mud balance, unit weight and Schupack pressure bleed test (ASTM C1741-12 Standard Method for Bleed Stability of Cementitious Post-tensioning Tendon Grout, 2012).

J.2 Modified Flow Cone

The modified ASTM C939 Flow Cone test was used to measure the fluidity of the grout while it was in fluid form. The modified flow cone test was developed for testing thixotropic grouts. The flow cone is filled completely, the plug at the bottom is pulled, and the time it takes to fill a 1000 mL beaker is recorded. Flow cone times should be between 5 seconds and 30

seconds for thixotropic PT grouts. The modified flow cone test was conducted before and after injecting all grouts, and was conducted before final additions of HRWR admixtures during plain grout testing. Figure J-3 and Figure J-4 show a schematic and photo of the modified flow cone, respectively.

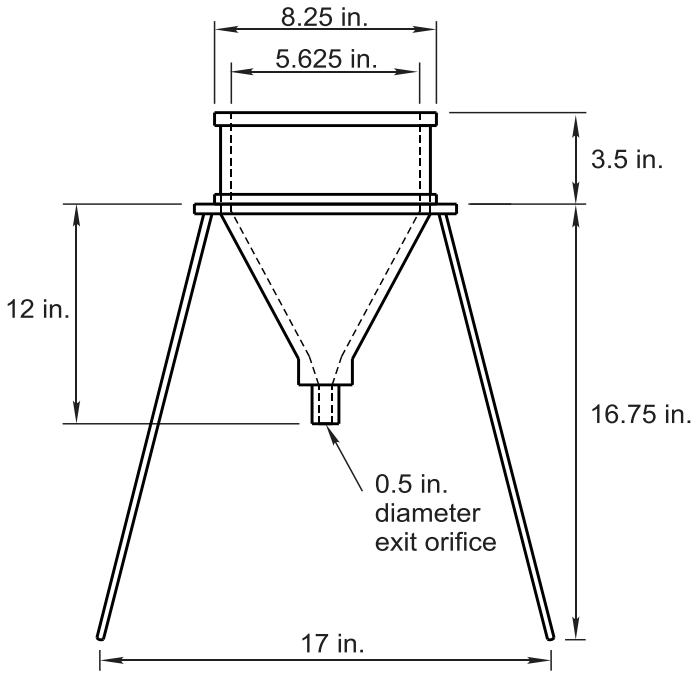

Figure J-3 ASTM C939 Modified Flow Cone schematic

Figure J-4 ASTM C939 Modified Flow Cone test

J.3 Unit Weight

The unit weight was measured using a cup with a known volume, and weighing the amount of grout needed to fill the cup completely. The inside volume of the cup was known to be 0.0141 ft^3. The grout was poured into the unit weight cup after zeroing the scale with the unit

weight cup and glass top. Then the excess grout was wiped off from the outside of the cup, and the configuration was weighed. The unit weight was simply the measured weight divided by the known volume. Figure J-5 below shows a photo of the empty unit weight cup.

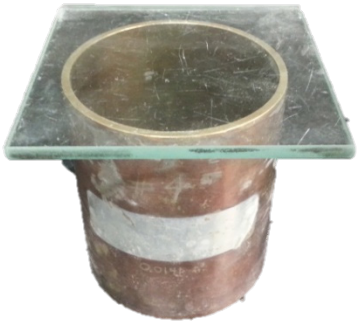

Figure J-5 Unit weight cup and glass plate

J.4 Mud Balance

The ASTM C185 “mud-balance” test was used to measure the density of the grout in fluid form. This test uses a beaker attached to a rod with a moveable counter balance on the opposite end of the beaker that is balanced on a fulcrum point. There is a level above the fulcrum point that allows the user to measure the density of the grout. The mud-balance test was conducted on all grout before and after injection. Figure J-6 below show a picture of the mud-balance being used during a grouting operation.

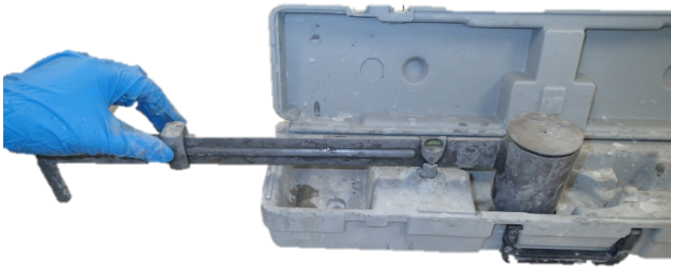

Figure J-6 ASTM C185 “Mud-balance” test

J.5 Schupack Pressure Bleed Test

The Schupack Pressure Bleed Test (ASTM C1741-12 Standard Method for Bleed Stability of Cementitious Post-tensioning Tendon Grout, 2012) was used to compare with data obtained from bleed measurements from the full-scale bleed test. The Schupack test uses air pressure and a fabric filter inside of a stainless steel cylinder to measure a grouts susceptibility to bleeding. Figure J-7 below shows a photo of the Schupack test. Figure J-8 shows the various components that make up the Schupack pressure bleed test.

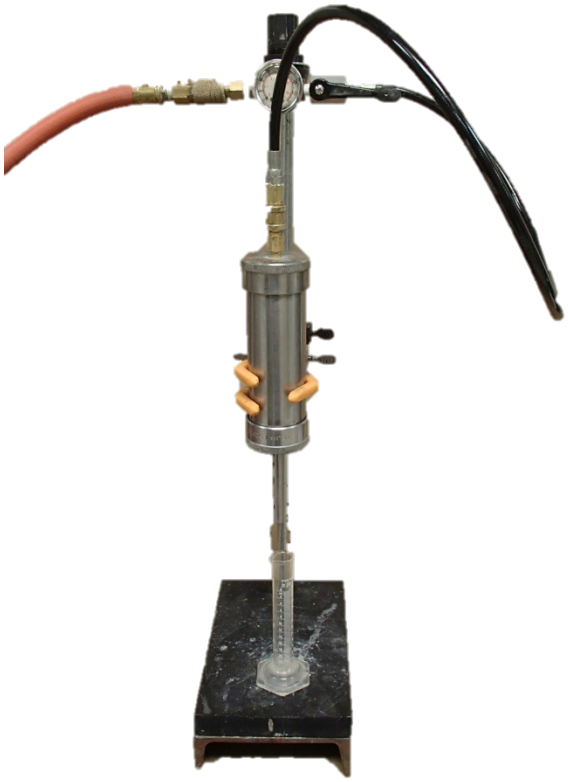

Figure J-7 Schupack pressure bleed test

Figure J-8 Schupack pressure bleed test components

Figure J-8 above shows the parts used to perform a pressurized Schupack bleed test. From left to right, the parts are: cylinder top cap, specimen cylinder, cylinder bottom bleed tube, metal screen, fabric filter, plastic filter ring. From Figure J-7 above, it can be seen that pressurized air is pumped through the top of the cylinder while the sample is inside of the cylinder for a finite amount of time. The scree, fabric filter, and plastic ring are all located under the sample, and above the bleed tube. The bleed water is collected in a beaker, and the volume is recorded.

J.6 Apparent Viscosity Test

The apparent viscosity of the grout was measured before and after injection using a dynamic shear rheometer (DSR). Figure J-9 below shows a photo of the DSR with the doors open. A helical ribbon geometry and cup were used to test the grout. Figure J-10 below shows the cup and ribbon next to each other. The DSR works by rotating the ribbon, which is attached to a threaded rod, using a frictionless air bearing. The rheometer measures the torque that results when the ribbon is submerged into fluid grout. The torque is then converted to shear stress based on a factor that must be determined by testing a standard reference material to calibrate the machine. The shear strain is determined by multiplying the angular velocity by a known shear strain factor that can be obtained from the manufacturer of the cup and ribbon. The apparent viscosity is then calculated by dividing the measured shear stress values by the calculated shear strain.

Figure J-9 Dynamic shear rheometer

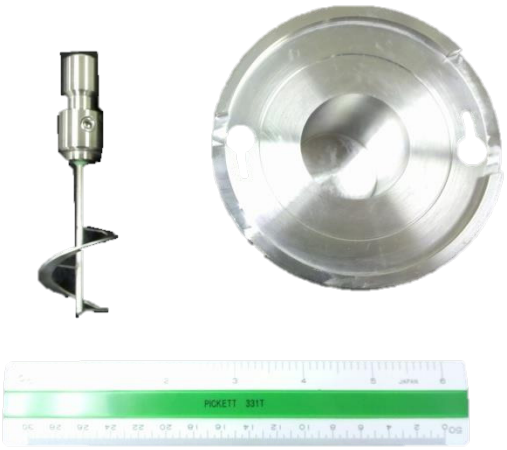

Figure J-10 Helical ribbon and cup

A schematic of both the helical ribbon geometry and the cup that the ribbon is lowered into that holds the fluid grout can be seen below in Figure J-11 and Figure J-12, respectively.

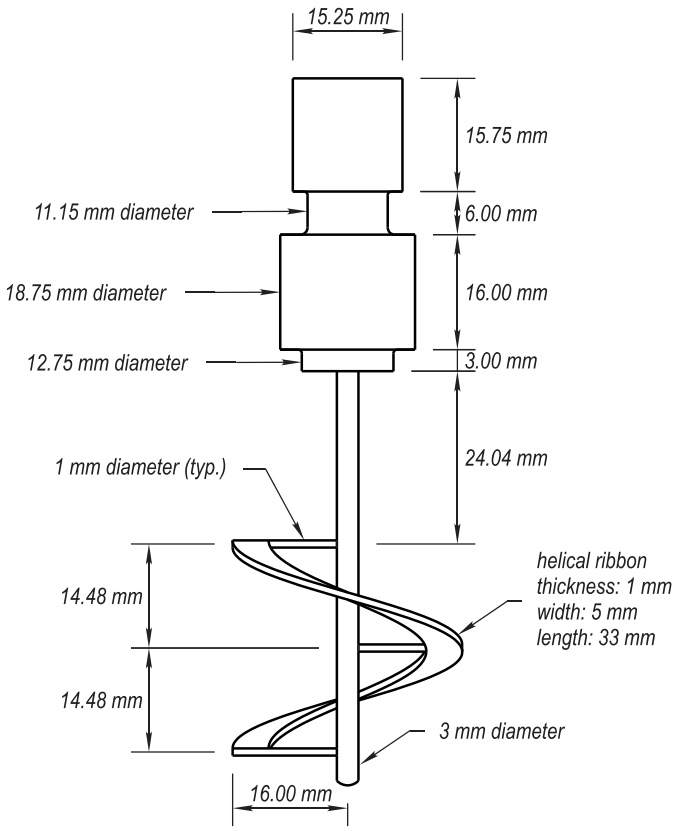

Figure J-11 Helical ribbon schematic

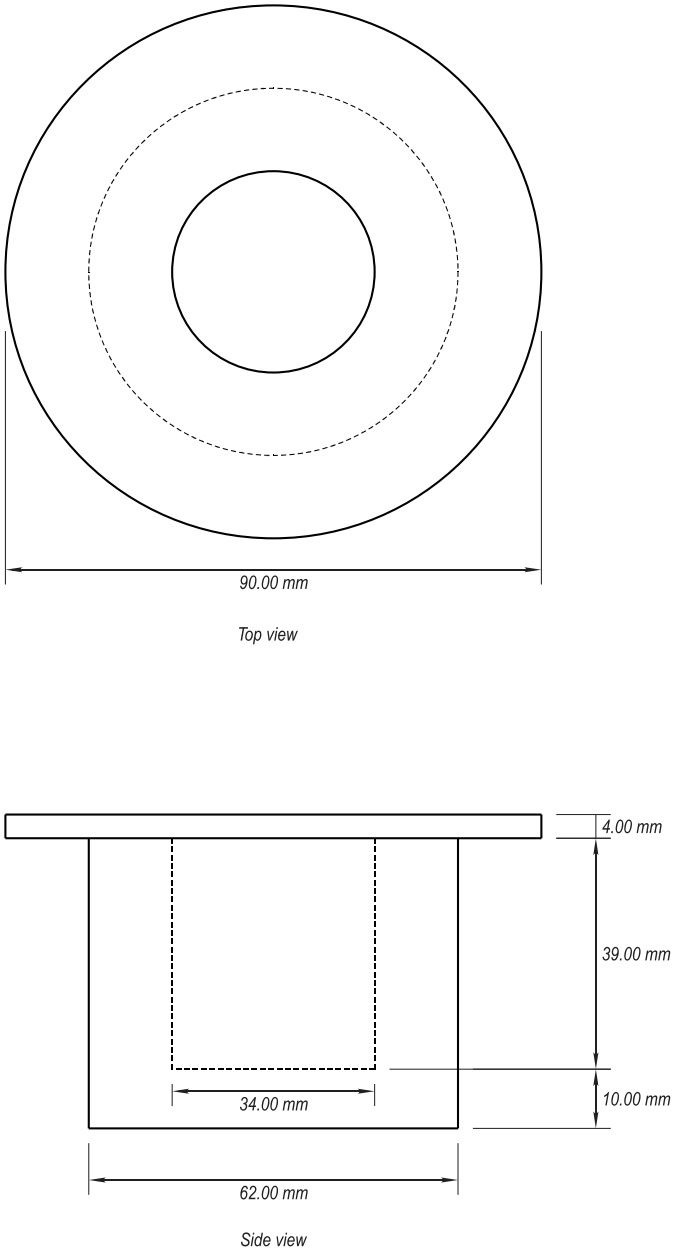

Figure J-12 DSR cup schematic

J.7 Bleed Water Measurement

The traditional inclined bleed test calls for bleed measurements immediately after injecting the inclined tube at specific time intervals, but for these tests bleed measurements were conducted after the grout had been allowed to harden for 24 h. This is because previous inclined bleed tests that were conducted before these tests resulted in no bleed immediately following grout injection. The ducts were removed from the inclined stand, and the top exit valve was removed by unscrewing it with a set of pliers. The duct was then carefully tilted so that any bleed water would pour into a large graduated cylinder that was placed under the exit. All bleed water was poured into the graduated cylinder, and the final volume was recorded.

J.8 Soft Grout Identification and Measurement

At approximately 24 h after injection, the region near the exit of the duct was cut open and inspected for soft grout. Soft grout was defined as grout that could be molded or deformed by hand and that appeared to have excessive moisture content. If bleed water was present, then that was measured separately. A flathead screwdriver was used to gently probe and scrape the grout in the exit region until all soft grout was removed. Soft grout was collected and weighed. Figure J-13 shows the exit region of a tendon during the MITT dissection process. If soft grout is formed during MITT it is always found at this location at the very top of the duct.

Figure J-13 Cross-section at top of duct where soft grout may be found during MITT

Based on Figure J-13, the soft grout can be seen occupying the top of the cross section of the exit region of the inclined test tube.

J.9 Moisture Content

Moisture content samples were gathered from the PT duct 24 h after grout injection. Figure J-14 shows the locations along the inclined test tube from which the moisture content samples were taken. These locations were selected to show the variation of moisture content along the length of the duct. The moisture content values were determined by measuring the moist weight of the grout, and then the grout samples were placed into an oven for 24 h. The samples were then weighed, and the moisture content was calculated. Figure J-15, Figure J-16, and Figure J-17 show the moisture content scale, samples, and samples inside of an oven, respectively.

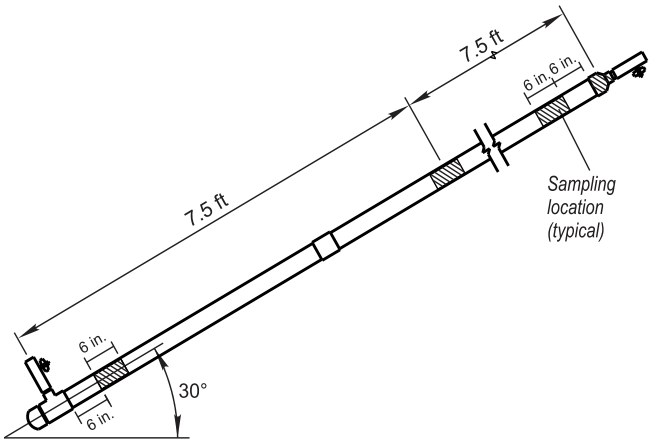

Figure J-14 MITT sampling locations

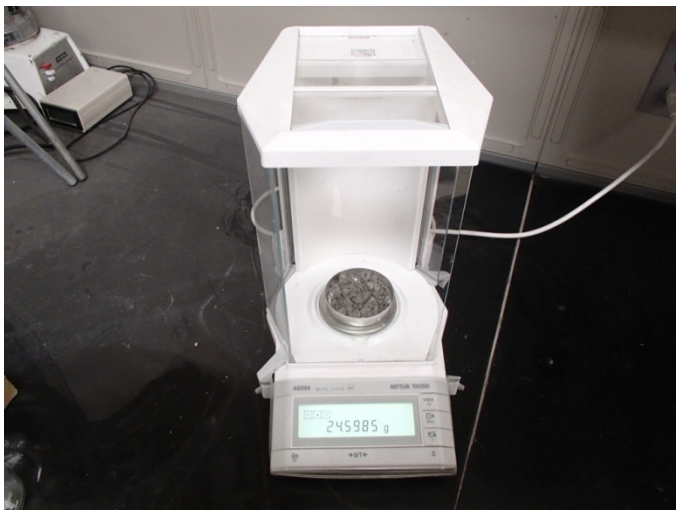

Figure J-15 Moisture content scale

Figure J-16 Moisture content samples

Figure J-17 Moisture content samples inside oven

Figure J-18 below shows the hand held band saw used to cut the incline tube for sampling the exit region. After using a cut-off wheel to remove the PVC duct, a jack hammer was used to gather a sample the hardened grout from the top and bottom of the cross-section as shown in Figure J-19. Although the volume of the samples varied, typically a sufficient quantity of grout to cover the bottom of the pan was gathered.

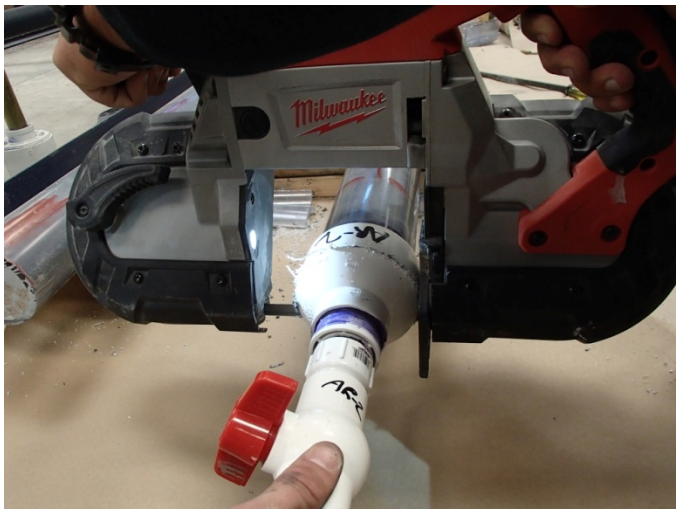

Figure J-18 Band saw used during dissection

Figure J-19 Jack hammer used during dissection

Appendix K—Screening Test Raw Data

Table K-1 Average mass gain percent from small-scale samples in *Field* and *Extreme* exposures

Time of Exposure	PT1-F	PT2-F	PT3-F	PT5-F	PT7-F
1 days	1.2	1.1	1.1	0.4	1.1
7 days	1.5	2.1	2.3	1.0	2.1
13 days	2.4	3.7	3.4	1.4	2.8
14 days	2.5	3.9	3.6	1.4	2.8
Time of Exposure	PT1-E	PT2-E	PT3-E	PT5-E	PT7-E
1 days	1.6	1.7	1.8	1.3	2.2
3 days	3.2	4.1	3.3	2.5	4.1
7 days	5.7	7.2	3.5	4.7	7.4
10 days	N/A	N/A	N/A	6.3	9.4
11days	8.7	N/A	N/A	N/A	N/A
14 days	N/A	10.9	N/A	N/A	N/A

Table K-2 Normalized dry PSA mean particle sizes for MITT samples of grout in *Field* and *Extreme* exposures

Time of Exposure	PT1-F	PT2-F	PT3-F	PT5-F	PT7-F
0 day	1	1	1	1	1
7 days	0.66	0.86	1	1	1.23
13 days	0.65	0.96	0.97	1.04	1.25
14 days	0.66	1.09	N/A	0.98	1.18
Time of Exposure	PT1-E	PT2-E	PT3-E	PT5-E	PT7-E
0 day	1	1	1	1	1
1 days	0.83	0.9	0.94	1	1.23
3 days	0.83	1.01	1	0.93	1.24
7 days	0.69	1	1.15	1.1	1.18
10 days	N/A	N/A	N/A	1.18	1.33
11 days	0.63	N/A	1.35	N/A	N/A
14 days	N/A	1.1	N/A	N/A	N/A

Table K-3 Normalized dry PSA mean particle sizes for small-scale samples of grouts in *Field* and *Extreme* exposures

Time of Exposure	PT1-F	PT2-F	PT3-F	PT5-F	PT7-F
0 day	1	1	1	1	1
7 days	0.69	0.93	1.04	1.03	1.26
13 days	0.64	1.04	1.08	1.08	1.26
14 days	0.74	1.10	1.23	1.09	1.44
Time of Exposure	PT1-E	PT2-E	PT3-E	PT5-E	PT7-E
0 day	1	1	1	1	1
1 days	0.65	0.93	0.63	1.11	1.30
3 days	1.49	1.17	1.08	1.32	1.56
7 days	0.90	1.37	1.31	1.39	1.99
10 days	N/A	N/A	N/A	1.77	2.80
11 days	1.23	N/A	N/A	N/A	N/A
14 days	N/A	1.84	N/A	N/A	N/A

Table K-4 BF_{ratio} for MITT samples of grout in *Field* and *Extreme* exposures

Time of Exposure	PT1-F	PT2-F	PT3-F	PT5-F	PT7-F
0 day	1.00	1.00	1.00	1.00	1.00
7 days	0.85	0.61	N/A	0.77	0.69
13 days	0.45	0.45	0.82	0.73	0.67
14 days	0.38	0.51	0.79	0.77	0.63
Time of Exposure	PT1-E	PT2-E	PT3-E	PT5-E	PT7-E
0 day	1.00	1.00	1.00	1.00	1.00
3 days	N/A	0.78	0.84	0.66	0.76
7 days	0.38	0.50	0.75	0.59	0.68
10 days	N/A	N/A	N/A	0.64	0.63
11 days	0.36	N/A	N/A	N/A	N/A
14 days	N/A	0.42	0.75	0.30	0.37

Table K-5 BF_{ratio} BF_{ratio} for small-scale samples of grout in *Field* and *Extreme* exposures

Time of Exposure	PT1-F	PT2-F	PT3-F	PT5-F	PT7-F
0 days	1.00	1.00	1.00	1.00	1.00
1 day	0.74	0.81	0.93	0.85	0.78
7 days	0.60	0.57	0.79	0.62	0.59
13 days	0.40	0.45	0.75	0.44	0.54
14 days	0.27	0.42	0.75	0.49	N/A
Time of Exposure	PT1-E	PT2-E	PT3-E	PT5-E	PT7-E
0 days	1.00	1.00	1.00	1.00	1.00
1 days	0.64	0.58	0.63	0.58	0.61
3 days	0.41	0.52	0.50	0.49	0.51
7 days	0.31	0.36	0.44	0.35	0.48
10 days	N/A	N/A	N/A	0.39	0.39
11 days	0.24	N/A	N/A	N/A	N/A
14 days	N/A	0.29	0.75	0.12	0.51

Table K-6 Normalized LOI mass loss from MITT grout samples in *Field* and *Extreme* exposures

Time of Exposure	PT1-F	PT2-F	PT3-F	PT5-F	PT7-F
0 days	1.00	1.00	1.00	1.00	1.00
7 days	1.03	1.10	1.43	1.12	1.09
13 days	1.05	1.32	1.63	1.20	1.16
14 days	1.16	1.33	1.65	1.24	1.17
Time of Exposure	PT1-E	PT2-E	PT3-E	PT5-E	PT7-E
0 days	1.00	1.00	1.00	1.00	1.00
1 day	1.01	0.95	1.20	1.04	1.09
3 days	1.03	N/A	1.42	1.18	1.13
7 days	1.10	1.13	1.60	1.26	1.20
10 days	N/A	N/A	N/A	1.44	1.32
11 days	1.34	N/A	N/A	N/A	N/A
14 days	N/A	1.43	N/A	N/A	N/A

Table K-7 Normalized LOI mass loss from small-scale grout samples in *Field* and *Extreme* exposures

Time of Exposure	PT1-F	PT2-F	PT3-F	PT5-F	PT7-F
0 days	1.00	1.00	1.00	1.00	1.00
1 day	1.19	1.09	1.58	1.14	1.18
7 days	1.26	1.32	2.11	1.41	1.29
13 days	1.44	1.88	2.40	1.72	N/A
14 days	1.52	1.96	N/A	1.77	1.40
Time of Exposure	PT1-E	PT2-E	PT3-E	PT5-E	PT7-E
0 day	1.00	1.00	1.00	1.00	1.00
1 day	1.24	1.19	1.77	1.43	1.32
3 days	1.55	1.94	2.53	2.03	1.59
7 days	2.70	3.10	2.91	3.54	N/A
10 days	N/A	N/A	N/A	6.25	2.49
11 days	3.28	N/A	N/A	N/A	N/A
14 days	N/A	3.72	N/A	N/A	N/A

Table K-8 TGA mass retention percent from MITT samples in *Field* and *Extreme* exposures

Mass Retention (%)												
Temperature °C	25	123	222	320	418	517	615	713	812	900	949	999
PT1-I-0	100.00	99.26	99.02	98.92	98.71	98.24	98.30	96.71	95.69	95.71	95.71	95.72
PT1-F-7	100.00	99.28	98.98	98.86	98.75	98.20	98.16	96.47	95.38	95.38	95.39	95.39
PT1-F-14	100.00	99.17	98.80	98.66	98.45	97.85	97.93	96.44	95.99	95.58	95.35	95.14
PT1-E-3	100.00	99.20	98.95	98.84	98.51	98.09	98.10	96.48	95.34	95.35	95.35	95.35
PT1-E-7	100.00	99.26	98.95	98.83	98.72	98.24	98.13	96.39	95.30	95.29	95.30	95.30
PT1-E-11	100.00	99.49	98.85	98.67	98.56	97.89	98.00	97.21	94.94	94.93	94.93	94.94
PT2-I-0	100.00	99.65	99.47	99.24	98.92	98.12	98.06	96.73	96.09	96.09	96.10	96.10
PT2-F-7	100.00	99.62	99.36	99.06	98.81	98.07	97.93	96.36	95.82	95.82	95.82	95.82
PT2-F-14	100.00	99.35	99.00	98.61	98.31	97.52	97.38	95.55	94.77	94.75	94.75	94.76
PT2-E-3	100.00	99.61	99.39	99.18	98.85	98.10	97.89	96.20	95.59	95.59	95.59	95.60
PT2-E-7	100.00	99.03	98.52	98.06	97.66	96.81	96.52	94.55	93.94	93.91	93.91	93.91
PT2-E-14	100.00	99.51	99.27	98.94	98.65	97.97	97.71	95.77	95.46	95.45	95.45	95.45
PT3-0	100.00	99.70	99.50	99.19	98.91	98.13	97.94	96.57	96.52	96.52	96.52	96.52
PT3-F-7	100.00	99.61	99.37	99.04	98.76	98.09	97.85	96.31	96.23	96.22	96.22	96.22
PT3-F-14	100.00	99.57	99.30	98.95	98.68	98.01	97.82	96.23	95.87	95.87	95.86	95.86
PT3-E-3	100.00	99.64	99.40	99.09	98.89	98.33	98.21	96.95	96.52	96.51	96.51	96.51
PT3-E-7	100.00	99.43	99.10	98.75	98.51	97.87	97.66	96.22	96.01	96.00	96.00	96.00
PT3-E-11	100.00	99.23	98.85	98.57	98.05	97.40	97.22	95.72	95.50	95.47	95.47	95.46
PT5-0	100.00	99.69	99.45	99.03	98.75	98.50	98.31	97.27	97.22	97.21	97.21	97.22
PT5-F-7	100.00	99.58	99.22	98.79	98.48	98.15	97.96	96.89	96.82	96.81	96.81	96.80
PT5-F-14	100.00	99.46	99.04	98.59	98.26	97.86	97.59	96.51	96.47	96.46	96.46	96.46
PT5-E-3	100.00	99.56	99.20	98.78	98.50	98.18	97.99	96.95	96.89	96.89	96.88	96.88
PT5-E-7	100.00	99.34	98.86	98.42	98.08	97.67	97.35	96.31	96.30	96.29	96.28	96.28
PT5-E-10	100.00	99.36	98.79	98.38	98.05	97.71	97.49	96.50	96.32	96.31	96.31	96.30
PT7-0	100.00	99.06	98.54	98.38	98.25	97.53	96.45	93.99	91.90	91.89	91.88	91.88
PT7-F-7	100.00	98.88	98.34	98.14	97.96	97.30	96.09	94.07	92.39	92.38	92.38	92.37
PT7-F-14	100.00	98.79	98.15	97.92	97.72	97.06	95.77	93.60	92.04	92.02	92.01	92.01
PT7-E-3	100.00	98.81	98.29	98.08	97.89	97.17	95.79	93.44	91.96	91.94	91.94	91.93
PT7-E-7	100.00	98.50	97.87	97.58	97.39	96.78	95.44	93.37	91.86	91.84	91.83	91.83
PT7-E-10	100.00	98.59	97.95	97.63	97.40	96.62	95.25	93.15	91.19	91.18	91.17	91.16

Table K-9 TGA mass retention from small-scale grout samples in *Field* and *Extreme* exposures

Mass Retention (%)												
Temperature °C	25	123	222	320	418	517	615	713	812	900	949	999
PT1-0	100.00	99.26	99.02	98.92	98.71	98.24	98.30	96.71	95.69	95.71	95.71	95.72
PT1-F-1	100.00	99.07	98.74	98.57	98.47	97.93	97.94	96.18	95.10	95.11	95.11	95.12
PT1-F-7	100.00	98.98	98.59	98.46	98.35	97.79	97.80	96.01	94.93	94.94	94.95	94.95
PT1-F-13	100.00	98.59	97.95	97.72	97.51	96.79	96.24	94.97	93.18	93.18	93.18	93.18
PT1-F-14	100.00	98.61	98.01	97.80	97.58	96.85	96.18	94.77	93.31	93.31	93.31	93.32
PT1-E-1	100.00	98.80	98.40	98.23	98.11	97.47	97.31	95.58	94.36	94.36	94.36	94.36
PT1-E-3	100.00	98.29	97.42	97.14	96.89	96.13	95.37	93.73	92.06	92.04	92.04	92.03
PT1-E-7	100.00	98.40	97.43	97.16	96.94	96.14	95.20	93.74	91.46	91.45	91.45	91.45
PT1-E-11	100.00	97.78	96.49	96.05	95.67	94.60	93.25	90.94	88.35	88.29	88.28	88.27
PT2-I-0,	100.00	99.65	99.47	99.24	98.92	98.12	98.06	96.73	96.09	96.09	96.10	96.10
PT2-F-1	100.00	99.39	99.12	98.78	98.53	97.78	97.67	96.05	95.20	95.20	95.21	95.21
PT2-F-7	100.00	99.24	98.93	98.56	98.31	97.66	97.57	96.00	95.12	95.11	95.11	95.12
PT2-F-13	100.00	98.35	97.55	97.03	96.55	95.87	95.59	93.83	92.06	91.99	91.98	91.98
PT2-F-14	100.00	98.29	97.45	96.91	96.45	95.71	95.45	93.73	91.89	91.83	91.82	91.82
PT2-E-1	100.00	99.33	99.03	98.63	98.32	97.61	97.41	95.61	94.92	94.91	94.92	94.93
PT2-E-3	100.00	98.63	98.06	97.62	97.21	96.44	96.15	94.02	93.17	93.14	93.14	93.15
PT2-E-7	100.00	98.12	97.32	96.86	96.43	95.58	95.29	93.48	92.75	92.71	92.70	92.71
PT2-E-14	100.00	96.25	94.52	93.74	92.96	92.15	91.17	89.07	83.00	82.81	82.76	82.75
PT3-0	100.00	99.70	99.50	99.19	98.91	98.13	97.94	96.57	96.52	96.52	96.52	96.52
PT3-F-7	100.00	99.20	98.79	98.45	98.17	97.50	97.21	95.53	95.05	95.02	95.02	95.02
PT3-F-14	100.00	99.03	98.63	98.30	98.05	97.32	97.03	95.65	95.60	95.59	95.58	95.58
PT3-E-3	100.00	99.09	98.58	98.23	97.96	97.28	97.02	95.38	95.08	95.07	95.06	95.06
PT3-E-7	100.00	99.05	98.53	98.16	97.89	97.21	96.98	95.28	94.66	94.65	94.64	94.64
PT3-E-11	100.00	98.07	97.18	96.65	96.18	95.46	95.06	92.92	91.87	91.80	91.79	91.78
PT5-0	100.00	99.69	99.45	99.03	98.75	98.50	98.31	97.27	97.22	97.21	97.21	97.22
PT5-F-7	100.00	99.37	98.93	98.50	98.20	97.84	97.51	96.45	96.37	96.36	96.38	96.38
PT5-F-14	100.00	99.23	98.56	98.10	97.72	97.34	96.94	95.95	95.64	95.63	95.62	95.62
PT5-E-3	100.00	98.81	98.09	97.60	97.15	96.76	96.36	95.18	95.04	95.01	94.99	94.98
PT5-E-7	100.00	98.84	98.05	97.55	97.11	96.72	96.30	95.14	94.83	94.81	94.80	94.79
PT5-E-10	100.00	98.65	97.71	97.21	96.73	96.31	95.89	94.81	94.25	94.21	94.19	94.18
PT7-0	100.00	99.06	98.54	98.38	98.25	97.53	96.45	93.99	91.90	91.89	91.88	91.88
PT7-F-7	100.00	98.24	97.48	97.17	96.93	96.01	94.65	92.45	90.23	90.22	90.21	90.21
PT7-F-14	100.00	98.30	97.42	97.12	96.88	95.89	94.52	92.17	90.17	90.15	90.15	90.14
PT7-E-3	100.00	97.99	96.96	96.62	96.34	95.28	93.75	91.53	89.20	89.16	89.14	89.13
PT7-E-7	100.00	97.45	96.06	95.64	95.31	94.25	92.62	90.49	87.78	87.62	87.60	87.59
PT7-E-10	100.00	97.34	95.64	95.21	94.84	93.63	91.95	89.50	86.88	86.80	86.78	86.76

Table K-10 MMC total mass loss percent for MITT grout samples from *Field* and *Extreme* exposures

	PT1-F	PT2-F	PT3-F	PT5-F	PT7-F
0days	0.21	0.04	0.04	0.10	0.62
7days	0.19	0.05	0.29	0.26	0.88
13days	0.30	0.06	0.38	0.32	0.99
14days	0.35	0.25	0.42	0.37	1.04
	PT1-E	PT2-E	PT3-E	PT5-E	PT7-E
0days	0.21	0.04	0.04	0.10	0.62
1days	0.19	0.23	0.04	0.13	0.60
3days	N/A	0.25	0.16	0.26	0.73
7days	0.33	0.65	0.27	0.45	0.95
10days	N/A	N/A	N/A	0.59	1.31
11days	0.63	N/A	N/A	N/A	N/A
14days	N/A	1.49	N/A	N/A	N/A

Table K-11 MMC total mass loss percent for small-scale grout samples from *Field* and *Extreme* exposures

	PT1-F	PT2-F	PT3-F	PT5-F	PT7-F
0days	0.21	0.04	0.04	0.10	0.62
7days	0.69	0.71	0.68	0.46	1.42
13days	0.86	0.99	0.75	0.57	1.71
14days	0.95	1.03	0.77	0.63	1.69
	PT1-E	PT2-E	PT3-E	PT5-E	PT7-E
0days	0.21	0.04	0.04	0.1	0.62
1days	N/A	0.47	0.49	0.56	1.34
3days	N/A	1.04	0.88	0.87	1.91
7days	1.63	1.58	1.09	1.29	2.76
10days	N/A	N/A	N/A	1.87	3.16
11days	2.35	N/A	N/A	N/A	N/A
14days	N/A	2.35	N/A	N/A	N/A

Appendix L—Screening Test Change with Exposure Data

Table L-1 Sensitivity of PSA (Dry)

Field Exposure					
	Days	Control	Soft Grout	Difference	% Difference
PT1	10	1	0.65	0.35	35
PT2	12	1	0.96	0.04	4
PT3	4	1	1.00	0.00	0
PT5	13	1	1.04	0.04	4
PT7	3	1	1.23	0.23	23
Average				0.13	13
Extreme Exposure					
	Days	Control	Soft Grout	Difference	% Difference
PT1	7	1	0.69	0.31	31
PT2	3	1	1.01	0.01	1
PT3	1	1	0.94	0.06	6
PT5	3	1	0.93	0.07	7
PT7	2	1	1.24	0.24	24
Average				0.14	14

Table L-2 Sensitivity of PSA (Wet)

Field Exposure					
	Days	Control	Soft Grout	Difference	% Difference
PT1	10	1	0.65	0.35	40
PT2	12	1	0.96	0.04	0
PT3	4	1	1.00	0.00	10
PT5	13	1	1.04	0.04	10
PT7	3	1	1.23	0.23	20
Average				0.13	16
Extreme Exposure					
	Days	Control	Soft Grout	Difference	% Difference
PT1	7	1	0.69	0.31	40
PT2	3	1	1.01	0.01	0
PT3	1	1	0.94	0.06	0
PT5	3	1	0.93	0.07	10
PT7	2	1	1.24	0.24	20
Average				0.14	14

Table L-3 Sensitivity of Blaine Fineness

Field Exposure					
	Days	Control	Soft Grout	Difference	% Difference
PT1	10	1	0.45	0.55	55
PT2	12	1	0.45	0.55	55
PT3	4	1	0.82	0.18	18
PT5	13	1	0.77	0.23	23
PT7	3	1	0.69	0.31	31
Average				0.36	36
Extreme Exposure					
	Days	Control	Soft Grout	Difference	% Difference
PT1	7	1	0.36	0.64	64
PT2	3	1	0.5	0.5	50
PT3	1	1	0.84	0.16	16
PT5	3	1	0.66	0.34	34
PT7	2	1	0.76	0.24	24
Average				0.38	37.6

Table L-4 Sensitivity of LOI

Field Exposure					
	Days	Control	Soft Grout	Difference	% Difference
PT1	10	1	1.05	0.05	5
PT2	12	1	1.31	0.31	31
PT3	4	1	1.42	0.42	42
PT5	13	1	1.19	0.19	19
PT7	3	1	1.08	0.08	8
Average				0.21	21
Extreme Exposure					
	Days	Control	Soft Grout	Difference	% Difference
PT1	7	1	1.09	0.09	9
PT2	3	1	1.12	0.12	12
PT3	1	1	1.2	0.2	20
PT5	3	1	1.17	0.17	17
PT7	2	1	1.12	0.12	12
Average				0.14	14

Table L-5 Sensitivity of TGA

Field Exposure					
	Days	Control	Soft Grout	Difference	% Difference
PT1	10	4.2	4.8	0.6	14
PT2	12	3.9	5.2	1.3	33
PT3	4	3.48	3.7	0.22	6
PT5	13	2.78	3.5	0.72	26
PT7	3	8.1	8.1	0	0
Average				0.57	16.0
Extreme Exposure					
	Days	Control	Soft Grout	Difference	% Difference
PT1	7	4.2	5	0.8	19
PT2	3	3.9	6.09	2.19	56
PT3	1	3.48	3.49	0.01	0
PT5	3	2.78	3.1	0.32	12
PT7	2	8.1	8.8	0.7	9
Average				0.80	19.1

Table L-6 Sensitivity of MMC

Field Exposure					
	Days	Control	Soft Grout	Difference	% Difference
PT1	0.21	0.3	0.09	35.3	43
PT2	0.04	0.06	0.02	40.0	50
PT3	0.04	0.29	0.25	151.5	625
PT5	0.1	0.37	0.27	114.9	270
PT7	0.62	0.88	0.26	34.7	42
Average				0.18	206
Extreme Exposure					
	Days	Control	Soft Grout	Difference	% Difference
PT1	7	0.21	0.63	0.42	200
PT2	3	0.04	0.65	0.61	1525
PT3	1	0.04	0.16	0.12	300
PT5	3	0.1	0.26	0.16	160
PT7	2	0.62	0.73	0.11	18
Average				0.28	441